I. Synthetic Studies towards NF00659B[1]

II. Design, Synthesis, and Characterization of Manassantin Analogues

by

Do Yeon Kwon

Department of Chemistry
Duke University

Date:_____

Approved:

_____
Jiyong Hong, Supervisor

_____
Steven W. Baldwin

_____
Katherine J. Franz

_____
Dewey G. McCafferty

Dissertation submitted in partial fulfillment of
the requirements for the degree of Doctor of Philosophy in the Department of
Chemistry in the Graduate School of
Duke University

2015

ABSTRACT

I. Synthetic Studies towards NF00659B1

II. Design, Synthesis, and Characterization of Manassantin Analogues

by

Do Yeon Kwon

Department of Chemistry
Duke University

Date:_____
Approved:

_____
Jiyong Hong, Supervisor

_____
Steven W. Baldwin

_____
Katherine J. Franz

_____
Dewey G. McCafferty

An abstract of a dissertation submitted in partial fulfillment of
the requirements for the degree of Doctor of Philosophy in the Department of
Chemistry in the Graduate School of
Duke University

2015

Abstract

Despite natural products play a crucial role in drug discovery and chemical biology, these compounds are often available in limited quantities. Therefore, there is a need for efficient methods that allow access to the natural products as well as analogues for the evaluation of biological activity, investigation of structure activity relationships, and generation of more improved bioactive molecules. This dissertation consists of two parts focused on synthetic studies towards biologically active natural products and their analogues.

Part I: Since bioactive diterpenoid pyrones produced by microbes have limitless potential in pharmaceutical applications, a considerable effort has been devoted to the synthesis of diterpenoid pyrones and the identification of their structure-activity relationships. This chapter describes our synthetic studies towards the first total synthesis of NF00659B$_1$, the 4,5-*seco*-tricyclic diterpene α-pyrone. Our synthetic efforts are focused on an efficient construction of the key intermediate oxepanol and installation of the α-pyrone moiety by Cu(I)-mediated intermolecular S_N2' reaction. Using efficient synthetic methods, we have been investigating the unknown absolute and relative stereochemistry of NF00659s. In addition, these synthetic strategies will contribute to a more thorough elucidation of their bioactivities. Due to their bioactivities, NF00659s are expected to be promising new anticancer drugs.

Part II: Hypoxia-inducible factor 1 (HIF-1) plays a significant role in the adaptation of tumor cells to hypoxia by activating the transcription of genes involved in critical aspects of cancer, making it a leading target for the treatment of cancer. Despite several small molecules have been reported to inhibit the HIF-1 signaling pathway, these compounds exhibit relatively low HIF-1 inhibitory activity. In addition, most of them lack the desired selectivity or toxicity profiles required for a useful therapeutic agent. Therefore, development of potent and selective HIF-1 inhibitors is urgently needed. Manassantin A, a dineolignan isolated from *Saururus cernuus* L. (Saururaceae) has been shown to be a potent inhibitor of HIF-1α *in vitro* with minimal cytotoxicity. Previously, we reported a convergent and efficient synthesis of manassantin A, which enables the creation of various analogues. This chapter describes our medicinal chemistry efforts for design, synthesis, and biological evaluation of manassantin analogues to establish structure-activity relationships of the natural product as well as identification of manassantin analogues with reduced structural complexity and improved drug-like properties. In addition, we have developed chemical probes by modifying structure of the natural product to determine the molecular mechanisms of manassantin-mediated HIF-1 inhibition.

In conclusion, we expect that these two projects will provide efficient synthetic approaches to the natural products and their analogues as well as invaluable tools to identify the mechanisms of action of the natural products.

Dedication

To my parents and my brothers for their unconditional love

Contents

List of Tables

List of Figures

List of Schemes

List of Abbreviations

4 Å MS	4 Å molecular sieves
AIBN	azobisisobutyronitrile
ATP	adenosine 5′-triphosphate
BEMP	2-*tert*-butylimino-2-diethylamino-1,3-dimethylperhydro-1,3,2-diazaphosphorine
Bn	benzyl
Boc	*tert*-butyloxycarbonyl
br s	broad singlet
brsm	based on recovered starting material
d	doublet
DBU	1,8-diazobicyclo[5,4,0]undec-7-ene
dd	double of doublet
ddd	doublet of doublet of doublet
DDQ	2,3-dichloro-5,6-dicyano-1,4-benzoquinone
ddt	doublet of doublet of triplet
DIBAL-H	diisobutylaluminium hydride
DMAP	4-(*N*,*N*-dimethylamino)-pyridine
DMDO	dimethyldioxirane
DMF	*N*,*N*-dimethylformamide

DMP	Dess–Martin periodinane
DMSO	dimethylsulfoxide
dq	doublet of quartet
dr	diastereomeric ratio
dt	doublet of triplet
EPO	erythropoietin
EVE	ethyl vinyl ether
GLUT1	glucose transporter 1
HIF-1	hypoxia inducible factor 1
HRE	hypoxia response element
HRMS	high-resolution mass spectrometry
IC_{50}	inhibitory concentration 50%
iNOS	inducible nitric oxide synthase
Kv1.3	voltage gated potassium channel 1.3
LAH	lithium aluminium hydride
LDH-A	lactate dehydrogenase A
LHMDS	lithium bis(trimethylsilyl)amide
m	multiplet
MAPK	mitogen-activated protein kinase
m-CPBA	*meta*-chloroperoxybenzoic acid

MOM	methoxy-*O*-methyl
Ms	methanesulfonyl
NaHMDS	sodium bis(trimethylsilyl)amide
NMO	*N*-methylmorpholine-*N*-oxide
NMR	nuclear magnetic resonance
NO	nitric oxide
ODD	oxygen-dependent degradation
OTf	trifluromethanesulfonate
p	pentet
$Pd(dba)_2$	bis(dibenzylideneacetone)palladium(0)
PHD	prolyl hydroxylase domain
PI3K	phosphatidylinositol 3-kinase
PPTS	pyridinium *p*-toluenesulfonate
q	quartet
RCM	ring closing metathesis
ROS	reactive oxygen species
s	singlet
SAR	structure activity relationship
sat.	saturated
t	triplet

TAD	transactivation domain
TBAB	tetra-*n*-butylammonium bromide
TBAF	tetra-*n*-butylammonium fluoride
TBAI	tetra-*n*-butylammonium iodide
TBDPS	*tert*-butyldiphenylsilyl
TBS	*tert*-butyldimethylsilyl
TFA	trifluoroacetic acid
THF	tetrahydrofuran
TLC	thin layer chromatography
TMEDA	tetramethylethylenediamine
TPAP	tetrapropylammonium perruthenate
Ts	*para*-toluenesulphonyl
UV	ultraviolet
VEGF	vascular endothelial growth factor
VHL	von Hippel Lindau

Acknowledgements

I would like to express my sincere gratitude to my research advisor, Professor Jiyong Hong for his excellent guidance, constant enthusiasm, and tremendous encouragement. I have enjoyed working on my great projects under his supervision and I believe my experiences here will be the cornerstone of my future career. I would also like to thank Professor Young-Ger Suh at Seoul National University in South Korea for his guidance in research for my master program and inspiring me to pursue this graduate career. I am also grateful to Professor Aree Moon at Duksung Women's University in South Korea for opening my eyes to the world of science. She is my role model as a female scientist. I would also like to thank my committee members, Professor Steven Baldwin, Professor Katherine Franz, and Professor Dewey McCafferty for their invaluable advice and support.

I would like to thank Dr. George Dubay for his help with mass spectrometry. I also sincerely thank my former and current lab colleagues, Dr. Joseph Baker, Dr. Heekwang Park, Dr. Kiyoun Lee, Dr. Jae-Hwan Kwak, Dr. Mijung Kim, Dr. Megan Lanier, Tesia Stephenson, Bumki Kim, Minhee Lee, Hyeri Park, and Hyunji Lee for their help, advice, and friendship. I would also like to thank my friends at Duke University.

Finally, I would like to express my deepest gratitude to my parents and brothers for their support, encouragement, and love.

1. Introduction

1.1 Natural Products in Drug Discovery and Chemical Biology

Nature takes advantage of the natural selection process, which enables generation of natural products with diversity, target affinity, and specificity.[1] As a consequence, natural products have been the major sources for drug discovery and chemical biology.

In 2012, Newman and co-workers summarized sources of new drugs from 1981 to 2010.[2] The sources of new chemical entities covering all diseases, countries, and sources were classified: biological (B), natural product (N), natural product botanical (NB), derived from a natural product and is usually a semisynthetic modification (ND), totally synthetic drug (S), made by total synthesis (S*), natural product mimic (NM), and vaccine (V). According to their report, 50% (N, NB, ND, S*, S*/NM, and S/NM) of 1355 new chemical entities are naturally derived or inspired (Figure 1). With the anticancer drugs, one of the major disease areas that have been investigated by pharmaceutical industry, approximately 65% have been related to natural products.

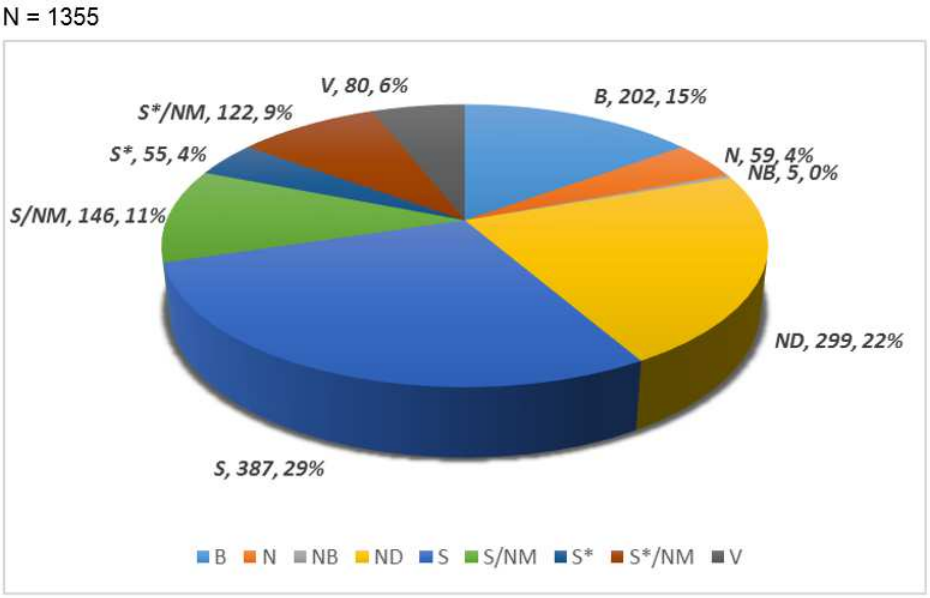

Figure 1: All new approved drugs[2]

There have been many examples of natural products being used for drug discovery.[3] Recent examples include dronabinol/cannabidiol, fumagillin, trabectedin, romidepsin, and capsaicin (Figure 2).[4] A mixture of dronabinol and cannabidiol, nabiximols (Sativex®), is an extract of cannabis plant[5] and used for neuropathic pain relief in multiple sclerosis.[6] Fumagillin (Flisint®) was isolated from *Aspergillus fumigatus* in 1949.[7] It has been used in the treatment of microsporidiosis.[8] Trabectedin (Yondelis®) was produced by *Ecteinascidia turbinate*[9] and have an interesting structure composed of tetrahydroisoquinoline moieties, 10-membered heterocyclic ring, and 7 stereogenic centers. It is used for advanced soft tissue sarcoma[10] and in Phase II trials against pediatric sarcoma[11], breast and prostate cancers.[12] Romidepsin (Istodax®) was isolated

from a culture of *Chromobacterium violaceum*.[13] It has been known as a histone deacetylase inhibitor[14] and used in the treatment of cutaneous and peripheral T-cell lymphoma (TCL).[15] As an active component of chili peppers, capsaicin (Qutenza®) is used for neuropathic pain combined with post-therapeutic neuralgia.[16]

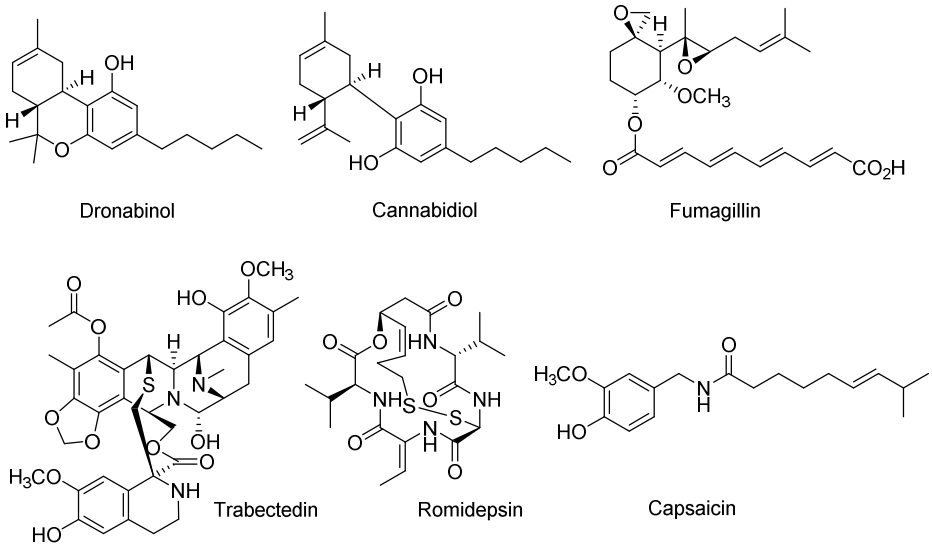

Figure 2: Natural products that have recently been developed as drugs

In addition to their crucial role in drug discovery, natural products play an important role in chemical biology by offering a wide range of biologically active molecules that can target various biological processes.[17] One representative example is FK506 (also known as tacrolimus). FK506 is a 23-membered macrolide lactone (Figure 3) and was isolated from the fermentation broth of *Streptomyces tsukubaensis* in 1987.[18] It was also reported to exhibit high levels of immunosuppressive activity *in vitro* and *in vivo*. These early studies showed that FK506 suppressed mixed lymphocyte reaction,

cytotoxic T cell generation, the production of T cell-derived soluble mediators such as interleukin 2 (IL-2), interleukin 3 (IL-3), gamma-interferon, and the expression of the IL-2 receptor.[19] In addition, this immunosuppressive effect was found to be more highly potent than that of cyclosporin A (CsA), a powerful immunosuppressive agent used in organ transplantation.[20] Subsequent investigations have demonstrated that the Ca^{2+} - and calmodulin-dependent phosphatase calcineurin is a common downstream biological target of CsA and FK506, revealing its previously unknown role in T cell receptor pathways.[21] Since its discovery, FK506 has provided a useful protein modulator in the elucidation of key immune-cell signal transduction mechanisms.

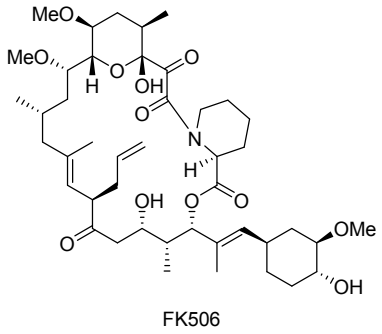

FK506

Figure 3: Structure of FK506

As previously mentioned, capsaicin is one of natural products that have been developed as drugs (Figure 2). Identification of vanilloid receptor 1 (VR1)[22], the first nociceptive receptor, using capsaicin as a molecular probe for pain/heat signal propagation is another example of natural product utilized in the study of important biological processes.

In order to use a natural product as a useful tool for studying biological systems or developing new drugs, it should be available in sufficient quantities. The availability of a compound is often limited from natural sources as shown in trabectedin (Figure 2). The Spanish company PharmaMar attempted to farm the sea squirt but yields were extremely low. It took 1 kilogram of animals to isolate 1 gram of trabectedin and about 5 grams were believed to be needed for a clinical trial. At that time, E. J. Corey was asked to search for a synthetic method of preparation and his group developed a method and published it in 1996.[23] After that, several other total syntheses of trabectedin were reported[24] and reviewed.[25] Currently, it is manufactured commercially by a semi-synthetic process from cyanosafracin B, the pioneering synthetic studies reported by Corey and co-workers.[23]

In addition to the sufficient availability, natural products should possess a certain level of specificity and potency to be used as drugs or modulators of biomolecular function. Therefore, development of efficient synthetic methods that allow access to the natural products as well as their analogues for the investigation of structure activity relationships (SARs) is the key issue in drug discovery and chemical biology.

1.2 Goals of Dissertation

Due to the crucial role of natural products in drug discovery and chemical biology, it is important to develop efficient synthetic methods to provide the natural products as well as their analogues for further studies. This dissertation will be focused on synthetic studies towards biologically active natural products and their analogues. In chapter 2, synthetic studies towards NF00659B$_1$, the 4,5-*seco*-tricyclic diterpene α-pyrone will be discussed. The synthetic strategies will contribute to a more thorough elucidation of their anticancer activities. In addition, we have been investigating the unknown absolute and relative stereochemistry of NF00659s. Chapter 3 will present our medicinal chemistry efforts to define the structural requirements of manassantins for HIF-1 inhibition. Furthermore, we have developed chemical probes by modifying structure of the natural product to determine the molecular mechanisms of manassantin-mediated HIF-1 inhibition.

2. Synthetic studies towards NF00659B$_1$

2.1 Introduction

2.1.1 Diterpenoid Pyrones

Terpenoids can be found in all classes of living things, and make up the largest group of natural products.[26] These terpenoids are derived from five-carbon units assembled and modified in a wide variety of ways. Most of them are multicyclic structures that differ from one another not only in their functional groups but also in their basic carbon skeletons. Moreover, the terpenoids from a variety of natural sources have played a significant role in traditional herbal remedies and are under investigation for antibacterial and other pharmaceutical functions. As a result, a considerable effort has been devoted to identification of the structure-activity relationships (SARs) of terpenoids.[27]

Diterpenoids, a member of the terpenoid family, with their twenty-carbon backbone constitute roughly a fourth of all known plant terpenoids, which currently are more than 12,000 (and counting) structures known.[28] It is well known that α- and γ-pyrones are privileged structural motifs frequently found in a number of natural products, pharmaceutical compounds, as well as useful building blocks in organic synthesis.[29] Within the last several years, a number of diterpenoid pyrones and related compounds have been isolated and reported to exhibit a wide variety of biological activities.[30] However, further biological studies including SARs are severely restricted.

Consequently, there is a need for efficient, stereo-, and enantioselective methods that allow access to these compounds as well as analogues for the evaluation of biological activities and SAR studies.

There have been several reports on structurally related and biologically interesting diterpenoid pyrones (Figure 4). Danishefsky and co-workers reported the first synthesis of (±)-sesquicillin[31], a glucocorticoid antagonist. In addition, the enantioselective synthesis of (−)-candelalide A-C[32], (−)-nalanthalide[33], (+)-sesquicillin[33b] was completed by Katoh and co-workers. Candelalides and nalanthalide are known as blockers of the voltage-gated potassium channel Kv1.3 and can be utilized as immunosuppressive agents.[30c, 30d] Hong and co-workers reported the first total synthesis of (−)-subglutinols A and B[34], which led to the determination of the absolute configuration of the natural products. Katoh and co-workers also accomplished the total synthesis of (−)-subglutinols A and B.[35] Subglutinols A and B exhibit the immunosuppressive activities *in vitro* and *in vivo*[36], as well as dose-dependent osteogenic activity.[34] In addition, recent study evaluated the antiestrogenic activity of subglutinol A.[37] Metarhizins have shown potent and selective antiproliferative activity against both insect and human cancer cell lines.[38] Viridoxins A and B have shown to be both potent insect toxins.[39]

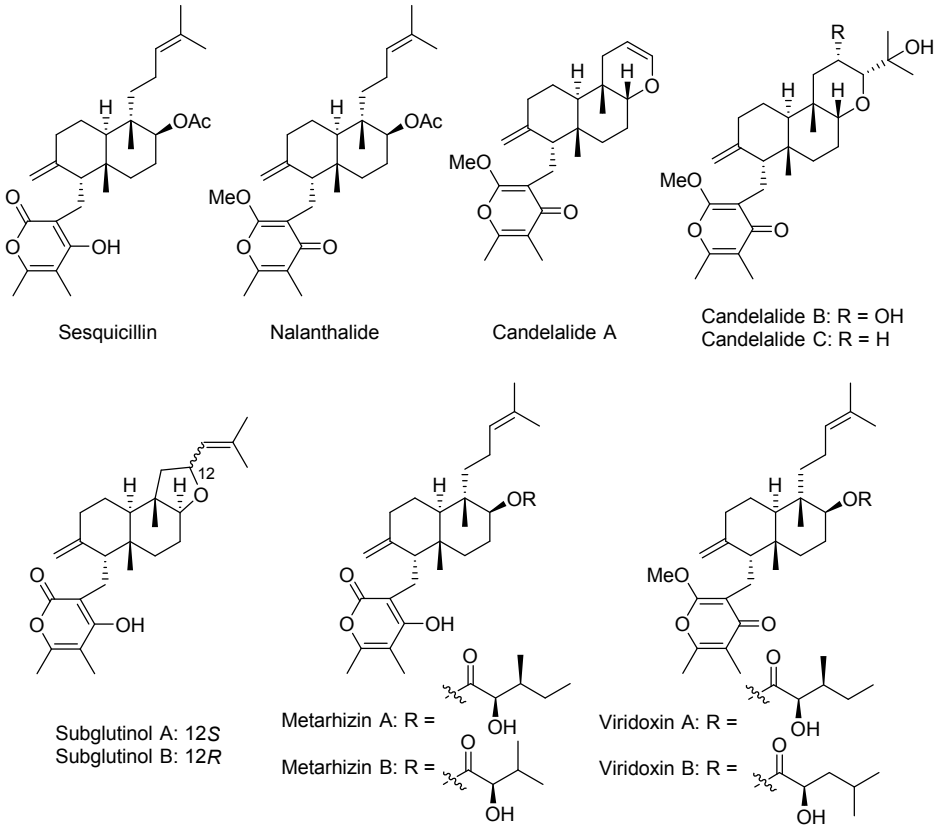

Figure 4: Structures of diterpenoid pyrones

Due to the unique structural features as well as the attractive biological activities, a considerable effort has been devoted to the total synthesis of the diterpenoid pyrones. In the subsequent section, brief overview of the previous syntheses focusing on the construction of *exo*-methylene group in the *trans*-decalin portion and the stereoselective installation of pyrones will be presented.

2.1.2 Synthetic Approaches to the Structurally Related Diterpenoid Pyrones

Danishefsky and co-workers reported the first total synthesis of (±)-sesquicillin (**2.08**) in 2002.[31] As shown in Scheme 1, the key features of the Danishefsky's synthesis are the stereoselective Eschenmoser–Claisen rearrangement of allyl alcohol **2.02** to construct *trans*-decalin portion **2.04** and the aldol-type coupling reaction of methyl ester **2.05** with the known aldehyde **2.06**[40] to generate the carbon framework for an α-pyrone formation.

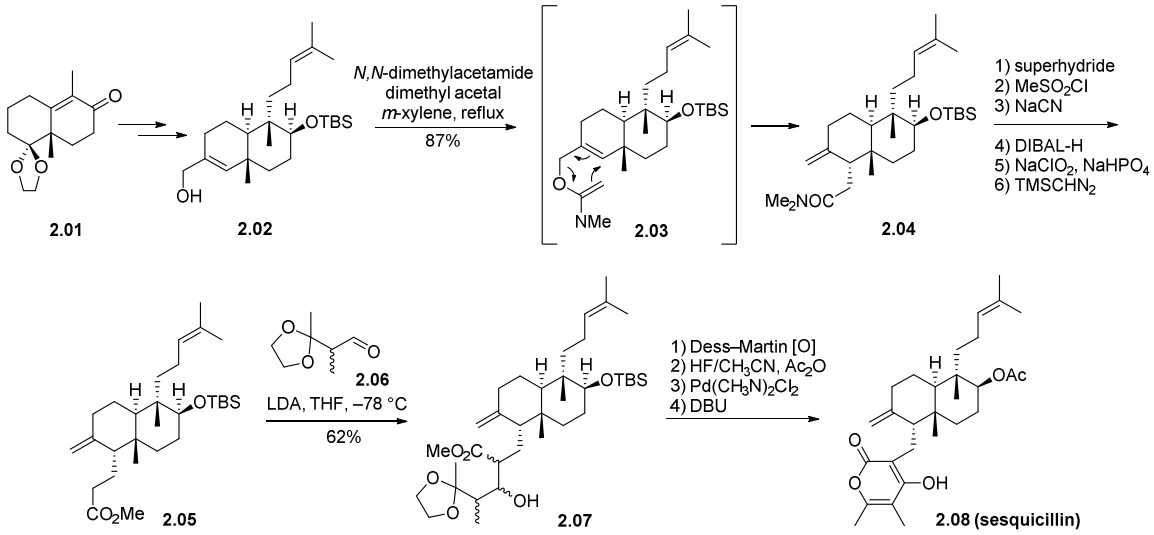

Scheme 1: Danishefsky's synthesis of (±)-sesquicillin

In 2006, Katoh and co-workers reported the first total synthesis of nalanthalide.[33a] As shown in Scheme 2, Katoh's synthesis relied on a convergent strategy with two requisite fragments **2.12** and **2.13**. With the key intermediate allyl alcohol **2.02** synthesized, stereocontrolled [2,3]-Wittig rearrangement of **2.09** was achieved. The

stereochemical outcome can be rationalized by considering that the attack of intermediate carbanion **2.10**, generated *in situ* by the tin/lithium exchange of stannane **2.09**, on the olefinic carbon preferentially occurs from the less hindered α-face, leading to **2.11**. After the Dess–Martin oxidation of **2.11**, the key coupling reaction of the resulting aldehyde **2.12** with bromo-γ-pyrone **2.13**[32-33] was accomplished. The desired coupling product was obtained as a mixture of epimeric alcohols **2.14** which were removed by Barton–McCombie deoxygenation reaction.

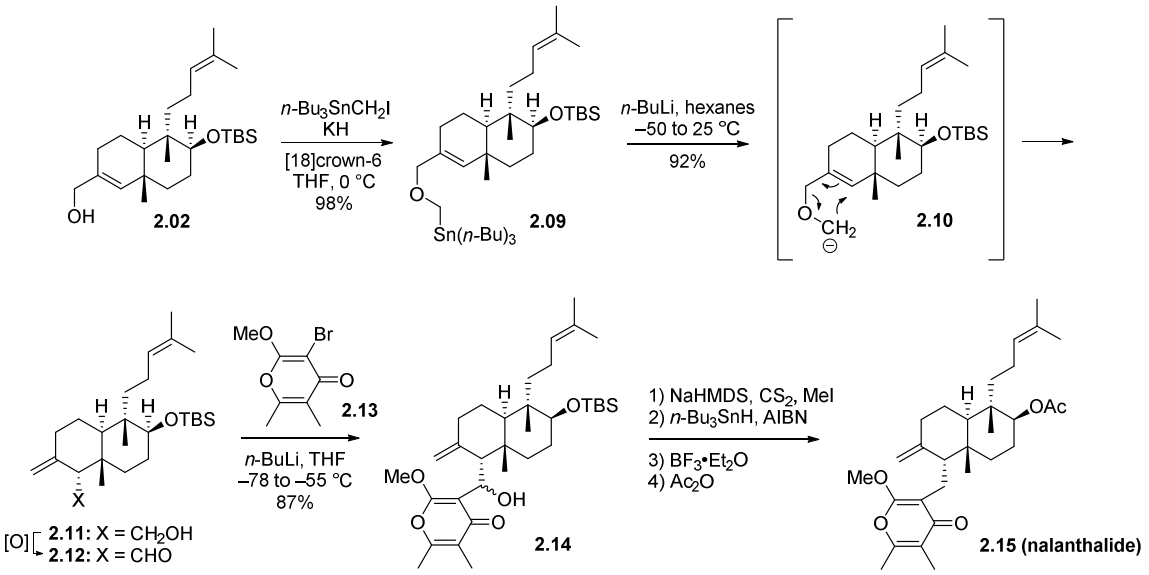

Scheme 2: Katoh's synthesis of nalanthalide

In addition to nalanthalide, Katoh and co-workers reported the first total synthesis of naturally occurring sesquicillin **2.08**.[33b] Because the γ-pyrone moiety present in nalanthalide **2.15** is considered to be an equivalent to vinylogous methyl ester, hydrolysis of this moiety followed by spontaneous tautomerization to α-pyrone would

provide **2.08**. However, the unfavorable deprotection of the acetyl group occurred under conventional basic conditions (1 N NaOH, MeOH, reflux). Therefore, completion of the synthesis of sesquicillin was achieved in a step-by step manner as shown in Scheme 3.

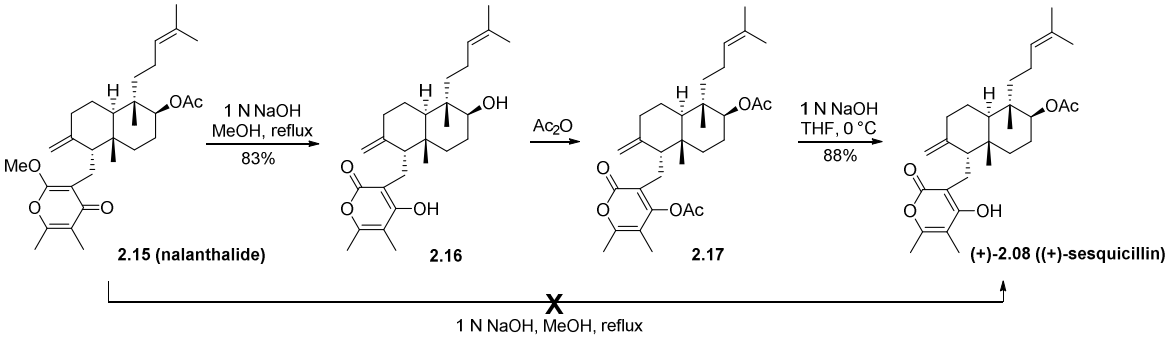

Scheme 3: Katoh's synthesis of (+)-sesquicillin

Using these synthetic strategies including [2,3]-Wittig rearrangement of stannylmethyl ethers, coupling reaction of decalin portions with a γ-pyrone, and the conversion of γ-pyrone moiety into α-pyrone, Katoh and co-workers successfully accomplished the total synthesis of (–)-candelalides A–C[32a], subglutinols A and B.[35]

In 2009, Hong and co-workers reported the first total synthesis of (–)-subglutinols A and B, which led to the determination of the absolute configuration of the natural products.[34] In their first generation synthesis of subglutinols A and B, a direct coupling of the activated decalin moiety **2.22** and the metallated α-pyrone moiety **2.23** was attempted to complete the synthesis (Scheme 4). However, the coupling reactions resulted in no reaction because of the steric congestion around the decalin moiety.

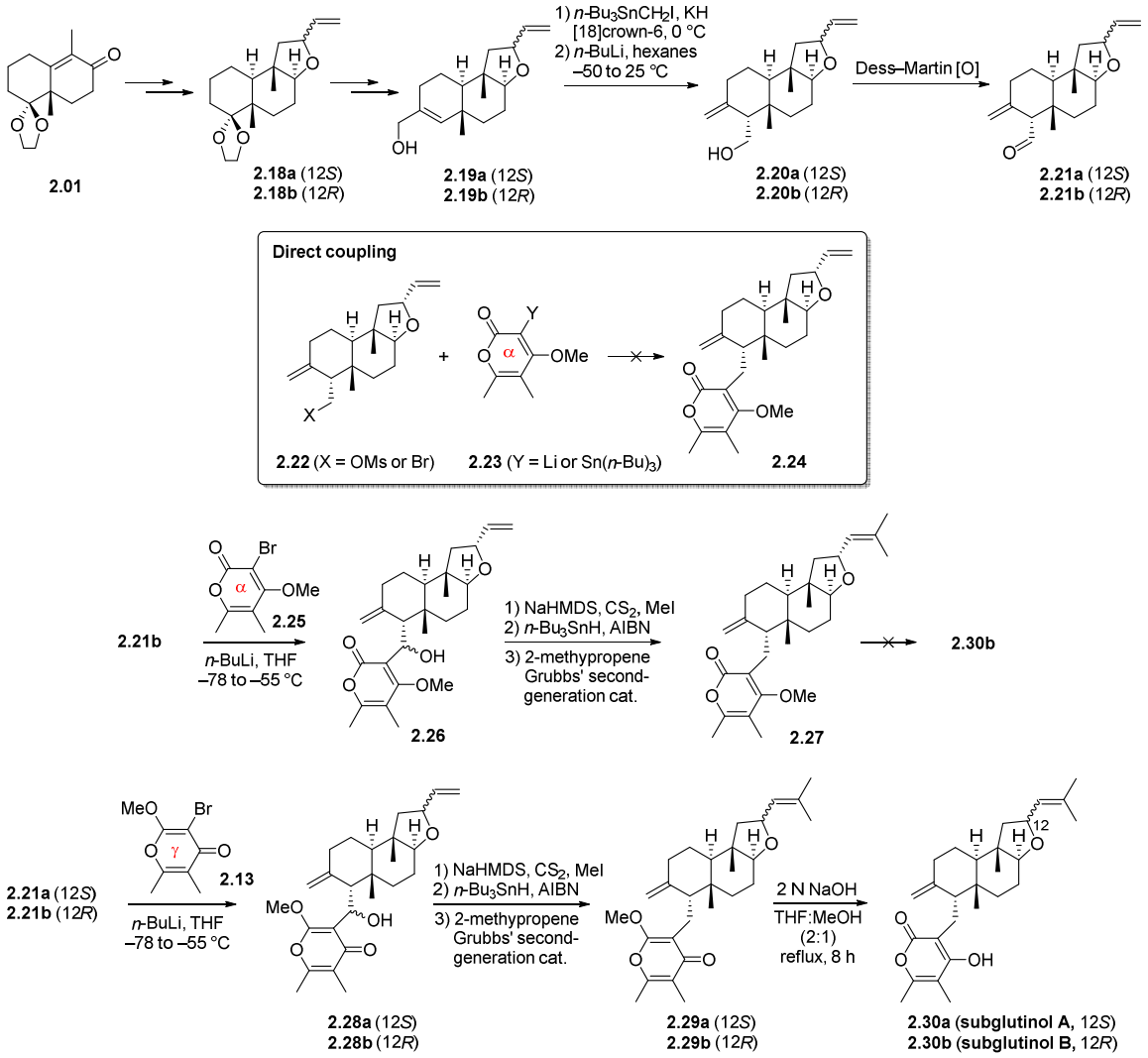

Scheme 4: Hong's first generation synthesis of subglutinols A and B

Next, they adopted Katoh's procedures.[32a] The coupling reaction of **2.21b** with the α-pyrone moiety **2.25**, Barton–McCombie deoxygenation, and olefin cross-metathesis successfully provided **2.27**. However, conversion of **2.27** to subglutinol B (**2.30b**) under various conditions (NaOH, HCl, BCl_3, BBr_3, or TMSI) led to no reaction or complex

reaction mixtures. Alternatively, the γ-pyrone moiety **2.13** was installed to the decalin portions **2.21a** and **2.21b**. Barton–McCombie deoxygenation of **2.21a** and **2.21b** followed by olefin cross-metathesis afforded **2.29a** and **2.29b**. Finally, hydrolysis and subsequent tautomerization of the γ-pyrone to the α-pyrone provided subglutinols A and B. Although Katoh's γ-pyrone installation method successfully complete the synthesis of subglutinols A and B, the first generation synthetic route was not highly straightforward and efficient for the generation of a variety of analogues for biological studies. Thus, Hong and co-workers established a more straightforward and efficient method for the installation of the α-pyrone and reported as a second generation synthesis of subglutinols A and B.[34]

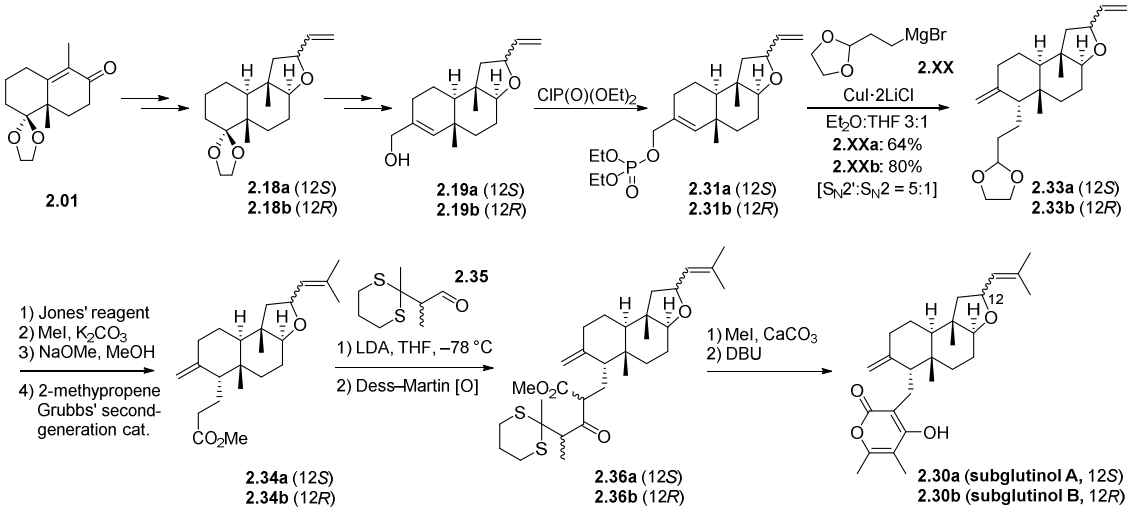

Scheme 5: Hong's second generation synthesis of subglutinols A and B

As shown in Scheme 5, the key step of Hong's second generation synthesis is the Cu(I)-mediated intermolecular S_N2' addition of **2.32** to **2.31a** and **2.31b**. With the appropriately functionalized alcohols **2.19a** and **2.19b** in hand, conversion to the phosphates **2.31a** and **2.31b** followed by Cu(I)-catalyzed intermolecular S_N2' addition of **2.32** to **2.31a** and **2.31b** in the presence of CuI·2LiCl provided **2.33a** and **2.33b**, respectively, as single diastereomers with good regioselectivity (S_N2':S_N2 = 5:1). Completion of the total synthesis of subglutinols A and B was accomplished by similar procedures including aldol-type coupling reaction and the pyrone ring formation established by Danishefsky.[31]

2.1.3 Background of NF00659s

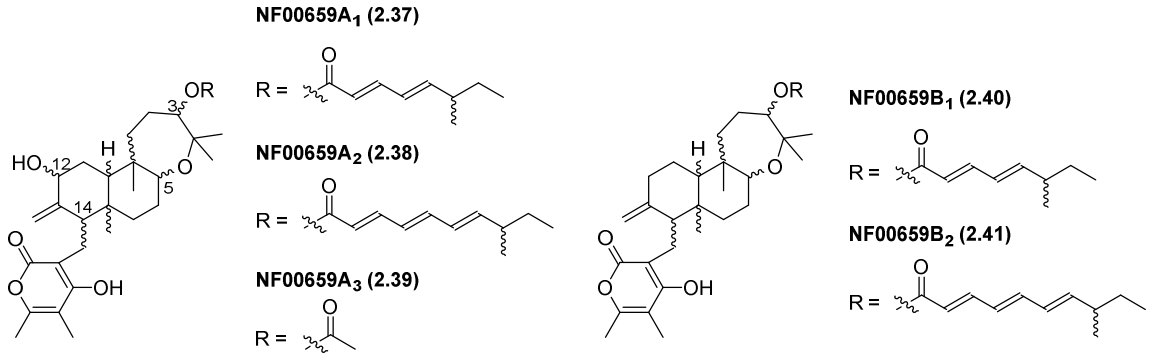

Figure 5: Structures of NF00659s

NF00659s (Figure 5) are 4,5-*seco*-tricyclic diterpene α-pyrone that were first isolated by Nakagawa and co-workers in 1997, from a culture mycelium of *Aspergillus* sp (Figure 6).[41] The novel structures of NF00659s were determined by extensive NMR spectroscopic studies, but the absolute and relative stereochemistries were not established.[41-42] NF00659s possess a tricyclic ring system comprised of a decalin framework and an oxepane, an α-pyrone appendage at C14 position, and side chains at C3 position. NF00659As and NF00659Bs differ only hydroxy group at C12 position.

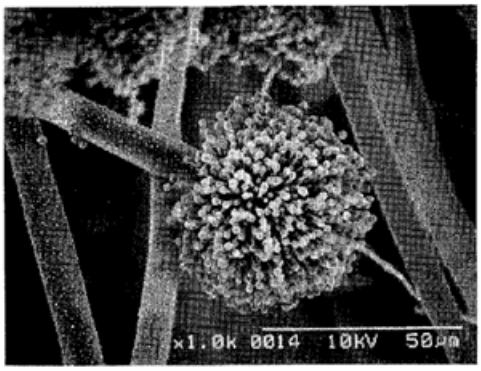

Figure 6: Scanning electron micrograph of *Aspergillus* sp. NF00659 grown on potato dextrose agar medium[41]

NF00659s have shown potent growth inhibitory activities against human ovarian carcinoma A2780 and human colorectal adenocarcinoma SW480 cells (Table 1) as well as insecticidal activities.[41] Interestingly, these compounds exhibit selectivity for SW480 over A2780 (95–840 fold). In addition, NF00659s with the longest side chain, **2.38** and **2.41**, are more potent than **2.37** and **2.40**, suggesting that the long side chain may have crucial interactions with the biological target.

Table 1: *In vitro* cytotoxicities of NF00659s[41]

***In vitro* cytotoxicity of NF00659s**

	IC_{50} (μM)[a]				
	A_1	A_2	A_3	B_1	B_2
SW480	0.005	0.0048	0.56	0.0034	0.005
A2780	4.2	3.2	53	1.55	0.99
A2780/SW480	840	667	95	456	198

[a] Concentration causing 50% inhibition of cell growth.

Due to their cytotoxicities, NF00659s have been expected to be promising new anticancer drugs. Nevertheless, their synthesis and molecular mechanisms of action have not been established. We embarked on a synthesis of NF00659B_1 with the aim of determining the unknown absolute and relative stereochemistries, elucidating the SARs, as well as disclosing the molecular mechanisms of action. In the following sections, synthetic studies towards NF00659B_1 will be discussed.

2.2 Results and Discussion

2.2.1 Proposed Structure of NF00659B$_1$

As shown in Figure 5, NF00659B$_1$ possesses seven unknown stereocenters. In view of common features of structurally related diterpenoid pyrones (Figure 4), the configuration of four stereocenters (C8, C9, C10, C14) in the decalin portion of NF00659B$_1$ was tentatively assigned as shown in Figure 7.

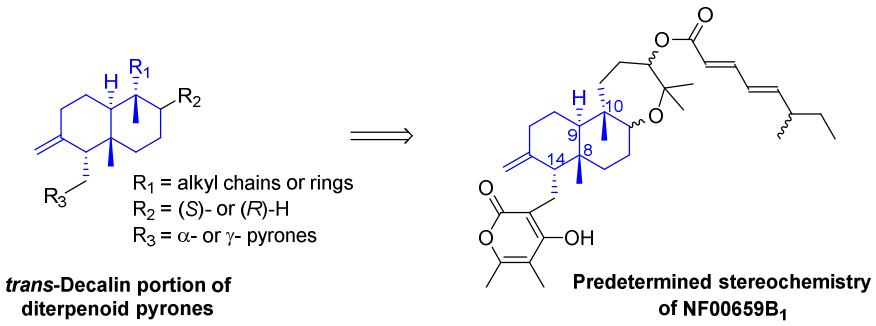

Figure 7: Predetermined stereochemistry of NF00659B$_1$

Next, we presumed that C5 has the same absolute stereochemistry as that of subglutinol A (Figure 8). This tentative stereochemical assignment can be rationalized on the basis of the dihedral angles between H5 and two H6s and the magnitude of their coupling constants in ^{1}H NMR spectrum. According to the Karplus equation[43], these couplings are generally smallest when the angle is close to 90° and largest when the angle is 0° or 180°. If H5 is an equatorial proton, dihedral angles between H5 and H6s can be 60°s, which leads to two similar small *J* values, as shown in candelalide A[32b] (Figure 8). If H5 is an axial proton, on the other hand, dihedral angles between H5 and

H6a and H6b can be 60° and 180°, respectively, which makes a big difference in the magnitude of these two *J* values, as shown in subglutinol A[34a] or sesquicillin C[30e] (Figure 8). Because NF00659B$_1$ was reported to have broad doublet with large *J* value,[42] we tentatively concluded that H5 is an axial proton.

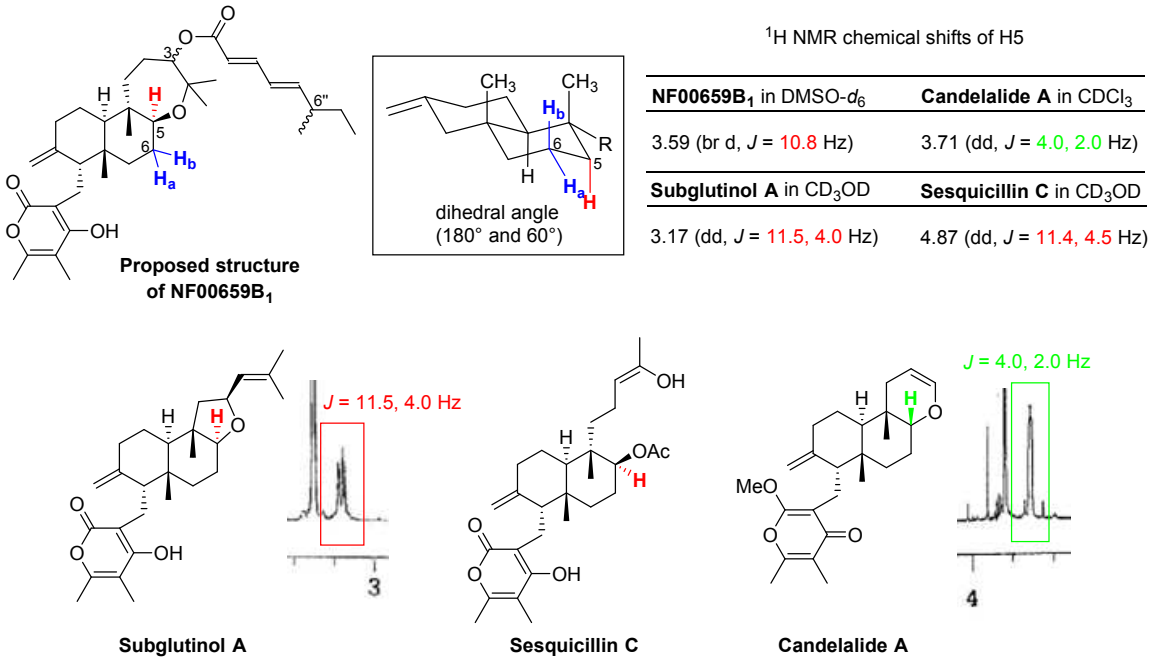

Figure 8: Configuration of C5 in NF00659B$_1$ determined by ^{1}H NMR analysis

To identify the configuration of C3 in NF00659B$_1$, we planned to prepare both (*R*)-OH and (*S*)-OH intermediates and coupled each compounds with a side chain-like carboxylic acid as a model study (Figure 9 top). Due to the unknown stereochemistry of side chain in NF00659B$_1$, the synthetic efficiency of the intermediates, and the structural similarity, we decided to use the commercially available sorbic acid. We anticipated that comparison of ^{1}H NMR data of H3 in the intermediates and that in the natural product

(Figure 9 bottom) would help to predict the configuration of C3 in NF00659B$_1$. In the subsequent sections, the synthesis of these intermediates, comparison of ^{1}H NMR spectrum, and determination of the configuration of C3 will be described in detail.

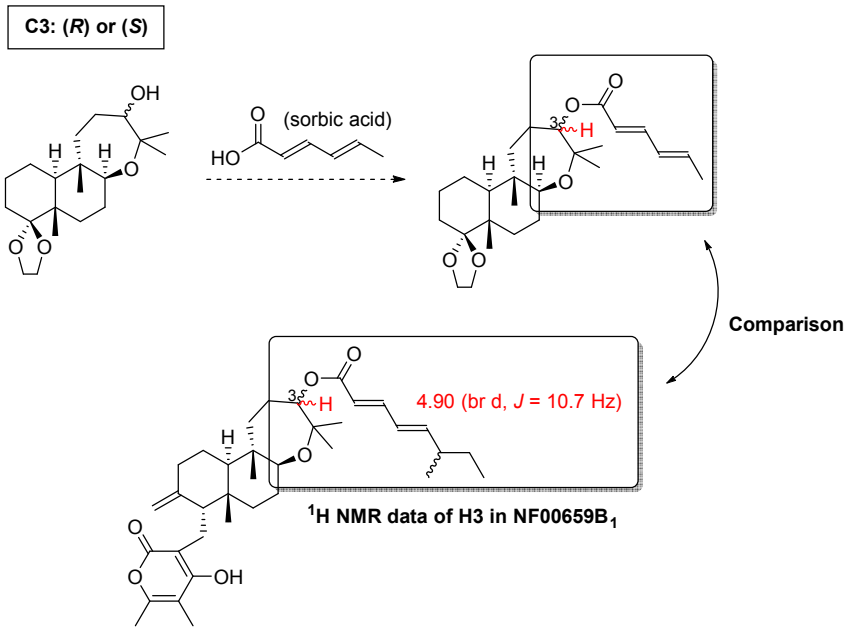

Figure 9: A plan for the determination of C3 in NF00659B$_1$

NF00659B$_1$ possess a side chain at C3 position. To predict the unknown configuration of C6″ in the side chain, an extensive literature search for the natural products that have structurally related side chains was carried out. We found that several natural products have the same branched C$_9$-side chains (Figure 10).[44] In addition, the configuration of their C6′ has been reported to be all (*S*), prompted us to consider the possibility that NF00659B$_1$ also has the configuration (*S*). Although no natural product containing (*R*)-C6′ has been found in our search, we planned to prepare

both (*R*)-C6″-side chain and (*S*)-C6″-side chain and esterified each compound with the key alcohol intermediate to complete the synthesis of NF00659B$_1$ and C6″-*epi*-NF00659B$_1$. Then, comparison of ^{1}H NMR or ^{13}C NMR data of these products with the reported data of NF00659B$_1$ will determine the configuration of C6″ in the side chain of NF00659B$_1$.

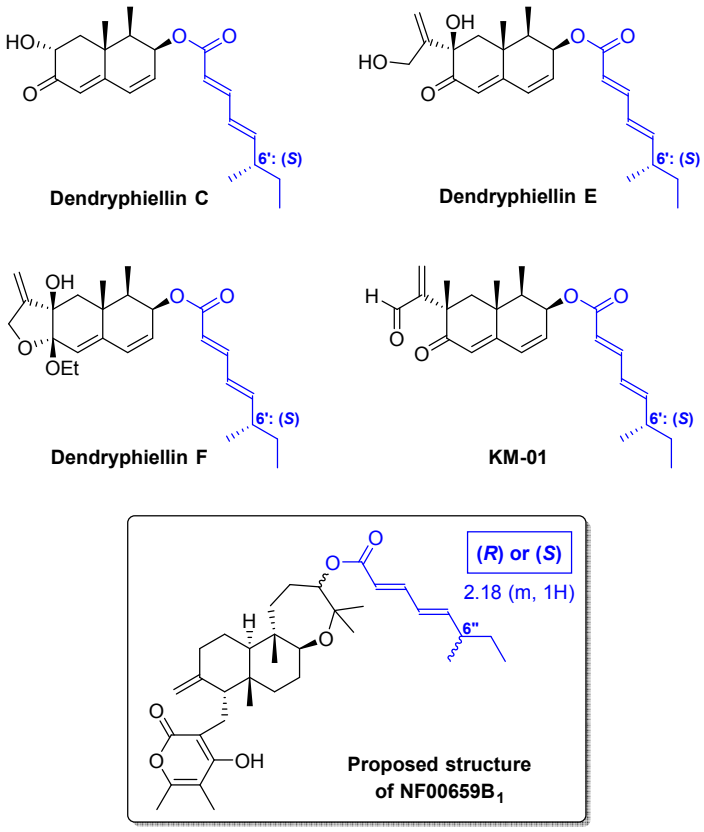

Figure 10: The same branched side chain-containing natural products and their stereochemistry in the side chain

2.2.2 Retrosynthetic Analysis

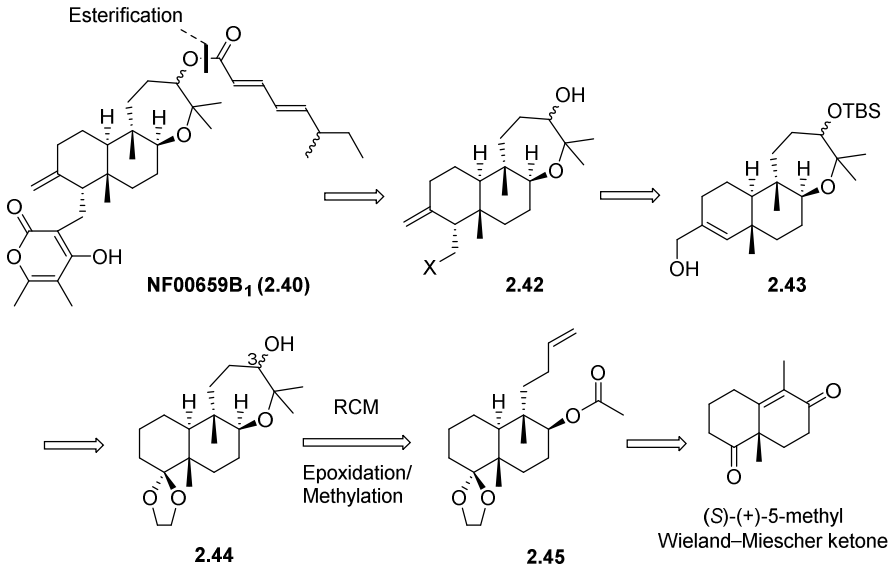

Scheme 6: Retrosynthetic analysis of NF00659B1

Scheme 6 summarizes our approach for the stereoselective synthesis of NF00659B1 from the common intermediate, (*S*)-(+)-5-methyl Wieland–Miescher ketone.[45] The strategy underlying our synthetic plan for NF00659B1 is to apply RCM of the olefinic ester followed by epoxidation and methylation to obtain the key intermediate oxepanol **2.44**. This key intermediate would then be subjected to the same sequence of reactions to obtain allyl alcohol **2.43**. With the appropriately functionalized alcohol **2.43**, installation of the α-pyrone moiety and esterification with side chain would complete the synthesis of NF00659B1. In the subsequent sections of this chapter, synthesis of the key intermediate oxepanol **2.44**, determination of the configuration of C3, and approaches to

the α-pyrone installation, which are the key issues for the synthesis of NF00659B1 will be described.

2.2.3 Attempts for the Synthesis of 7-Membered Cyclic Enol Ether

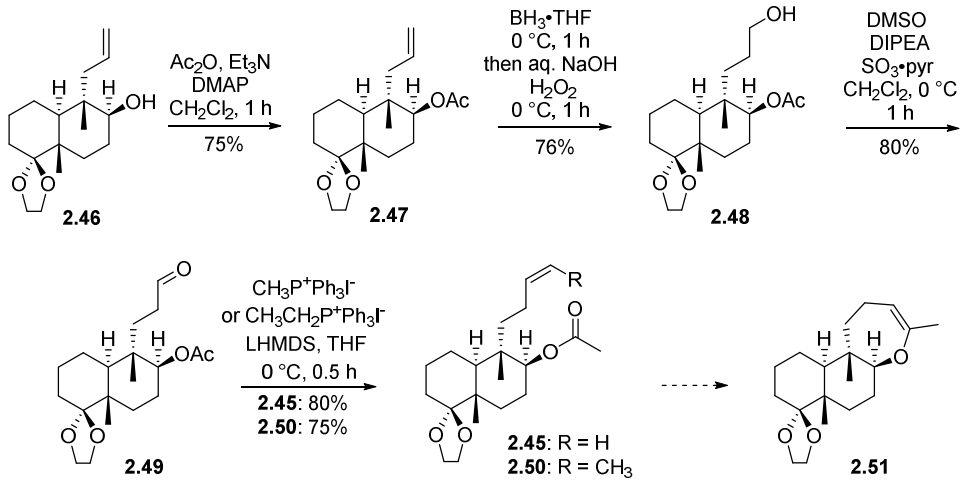

Scheme 7: Synthesis of olefinic esters 2.45 and 2.50

As shown in Scheme 7, the synthesis of olefinic esters **2.45** and **2.50**, precursors to the 7-membered cyclic enol ether **2.51**, began with acetylation of the known alcohol **2.46**[46], the common intermediate readily prepared from the enantiomerically pure (*S*)-(+)-5-methyl Wieland–Miescher ketone.[45] Hydroboration followed by hydrogen peroxide oxidation to give the requisite alcohol **2.48**. Parikh–Doering oxidation of terminal alcohol to aldehyde **2.49** and Wittig reaction proceeded smoothly to provide olefinic esters **2.45** and **2.50**.

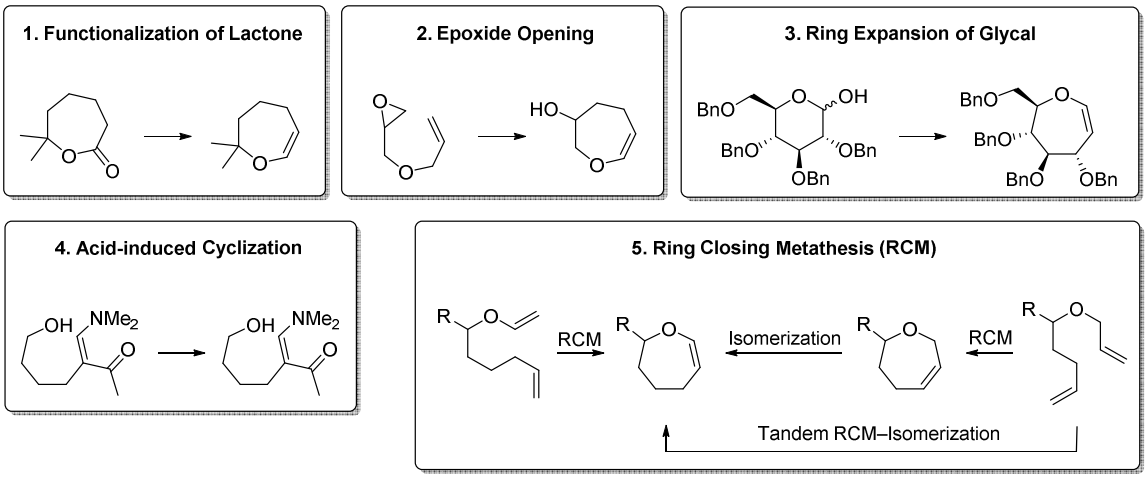

Figure 11: Approaches to the synthesis of 7-membered cyclic enol ether

There have been many reports on the synthesis of 7-membered cyclic enol ether including functionalization of lactone[47], epoxide opening of carbanion generated from allylic alcohol[48], ring expansion of glycal[49], acid induced intramolecular cyclization[50], and various ring closing metathesis (RCM) reactions[51] (Figure 11).

Our attempts to the synthesis of 7-membered cyclic enol ether relied on RCM (Scheme 8). First, we used a direct conversion of olefinic ester **2.50** to the cyclic enol ether **2.51** using Tebbe reagent. This condition was reported by Nicolaou and co-workers in 1996 and is known as a powerful tool for the construction of polycyclic frameworks.[51b] Based on the TLC monitoring, this strategy seemed to form cyclic enol ether via initially formed methylenation intermediate **2.52**. The intermediacy of compound was proven by isolation and spectral characterization. However, we failed to isolate the resulting cyclic enol ether. We speculated that the conversion of methylenation intermediate to cyclic

enol ether required harsh conditions such as reflux and excessive use of Tebbe reagent, which led to decomposition of the desired product. Our next attempt was RCM of the methylenation intermediate **2.52** using Hoveyda–Grubbs' second-generation catalyst.[52] However, no desired product was obtained.

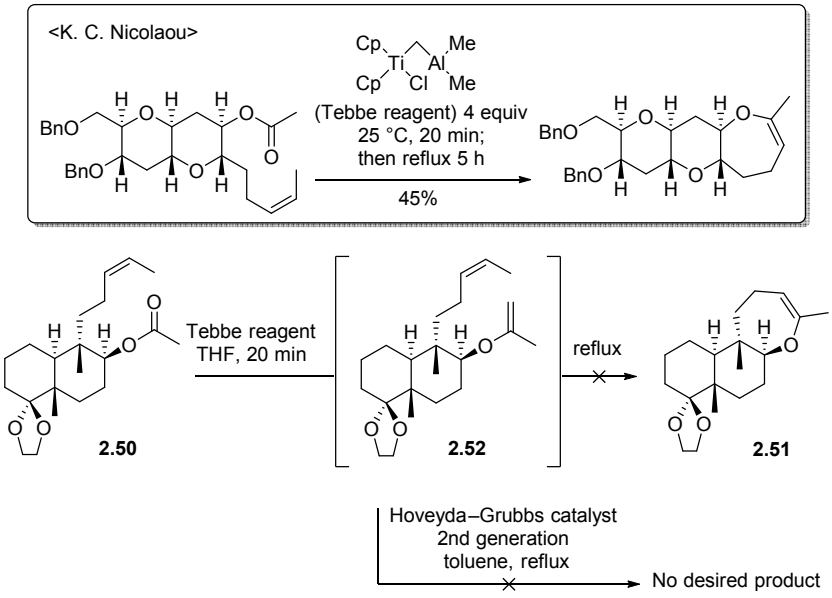

Scheme 8: Attempts for RCM of olefinic ester 2.50

After an extensive investigation of RCM reaction conditions, we adopted the reduced titanium protocol (Scheme 9), modified from the Takai–Utimoto condition[53] by Rainier and co-workers.[54] Rainier's procedure for olefinic ester cyclization used the Takai–Utimoto reduced titanium reagent because of its *in situ* preparation, its increased reactivity relative to the Petasis reagent, and its diminished Lewis acidity relative to the

Tebbe reagent. Finally, the conversion of olefinic esters to the cyclic enol ether **2.51** was achieved in moderate yield.

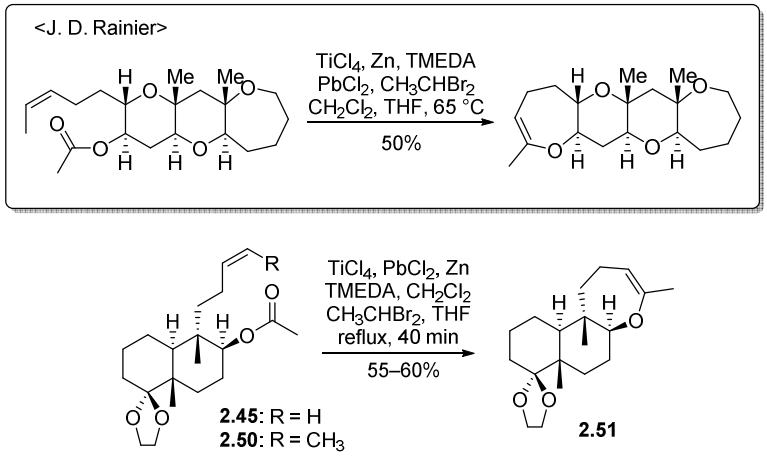

Scheme 9: Conversion of olefinic esters to cyclic enol ether 2.51

We found that the 7-membered cyclic enol ether **2.51** is acid-labile enough to be easily hydrolyzed even in $CDCl_3$ (Figure 12). When it is exposed to an acid, oxocarbenium ion formation occurs which is attacked by water followed by the ring opening to give the hydrolyzed product **2.56**, which was identified by ^1H NMR and single-crystal X-ray diffraction analysis.

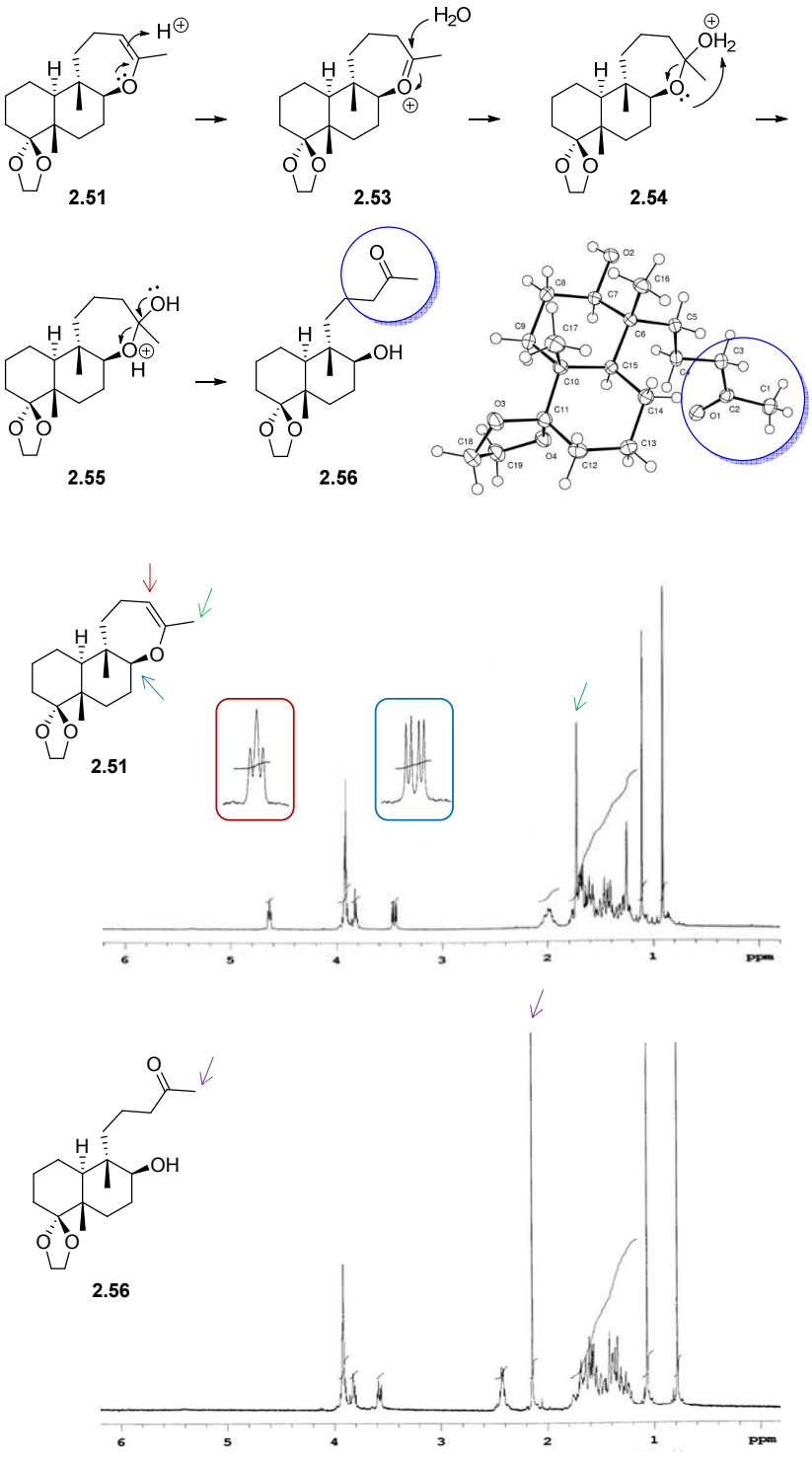

Figure 12: Acid-labile cyclic enol ether 2.51

Although the synthesis of **2.51** from **2.46** was successful, this synthetic route is somewhat lengthy and complicated. After an extensive search for an efficient way to obtain **2.51**, we chose tandem RCM–isomerization method.[51a] Several reports indicated that the decomposition products of Ru-metathesis catalysts (generally Ru-hydride complexes) may be responsible for undesired side products, which are isomerized alkene products.[55] We anticipated that cyclic enol ether **2.51** could be easily obtained by these side reactions because the desired product has more substituted and stable alkene. With this strategy in mind, alcohol **2.46** was converted to **2.57** using the conditions reported by Chattopadhyay and co-workers[56] as shown in Table 2. Then, **2.57** was employed to the tandem RCM–isomerization conditions. However, our desired product as well as RCM product were not observed.

Table 2: Attempts for tandem RCM–isomerization

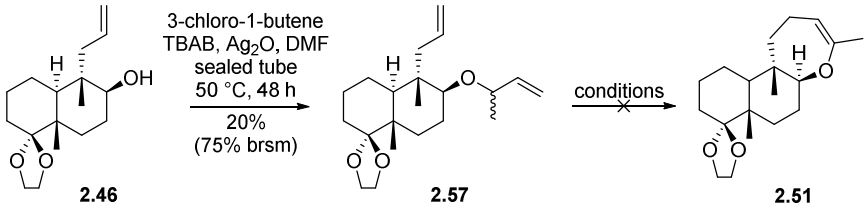

2.46 **2.57** **2.51**

conditions	solvent	temperature	yield
Grubbs 2nd	toluene	25 °C	SM major, unidentified P
Grubbs 2nd	toluene	25 to 50 °C	SM major, unidentified P
Grubbs 2nd	toluene	110 °C	SM major, unidentified P

2.2.4 Synthesis of a Key Intermediate Oxepanol

To obtain the key intermediate oxepanol **2.44**, cyclic enol ether **2.51** was subject to an enol ether epoxidation and nucleophilic addition sequence[57] (Scheme 10). Due to the instability of cyclic enol ether when exposed to the acid, epoxidation was carried out using DMDO[58] under neutral condition. We anticipated that oxepanol **2.44** would be obtained from 7-membered cyclic enol ether through epoxidation and nucleophilic addition of Grignard reagent.

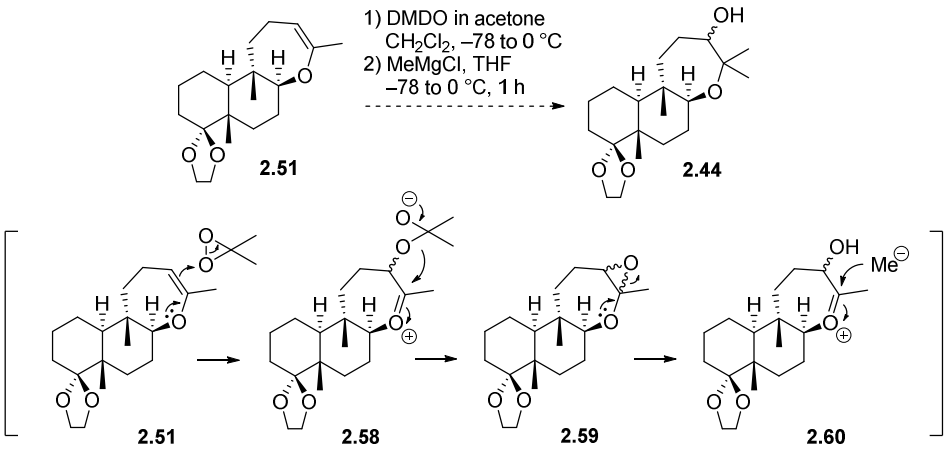

Scheme 10: Epoxidation and nucleophilic addition sequence

However, only hydrolyzed products, diol **2.61** and triol **2.65** were obtained through the reaction (Scheme 11). Our proposed rationales for the hydrolyzed products can be explained via two different mechanisms. The rationale behind the observed diol **2.61** is that cyclic enol ether **2.51** first undergoes hydrolysis followed by nucleophilic addition of the Grignard reagent. On the other hand, formation of triol **2.65** can be

achieved by hydrolysis of epoxide **2.59** followed by nucleophilic addition of the Grignard reagent. To circumvent the problems associated with hydrolysis of intermediates, rapid work up, low temperature, and minimal use of dry solvent as well as rapid addition of Grignard reagent were applied. Finally, oxepanol **2.71** was obtained in 62% yield (Scheme12).

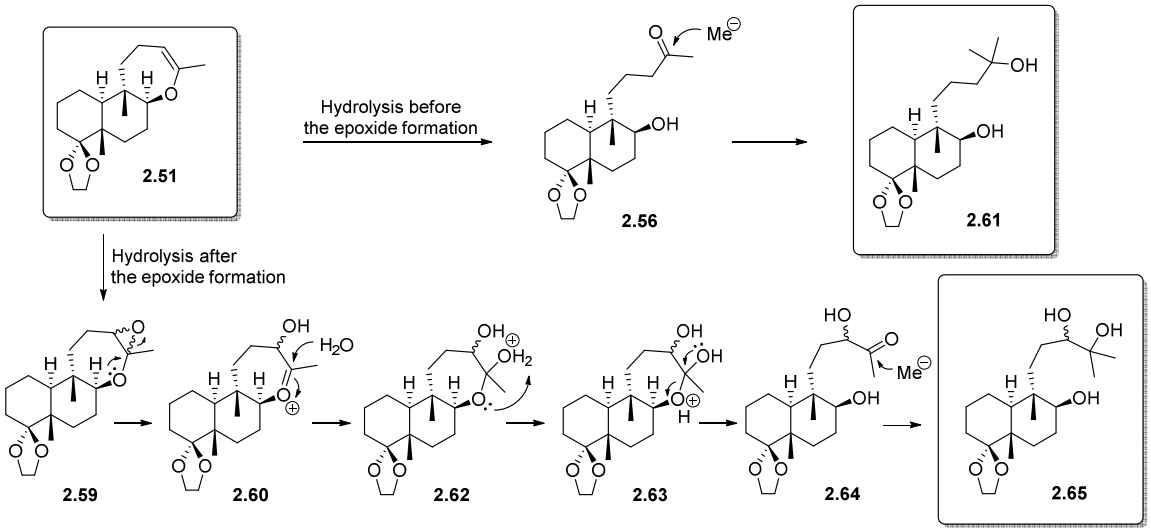

Scheme 11: Hydrolyzed products during the epoxidation/nucleophilic addition sequence

As we had been able to successfully overcome the problems through careful controls, we were confident that the epoxidation/nucleophilic addition sequence provided **2.71** in good yield (Scheme 12). However, we sometimes isolated **2.71** in 15% yield along with the rearrangement product **2.69** in 60% yield. We believed that **2.69** comes from a stereoselective epoxidation to give **2.66**. Subsequently, MeMgCl acts as a Lewis acid to give intermediate oxonium ion **2.68**. Oxonium **2.68** then undergoes a syn-

facial [1,2]-hydride migration to give ketone **2.69**. After an extensive search for a more direct solution, we realized that Grignard reagent in an aged bottle increases the reactivity as a Lewis acid.[59] Thus, we used a new bottle of MeMgCl to suppress hydride migration and successfully overcome rearrangement. Single-crystal X-ray diffraction analysis indicated that **2.71** had the configuration (*S*), thus confirming the stereoselectivity of the epoxidation.

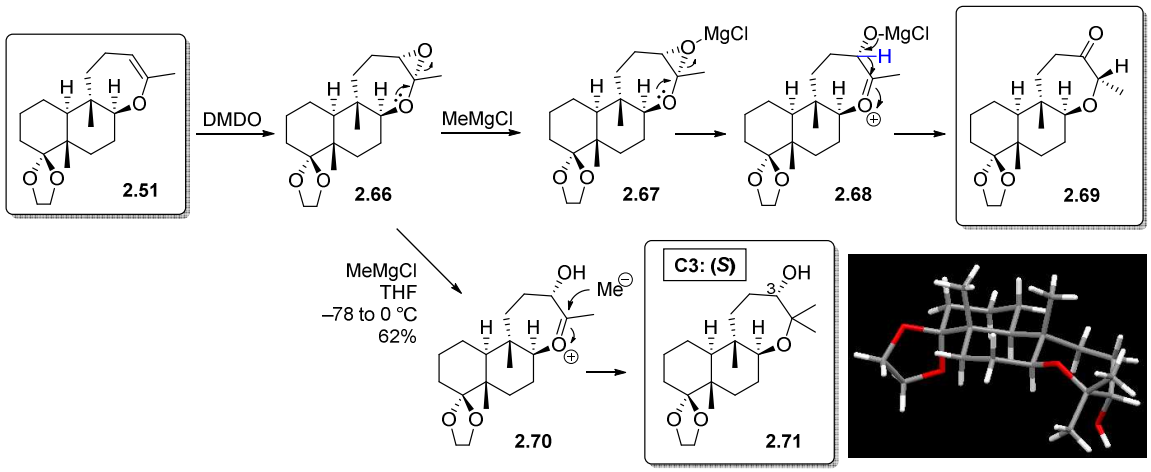

Scheme 12: Rearrangement vs nucleophilic addition

Having achieved the critical oxepanol **2.71**, we turned our attention to the configuration of C3 present in NF00659B1 (Scheme 13). To determine the configuration of C3, we decided to prepare both (*S*)-OH and (*R*)-OH and esterified with a side chain-like carboxylic acid. **2.71** was converted to **2.71** and **2.73** through Dess–Martin oxidation followed by DIBAL-H reduction. Then, Yamaguchi esterification[60] of the commercially available sorbic acid **2.74** with **2.71** and **2.73** provided **2.75** and **2.76**, respectively. Due to

the structural similarity between two esters, **2.75** and **2.76**, and the natural product, the configuration of C3 was tentatively determined to be (*R*) by comparison of ^{1}H NMR spectrum between them.

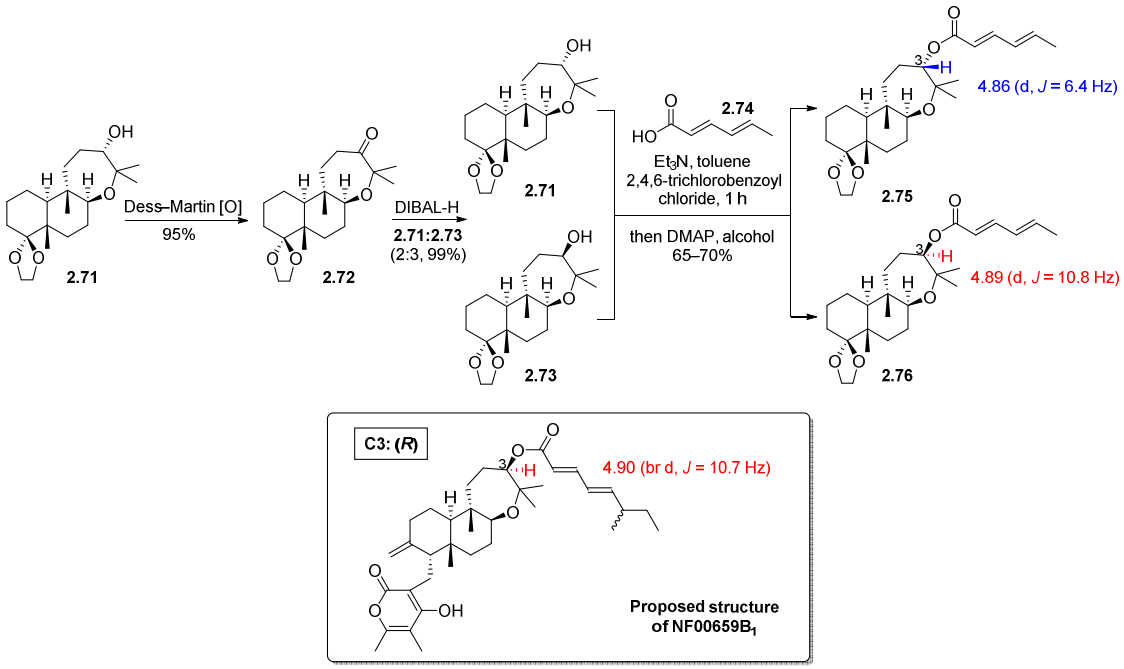

Scheme 13: Determination of the configuration of C3 in NF00659B$_1$

2.2.5 Approaches to α-Pyrone Installation

Having secured a successful route to the preparation of the key intermediate oxepanol **2.73**, we embarked on the installation of the α-pyrone moiety. Although much efforts have been reported to install precursors to α- or γ-pyrones, we needed a more straightforward and efficient method for the installation of α-pyrone. In the subsequent sections, our extensive investigation of the installation of α-pyrone will be described.

2.2.5.1 Attempts for Direct Installation of α-Pyrone

The key intermediate oxepanol **2.73** was converted to the appropriately functionalized allyl alcohol **2.80** following the procedures established by Danishefsky[31] and Katoh[32a] (Scheme 14). Acid-catalyzed ketal-deprotection of **2.73** followed by TBS-protection provided **2.75**. Formylation of **2.75** followed by ethoxyethyl-protection smoothly proceeded to give **2.77** in excellent yield. The α,β-unsaturated ketone was then reduced to the alcohol **2.78** followed by dehydration, which was subjected to sodium borohydride reduction to form **2.80**.

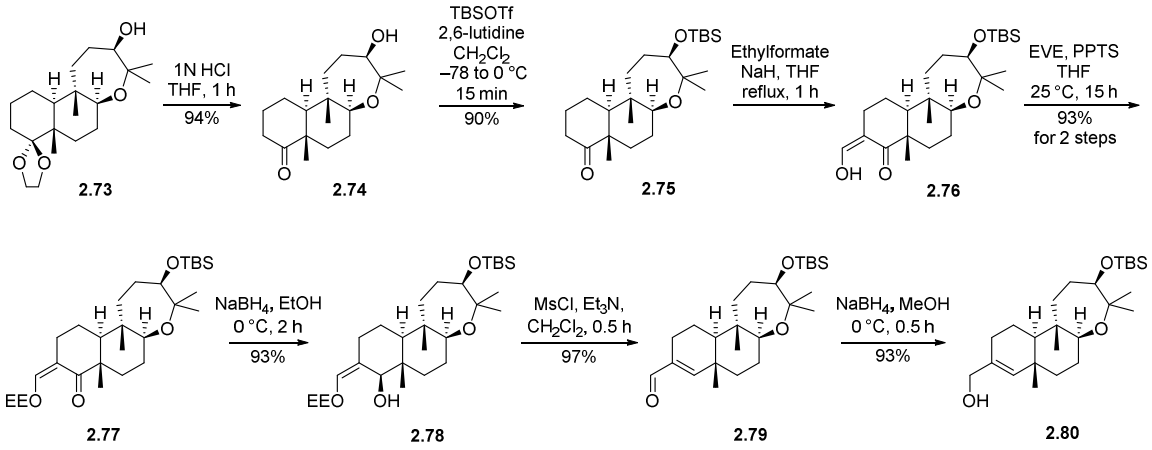

Scheme 14: Synthesis of appropriately functionalized allyl alcohol 2.80

First, we chose direct coupling of the phosphate **2.81** and the α-pyrone moiety. We anticipated that the installation of the α-pyrone moiety could be achieved by a direct coupling of the *in situ*-generated benzylic anion-containing α-pyrone moiety with the decalin phosphate **2.81** (Figure 13).

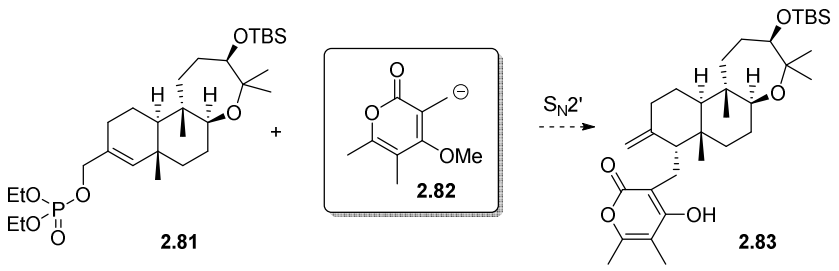

Figure 13: Initial strategy for direct coupling of decalin and α-pyrone

As shown in Scheme 15, the known α-pyrone **2.84**[61] was phenylthiomethylated to provide **2.85**, which was subjected to methylation to provide separable α-pyrone **2.86** and γ-pyrone **2.87**. Each compound was then oxidized, trifluoroacetylated, and hydrolyzed to give **2.88** and **2.90**, respectively under the conditions reported by Hagiwara and co-workers.[62] We expected hydroxymethylated compounds could be converted to the corresponding bromide using Appel reaction.[63] However, the desired pyrone moieties were not obtained due to the instability of benzylic bromide. Alternatively, **2.84** was ethylthiomethylated followed by methylation to provide separable α-pyrone **2.93** and γ-pyrone **2.94**. Each compound was then treated with methyl iodide to provide iodomethyl pyrones, resulting in no reaction or decomposition of the product.

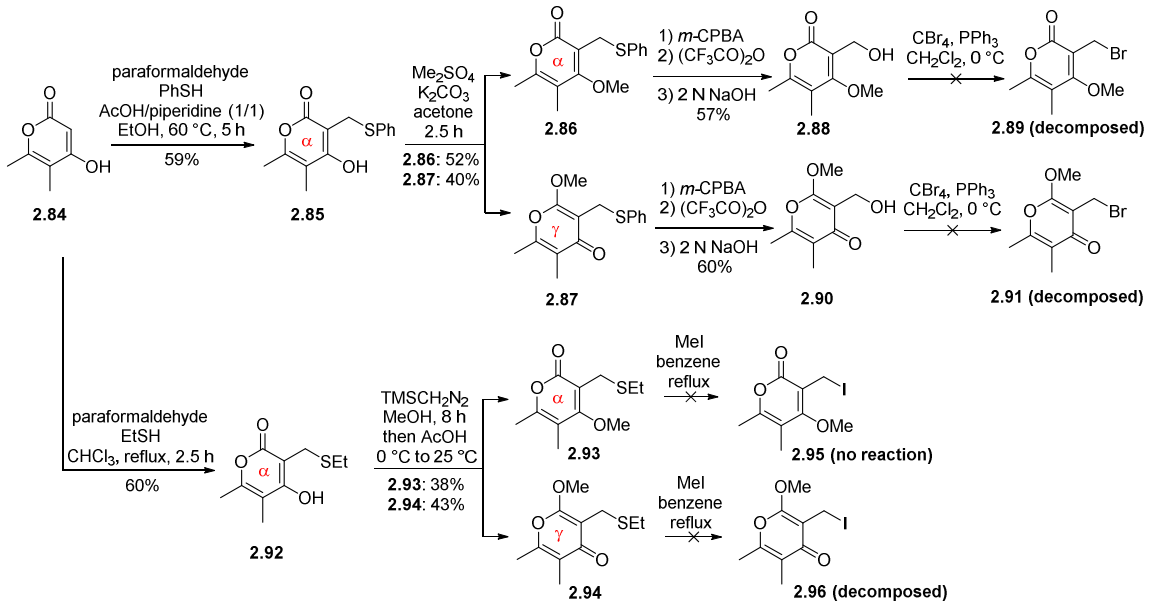

Scheme 15: Attempts for the preparation of pyrone moieties

Our next approach is depicted in Figure 14. We anticipated that the installation of the α-pyrone moiety could be achieved by a Hosomi–Sakurai[64] type direct coupling of the activated decalin **2.97** with the α-pyrone moiety generated *in situ*.[65]

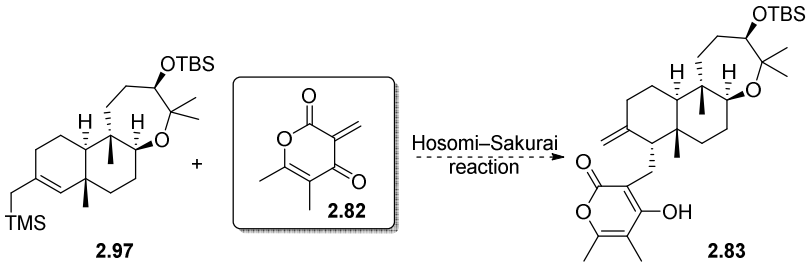

Figure 14: Hosomi–Sakurai type direct coupling of decalin and α-pyrone

With this strategy in mind, allyl alcohol **2.98** was converted to allyl silane **2.100**, a substrate for the model study as shown in Scheme 16.

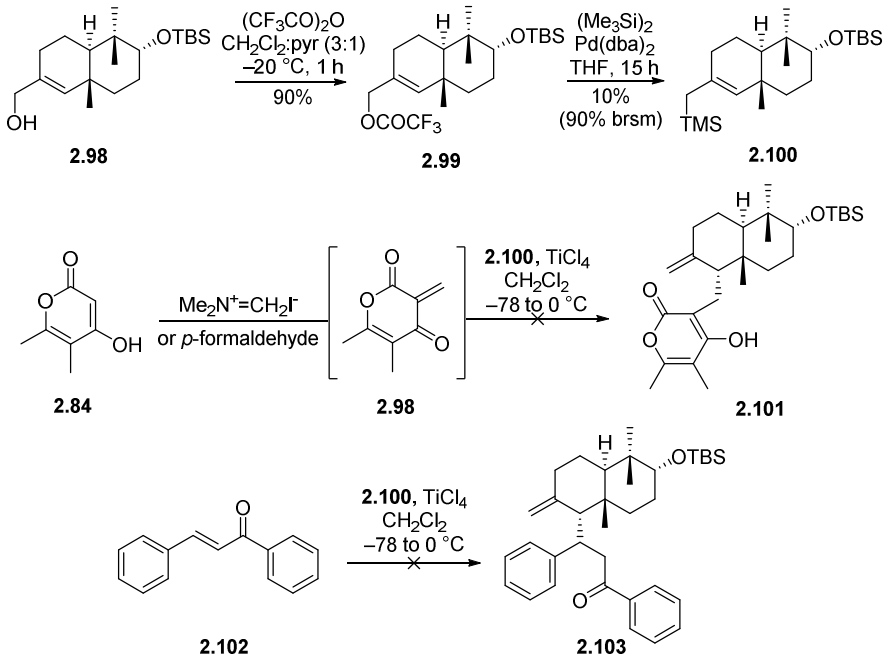

Scheme 16: Model study for direct coupling by Hosomi–Sakurai reaction

Unfortunately, our efforts for direct coupling reactions resulted in no reaction due to the poor reactivity of allylsilane **2.100**, which was confirmed by the reaction with **2.102**, a known substrate[64] for Hosomi–Sakurai reaction. Thus, we decided to adopt Katoh's procedures for the installation of α-pyrone moiety.

2.2.5.2 Adoption of Katoh's Procedure

All attempts to direct coupling of the α-pyrone moiety with the activated decalin portions failed, leading us to apply Katoh's method[32a] of γ-pyrone installation (Scheme 17). This method was also used for Hong's first generation synthesis of subglutinols A and B.[34b] Stannylmethylation of **2.80** followed by Wittig rearrangement proceeded to provide **2.105** (diastereomeric ratio > 5:1). Dess–Martin oxidation of the rearrangement product **2.105** afforded the decalin aldehyde **2.106** in 96% yield. Addition of the 3-lithio-γ-pyrone to **2.106** furnished a mixture of epimeric alcohols **2.107** in low yield (10–37%). Prolonged reaction time or changing of the reaction temperature did not improve the coupling yield, but only significant decomposition of aldehyde was observed. To remove the sterically hindered hydroxy group from **2.107**, Barton–McCombie deoxygenation procedure was applied. After forming methyl xanthate intermediate **2.108**, only trace amount of unidentified product was obtained. At this point, we assumed that the presence of 7-membered ring significantly affects the reactivity for the γ-pyrone addition and Barton–McCombie deoxygenation.

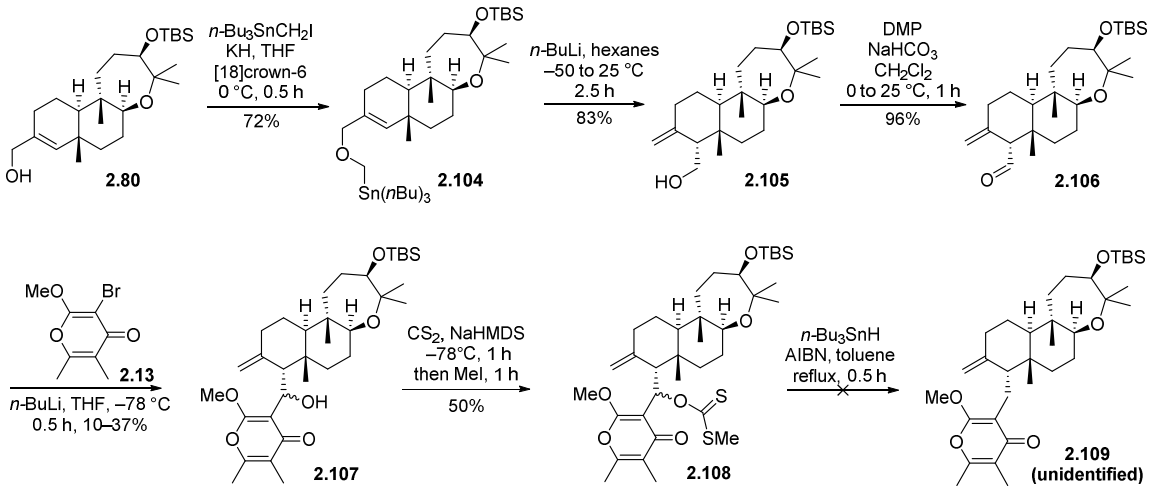

Scheme 17: Installation of γ-pyrone by Katoh's procedures

2.2.5.3 S_N2' Reaction of Phosphate with an Orthoester

As described in section 2.1.2, Cu(I)-mediated intermolecular S_N2' alkylation of phosphate **2.31a** or **2.31b** with Grignard reagent **2.32** successfully provided **2.33a** or **2.33b** as a single diastereomer in good regioselectivity (S_N2':S_N2 = 5:1) in Hong's synthesis of subglutinols A and B.[34] Although this method is straightforward and efficient for the installation of the α-pyrone moiety, it also has limitations such as the low yield in the conversion of **2.33a** or **2.33b** to **2.34a** or **2.34b**. Therefore, we considered an alternative precursor to α-pyrone, an orthoester **2.111**[66], to avoid the problematic oxidation step.

With the prepared orthoester **2.111** in hand, we next examined the reaction conditions for the coupling of **2.110** and **2.111** through the Cu(I)-mediated S_N2' reaction. It should be noted that this model study was conducted by the Hong lab's former

graduate student Kiyoun Lee. As shown in Table 3, a series of copper reagents, reaction temperature, as well as solvent systems were explored. Pleasingly, we found that conversion of the phosphate **2.110** to the alkylation product **2.112** was accomplished with good regioselectivity in the presence of $CuBr{\cdot}SMe_2$.

Table 3: Model study for S_N2' alkylation of 2.111

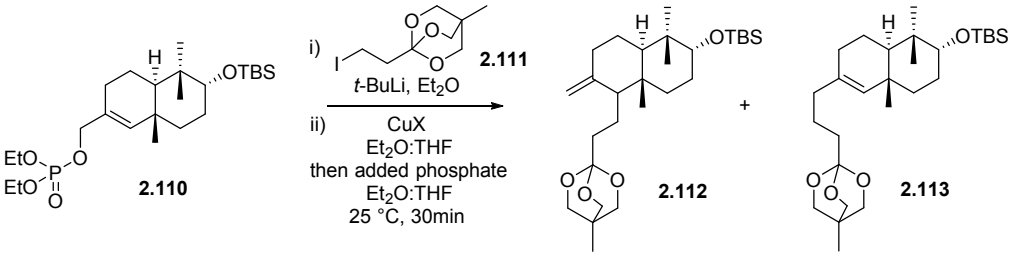

lithiation condition	Cu source in THF	cuprate generation temperature	solvent (Et_2O:THF)	2.112:2.113 (S_N2':S_N2)[a]	yield[b]
–78 °C, 2h to 25 °C 20min	CuI•2LiCl	–78 °C (20min) to 25 °C (20min)	3:1	~1.5 : 1	~85%
–78 °C, 2h to 25 °C 20min	CuI•2LiCl	25 °C (20min)	3:1	~1.5 : 1	~50%
–78 °C, 2h to 25 °C 20min	CuI	–78 °C (20min) to 25 °C (20min)	3:1	~1 : 1	~38%
–78 °C, 2h to 25 °C 20min	CuI	25 °C (20min)	Et_2O only	~1 : 1	~35%
–78 °C, 2h to 25 °C 20min	CuCN•thienyllithium	–78 °C (20min) to 25 °C (20min)	3:1	~1 : 2	~55%
–78 °C, 2h to 25 °C 20min	CuCN•thienyllithium	25 °C (20min)	3:1	~1 : 1	~52%
–78 °C, 2h to 25 °C 20min	CuCN•2LiCl	–78 °C (20min) to 25 °C (20min)	3:1	~1 : 1	~85%
–78 °C, 2h to 25 °C 20min	CuCN•2LiCl	25 °C (20min)	3:1	~1 : 1	~50%
–78 °C, 2h to 25 °C 20min	CuCN	–78 °C (20min) to 25 °C (20min)	3:1	~1 : 1	~38%
–78 °C, 2h to 25 °C 20min	CuCN	–78 °C (20min) to 25 °C (20min)	Et_2O only	~2 : 1	~35%
–78 °C, 2h to 25 °C 20min	CuCN	–78 °C (20min) to 25 °C (20min)	Et_2O only	~1 : 1 (inverse additon[c])	~32%
–78 °C, 2h to 25 °C 20min	$CuBr•SMe_2$	25 °C (20min)	3:1	~3 : 1	~80%
–78 °C, 2h to 25 °C 20min	$CuBr•SMe_2$	–78 °C (20min) to 25 °C (20min)	3:1	~4 : 1	~65%

[a] Determined by integration of the ^{1}H NMR spectrum of the crude product. [b] Combined yield of isolated **2.112** and **2.113**. [c] lithiated orthoester was transferred to CuX via cannula.

Encouraged by the results from the model study, we applied this method to the synthesis of NF00659B1 (Scheme 18). Conversion of allyl alcohol **2.80** to the phosphate **2.81** followed by Cu(I)-mediated intermolecular S_N2' addition of **2.111** to **2.81** provided

2.114 as a single diastereomer in good regioselectivity (S_N2':S_N2 = 5:1). Deprotection of **2.114** followed by methylation led to methyl ester **2.115**. Aldol reaction of **2.115** with **2.06**[40] followed by Dess–Martin oxidation set the stage for final cylization to the α-pyrone. Deprotection of 1,3-dioxolane in **2.117** and subsequent DBU-mediated cyclization to give **2.119**.

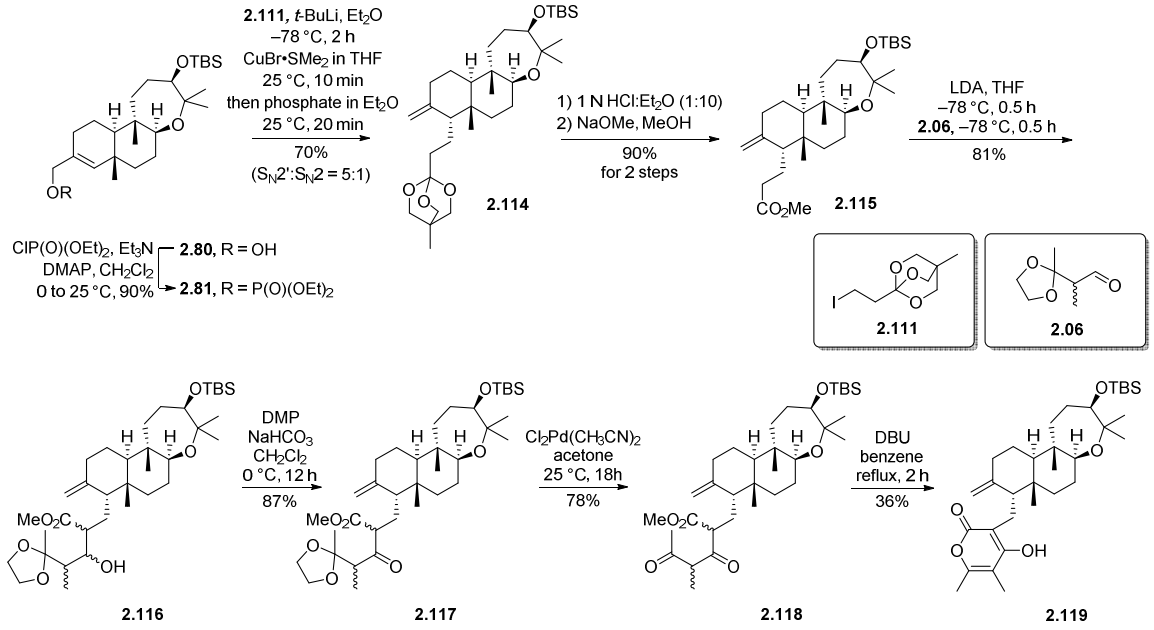

Scheme 18: Installation of α-pyrone by S_N2' alkylation of 2.111

2.2.6 Synthesis of Side Chains

As discussed in sections 2.2.1 and 2.2.4, the configuration of stereocenters in the key intermediate **2.71** was tentatively determined through ^{1}H NMR analysis. One remaining stereocenter to be elucidated is C6'' in the side chain of NF00659B$_1$. To determine its configuration, we decided to prepare (*R*)- and (*S*)- side chains. First, the

synthesis of (*S*)-**2.126** was achieved according to the reported procedure[44b] with slight modification (Scheme 19).

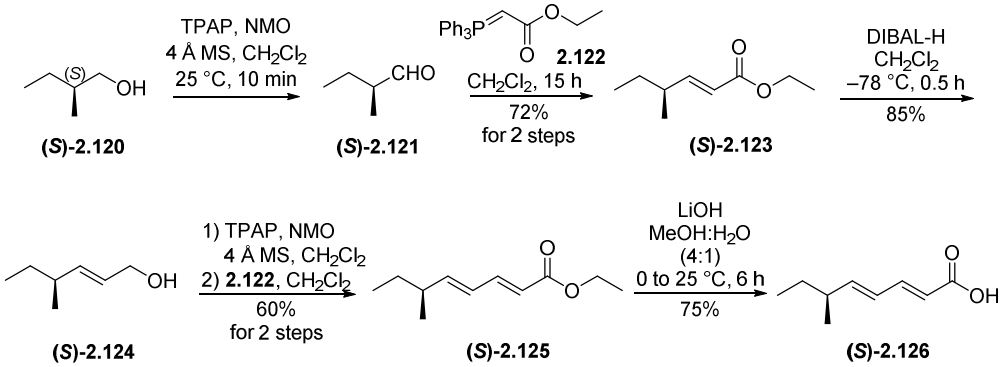

Scheme 19: Synthesis of (*S*)-2.126

The commercially available (*S*)-(–)-2-methylbutanol was converted into aldehyde **2.121** followed by Wittig reaction with **2.122** to provide **2.123**. DIBAL-H reduction of **2.123** gave an allyl alcohol **2.124**, which was subjected to similar processes to produce **2.125**. Hydrolysis of **2.125** yielded carboxylic acid **2.126**. Through this route, **(*R*)-2.126** was also prepared from the commercially available (*R*)-(+)-2-methylbutanol.

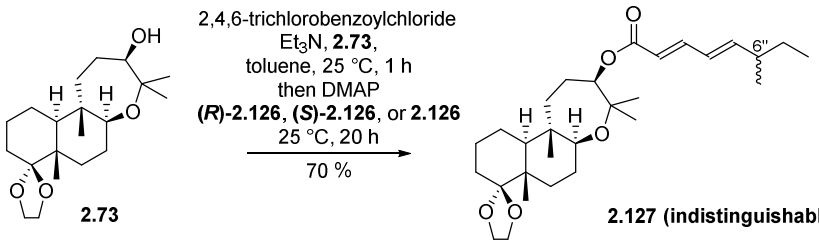

Scheme 20: Attempts to determine the configuration of C6''

With (*S*)- or (*R*)- carboxylic acid in hand, we coupled each compound with **2.73**, a model substrate, by Yamaguchi esterification (Scheme 20). Unfortunately, the two esterification products were not distinguishable based on ^{1}H NMR or ^{13}C NMR spectrum. Although a racemic mixture of carboxylic acids **2.126** or 1:1 mixture of **(*S*)-2.126** and **2.126** was also coupled with **2.73**, the products were not distinguishable.

2.3 Future Work

We have synthesized **2.119**, which will be subjected to TBS-deprotection and esterification with side chains to complete the synthesis of NF00659B$_1$ (Figure 15). In addition, the configuration of C6'' will be determined. If the esterification products are not distinguishable, NF00659B$_1$ and C6"-*epi*-NF00659B$_1$ will be synthesized.

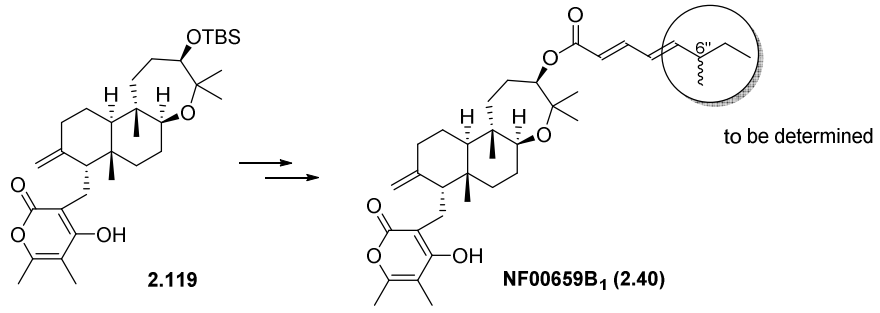

Figure 15: Future work to complete the synthesis of NF00659B$_1$

After the synthesis of NF00659B$_1$, its biological activity will be evaluated. In addition to the known anticancer activity, we will explore another bioactivities such as immunosuppressive effect that other diterpenoid pyrones possess. With the synthetic

approaches to NF00659B$_1$, we expect that NF00659As can be easily obtained by allylic oxidation using selenium dioxide. Furthermore, we will systemically explore the structure of NF00659s to complete the SAR studies and to develop their analogues with desirable drug-like properties. The side chain region, oxepane region, decalin region, and α-pyrone region will be explored to generate a variety of analogues. Moreover, molecular target and mechanisms of action of NF00659B$_1$ will be explored. One possibility to identify the molecular target would be to develop an affinity probe by modifying the natural product by attaching a handle that could "fish out" the target from cell lysate.

2.4 Conclusion

In summary, we have been investigating the first stereoselective synthesis of NF00659B$_1$, the 4,5-*seco*-tricyclic diterpene α-pyrone. During the synthetic studies, the stereochemistry of C3 and C5 were determined by ^{1}H NMR analysis. Our synthetic efforts are focused on an efficient construction of the key intermediate oxepanol **2.73** and installation of the α-pyrone moiety by Cu(I)-mediated intermolecular S$_N$2′ addition of **2.111** to **2.81**. In particular, use of orthoester **2.111** improved the yield from **2.114** to **2.115** by avoiding the problematic oxidation step shown in the previous method.

2.5 Experimental Section

General Methods

All reactions were conducted in oven-dried glassware under nitrogen. Unless otherwise stated all reagents were purchased from Sigma–Aldrich, Acros, or Fisher and were used without further purification. All solvents were ACS grade or better and used without further purification except tetrahydrofuran (THF) which was freshly distilled from sodium/benzophenone each time before use. Analytical thin layer chromatography (TLC) was performed with glass backed silica gel (60 Å) plates with fluorescent indication (Whatman). Visualization was accomplished by UV irradiation at 254 nm and/or by staining with *para*-anisaldehyde solution. Flash column chromatography was performed by using silica gel (particle size 230–400 mesh, 60 Å). All ^{1}H NMR and ^{13}C NMR spectrum were recorded with a Varian 400 (400 MHz) and a Bruker 500 (500 MHz) spectrometer in $CDCl_3$ by using the signal of residual $CHCl_3$, as an internal standard. All NMR δ values are given in ppm, and all J values are in Hz. Electrospray ionization (ESI) mass spectra (MS) were recorded with an Agilent 1100 series (LC/MSD trap) spectrometer and were performed to obtain the molecular masses of the compounds. Infrared (IR) absorption spectra were determined with a Thermo–Fisher (Nicolet 6700) spectrometer. Optical rotation values were measured with a Rudolph Research Analytical (A21102. API/1W) polarimeter.

Preparation of Acetate 2.47

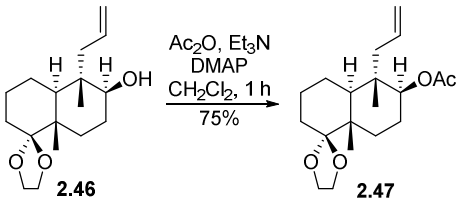

To a solution of the known alcohol **2.46**[46] (2.8 g, 10 mmol) in dry CH_2Cl_2 (50 mL, 0.2 M) were added Et_3N (4.2 mL, 30 mmol), Ac_2O (1.89 mL, 20 mmol), and DMAP (122 mg, 1 mmol) at 25 °C. After stirring for 1 h, the reaction was quenched by addition of MeOH and saturated aqueous $NaHCO_3$, diluted with CH_2Cl_2. The layers were separated, and the aqueous layer was extracted with CH_2Cl_2. The combined organic layers were washed with brine, dried over anhydrous Na_2SO_4, and concentrated *in vacuo*. The residue was purified by column chromatography (silica gel, hexanes/EtOAc, 8/1) to afford **2.47** as a white powder (2.41 g, 75%): $[\alpha]^{23.4}_D$ = 5.12 (*c* 1.22, $CHCl_3$); ^{1}H NMR (400 MHz, $CDCl_3$) δ 5.78 (ddt, *J* = 7.6, 10.0, 17.2 Hz, 1H), 5.06 (dd, *J* = 2.0, 10.0 Hz, 1H), 4.93 (dd, *J* = 2.0, 16.8 Hz, 1H), 4.70−4.66 (m, 1H), 3.93−3.86 (m, 3H), 3.84−3.78 (m, 1H), 2.03 (s, 3H), 1.98 (dd, *J* = 6.4, 8.0 Hz, 2H), 1.75−1.70 (m, 1H), 1.68−1.59 (m, 4H), 1.58−1.56 (dd, *J* = 3.2, 3.2 Hz, 1H), 1.52−1.33 (m, 2H), 1.30 (dd, *J* = 3.6, 3.6 Hz, 1H), 1.08 (s, 3H), 0.90 (s, 3H); ^{13}C NMR (125 MHz, $CDCl_3$) δ 170.6, 134.1, 117.8, 113.2, 76.3, 65.4, 64.9, 43.2, 43.0, 42.3, 40.8, 30.5, 28.3, 23.3, 22.8, 21.4, 20.2, 17.3, 17.1.

Preparation of Alcohol 2.48

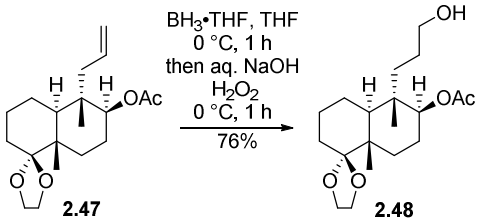

To a cooled (0 °C) solution of acetate **2.47** (1.78 g, 5.52 mmol) in dry THF (35 mL, 0.16 M) was added dropwise BH_3·THF in THF (1.0 M in THF, 16.6 mL, 16.6 mmol). After stirring for 1 h at the same temperature, 2 N NaOH (19 mL) and 50% aqueous H_2O_2 (9.5 mL) were added to the reaction mixture at 0 °C. After stirring for 1 h at the same temperature, the reaction was quenched by addition of H_2O at 0 °C and extracted with EtOAc. The combined organic layers were washed with brine, dried over anhydrous Na_2SO_4, and concentrated *in vacuo*. The residue was purified by column chromatography (silica gel, hexanes/EtOAc, 2/1) to afford **2.48** as a white foam (1.43 g, 76%): $[\alpha]^{23.5}_D$ = –3.32 (*c* 1.03, $CHCl_3$); ^{1}H NMR (400 MHz, $CDCl_3$) δ 4.78 (dd, *J* = 5.6, 8.8 Hz, 1H), 3.93−3.77 (m, 3H), 3.82−3.77 (m, 1H), 3.59−3.46 (m, 2H), 2.03 (s, 3H), 1.68−1.12 (m, 16H), 1.07 (s, 3H), 0.87 (s, 3H); ^{13}C NMR (125 MHz, $CDCl_3$) δ 171.2, 113.2, 75.6, 65.4, 64.9, 63.3, 42.9, 42.6, 39.9, 33.6, 30.5, 28.4, 26.3, 23.6, 22.9, 21.4, 20.1, 18.0, 17.1.

Preparation of Aldehyde 2.49

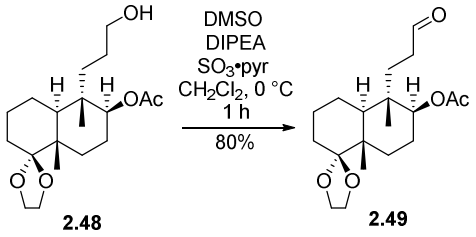

To a cooled (0 °C) solution of alcohol **2.48** (216 mg, 0.63 mmol) in dry CH_2Cl_2 (7 mL, 0.09 M) were added DIPEA (0.23 mL, 1.27 mmol), dry DMSO (0.18 mL, 2.54 mmol), and SO_3·pyr (202 mg, 1.27 mmol). After stirring for 1 h at the same temperature, the reaction was quenched by addition of H_2O and extracted with CH_2Cl_2. The combined organic layers were washed with brine, dried over anhydrous Na_2SO_4, and concentrated *in vacuo*. The residue was purified by column chromatography (silica gel, hexanes/EtOAc, 4/1) to afford **2.49** as a colorless oil (172 mg, 80%): $[\alpha]^{23.4}_D$ = –2.86 (*c* 1.17, $CHCl_3$); ^{1}H NMR (400 MHz, $CDCl_3$) δ 9.72 (s, 1H), 4.68 (m, 1H), 3.94−3.86 (m, 3H), 3.84−3.80 (m, 1H), 2.56−2.48 (m, 1H), 2.31−2.22 (m, 1H), 2.03 (s, 3H), 1.70−1.31 (m, 13H), 1.08 (s, 3H), 0.92 (s, 3H); ^{13}C NMR (125 MHz, CDCl3) δ 202.3, 170.9, 113.1, 75.3, 65.4, 64.9, 42.9, 42.8, 39.7, 38.2, 30.4, 28.9, 28.4, 23.5, 22.9, 21.3, 20.1, 17.8, 17.1.

Preparation of Olefinic Ester 2.45

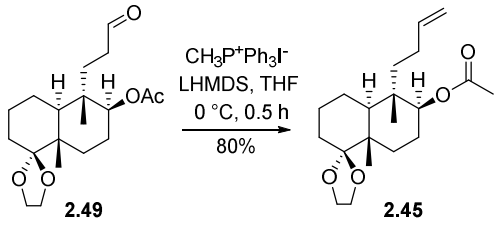

To a cooled (0 °C) suspension of methyltriphenylphosphonium iodide (3.9 g, 9.59 mmol) in dry THF (120 mL) was added dropwise LHMDS (1.0 M in THF, 8 mL, 8 mmol). The resulting mixture was stirred at the same temperature for 30 min before aldehyde **2.49** (1.08 g, 3.2 mmol) in dry THF (25 mL, 0.13 M) was added dropwise. After stirring for 30 min at 0 °C, the reaction was quenched by addition of saturated aqueous NH_4Cl and diluted with EtOAc. The layers were separated, and the aqueous layer was extracted with EtOAc. The combined organic layers were washed with brine, dried over anhydrous Na_2SO_4, and concentrated *in vacuo*. The residue was purified by column chromatography (silica gel, hexanes/EtOAc, 8/1) to afford **2.45** as a white powder (860 mg, 80%): $[\alpha]^{23.7}_D$ = 7.91 (*c* 1.17, $CHCl_3$); ^{1}H NMR (400 MHz, $CDCl_3$) δ 5.71 (ddt, *J* = 6.8, 10.0, 17.2 Hz, 1H), 4.96 (dd, *J* = 2.0, 17.2 Hz, 1H), 4.87 (dd, *J* = 2.0, 10.0 Hz, 1H), 4.76 (q, *J* = 5.6 Hz, 1H), 3.93–3.86 (m, 3H), 3.83–3.79 (m, 1H), 2.02 (s, 3H), 1.88–1.79 (m, 1H), 1.56–1.72 (m, 6H), 1.49–1.14 (m, 8H), 1.08 (s, 3H), 0.87 (s, 3H); ^{13}C NMR (125 MHz, $CDCl_3$) δ 170.7, 139.2, 114.1, 113.2, 75.7, 65.4, 64.9, 43.0, 42.6, 40.0, 37.1, 30.5, 28.4, 27.4, 23.5, 22.9, 21.3, 20.2, 17.9, 17.1.

Preparation of Olefinic Ester 2.50

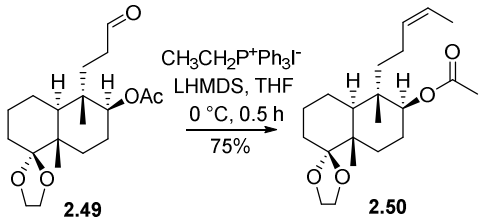

To a cooled (0 °C) suspension of ethyltriphenylphosphonium iodide (1.33 g, 3.2 mmol) in dry THF (60 mL) was added dropwise LHMDS (1.0 M in THF, 2.7 mL, 2.7 mmol). The resulting mixture was stirred at the same temperature for 30 min before aldehyde **2.49** (360 mg, 1.06 mmol) in dry THF (20 mL, 0.05 M) was added dropwise. After stirring for 30 min at 0 °C, the reaction was quenched by addition of saturated aqueous NH_4Cl and diluted with EtOAc. The layers were separated, and the aqueous layer was extracted with EtOAc. The combined organic layers were washed with brine, dried over anhydrous Na_2SO_4, and concentrated *in vacuo*. The residue was purified by column chromatography (silica gel, hexanes/EtOAc, 8/1) to afford **2.50** (289 mg, 75%): ^{1}H NMR (400 MHz, $CDCl_3$) δ 5.42−5.24 (m, 2H), 4.82−4.78 (m, 1H), 4.94−3.88 (m, 3H), 3.83−3.80 (m, 1H), 2.02 (s, 3H), 2.01−1.97 (m, 1H), 1.88−1.78 (m, 1H), 1.56−1.72 (m, 8H), 1.50−1.14 (m, 8H), 1.08 (s, 3H), 0.87 (s, 3H).

Preparation of Cyclic Enol Ether 2.51

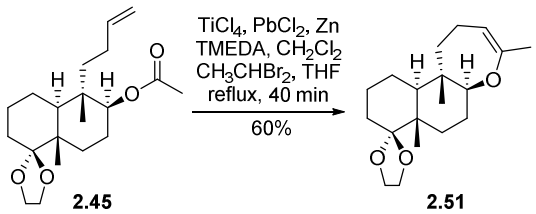

An oven dried two-necked flask fitted with a condenser was cooled to 0 °C and charged with dry CH_2Cl_2 (17 mL), followed by $TiCl_4$ (1.0 M in CH_2Cl_2, 4.6 mL, 4.6 mmol). To the resulting solution was added dropwise THF (2.2 mL, 27.4 mmol) at which time the solution turned yellow. The addition of THF was followed by the dropwise addition of TMEDA (4.08 mL, 27.4 mmol) resulting in the formation of a brown solution. The ice bath was removed and the reaction mixture was allowed to stir for 20 min. Activated Zn dust (669 mg, 10.22 mmol) and $PbCl_2$ (150 mg, 0.54 mmol) were then added. The resulting mixture went through a series of color changes from brown to green to purple and finally to blue–green over the course of 3–5 min. To the slurry as transferred a solution of ester **2.45** (50 mg, 0.14 mmol) and CH_3CHBr_2 (0.42 mL, 4.57 mmol) in CH_2Cl_2 (3 mL) via cannula. After stirring for 45 min at reflux, the reaction mixture was cooled to 0 °C, quenched by addition of saturated aqueous K_2CO_3. The resulting mixture was filtered through Celite and extracted with EtOAc. The combined organic layers were washed with brine, dried over anhydrous Na_2SO_4, and concentrated *in vacuo*. The residue was purified by column chromatography (silica gel, hexanes/EtOAc, 100/1 with 1% Et_3N) to afford **2.51** as a colorless oil (26 mg, 60%): $[\alpha]^{23.1}_D$ = –25.48 (*c* 2.6, acetone); ^1H

NMR (400 MHz, acetone-d_6) δ 4.62 (dd, *J* = 6.0, 6.0 Hz, 1H), 3.94–3.87 (m, 3H), 3.83–3.77 (m, 1H), 3.40 (dd, *J* = 4.4, 11.6 Hz, 1H), 2.01−1.93 (m, 2H), 1.67 (s, 3H), 1.73−1.22 (m, 12H), 1.27−1.20 (ddd, *J* = 4.0, 10.0, 14.0 Hz, 1H) 1.10 (s, 3H), 0.89 (s, 3H); ^{13}C NMR (125 MHz, acetone-d_6) δ 157.8, 113.7, 105.5, 88.4, 66.0, 65.5, 48.3, 44.0, 42.5, 41.0, 31.1, 29.9, 26.7, 24.0, 22.4, 21.9, 21.4, 17.7, 14.5; HRMS (ESI) *m*/*z* 307.2272 [(M+H)$^+$, $C_{19}H_{30}O_3$ requires 307.2268].

Preparation of Alkene 2.57

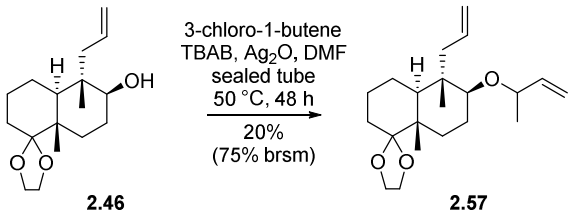

To a solution of alcohol **2.46** (50 mg, 0.18 mmol) in DMF (2 mL, 0.09 M), were added 3-chloro-1-butene (0.07 mL, 0.71 mmol), TBAB (57.5 mg, 0.18 mmol), and Ag_2O (62 mg, 0.27 mmol) at 25 °C. After stirring for 48 h at 50 °C in a sealed tube, the reaction mixture was cooled to 25 °C and filtered through Celite. The filtrate was diluted with EtOAc and H_2O and extracted with EtOAc. The combined organic layers were washed with brine, dried over anhydrous Na_2SO_4, and concentrated *in vacuo*. The residue was purified by column chromatography (silica gel, hexanes/EtOAc, 6/1) to afford **2.57** (12 mg, 20%): ^{1}H NMR (400 MHz, $CDCl_3$) δ 5.92–5.73 (m, 2H), 5.30–5.15 (m, 2H), 5.10–5.06 (m, 1H), 4.99–4.93 (m, 1H), 4.56–4.51 (m, 1H), 3.93–3.84 (m, 3H), 3.83–3.79 (m, 1H), 2.09–1.98 (m, 2H),

1.08 (s, 3H), 0.92 (s, 3H), 1.83–1.59 (m, 7H), 1.52–1.46 (m, 2H), 1.37 (dd, *J* = 2.0, 6.8 Hz, 1H) 1.42–1.28 (m, 2H).

Preparation of Alcohol 2.71

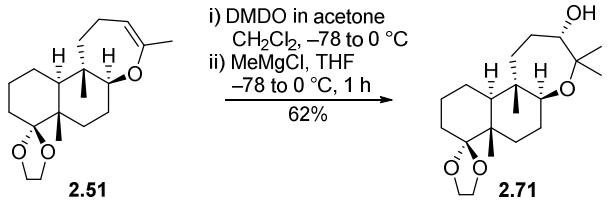

To a cooled (−78 °C) solution of ether **2.51** (30 mg, 0.1 mmol) in dry CH_2Cl_2 (1 mL, 0.1 M) was added dropwise the freshly prepared DMDO (0.1 M in acetone, 1.5 mL, 0.15 mmol). The resulting mixture was slowly warmed to 0 °C and stirred for 5 min. The mixture was concentrated by placing it under vacuum for 30 sec. The residue was cooled to −78 °C and dissolved in a cooled (−78 °C) THF (1 mL). To the resulting mixture was added MeMgCl (3.0 M in THF, 0.13 mL) in one portion. After stirring for 1 h at the same temperature, the reaction mixture was allowed to slowly warm to 0 °C for 1 h. The reaction was quenched by addition of saturated aqueous NH_4Cl and diluted with EtOAc. The layers were separated, and the aqueous layer was extracted with EtOAc. The combined organic layers were washed with brine, dried over anhydrous Na_2SO_4, and concentrated *in vacuo*. The residue was purified by column chromatography (silica gel, hexanes/EtOAc, 4/1) to afford **2.71** as a white powder (20.5 mg, 62%): $[\alpha]^{23.7}_D$ = –11.34 (*c* 0.92, $CHCl_3$); ^{1}H NMR (400 MHz, $CDCl_3$) δ 3.93–3.86 (m, 3H), 3.84–3.79 (m, 1H), 3.77 (d, *J*

= 7.2 Hz, 1H), 3.49 (dd, *J* = 4.8, 11.2 Hz, 1H), 1.97 (ddd, *J* = 3.2, 11.6, 12.4 Hz, 1H), 1.27−1.71 (m, 15H), 1.25 (s, 3H), 1.10 (s, 3H), 1.03 (s, 3H), 0.84 (s, 3H); ^{13}C NMR (125 MHz, $CDCl_3$) δ 113.4, 77.8, 76.9, 65.2, 64.7, 49.7, 42.9, 41.1, 35.4, 30.5, 29.1, 29.0, 26.9, 25.8, 23.2, 21.5, 20.6, 16.6, 13.7; HRMS (ESI) *m*/*z* 339.2532 [$(M+H)^+$, $C_{20}H_{34}O_4$ requires 339.2530].

Preparation of Ketone 2.72

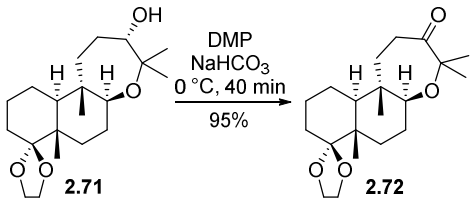

To a cooled (0 °C) solution of alcohol **2.71** (736 mg, 2.17 mmol) in dry CH_2Cl_2 (20 mL, 0.11 M) were added Dess–Martin periodinane (1.85 g, 4.35 mmol) and $NaHCO_3$ (730 mg, 8.7 mmol). After stirring for 40 min at the same temperature, the reaction was quenched by addition of saturated aqueous $NaHCO_3$ and extracted with CH_2Cl_2. The combined organic layers were washed with brine, dried over anhydrous Na_2SO_4, and concentrated *in vacuo*. The residue was purified by column chromatography (silica gel, hexanes/EtOAc, 8/1) to afford **2.72** as a white powder (695 mg, 95%): $[\alpha]^{22.9}_D$ = 25.28 (*c* 2.05, $CHCl_3$); ^{1}H NMR (400 MHz, $CDCl_3$) δ 3.90−3.83 (m, 3H), 3.80−3.74 (m, 1H), 3.12 (ddd, *J* = 3.2, 11.2, 14.0 Hz, 1H), 2.84 (dd, *J* = 4.4, 11.6 Hz, 1H), 2.05 (ddd, *J* = 2.4, 6.4, 10.8 Hz, 1H), 1.81 (ddd, *J* = 3.2, 6.0, 13.6 Hz, 1H), 1.65−1.27 (m, 10H) 1.26 (s, 3H), 1.20 (s, 3H), 1.04 (s, 3H), 0.96 (s, 3H) ; ^{13}C NMR (125 MHz, $CDCl_3$) δ 217.8, 113.2, 82.4, 81.9, 65.3, 64.9,

49.6, 42.9, 40.8, 40.5, 35.4, 30.3, 28.8, 26.7, 26.6, 23.1, 20.9, 20.6, 16.7, 13.0; HRMS (ESI) *m*/*z* 337.2367 [$(M+H)^+$, $C_{20}H_{32}O_4$ requires 337.2373].

Preparation of Alcohol 2.73

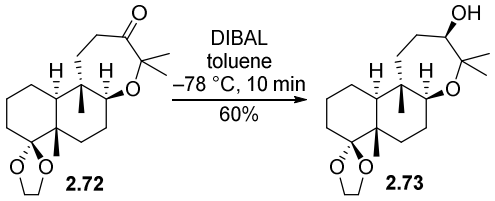

To a cooled (–78 °C) solution of ketone **2.72** (970 mg, 2.88 mmol) in dry toluene (28 mL, 0.1 M) was added DIBAL-H (1.0 M in toluene, 4.5 mL, 4.5 mmol). After stirring for 10 min at the same temperature, the reaction was quenched by addition of MeOH followed by aqueous Rochelle's salt, diluted with EtOAc, and stirred for 1 h at 25 °C. The layers were separated, and the aqueous layer was extracted with EtOAc. The combined organic layers were washed with brine, dried over anhydrous Na_2SO_4, and concentrated *in vacuo*. The residue was purified by column chromatography (silica gel, hexanes/EtOAc, 6/1) to afford **2.73** as a white foam (586 mg, 60%): $[\alpha]^{23.5}_D$ = –5.71 (*c* 0.95, $CHCl_3$); ^{1}H NMR (400 MHz, $CDCl_3$) δ 3.96–3.87 (m, 3H), 3.84–3.78 (m, 1H), 3.63 (d, *J* = 10.4 Hz, 1H), 3.13 (dd, *J* = 4.0, 10.4 Hz, 1H), 2.08–1.99 (m, 1H), 1.75–1.26 (m, 15H), 1.24 (s, 3H), 1.08 (s, 3H), 1.03 (s, 3H), 0.81 (s, 3H) ; ^{13}C NMR (125 MHz, $CDCl_3$) δ 113.5, 79.3, 76.6, 76.1, 65.3, 64.8, 50.1, 42.9, 42.2, 40.6, 30.4, 30.2, 29.0, 26.8, 24.7, 23.3, 22.0, 20.7, 16.7, 14.1.

Preparation of Ketone 2.74

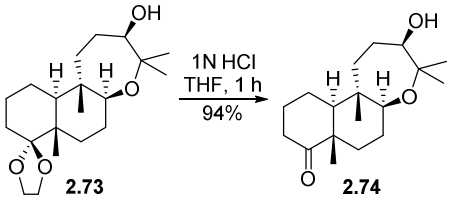

To a solution of alcohol **2.73** (75 mg, 0.22 mmol) in THF/H_2O (2/1, 4.5 mL, 0.05 M) was added 1 N HCl (2.8 mL) at 25 °C. After stirring for 1 h, the reaction mixture was cooled to 0 °C, quenched by addition of saturated aqueous $NaHCO_3$, and diluted with CH_2Cl_2. The layers were separated, and the aqueous layer was extracted with CH_2Cl_2. The combined organic layers were washed with brine, dried over anhydrous Na_2SO_4, and concentrated *in vacuo*. The residue was purified by column chromatography (silica gel, hexanes/EtOAc, 3/1) to afford **2.74** as a white powder (61 mg, 94%): $[\alpha]^{22.9}_D$ = –13.71 (*c* 1.75, $CHCl_3$); ^{1}H NMR (400 MHz, $CDCl_3$) δ 3.60 (d, *J* = 10.8 Hz, 1H), 3.07–3.04 (m, 1H), 2.53 (ddd, *J* = 6.8, 13.6, 13.6 Hz, 1H), 2.15 (dd, *J* = 3.6, 14.0 Hz, 1H), 2.08–1.98 (m, 2H), 1.83 (s, 1H), 1.77–1.60 (m, 3H), 1.58–1.36 (m, 6H), 1.23 (s, 3H), 1.10 (s, 3H), 1.07 (s, 3H), 1.03–0.99 (m, 2H), 0.89 (s, 3H); ^{13}C NMR (125 MHz, $CDCl_3$) δ 215.5, 79.1, 76.7, 75.5, 54.3, 48.5, 42.2, 41.5, 37.6, 31.6, 30.0, 26.6, 26.4, 24.6, 21.9, 20.9, 18.8, 14.5.

Preparation of 2.75

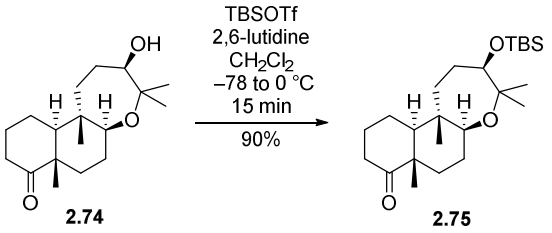

To a cooled (−78 °C) solution of ketone **2.74** (75 mg, 0.25 mmol) in dry CH_2Cl_2 (2 mL, 0.12 M) were added 2,6-lutidine (0.04 mL, 0.38 mmol) and TBSOTf (0.07 mL, 0.3 mmol). The resulting mixture was stirred for 15 min at 0 °C. The reaction was quenched by addition of saturated aqueous $NaHCO_3$ and extracted with CH_2Cl_2. The combined organic layers were washed with brine, dried over anhydrous Na_2SO_4, and concentrated *in vacuo*. The residue was purified by column chromatography (silica gel, hexanes/EtOAc, 20/1) to afford **2.75** as a white powder (93.4 mg, 90%): $[\alpha]^{23.1}_D$ = –13.64 (*c* 1.47, $CHCl_3$); ^{1}H NMR (400 MHz, $CDCl_3$) δ 3.54 (d, *J* = 10.4 Hz, 1H), 3.09–3.05 (m, 1H), 2.53 (ddd, *J* = 7.2, 14.0, 14.0 Hz, 1H), 2.16 (dd, *J* = 3.6, 14.4 Hz, 1H), 2.07–1.98 (m, 2H), 1.74–1.42 (m, 8H), 1.30–1.25 (m, 1H), 1.16 (s, 3H), 1.11 (s, 3H), 1.05 (s, 3H), 1.03–0.92 (m, 2H), 0.89 (s, 3H), 0.84 (s, 9H), 0.005 (d, *J* = 2.0 Hz, 6H); ^{13}C NMR (125 MHz, $CDCl_3$) δ 215.3, 79.6, 75.4, 54.4, 48.6, 42.3, 41.5, 37.6, 31.6, 29.8, 26.6, 26.5, 25.8, 24.7, 22.5, 21.0, 18.8, 17.9, 14.6, –4.0, –4.8.

Preparation of EE-protected Enol Ketone 2.77

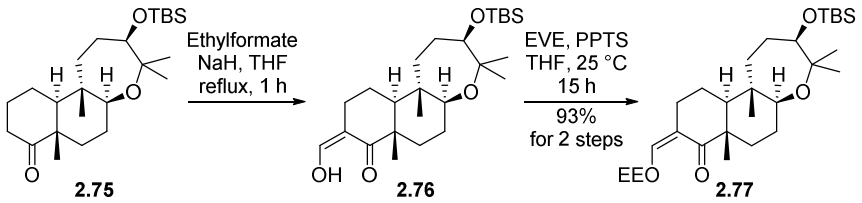

[**Formylation**] To a cooled (0 °C) solution of ketone **2.75** (88 mg, 0.22 mmol) in dry THF (4 mL, 0.06 M) were added ethylformate (0.17 mL, 2.15 mmol) and NaH (60% dispersion in mineral oil, 50 mg, 1.29 mmol). After stirring for 1 h at reflux, the reaction mixture was cooled to 0 °C, quenched by addition of saturated aqueous NH_4Cl and extracted with EtOAc. The combined organic layers were washed with brine, dried over anhydrous Na_2SO_4, and concentrated *in vacuo*. The residue was purified by column chromatography (silica gel, hexanes/EtOAc, 20/1) to afford **2.76**. [**EE-protection**] To a solution of enol ketone **2.76** (96 mg, 0.22 mmol) in dry THF (5 mL, 0.04 M) were added ethyl vinyl ether (0.2 mL, 2.06 mmol) and PPTS (11 mg, 0.04 mmol) at 25 °C. After stirring for 15 h, the reaction was quenched by addition of saturated aqueous $NaHCO_3$ and extracted with EtOAc. The combined organic layers were washed with brine, dried over anhydrous Na_2SO_4, and concentrated *in vacuo*. The residue was purified by column chromatography (silica gel, hexanes/EtOAc, 100/1 with 1% Et_3N) to afford **2.77** as a white powder (104 mg, 93% for 2 steps).

Preparation of Alcohol 2.78

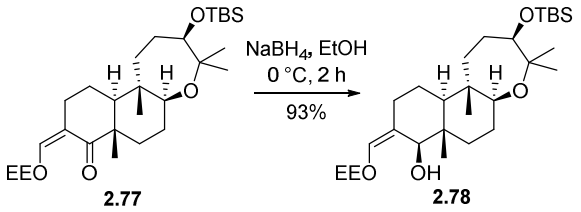

To a cooled (0 °C) solution of EE-protected enol ketone **2.77** (105 mg, 0.21 mmol) in EtOH (5 mL, 0.04 M) was added $NaBH_4$ (117 mg, 3.09 mmol) in four portions over a period of 2 h. The reaction was quenched by addition of saturated aqueous $NaHCO_3$ and extracted with EtOAc. The combined organic layers were washed with brine, dried over anhydrous Na_2SO_4, and concentrated *in vacuo*. The residue was purified by column chromatography (silica gel, hexanes/EtOAc, 6/1) to afford **2.78** (98 mg, 93%).

Preparation of Aldehyde 2.79

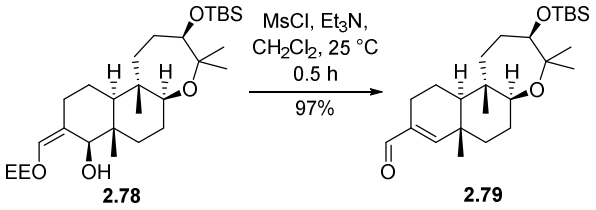

To a cooled (0 °C) solution of alcohol **2.78** (110 mg, 0.22mmol) in CH_2Cl_2 (4 mL, 0.06 M) were added Et_3N (0.09 mL, 0.65 mmol) and MsCl (0.03 mL, 0.43 mmol). After stirring for 30 min at the same temperature, the reaction was quenched by addition of saturated aqueous $NaHCO_3$ and extracted with CH_2Cl_2. The combined organic layers were washed with brine, dried over anhydrous Na_2SO_4, and concentrated *in vacuo*. The residue was

purified by column chromatography (silica gel, hexanes/EtOAc, 12/1) to afford **2.79** (88 mg, 97%).

Preparation of Alcohol 2.80

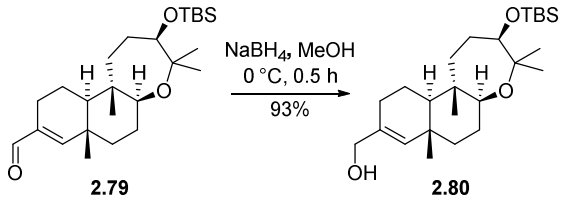

To a cooled (0 °C) solution of enal **2.79** (27 mg, 0.06 mmol) in EtOH (2 mL, 0.03 M) was added $NaBH_4$ (13 mg, 0.32 mmol). After stirring for 30 min at the same temperature, the reaction was quenched by addition of saturated aqueous NH_4Cl and extracted with EtOAc. The combined organic layers were washed with brine, dried over anhydrous Na_2SO_4, and concentrated *in vacuo*. The residue was purified by column chromatography (silica gel, hexanes/EtOAc, 6/1) to afford **2.80** as a white powder (25 mg, 93%): ^{1}H NMR (500 MHz, $CDCl_3$) δ 5.32 (s, 1H), 3.95 (s, 2H), 3.60 (d, *J* = 10.5 Hz, 1H), 3.15 (dd, *J* = 4.0, 11.5 Hz, 1H), 2.16–1.96 (m, 4H), 1.78–1.72 (m, 2H), 1.50–1.42 (m, 3H), 1.34–1.22 (m, 3H), 1.19 (s, 3H), 1.09 (s, 3H), 1.02–0.99 (m, 2H), 0.95 (s, 3H), 0.87 (s, 9H), 0.83 (s, 3H), 0.04 (d, *J* = 7.0 Hz, 6H).

Preparation of 2.85

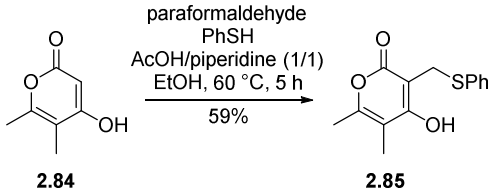

To a solution of paraformaldehyde (1.5 g), PhSH (4.3 mL, 42.8 mmol), AcOH:pyridine (1:1, 2.4 mL) in EtOH (50mL, 0.86 mmol) was added the known α-pyrone **2.84**[61] (1.5 g, 10.7 mmol) in EtOH (70 mL, 0.15 M) at 25 °C. After stirring for 5 h at 60 °C, the reaction mixture was concentrated *in vacuo*. The residue was purified by column chromatography (silica gel, hexanes/EtOAc, 3/1 to CH_2Cl_2/MeOH, 10/1) to afford **2.85** (1.6 g, 59%): ^{1}H NMR (400 MHz, $CDCl_3$) δ 7.38–7.36 (m, 2H), 7.31–7.22 (m, 3H), 4.17 (s, 2H), 2.18 (s, 3H), 1.88 (s, 3H).

Preparation of 2.86 and 2.87

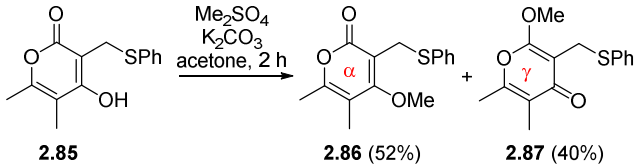

To a solution of **2.85** (170 mg, 0.65 mmol) in acetone (6 mL, 0.1 M) were added K_2CO_3 (448 mg, 3.24 mmol) and Me_2SO_4 (0.31 mL, 3.24 mmol) at 25 °C. After stirring for 2 h at the same temperature, the reaction mixture was concentrated *in vacuo*. The residue was purified by column chromatography (silica gel, hexanes/EtOAc, 3/1) to afford **2.86** (93 mg, 52%) and **2.87** (72 mg, 40%): [**For 2.86**] ^{1}H NMR (400 MHz, $CDCl_3$) δ 7.46–7.43 (m,

2H), 7.30–7.26 (m, 2H), 7.22–7.17 (m, 1H), 4.05 (s, 2H), 3.83 (s, 3H), 2.23 (s, 3H), 1.92 (s, 3H). [**For 2.87**] ^{1}H NMR (400 MHz, $CDCl_3$) δ 7.46–7.43 (m, 2H), 7.27–7.24 (m, 2H), 7.18–7.14 (m, 1H), 3.97 (s, 2H), 3.82 (s, 3H), 2.26 (s, 3H), 1.94 (s, 3H).

Preparation of 2.88

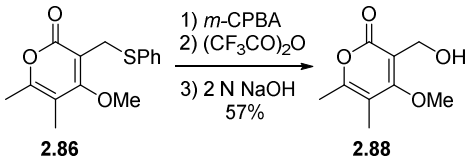

2.86 **2.88**

To a cooled (0 °C) solution of sulfide **2.86** (47 mg, 0.17 mmol) in CH_2Cl_2 (3 mL, 0.06 M) was added *m*-CPBA (77%, 38 mg, 0.17 mmol). After stirring for 20 min at the same temperature, $(CF_3CO)_2O$ (0.09 mL, 0.68 mmol) was added to the above mixture. After stirring for 1 h, the resulting mixture was diluted by addition of THF (3mL) to make the solution homogeneous during hydrolysis, and then 2 N NaOH (1.5 mL) was added at 0 °C. After stirring for 5 min at the same temperature, the reaction was quenched by addition of saturated aqueous NH_4Cl and extracted with CH_2Cl_2. The combined organic layers were washed with brine, dried over anhydrous Na_2SO_4, and concentrated *in vacuo*. The residue was purified by column chromatography (silica gel, hexanes/EtOAc, 1/1 to EtOAc) to afford **2.88** (18 mg, 57%): ^{1}H NMR (400 MHz, CDCl3) δ 4.51 (s, 2H), 4.15 (s, 3H), 2.20 (s, 3H), 1.86 (s, 3H).

Preparation of 2.90

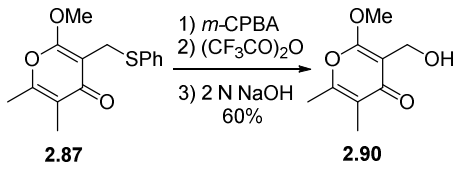

2.87 **2.90**

To a cooled (0 °C) solution of sulfide **2.87** (42 mg, 0.15 mmol) in CH_2Cl_2 (3 mL, 0.05 M) was added *m*-CPBA (77%, 33 mg, 0.15 mmol). After stirring for 20 min at the same temperature, $(CF_3CO)_2O$ (0.09 mL, 0.6 mmol) was added to the above mixture. After stirring for 1 h, the resulting mixture was diluted by addition of THF (3mL) to make the solution homogeneous during hydrolysis, and then 2 N NaOH (1.5 mL) was added at 0 °C. After stirring for 5 min at the same temperature, the reaction was quenched by addition of saturated aqueous NH_4Cl and extracted with CH_2Cl_2. The combined organic layers were washed with brine, dried over anhydrous Na_2SO_4, and concentrated *in vacuo*. The residue was purified by column chromatography (silica gel, hexanes/EtOAc, 1/1 to EtOAc) to afford **2.90** (17 mg, 60%): ^{1}H NMR (400 MHz, $CDCl_3$) δ 4.57 (s, 2H), 3.98 (s, 3H), 2.81 (bs, 1H), 2.23 (s, 3H), 1.91 (s, 3H).

Preparation of 2.92

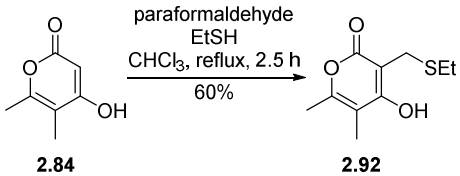

2.84 **2.92**

To a solution of paraformaldehyde (1.1 g) and EtSH (1.8 mL, 24.19 mmol) in $CHCl_3$ (20mL, 1.21 mmol) was added the known α-pyrone **2.84**[61] (1.13 g, 8.06 mmol) in $CHCl_3$ (25 mL, 0.32 M) at 25 °C. After stirring for 4 h at reflux, the reaction mixture was concentrated, dissolved in EtOAc, and cooled to −20 °C. After cooling for 2 h, white precipitate was removed by filtration and the filtrate was concentrated. The residue was purified by column chromatography (silica gel, hexanes/EtOAc, 1/1 to EtOAc) to afford **2.92** (17 mg, 60%): ^{1}H NMR (400 MHz, $CDCl_3$) δ 9.21 (s, 1H), 3.78 (s, 2H), 2.50 (q, J = 7.2 Hz, 2H), 2.21 (s, 3H), 1.91 (s, 3H), 1.25 (t, J = 7.2 Hz, 3H).

Preparation of 2.93 and 2.94

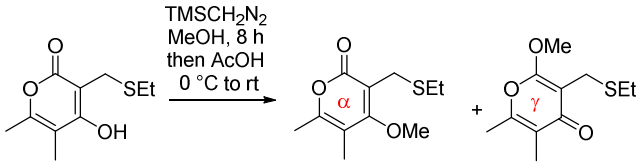

2.92 **2.93** (38%) **2.94** (43%)

To a cooled (0 °C) solution of **2.92** (44 mg, 0.21 mmol) in MeOH (2 mL, 0.1 M), was added $TMSCH_2N_2$ (2.0 M in hexanes, 0.41 mL, 0.82 mmol). After stirring for 8 h at 25 °C, the reaction was quenched by addition of AcOH at 0 °C. The resulting mixture was stirred for 10 min at 25 °C and extracted with EtOAc. The combined organic layers were washed with 2 N NaOH, dried over anhydrous Na_2SO_4, and concentrated *in vacuo*. The residue was purified by column chromatography (silica gel, hexanes to hexanes/EtOAc, 2/1) to afford **2.93** (18 mg, 38%) and **2.94** (20 mg, 43%): [**For 2.93**] ^{1}H NMR (400 MHz,

$CDCl_3$) δ 3.91 (s, 3H), 3.63 (s, 2H), 2.66 (q, *J* = 7.2 Hz, 2H), 2.23 (s, 3H), 1.94 (s, 3H), 1.29 (t, *J* = 7.6 Hz, 3H). [**For 2.94**] ^{1}H NMR (400 MHz, $CDCl_3$) δ 3.98 (s, 3H), 3.55 (s, 2H), 2.60 (q, *J* = 7.2 Hz, 2H), 2.27 (s, 3H), 1.93 (s, 3H), 1.28 (t, *J* = 7.2 Hz, 3H).

Preparation of 2.99

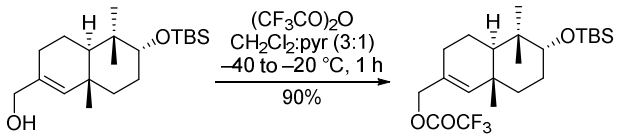

2.98 **2.99**

To a cooled (−40 °C) solution of alcohol **2.98** (35 mg, 0.1 mmol) in CH_2Cl_2:pyridine (3:1, 8 mL) was added $(CF_3CO)_2O$ (0.02 mL, 0.13 mmol). After stirring for 1 h at −20 °C, the reaction was quenched by addition of H_2O and extracted with CH_2Cl_2. The combined organic layers were washed with brine, dried over anhydrous Na_2SO_4, and concentrated *in vacuo*. The residue was purified by column chromatography (silica gel, hexanes) to afford **2.99** (41 mg, 90%): ^{1}H NMR (400 MHz, $CDCl_3$) δ 5.50 (s, 1H), 4.67 (s, 2H), 3.40 (s, 1H), 2.14–1.98 (m, 2H), 1.94–1.86 (m, 1H), 1.74–1.63 (m, 2H), 1.61–1.58 (m, 1H), 1.51–1.42 (m, 2H), 1.15 (ddd, *J* = 3.2, 3.6, 12.4 Hz, 1H), 0.95 (s, 3H), 0.89 (s, 9H), 0.87 (s, 3H), 0.83 (s, 3H), 0.03 (d, *J* = 3.6 Hz, 6H).

Preparation of 2.100

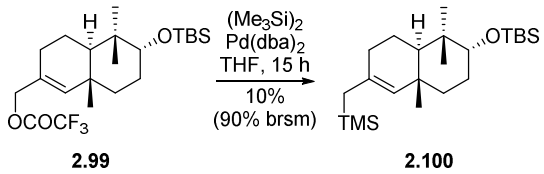

2.99 **2.100**

To a solution of $Pd(dba)_2$ (23 mg, 0.04 mmol) in dry THF (1 mL, 0.04 M) were added Si_2Me_6 (0.03 mL, 0.16 mmol) and **2.99** (35 mg, 0.08 mmol) in THF (1 mL, 0.08 M) at 25 °C. After stirring for 15 h at the same temperature, the reaction was quenched by addition of saturated aqueous $NaHCO_3$ and extracted with Et_2O. The combined organic layers were washed with brine, dried over anhydrous Na_2SO_4, and concentrated *in vacuo*. The residue was purified by column chromatography (silica gel, hexanes) to afford **2.100** (3.2 mg, 10%): ^{1}H NMR (400 MHz, $CDCl_3$) δ 4.89 (s, 1H), 3.38 (s, 1H), 1.97–1.93 (m, 2H), 1.91–1.82 (m, 1H), 1.68 (dt, *J* = 2.8, 12.8 Hz, 1H), 1.60 (dd, *J* = 2.0, 12.8 Hz, 1H), 1.53–1.50 (m, 1H), 1.46–1.35 (m, 2H), 1.32 (d, *J* = 4.4 Hz, 2H), 1.09 (dd, *J* = 3.2, 3.6, 12.8 Hz, 1H), 0.92 (s, 3H), 0.88 (s, 9H), 0.85 (s, 3H), 0.81 (s, 3H), 0.02 (d, *J* = 4.8 Hz, 6H), –0.01 (s, 9H).

Preparation of 2.104

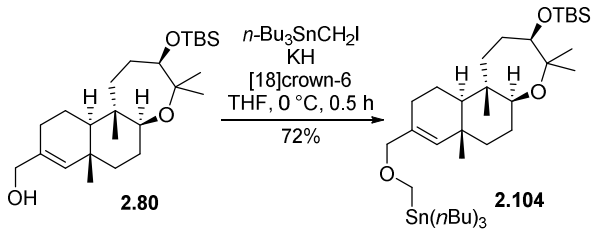

2.80 **2.104**

To a cooled (0 °C) solution of allylic alcohol **2.80** (22 mg, 0.05 mmol) in dry THF (1.5 mL, 0.03 M) were added KH (30% dispersion in mineral oil, 21 mg, 0.16 mmol) in THF (0.2 mL), (n-Bu)$_3$SnCH$_2$I (0.02 mL, 0.06 mmol), and 18-crown-6 (27.5 mg, 0.1 mmol). After stirring for 30 min at the same temperature, the reaction was quenched by addition of saturated aqueous NH_4Cl and extracted with EtOAc. The combined organic layers were washed with brine, dried over anhydrous Na_2SO_4, and concentrated *in vacuo*. The residue was purified by column chromatography (silica gel, hexanes to hexanes/EtOAc, 100/1) to afford **2.104** (28 mg, 74%): ^{1}H NMR (400 MHz, $CDCl_3$) δ 5.28 (s, 1H), 3.66–3.64 (m, 4H), 3.60 (d, J = 10.4 Hz, 1H), 3.15 (dd, J = 4.4, 11.6 Hz, 1H), 2.13–2.04 (m, 2H), 1.99–1.89 (m, 1H), 1.78–1.57 (m, 5H), 1.54–1.42 (m, 9H), 1.35–1.26 (m, 12H), 1.10–0.98 (m, 2H), 1.18 (s, 3H), 1.09 (s, 3H), 0.95 (s, 3H), 0.89 (dd, J = 7.2, 7.2 Hz, 9H), 0.87 (s, 9H), 0.82 (s, 3H), 0.04 (d, J = 6.0 Hz, 6H).

Preparation of Homoallylic Alcohol 2.105

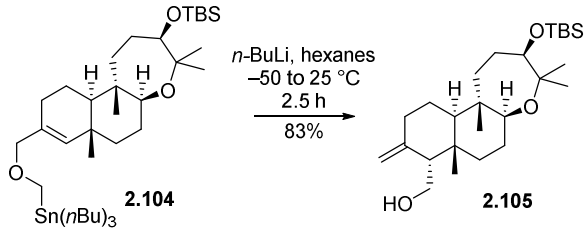

To a cooled (−50 °C) solution of **2.104** (28 mg, 0.04 mmol) in hexanes was added dropwise n-BuLi (2.5 M in hexanes, 0.15 mL, 0.39 mmol). After stirring for 10 min at the same temperature, the reaction mixture was slowly warmed to 25 °C for 2.5 h. The

reaction was quenched by addition of saturated aqueous NH_4Cl at 0 °C and diluted with EtOAc. The layers were separated, and the aqueous layer was extracted with EtOAc. The combined organic layers were washed with brine, dried over anhydrous Na_2SO_4, and concentrated *in vacuo*. The residue was purified by column chromatography (silica gel, hexanes/EtOAc, 15/1) to afford **2.105** as a white foam (14 g, 83%): ^1H NMR (400 MHz, $CDCl_3$) δ 4.93 (s, 1H), 4.76 (s, 1H), 3.76 (dd, *J* = 4.0, 9.2 Hz, 1H), 3.62–3.57 (m, 1H), 3.08 (dd, *J* = 4.4, 12.0 Hz, 1H), 2.30–2.25 (m, 1H), 2.13–1.98 (m, 2H), 1.90 (dd, *J* = 4.8, 10.8 Hz, 1H), 1.76–1.70 (m, 1H), 1.68–1.60 (m, 3H), 1.50–1.38 (m, 4H), 1.32–1.22 (m, 4H), 1.19 (s, 3H), 1.18–1.12 (m, 2H), 1.07 (s, 3H), 0.95 (s, 1H), 0.87 (s, 9H), 0.81 (s, 3H), 0.06–0.04 (m, 6H).

Preparation of Aldehyde 2.106

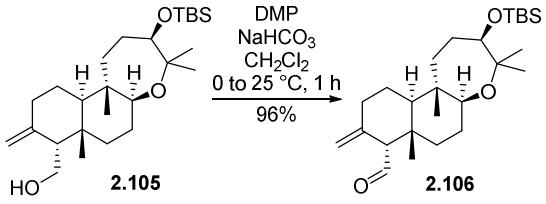

To a cooled (0 °C) solution of homoallylic alcohol **2.105** (13 mg, 0.03 mmol) in dry CH_2Cl_2 (2 mL, 0.01 M) were added Dess–Martin periodinane (26 mg, 0.06 mmol) and $NaHCO_3$ (10 mg, 0.12 mmol). After stirring for 1 h at 25 °C, the reaction was quenched by addition of saturated aqueous $Na_2S_2O_3$ and saturated aqueous $NaHCO_3$, diluted with CH_2Cl_2, and stirred vigorously for 1 h. The layers were separated, and the aqueous layer

was extracted with CH_2Cl_2. The combined organic layers were washed with brine, dried over anhydrous Na_2SO_4, and concentrated *in vacuo*. The residue was purified by column chromatography (silica gel, hexanes/EtOAc, 15/1) to afford **2.106** (12.5 mg, 96%): ^{1}H NMR (400 MHz, $CDCl_3$) δ 9.87 (d, *J* = 4.0 Hz, 1H), 4.94 (s, 1H), 4.77 (s, 1H), 3.60 (d, *J* = 10.0 Hz, 1H), 3.17–3.12 (m, 1H), 2.62 (d, *J* = 3.2 Hz, 1H), 2.46–2.40 (m, 1H), 2.29–2.20 (m, 1H), 2.09–1.99 (m, 1H), 1.78–1.73 (m, 2H), 1.67–1.32 (m, 8H), 1.18 (s, 3H), 1.08 (s, 3H), 0.94 (s, 3H), 0.87 (s, 9H), 0.82 (s, 3H), 0.05 (s, 6H).

Preparation of Alcohols 2.107

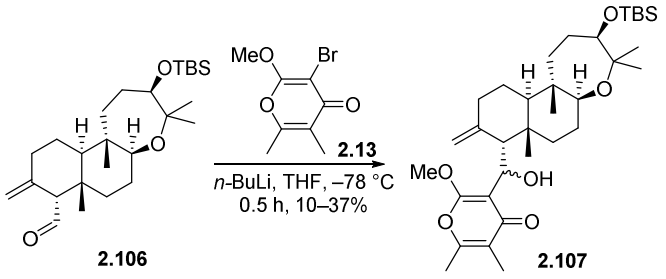

To a cooled (−78 °C) solution of bromo-γ-pyrone **2.13** (70 mg, 0.3 mmol) in dry THF (15 mL, 0.02 M) was added dropwise *n*-BuLi (2.5 M in hexanes, 0.1 mL, 0.24 mmol). The resulting mixture was stirred at the same temperature for 5 min before aldehyde **2.106** (26 mg, 0.06 mmol) in THF (3 mL, 0.02 M) was added dropwise. After stirring for 30 min at the same temperature, the reaction was quenched by addition of saturated aqueous NH_4Cl at 0 °C and diluted with EtOAc. The layers were separated, and the aqueous layer was extracted with EtOAc. The combined organic layers were washed with brine,

dried over anhydrous Na_2SO_4, and concentrated *in vacuo*. The residue was purified by column chromatography (silica gel, hexanes/CH_2Cl_2/EtOAc, 7/1/1) to afford alcohols **2.107** (13 mg, 37%): [**For major alcohol**] ^{1}H NMR (400 MHz, $CDCl_3$) δ 5.05 (d, *J* = 7.6 Hz, 1H), 4.54 (s, 1H), 4.49 (s, 1H), 3.87 (s, 3H), 3.65 (d, *J* = 10.0 Hz, 1H), 3.26–3.21 (m, 1H), 2.43 (d, *J* = 8.0 Hz, 1H), 2.37–2.32 (m, 1H), 2.21 (s, 3H), 2.08–2.01 (m, 2H), 1.93 (s, 3H), 1.81–1.44 (m, 9H), 1.31–1.24 (m, 2H), 1.23 (s, 3H), 1.09 (s, 3H), 0.95 (s, 3H), 0.88 (s, 9H), 0.82 (s, 3H), 0.06–0.03 (m, 6H). [**For minor alcohol**] ^{1}H NMR (400 MHz, $CDCl_3$) δ 5.41–5.23 (m, 1H), 4.76 (s, 1H), 4.27 (s, 1H), 3.82 (s, 3H), 3.65 (d, *J* = 10.0 Hz, 1H), 3.26–3.21 (m, 1H), 2.43 (d, *J* = 8.0 Hz, 1H), 2.37–2.32 (m, 1H), 2.23 (s, 3H), 2.08–2.01 (m, 2H), 1.96 (s, 3H), 1.81–1.44 (m, 9H), 1.31–1.24 (m, 2H), 1.20 (s, 3H), 1.08 (s, 3H), 0.90 (s, 3H), 0.87 (s, 9H), 0.81 (s, 3H), 0.06–0.03 (m, 6H).

Preparation of Xanthates 2.108

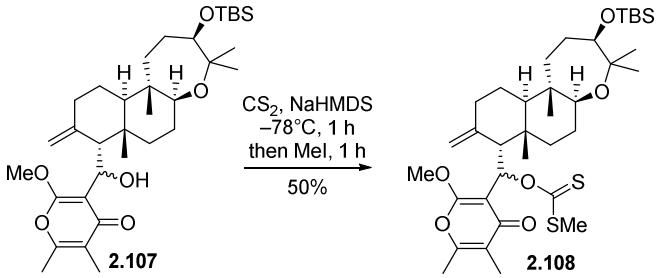

To a cooled (−78 °C) solution of alcohols **2.107** (11 mg, 0.02 mmol) in dry THF (2 mL, 0.01 M) was added CS_2 (0.01 mL, 0.2 mmol). The resulting mixture was stirred at the same temperature for 10 min before NaHMDS (1.0 M in THF, 0.03 mL, 0.03 mmol) was added

dropwise. After stirring for 1 h at the same temperature, MeI (0.01 mL, 0.2 mmol) was added in one portion. After stirring for 1 h at the same temperature, the reaction was quenched by addition of saturated aqueous NH_4Cl and diluted with EtOAc. The layers were separated, and the aqueous layer was extracted with EtOAc. The combined organic layers were washed with brine, dried over anhydrous Na_2SO_4, and concentrated *in vacuo*. The residue was purified by column chromatography (silica gel, hexanes/EtOAc, 3/1) to afford xanthates **2.108** (6 mg, 50%): [**For major xanthate**] ^{1}H NMR (400 MHz, $CDCl_3$) δ 5.35 (d, *J* = 9.2 Hz, 1H), 4.62 (s, 1H), 4.56 (s, 1H), 3.89 (s, 3H), 3.73 (d, *J* = 10.8 Hz, 1H), 3.21–3.16 (m, 1H), 2.65 (d, *J* = 9.2 Hz, 1H), 2.41 (s, 3H), 2.19 (s, 3H), 1.95 (s, 3H), 1.84–1.54 (m, 10H), 1.49–1.40 (m, 3H), 1.21 (s, 3H), 1.09 (s, 3H), 0.93 (s, 3H), 0.90 (s, 9H), 0.81 (s, 3H), 0.11–0.08 (m, 6H).

Preparation of Phosphate 2.81

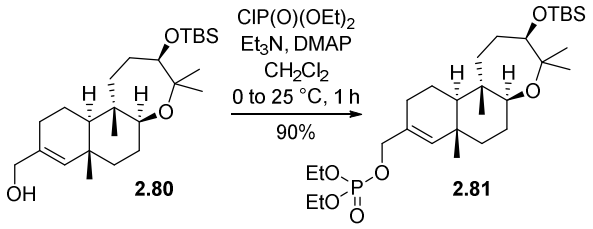

To a cooled (0 °C) solution of allylic alcohol **2.80** (152 mg, 0.36 mmol) in CH_2Cl_2 (6 mL, 0.06 M) were added Et_3N (0.1 mL, 0.72 mmol), DMAP (4.4 mg, 0.04 mmol), and diethylchlorophosphate (0.06 mL, 0.43 mmol). After stirring for 1 h at 25 °C, the reaction was quenched by addition of saturated aqueous $NaHCO_3$ and extracted with CH_2Cl_2.

The combined organic layers were washed with brine, dried over anhydrous Na_2SO_4, and concentrated *in vacuo*. The residue was purified by column chromatography (silica gel, hexanes/EtOAc, 3/1) to afford **2.81** (181 mg, 90%): ^{1}H NMR (400 MHz, $CDCl_3$) δ 5.40 (s, 1H), 4.38–4.29 (m, 2H), 4.14–4.07 (m, 4H), 3.60 (d, *J* = 10.4 Hz, 3.15 (dd, *J* = 4.4, 11.6 Hz, 1H), 2.19–1.97 (m, 3H), 1.77–1.72 (m, 2H), 1.67–1.63 (m, 1H), 1.48–1.44 (m, 3H), 1.34 (dd, *J* = 6.8, 7.2 Hz, 6H), 1.30–1.25 (m, 2H), 1.18 (s, 3H), 1.08 (s, 3H), 1.02–0.97 (m, 2H), 0.94 (s, 3H), 0.87 (s, 9H), 0.82 (s, 3H), 0.04 (d, *J* = 5.6 Hz, 6H).

Preparation of 2.114

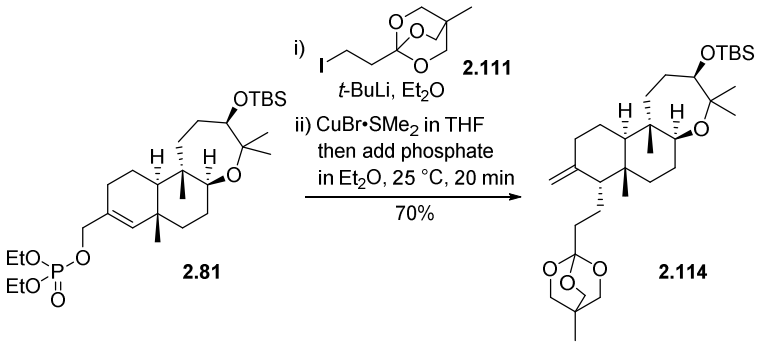

To a cooled (−78 °C) solution of orthoester **2.111** (295 mg, 1.04 mmol) in dry Et_2O (3 mL, 0.35 M) was added *t*-BuLi (1.7 M in pentane, 1.16 mL, 1.97 mmol). After stirring for 2 h at the same temperature, the reaction mixture was slowly warmed to 25 °C, and stirred for 20 min. CuBr·SMe_2 (213 mg, 1.04 mmol) in THF (2 mL) was added quickly to the above mixture and the resulting mixture was stirred for 10 min at 25 °C. Phosphate **2.81** (29 mg, 0.05 mmol) in dry Et_2O (3 mL) was added quickly to the above mixture and the

resulting mixture was stirred for 20 min at 25 °C. The reaction was quenched by addition of saturated aqueous NH_4OH and saturated aqueous NH_4Cl, diluted with EtOAc. The resulting mixture was stirred vigorously until the aqueous layer turned blue. The layers were separated, and the aqueous layer was extracted with EtOAc, and concentrated *in vacuo*. The residue was purified by column chromatography (silica gel, hexanes/EtOAc, 10/1) to afford **2.114** (20 mg, 70%): ^{1}H NMR (400 MHz, $CDCl_3$) δ 4.66 (s, 1H), 4.48 (s, 1H), 3.91 (s, 6H), 3.62 (d, *J* = 10.4 Hz, 1H), 3.19–3.13 (m, 1H), 2.12–1.98 (m, 3H), 1.71–1.30 (m, 15H), 1.20 (s, 3H), 1.08 (s, 3H), 0.88 (s, 12H), 0.81 (s, 3H), 0.79 (s, 3H), 0.08–0.07 (m, 6H).

Preparation of Ester 2.115

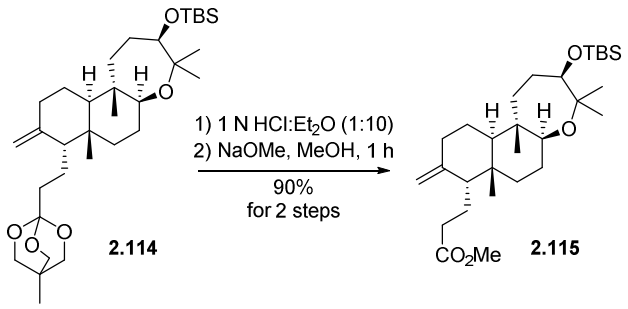

[**Hydrolysis**] To a solution of **2.114** (26 mg, 0.05 mmol) in Et_2O (5 mL) was added 1 N HCl (0.5 mL) at 25 °C. After stirring for 10 min at the same temperature, the reaction was quenched by addition of saturated aqueous $NaHCO_3$, diluted with $CHCl_3$. The layers were separated, and the aqueous layer was extracted with CH_2Cl_2. The combined organic layers were washed with brine, dried over anhydrous Na_2SO_4, and concentrated

in vacuo. The crude compound was employed in the next step without further purification. [**Esterification**] To a solution of the crude hydrolyzed intermediate (35 mg, 0.06 mmol) in MeOH (2.5 mL, 0.02 M) was added NaOMe (32 mg, 0.6 mmol) at 25 °C. After stirring for 1 h at the same temperature, the reaction was quenched by addition of saturated aqueous NH_4Cl and extracted with EtOAc. The combined organic layers were washed with brine, dried over anhydrous Na_2SO_4, and concentrated *in vacuo*. The residue was purified by column chromatography (silica gel, hexanes/EtOAc, 30/1) to afford **2.115** (22 mg, 90% for 2 steps): ^{1}H NMR (400 MHz, $CDCl_3$) δ 4.72 (s, 1H), 4.52 (s, 1H), 3.66 (s, 3H), 3.62 (d, *J* = 10.0 Hz, 1H), 3.11 (dd, *J* = 4.4, 10.4 Hz, 1H), 2.26–1.85 (m, 7H), 1.74–1.52 (m, 8H), 1.47–1.43 (m, 1H), 1.36 (dd, *J* = 4.4, 12.8 Hz, 1H), 1.32–1.20 (m, 4H), 1.20 (s, 3H), 1.10–0.96 (m, 3H), 1.08 (s, 3H), 0.91 (s, 3H), 0.88 (s, 9H), 0.80 (s, 3H).

Preparation of 2.116

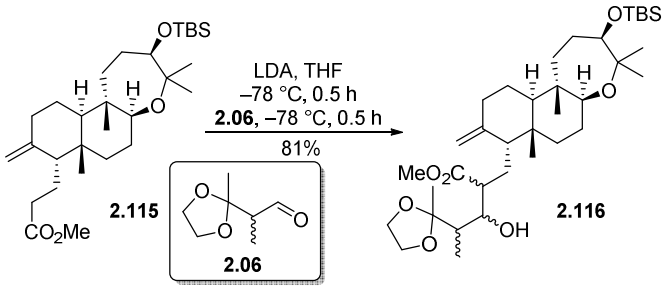

To a cooled (−78 °C) solution of diisopropylamine (0.03 mL, 0.21 mmol) in THF (1 mL, 0.21 M) was dropwise *n*-BuLi (2.5 M in hexanes, 0.08 mL, 0.2 mmol). After stirring for 5 min at the same temperature, the resulting mixture was warmed to 25 °C for 20 min.

Ester **2.115** (21 mg, 0.04 mmol) in THF (0.9 mL) was added dropwise to the above mixture at −78 °C and the resulting mixture was stirred for 30 min before aldehyde **2.06** in THF (0.5 mL) was added dropwise. After stirring for 30 min at the same temperature, the reaction was quenched by addition of saturated aqueous NH_4Cl and diluted with EtOAc. The layers were separated, and the aqueous layer was extracted with EtOAc. The combined organic layers were washed with brine, dried over anhydrous Na_2SO_4, and concentrated *in vacuo*. The residue was purified by column chromatography (silica gel, hexanes/EtOAc, 6/1) to afford **2.116** (22 mg, 81%).

Preparation of 2.117

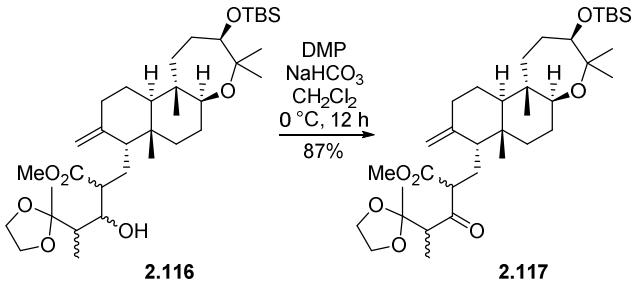

2.116 **2.117**

To a cooled (0 °C) solution of alcohol **2.116** (22 mg, 0.03 mmol) in dry CH_2Cl_2 (3 mL, 0.01 M) were added Dess–Martin periodinane (30 mg, 0.07 mmol) and $NaHCO_3$ (12 mg, 0.14 mmol). After stirring for 12 h at 25 °C, the reaction was quenched by addition of saturated aqueous $NaHCO_3$ and extracted with CH_2Cl_2. The combined organic layers were washed with brine, dried over anhydrous Na_2SO_4, and concentrated *in vacuo*. The

residue was purified by column chromatography (silica gel, hexanes/EtOAc, 6/1) to afford **2.117** (19 mg, 87%).

Preparation of 2.118

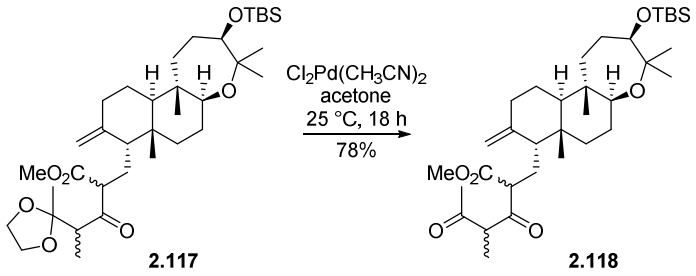

To a solution of **2.117** (19 mg, 0.03 mmol) in acetone (1.5 mL, 0.02) was added $Cl_2Pd(CH_3CN)_2$ (0.8 mg, 0.003 mmol) 25 °C. After stirring for 18 h at the same temperature, the reaction mixture was concentrated *in vacuo*. The residue was purified by column chromatography (silica gel, hexanes/EtOAc, 2/1) to afford **2.118** (13.8 mg, 78%).

Preparation of 2.119

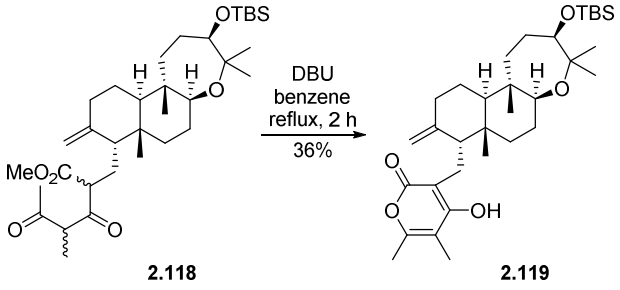

To a solution of 1,3-diketone **2.118** (18 mg, 0.03 mmol) in benzene (3 mL, 0.01 M) was added DBU (0.05 mL, 0.3 mmol) 25 °C. After stirring for 2 h at reflux, the reaction

mixture was neutralized carefully with 2 N HCl, diluted with EtOAc and H_2O, and extracted with EtOAc. The combined organic layers were washed with brine, dried over anhydrous Na_2SO_4, and concentrated *in vacuo*. The residue was purified by column chromatography (silica gel, hexanes/EtOAc, 3/1) to afford **2.119** (19 mg, 87%): ^{1}H NMR (400 MHz, $CDCl_3$) δ 5.78 (bs, 1H), 4.71 (s, 1H), 4.53 (s, 1H), 3.63 (d, *J* = 10.0 Hz, 1H), 3.18 (dd, *J* = 4.4, 11.6 Hz, 1H), 2.86 (dd, *J* = 3.2, 14.4 Hz, 1H), 2.44 (dd, *J* = 9.6, 14.8 Hz, 1H), 2.38–2.31 (m, 1H), 2.20 (s, 3H), 1.91 (s, 3H), 1.84–1.72 (m, 3H), 1.66–1.60 (m, 3H), 1.54–1.48 (m, 2H), 1.43–1.38 (m, 1H), 1.32–1.24 (m, 4H), 1.21 (s, 3H), 1.08 (s, 3H), 0.90 (s, 3H), 0.88 (s, 9H), 0.82 (s, 3H), 0.07 (s, 6H).

Preparation of Ester (*S*)-2.123

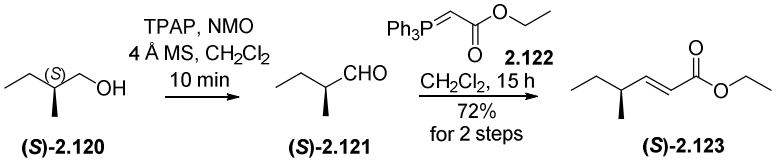

[**Oxidation**] To a solution of (*S*)-(–)-2-methylbutanol **(*S*)-2.120** (0.25 mL, 2.27 mmol) in CH_2Cl_2 (8 mL, 0.03 M) were added 4 Å molecular sieves (1.13 g, 0.5 g/mmol substrate), NMO (531.6 mg, 4.53 mmol), and TPAP (79.8 mg, 0.23 mmol) at 25 °C. After stirring for 10 min at the same temperature, the reaction mixture was filtered through a short SiO_2 pad with CH_2Cl_2. The combined crude aldehyde **(*S*)-2.121** in CH_2Cl_2 (8 mL) was employed in the next step without further purification. [**Wittig reaction**] To a solution of crude **(*S*)-2.121** (196 mg, 2.27 mmol) in CH_2Cl_2 (8 mL, 0.03 M) was added

carbethoxymethylene)triphenylphosphorane (791 mg, 2.27 mmol) at 25 °C. After stirring for 15 h at the same temperature, the reaction mixture was concentrated. The residue was purified by column chromatography (silica gel, hexanes/EtOAc, 15/1) to afford **(*S*)-2.123** as a colorless oil (255 mg, 72% for 2 steps): ^{1}H NMR (400 MHz, $CDCl_3$) δ 6.85 (dd, *J* = 8.0, 16.0 Hz, 1H), 5.76 (d, *J* = 15.6 Hz, 1H), 4.17 (q, *J* = 7.2 Hz, 2H), 2.20 (septet, *J* = 6.8 Hz, 1H), 1.42–1.35 (m, 2H), 1.28 (t, *J* = 7.2 Hz, 3H), 1.03 (d, *J* = 6.8 Hz, 3H), 0.87 (t, *J* = 7.6 Hz, 3H).

Preparation of Alcohol (*S*)-2.124

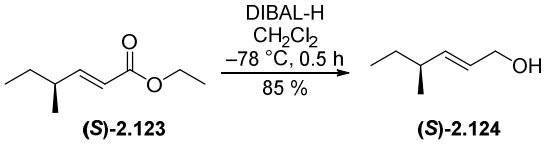

To a cooled (−78 °C) solution of ester **(*S*)-2.123** (280 mg, 1.79 mmol) in CH_2Cl_2 (3 mL, 0.6 M) was added DIBAL-H (5.4 mL, 1.0 M in toluene, 5.4 mmol). After stirring for 30 min at the same temperature, the reaction was quenched by addition of MeOH followed by aqueous Rochelle's salt, diluted with CH_2Cl_2, and stirred for 1 h at 25 °C. The layers were separated, and the aqueous layer was extracted with CH_2Cl_2. The combined organic layers were washed with brine, dried over anhydrous Na_2SO_4, and concentrated *in vacuo*. The residue was purified by column chromatography (silica gel, hexanes/EtOAc, 6/1) to afford **(*S*)-2.124** (174 mg, 85%): ^{1}H NMR (400 MHz, $CDCl_3$) δ

5.63–5.52 (m, 2H), 4.09 (d, *J* = 4.8 Hz, 2H), 2.07–2.01 (m, 1H), 1.42 (bs, 1H), 1.31 (p, *J* = 7.2 Hz, 2H), 0.98 (d, *J* = 6.8 Hz, 3H), 0.85 (t, *J* = 7.2 Hz, 3H).

Preparation of Ester (*S*)-2.125

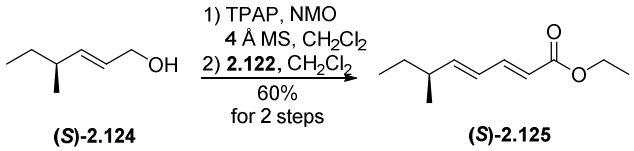

[**Oxidation**] To a solution of alcohol **(*S*)-2.124** (170 mg, 1.49 mmol) in CH_2Cl_2 (6 mL, 0.25 M) were added 4 Å molecular sieves (745 mg, 0.5 g/mmol substrate), NMO (349 mg, 2.98 mmol), and TPAP (52 mg, 0.15 mmol) at 25 °C. After stirring for 10 min at the same temperature, the reaction mixture was filtered through a short SiO_2 pad with CH_2Cl_2. The combined crude aldehyde in CH_2Cl_2 (5 mL) was employed in the next step without further purification. [**Wittig reaction**] To a solution of crude aldehyde (167 mg, 1.49 mmol) in CH_2Cl_2 (5 mL, 0.3 M) was added (carbethoxymethylene)triphenylphosphorane (519 mg, 1.49 mmol) at 25 °C. After stirring for 15 h at the same temperature, the reaction mixture was concentrated. The residue was purified by column chromatography (silica gel, hexanes/EtOAc, 100/1) to afford **(*S*)-2.125** as a colorless oil (162 mg, 60% for 2 steps): ^{1}H NMR (400 MHz, $CDCl_3$) δ 7.26 (dd, *J* = 10.8, 15.2 Hz, 1H), 6.14 (dd, *J* = 10.8, 15.2 Hz, 1H), 6.00 (dd, *J* = 7.6, 15.2 Hz, 1H), 5.79 (d, *J* = 15.2 Hz, 1H), 4.20 (q, *J* = 7.2 Hz, 1H), 2.20–2.13 (m, 1H), 1.42–1.32 (m, 2H), 1.28 (t, *J* = 7.2 Hz, 3H), 1.03 (d, *J* = 6.8 Hz, 3H), 0.87 (t, *J* = 7.6 Hz, 3H).

Preparation of Carboxylic Acid (*S*)-2.126

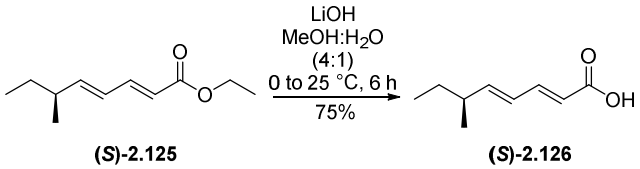

To a cooled (0 °C) solution of ester **(*S*)-2.125** (45 mg, 0.25 mmol) in MeOH:H_2O (4:1, 4mL, 0.06 M) was added LiOH (180 mg, 7.5 mmol). After stirring for 6 h at 25 °C, the reaction mixture was neutralized with AcOH and concentrated to remove MeOH. The residue was extracted with EtOAc/H_2O mixture, dried over anhydrous Na_2SO_4, and concentrated *in vacuo*. The residue was purified by column chromatography (silica gel, hexanes/EtOAc, 6/1) to afford **(*S*)-2.126** as a colorless oil (28.6 mg, 75%): ^{1}H NMR (400 MHz, $CDCl_3$) δ 7.34 (dd, *J* = 10.8, 15.6 Hz, 1H), 6.18 (dd, *J* = 10.8, 14.8 Hz, 1H), 6.07 (dd, *J* = 7.6, 15.2 Hz, 1H), 5.80 (d, *J* = 15.6 Hz, 1H), 2.22–2.15 (m, 1H), 1.38 (p, *J* = 7.2 Hz, 2H), 1.04 (d, *J* = 6.8 Hz, 3H), 0.87 (dd, *J* = 7.2, 8.0 Hz, 3H).

Preparation of Ester 2.127

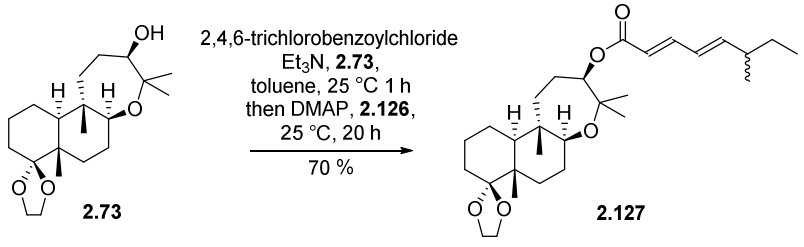

To a solution of carboxylic acid **2.126** (46 mg, 0.3 mmol) in dry toluene (1 mL, 0.3 M) was added Et_3N (0.12 mL, 0.89 mmol) and 2,4,6-trichlorobenzoyl chloride (0.05 mL, 0.3

mmol) at 25 °C. After stirring for 1 h at the same temperature, a solution of alcohol **2.73** (10 mg, 0.03 mmol) and DMAP (10.8 mg, 0.09 mmol) in toluene (1mL, 0.03 M) was added to the above reaction mixure. After stirring for 20 h, the reaction was quenched by addition of saturated aqueous $NaHCO_3$ and extracted with EtOAc. The combined organic layers were washed with brine, dried over anhydrous Na_2SO_4, and concentrated *in vacuo*. The residue was purified by column chromatography (silica gel, hexanes/EtOAc, 15/1) to afford **2.127** (9.8 mg, 70%): ^{1}H NMR (400 MHz, $CDCl_3$) δ 7.21 (dd, *J* = 10.0, 15.2 Hz, 1H), 6.13 (dd, *J* = 10.8, 15.2 Hz, 1H), 6.01 (dd, *J* = 7.6, 15.2 Hz, 1H), 5.77 (d, *J* = 15.2 Hz, 1H), 4.89 (d, *J* = 10.4 Hz, 1H), 3.96–3.88 (m, 3H), 3.85–3.79 (m, 1H), 3.30–3.25 (m, 1H), 2.20–2.13 (m, 1H), 2.08–2.99 (m, 1H), 1.76–1.25 (m, 16H), 1.18 (s, 6H), 1.05 (s, 3H), 1.02 (d, *J* = 6.8 Hz, 3H), 0.86 (t, *J* = 6.8 Hz, 3H), 0.85 (s, 3H).

3. Design, Synthesis, and Characterization of Manassantin Analogues

3.1 Introduction

3.1.1 Hypoxia

Molecular oxygen (O_2) is required for aerobic metabolism to maintain intracellular bioenergetics and to serve as an electron acceptor in many biochemical reactions.[67] Eukaryotic organisms have the ability to oxidize glucose into carbon dioxide and water, which produces energy for aerobic metabolism in the form of adenosine 5'-triphosphate (ATP). The use of O_2 as a substrate for energy production allows cells to become multicellular organisms, leading to the evolution of more specialized and complex O_2 delivery systems. Acute increases or decreases in O_2 levels can threaten energy production and result in increased oxidative stress through the generation of excessive reactive oxygen species (ROS).[68] As a result, O_2 homeostasis is an essential physiological requirement to all organisms for maintaining metabolic processes. Ambient air contains 21% of O_2; however, most mammalian tissues exist at 2–9% of O_2.

Hypoxia, usually defined as ≤ 2% of O_2, occurs in a variety of pathological conditions, including stroke, tissue ischemia, inflammation, and tumor growth.[69] Cells have developed a number of essential mechanisms to cope with the stress of hypoxia. Among these coping mechanisms is the response mediated by the hypoxia-inducible transcription factor 1 (HIF-1).[70] As will be described, hypoxia causes an increased

expression of HIF-1 and the up-regulation of genes involved in cellular processes that compensate for the decrease in O_2 availability. As a main regulator of hypoxia, HIF-1 stabilization mechanisms and the consequences of its increased activity will be presented in the subsequent section.

3.1.2 Hypoxia Inducible Factor 1 (HIF-1)

In 1991, Sememza and co-workers identified HIF-1 while investigating its binding to the gene of erythropoietin (EPO) which regulates the production of red blood cells and thus oxygen delivery to tissues.[71] HIF-1 is a basic helix-loop-helix-PER-ARNT-SIM (bHLH-PAS) family protein that forms a heterodimer with its α and β subunits and functions as a transcription factor (Figure 16).[72] While HIF-1β, also known as ARNT (aryl hydrocarbon receptor nuclear translocator) is constitutively active, HIF-1 is regulated by oxygen status. Thus, the overall activity of HIF-1 is dependent on the availability of its α subunit.

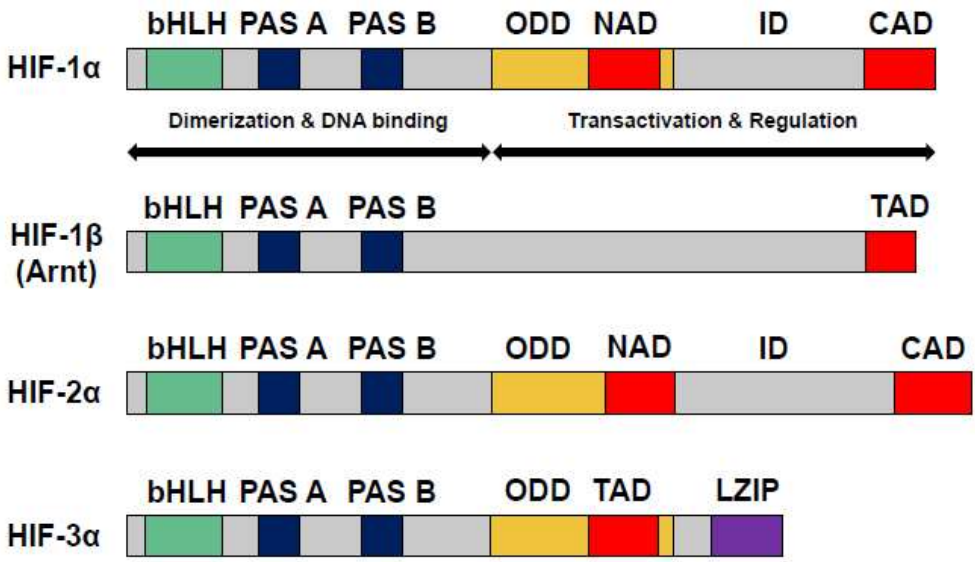

Figure 16: Domain structures of HIF-1α, HIF-1β, HIF-2α, and HIF-3α

In addition to HIF-1α, two closely-related HIF-2α and HIF-3α are currently known (Figure 16). Both HIF-1α and HIF-2α are O_2-labile α-subunits and heterodimeric complexes composed of bHLH-PAS proteins. Furthermore, both of them can bind to HIF-1β to form a functional heterodimer and mediate transcription. However, increasing evidence has indicated that HIF-2α is distinct or even opposite in many ways from HIF-1α.[73] First, HIF-2α expression has been shown to differ from that of HIF-1α expression in various tissues.[74] In contrast to HIF-1α that appears to be expressed in nearly all cell types, HIF-2α expression is restricted to specific types, including endothelial cells, gial cells, type II pneumocytes, cardiomyocytes, kidney fibroblasts, interstitial cells of the pancreas and duodenum and hepatocytes. In addition, HIF-1α is observed by cytoplasmic staining in addition to nuclear accumulation: however, HIF-2α

is confined to the cell nucleus and expressed only under hypoxic stimulation. The second difference can be found in the oxygen conditions needed for expression. More severe hypoxia is required to induce HIF-1α compared with HIF-2α in liver and kidney.[75] Furthermore, HIF-1α is most active during short periods (2–24 h) of intense hypoxia or anoxia (<0.1% O_2), whereas HIF-2α is shown to be active under mild or physiological hypoxia (<5% O_2) in both SK-N-BE(2)-C and KCN-69n neuroblastoma cell lines.[76] These findings suggest that HIF-2α plays an important role in driving the hypoxic response, whereas HIF-1α controls the initial response to hypoxia in certain contexts. Another difference can be found in the time needed for activation and duration of activity. HIF-1α induction in kidney and liver is shown to be transient: however, HIF-2α expression is sustained.[75] In addition, HIF-1α is transiently stabilized and primarily mediated acute responses, whereas HIF-2α gradually accumulates and manages prolonged hypoxic gene activation under hypoxia in neuroblastoma.[76]

It has been reported that the majority of hypoxia-induced genes contain HIF-1 binding sites, and gene expression is dependent on HIF-1α expression. HIF-2α binding is redundant for many genes, but knockdown of HIF-2α levels does not affect gene expression.[77] A number of studies have shown that HIF-1α and HIF-2α regulate different target genes with non-redundant and even opposite biological functions.[78] In addition, HIF-2α and HIF-1α regulate conversely some key downstream genes. HIF-2α increases

c-Myc,[78b, 79] *mTOR*[80] and *β-catenin*[81] activity and decreases *p53*[82], whereas HIF-1α exerts opposite effects.[78b, 81-83]

HIF-3α differs from HIF-1α and HIF-2α in protein structure and regulation of gene expression. Whereas HIF-1α and HIF-2α have two transactivation domains (TADs), HIF-3α has only one TAD (Figure 16).[84] HIF-3α has a unique leucine zipper domain (LZIP) and an LXXLL motif, and these unique structural features are evolutionarily conserved.[85] Despite HIF-3α is not fully characterized, it has been considered as a negative mediator of HIF-regulated genes. It has been shown that some splicing variants of the HIF-3α gene are able to dimerize with HIF-1α or HIF-1β and prevent target gene transcription.[86]

HIF-1α is the most characterized of all isoforms in the molecular response to hypoxia. Figure 17 shows the regulation of HIF-1α under normoxic and hypoxic conditions. In well-oxygenated states, constitutively synthesized HIF-1α undergoes continuous degradation.[87] During this process, two proline sites (Pro402 and Pro564) in the oxygen-dependent degradation (ODD) domain are hydroxylated by prolyl hydroxylase.[88] Of the three prolyl hydroxylase-domains (PHD1, PHD2, and PHD3) identified in mammalian cells, PHD2 is known to play a major role. Under normoxic conditions, PHD2 uses molecular oxygen and 2-oxoglutarate (α-ketoglutarate) as co-substrates for proline hydroxylation of HIF-1α. Hydroxylated HIF-1α is then recognized

by the tumor suppressor gene von Hippel Lindau (VHL), subsequently ubiquitinated, and degraded.

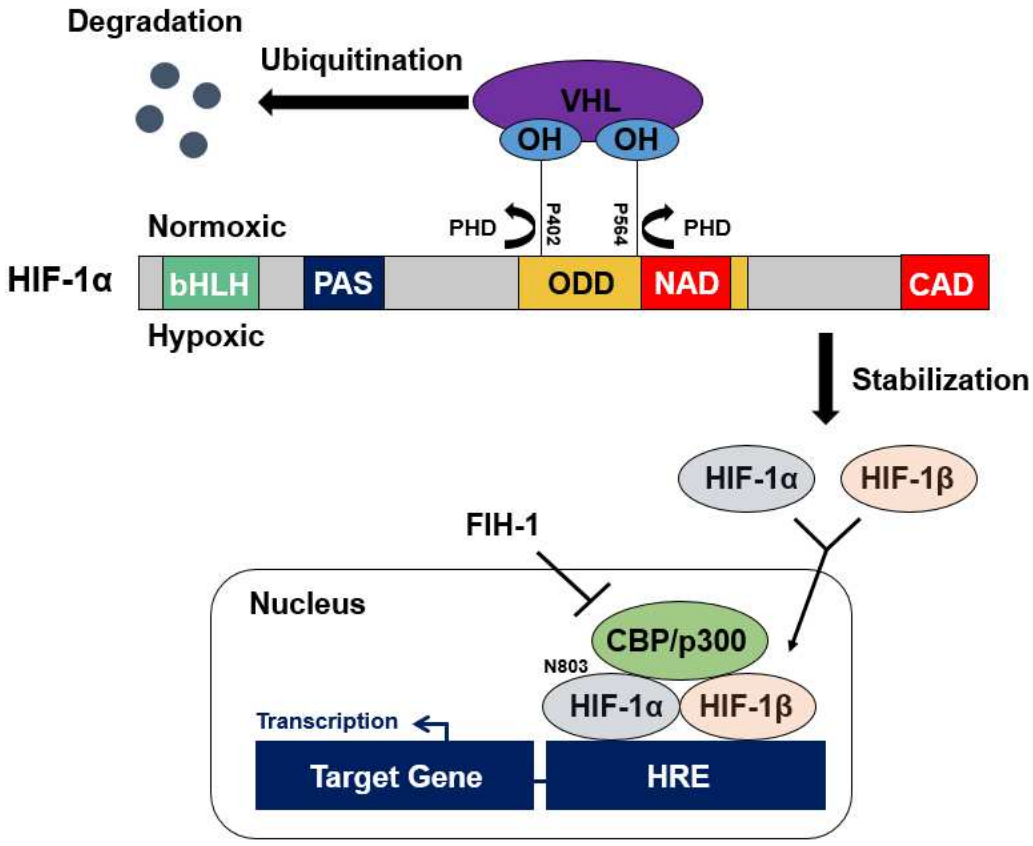

Figure 17: Regulation of HIF-1α under normoxic and hypoxic conditions

However, hypoxic O_2 levels limit the ability of PHD2 to function and result in enhanced stability of HIF-1α. Stabilized HIF-1α forms a heterodimer with its β subunit and translocates into the nucleus where it binds to its target gene promoters known as hypoxia response elements (HREs) and activates gene transcription. Dimerization process is prerequisite for binding of DNA and is mediated by the bHLH and PAS

domains of each subunit (Figure 16).[89] In order to transactivate, HIF-1 interacts with co-factors such as CBP/p300 that bind to its transactivation domain (TAD). HIF-1α contains two transactivation domains (C-TAD and N-TAD), whereas HIF-1β has only one TAD (Figure 16). Of the two, CAD appears to be the predominate domain contributing significantly to the regulation of HIF-1 target genes.[90] NAD has been implicated in the regulation of HIF-1 target gene specificity.

Similar to the regulation of HIF-1α stability via prolyl hydroxylation, the asparaginyl residue (Asn803) of TAD is hydroxylated by the factor inhibiting HIF-1 (FIH-1) whose activity is also dependent on O_2 levels. When FIH-1 is active, the interaction of HIF-1α with its co-activators is prevented. In addition to oxygen, FIH-1 require Fe^{2+} and 2-oxoglutarate for activation like PHDs.[91] Therefore, the stabilization of HIF-1α is regulated not only by oxygen but also by iron chelators such as cobalt chloride ($CoCl_2$), desferrioxamine (DFO), and 1,10-phenanthroline. As an oxygen-independent stabilization, HIF-1 is also regulated by nitric oxide (NO)[92], reactive oxygen species (ROS)[93], and growth factors[94] as well as signaling pathways including the phosphatidylinositol 3-kinase (PI3K)/Akt pathway[95] and the mitogen-activated protein kinase (MAPK) pathway.[96]

HIF-1 is a main regulator of hypoxia, activating more than several hundred genes involved in angiogenesis (VEGF), glucose transport (GLUT1), glycolytic pathway (LDH-A), ROS signals (iNOS), erythropoiesis (EPO), and a variety of other processes.[89]

Considering the scope of metabolic pathways as well as wide range of hypoxia-related pathologies, HIF has become an attractive target for drug development. As will be presented in the subsequent section, one of the most significant associations between HIF-1 and patient mortality have been shown in many cancers.

3.1.3 HIF-1 and Cancer

Tumors adapt to hypoxia by increasing angiogenesis and metastatic potential, altering apoptosis, and regulating metabolism.[97] These adaptations mediated by HIF-1 make tumors both more aggressive and treatment-resistant, resulting in poor clinical outcomes.[98] Immunohistochemical analyses have revealed that HIF-1α is overexpressed in many human cancers and closely associated with patient mortality.[99] HIF-1 overexpression is not only involved in tumor progression but also associated with resistance to radiation[100] and chemotherapy.[101] Tumor hypoxia is correlated with radioresistance due to the role of oxygen in DNA fixation. Exposure of cells to ionizing radiation generates free radicals in DNA, which can react with available O_2, forming peroxy radical species (DNA-OO·) that chemically modify the DNA. In the absence of oxygen, free radical production is reduced and the target cells can repair the damage by restoring the DNA to its original composition.[69] Hypoxic tumor cells are also resistant to chemotherapy. Because hypoxic cells are usually distantly located from blood vessels, they receive inefficient drug delivery. In addition, the slow proliferation rate of hypoxic

cells impedes the effect of anticancer drugs that target dividing cells. Furthermore, hypoxia mediates the up-regulation of the multidrug resistance gene (MDR1)[102], resulting in the efflux of the drugs and reduction in their effects. Therefore, inhibition of HIF-1 activity destroys blood vessels, suppresses tumor growth, enhances tumor apoptosis, and increases tumor radiosensitivity[100b, 103], making HIF-1 an excellent target for the treatment of cancer.

3.1.4 HIF-1 Inhibitors

Due to the importance of HIF-1 in tumor development, progression, and resistance to treatment a considerable effort has been devoted to identifying HIF-1 inhibitors for the treatment of cancer.[104] Despite a variety of anticancer drugs have been reported to inhibit HIF-1, these compounds possess relatively low HIF-1 inhibitory activity (≥ micromolar range). In addition, most of them lack the desired selectivity for the HIF-1 signaling pathway or toxicity profiles to become useful therapeutic agents. For example, rotenone is known to downregulate HIF-1 by inhibiting the electron transport chain complex I in mitochondria.[105] However, it is not selective for the HIF-1 signaling pathway and possesses a severe neurotoxicity.[106] Currently, there are no HIF-1 selective small molecules approved by the FDA.

3.1.5 Background of Manassantins A and B

3.1.5.1 Isolation and Biological Activity of Manassantins A and B

Saururus cernuus L. (Saururaceae), an aquatic plant found throughout the eastern half of the United States, has a long history of medicinal use in the treatment of tumors by both native Americans and early colonists. The dineolignans manassantin A (**1**), manassantin B (**2**), 4-*O*-demethylmanassantin B (**3**), and manassantin B_1 (**4**) are natural products isolated from *Saururus cernuus* (Figure 18).[107]

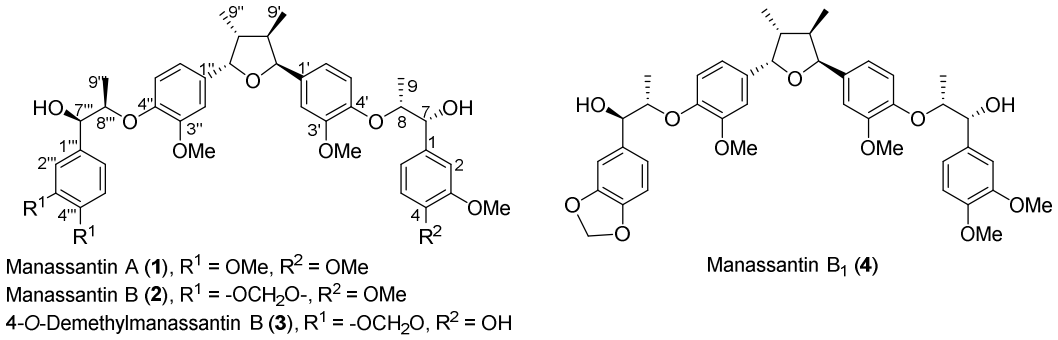

Figure 18: Structure of dineolignans from *Saururus cernuus*

Manassantins A (**1**) and B (**2**) have been shown to be potent inhibitors of HIF-1 (IC_{50} = ~10 nM) *in vitro* with minimal cytotoxicity.[107c, 108] Despite their potent inhibition of HIF-1, low toxicity, and selectivity for cancer cells, the molecular mechanisms of action for manassantins A and B are not established. To date, two total syntheses have been reported. In the subsequent sections, these two approaches will be briefly described.

3.1.5.2 Hanessian's Synthesis of Manassantins A and B

In 2006, Hanessian and co-workers reported the first total synthesis of **1** and **2** and confirmed the absolute configuration of the natural products.[109] As shown in Scheme 21, cyanohydrin **3.01** was converted to enoate **3.02** through methylester formation, TBS-protection, DIBAL-H reduction, and Wittig reaction. Treatment of **3.02** with lithium dimethylcuprate in the presence of TMSCl afforded the *anti*-*C*-methyl adduct, which was converted to the K-enolate and alkylated with MeI to give **3.03**. The ester group in **3.03** was reduced to alcohol and was back oxidized to provide aldehyde **3.04**. The addition of (4-benzyloxy-3-methoxyphenyl)magnesium bromide to **3.04** afforded a 2.5:1 mixture of epimeric alcohols **3.05**, which was MOM-protected followed by TBS-deprotection and de-*O*-allylation to give a separable mixture of **3.06** and **3.07**. The key intramolecular etherification was achieved using *p*-nitrobenzoate ester **3.08** as a precursor. Treatment of **3.08** with mesyl chloride provided the THF isomer **3.09**, which was converted to the THF core **3.12** by Bn-deprotection. A BEMP-mediated S_N2 reaction[110] of **3.12** with the triflate ester of *S*-methyl lactate provided **3.13**. Conversion of **3.13** to the corresponding Weinreb amide[111] followed by treatment with (3,4-dimethoxyphenyl)magnesium bromide afforded **MA05**. Finally, the stereocontrolled reduction of **MA05** using polymer-supported BH_4 completed the synthesis of **1**. In order to accomplish the synthesis of **2**, **3.11** was subjected to the BEMP-mediated S_N2 reaction with the triflate ester of *S*-methyl lactate to obtain **3.14**. Conversion of **3.14** to the

Weinreb amide, treatment with the Grignard reagent prepared from 3,4-methylenedioxy-1-bromobenzene, the stereocontrolled reduction, and Bn-deprotection provided **3.15**. **3.15** was applied to the same protocol as described above to complete the synthesis of **2**.

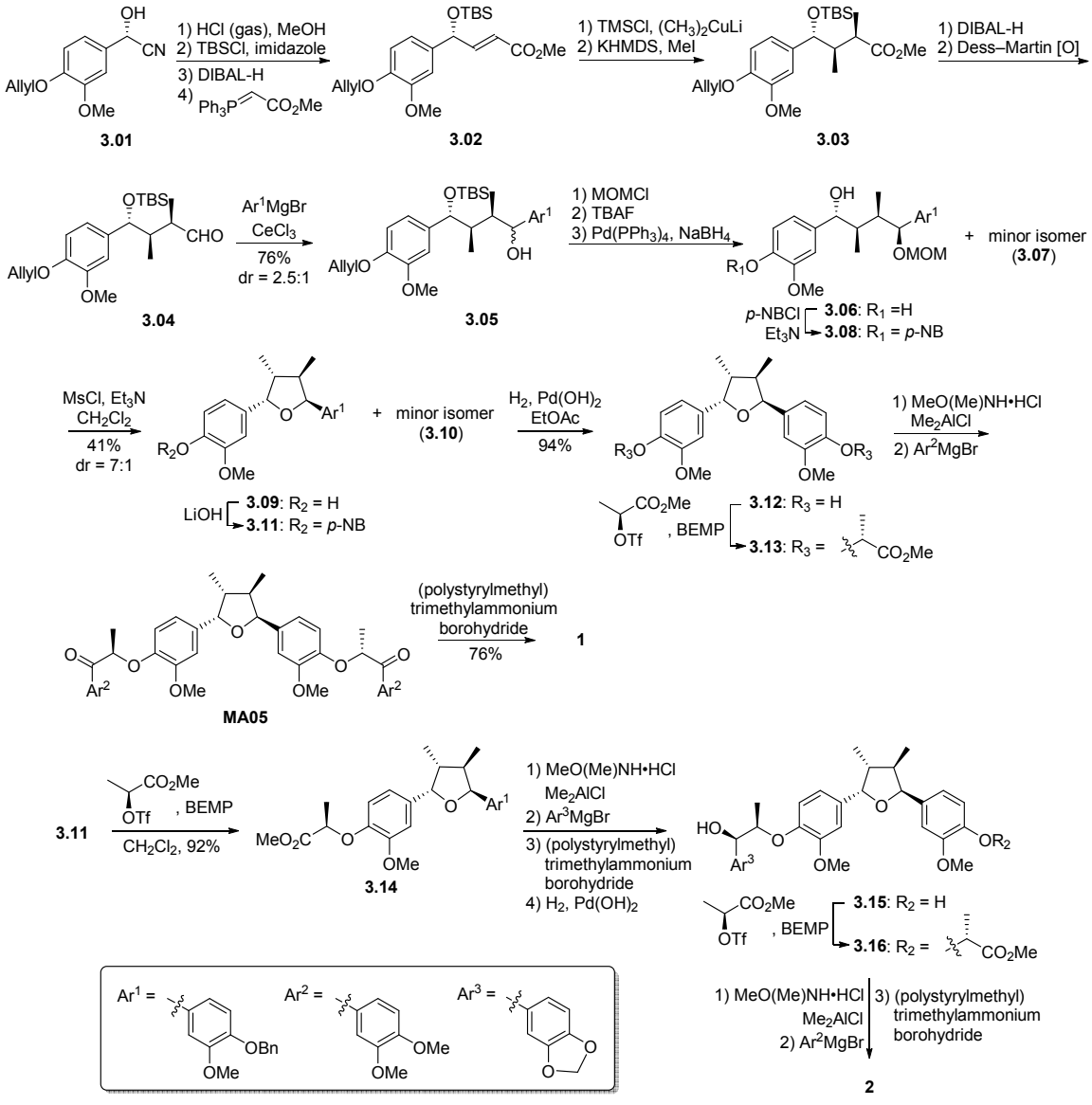

Scheme 21: Hanessian's synthesis of manassantins A and B

3.1.5.3 Hong's Synthesis of Manassantins A and B

In 2009, Hong and co-workers reported a convergent synthetic route to **1** and **2** that would be easily amenable to the development of analogues for biological studies.[108] As shown in Scheme 22, alkylation of the known **3.17**[108] with Eschenmoser's salt and *m*-CPBA oxidation, DIBAL-H reduction, and treatment with $PhSO_2H$ provided **3.19**. The addition of (4-benzyloxy-3-methoxyphenyl)zinc(II) bromide to **3.20** followed by asymmetric hydrogenation furnished **3.21** and **3.22**. Alternatively, methylation, DIBAL-H reduction, and sulfonylation of **3.17** provided **3.23**. The addition of (4-benzyloxy-3-methoxyphenyl)zinc(II) bromide to **3.23** afforded **3.21** and **3.24**. After Bn-deprotection of **3.21**, a BEMP-mediated S_N2 reaction[109-110] of **3.12** with **3.25** followed by stereocontrolled reduction using polymer-supported BH_4 completed the synthesis of **1**. In order to accomplish the synthesis of **2**, **3.12** was subjected to the BEMP-mediated S_N2 reaction with 1 eqivalent of **3.25** to form **3.26** with **MA05**. **3.26** was then subjected to a second BEMP-mediated S_N2 reaction with **3.27** to give **3.28**. Reduction of **3.28** with polymer-supported BH_4 afforded **2**.

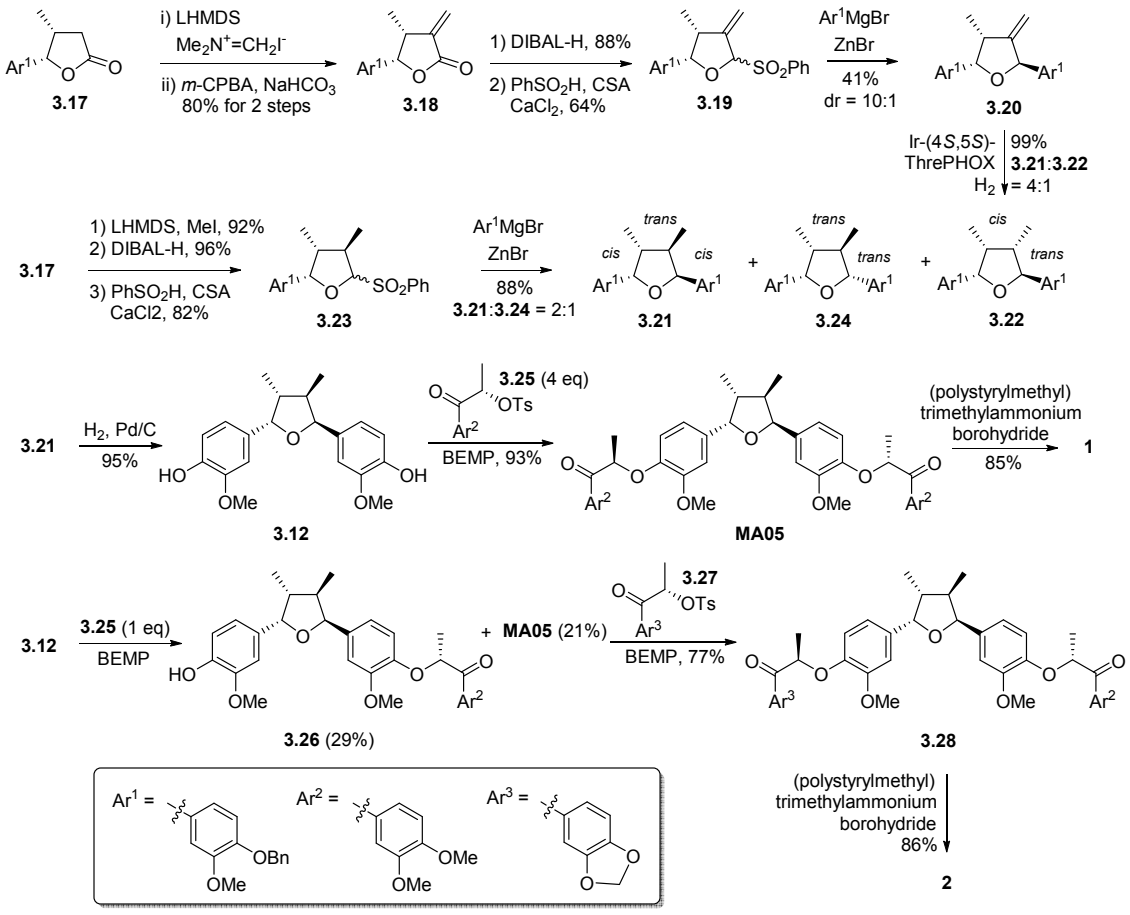

Scheme 22: Hong's synthesis of manassantins A and B

3.1.5.4 Biological Evaluation of Manassantins A and B

After completing the synthesis of **1** and **2**, the effect of these manassantins on HIF-1 and VEGF expression was determined.[108, 112] The luciferase assay of manassantin A (**1**) using 4T1/ODD-Luc cells revealed that **1** is a potent inhibitor of HIF-1 activity. Western blots of 4T1 cells exposed to **1** under hypoxic conditions showed that hypoxia-induced HIF-1 expression was significantly inhibited at concentrations between 10–100

nM (Figure 19a). In addition, the inhibition effect of HIF-1 by **1** is not cell-type specific (Figure 19b).

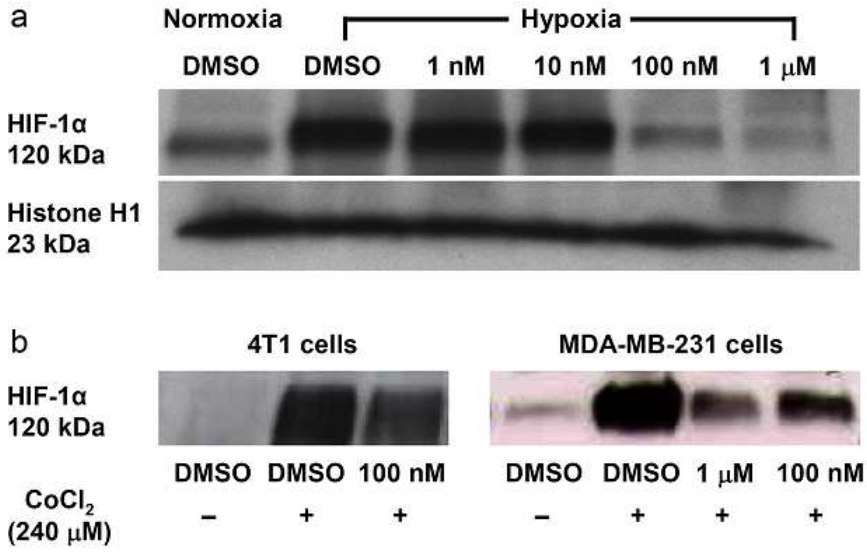

Figure 19: Inhibition of HIF-1α expression by 1[112]

Furthermore, HIF-1 regulated VEGF secretion was dramatically reduced by **1** (Figure 20). Evaluation of **1** in the National Cancer Institute's 60-Cell Line Screen30 showed that **1** possesses strong differential cytotoxicities against several breast, leukemia, and melanoma cell lines.[113]

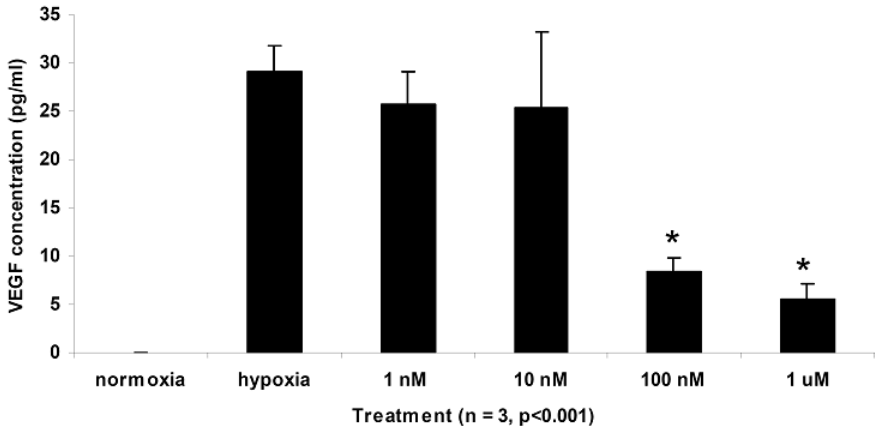

Figure 20: Inhibition of VEGF secretion by 1[112]

For preliminary SAR study of manassantins, several structurally related analogues were also synthesized and evaluated.[108, 112] ODD-Luc assay revealed that **MA05**, **1**, and *anti*-diol diastereomer ((7*S*,7′′′*S*)-epimer) **3.29** revealed that these three compounds exhibited similar levels of HIF-1 inhibitory activity (IC_{50} = 1–10 nM), suggesting that the (*R*)-configuration at C-7 and C-7′′′ is not critical for HIF-1 inhibition (Figure 21). In addition, the hydroxyl group at C-7 and C-7′′′ can be replaced with carbonyl group without significant loss of activity.

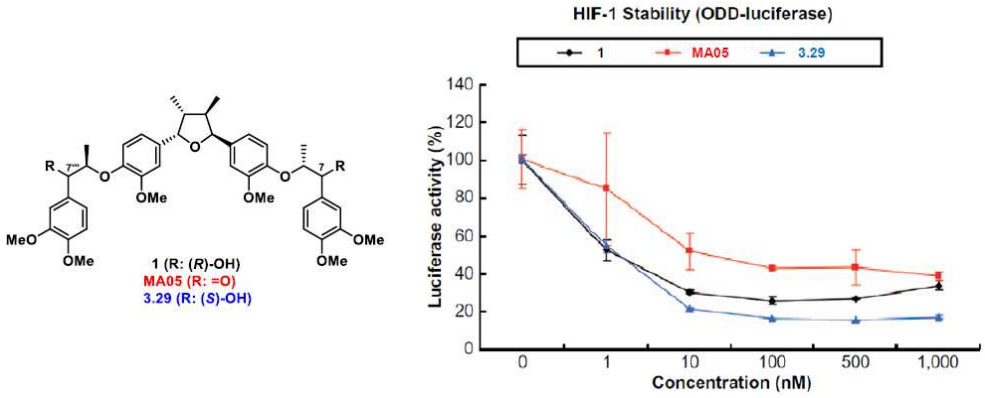

Figure 21: Inhibition of HIF-1 by 1, MA05, 3.29[108]

HIF-1 inhibitory activity of analogues with 2,3-*cis*-3,4-*trans*-4,5-*trans*- and 2,3-*trans*-3,4-*trans*-4,5-*trans*-tetrahydrofuran cores was nearly inactive and less active than **1** by 10-fold (IC_{50} = 47 nM), respectively, suggesting that the 2,3-*cis*-3,4-*trans*-4,5-*cis*-configuration of the tetrahydrofuran core is critical for HIF-1 inhibition (Figure 22).

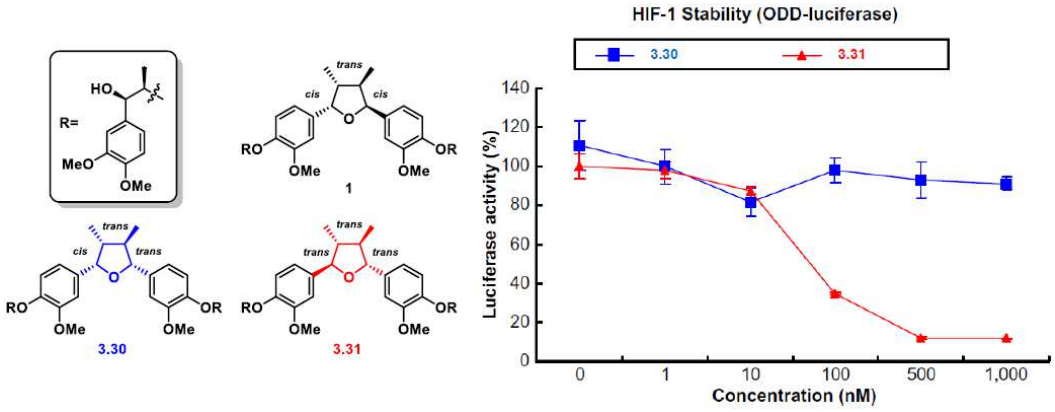

Figure 22: Inhibition of HIF-1 by 3.30 and 3.31[112]

3.2 Results and Discussion

3.2.1 SAR Plan

We investigated design and synthesis of a series of analogues based on Hong's synthesis which is easily amenable to the development of analogues for biological studies. Manassantins A and B consist of two regions (Figure 23): tetrahydrofuran core region and side chain region. Since manassantins A and B are equally potent, our SAR studies are focused on the structure of manassantin A. The 2,3-*cis*-3,4-*trans*-4,5-*cis*-configuration of the tetrahydrofuran core is critical for HIF-1 inhibition.[112] Thus, we envisioned the preparation of a series of analogues with modification of the substituents and the length of the side chains in an effort to establish a more comprehensive SAR and identify manassantin analogues with improved drug-like properties. The manassantin analogues could be easily prepared from the known tetrahydrofuran core **3.12**[108] following the convergent synthetic approach shown in Figure 23.

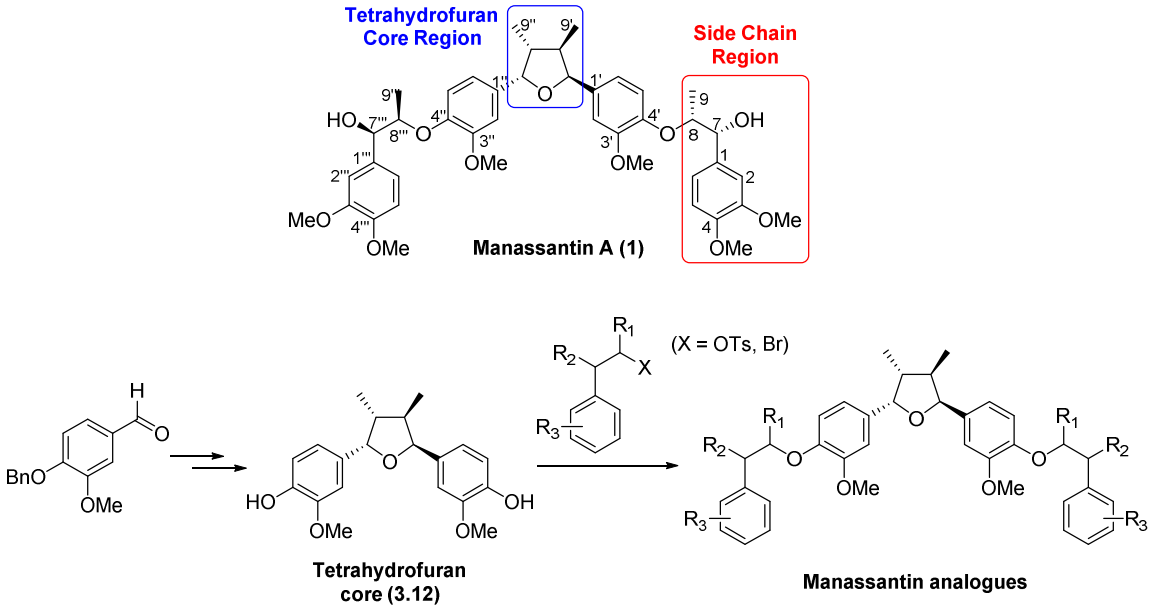

Figure 23: A convergent synthetic approach to manassantin analogues

We anticipated that SAR studies would identify structural motifs and minimal structural requirements required for HIF-1 inhibition. Such information will allow structural modifications to increase specificity, decrease off-target effects, and improve drug performance.

3.2.2 Synthesis of 1st Generation Analogues

3.2.2.1 Synthesis of Extended Chain Analogues

First, we prepared an extended side chain analogue **MA02** to gain insights into the importance of side chain length in HIF-1 inhibition. The synthesis of **MA02** started with the preparation of tosylate **3.36** and α-bromoketone **3.39** for coupling reactions

(Scheme 23). Bn-protection of the known trans-*m*-propenyl guaiacol **3.32**[114] followed by asymmetric dihydroxylation[115] of **3.33** provided diol **3.34**. Selective DDQ-oxidation of the benzylic hydroxyl group of **3.35** followed by tosylation successfully afforded **3.36**. α-Bromoketone **3.39** was prepared by treatment of the commercially available 3',4'-dimethyoxyacetophenone **3.38** with Br_2.[116] BEMP-mediated coupling of tetrahydrofuran core **3.12**[108] and tosylate **3.36** and Bn-deprotection provided **MA01** in excellent overall yield. Final coupling of **MA01** with **3.39** completed the synthesis of **MA02**. It is worthwhile to note that over-reduction of the benzylic carbonyl group in **MA01** was observed during the Bn-deprotection of **3.37**.

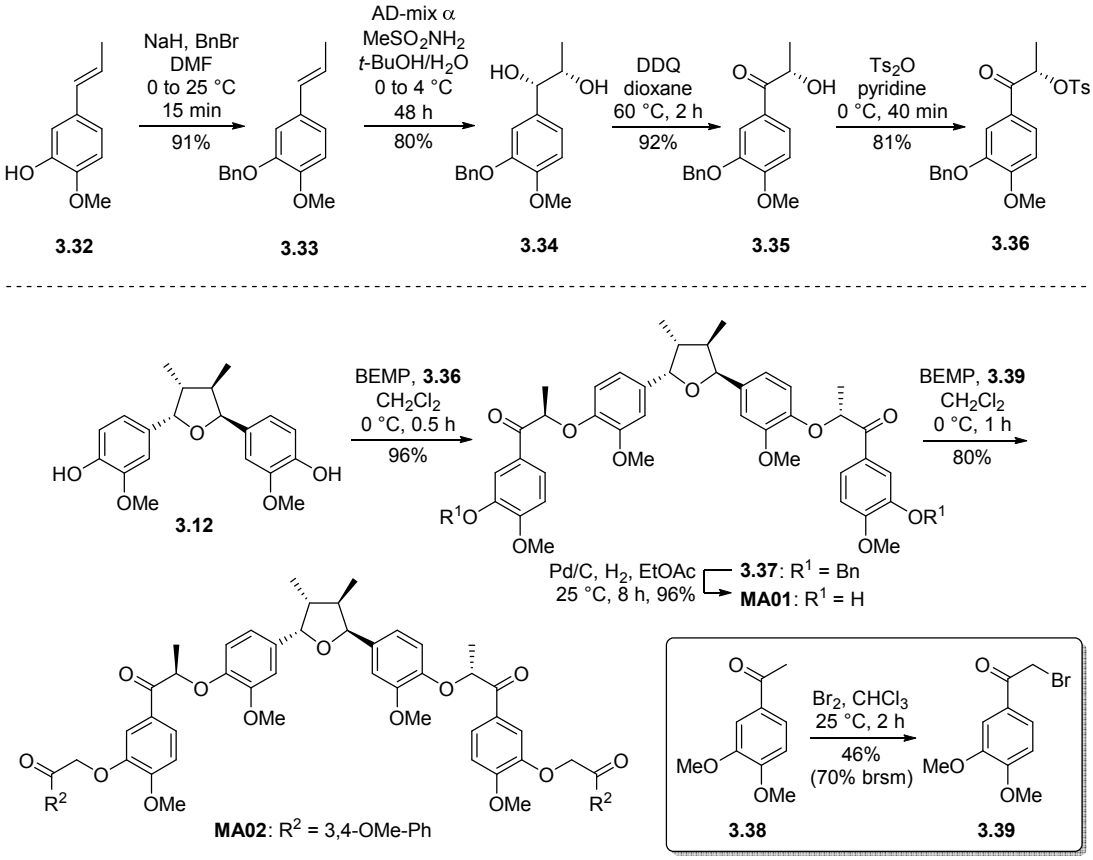

Scheme 23: Synthesis of extended analogue

3.2.2.2 Synthesis of Truncated Analogues

As shown in Scheme 24, truncated analogue **MA03** was prepared by monoalkylation of **3.12** (48%) with the known tosylate **3.25**[108] followed by methylation (K_2CO_3, MeI, 93%). Stereoselective reduction of **MA03** with polymer-supported BH_4 afforded the desired truncated analogue **MA04** in 80% yield.

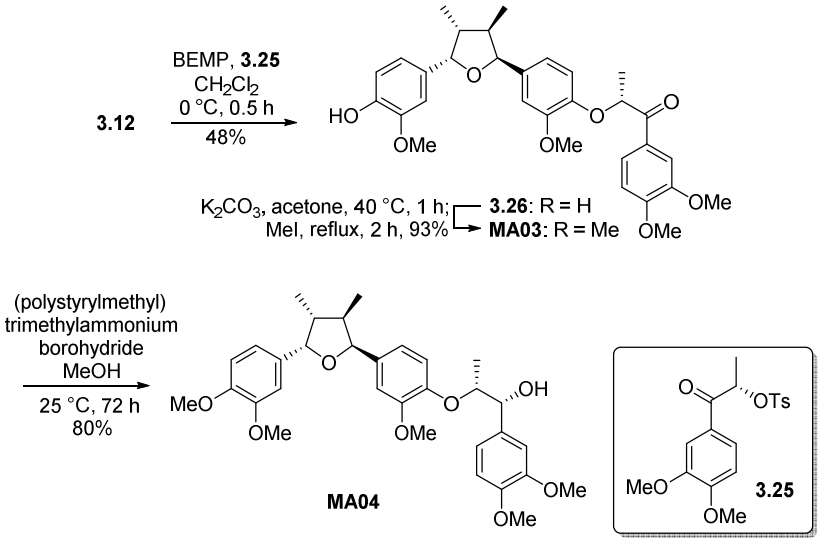

Scheme 24: Synthesis of truncated analogues

3.2.2.3 Synthesis of Keto and Methoxy Analogues

We believed that the C7 and C7''' hydroxyl groups could play an important role by providing hydrogen bonds to the binding target(s) or influencing the conformation of the side chains via intramolecular hydrogen bonds with the neighboring ether oxygen atom. To assess the role of the C7/C7''' hydroxyl groups, we synthesized the corresponding keto analogue **MA05**[108] by coupling **3.12** and **3.25** (Scheme 25). Methoxy analogue **MA06** was prepared by methylation of manassantin A (**1**) with NaH and MeI.

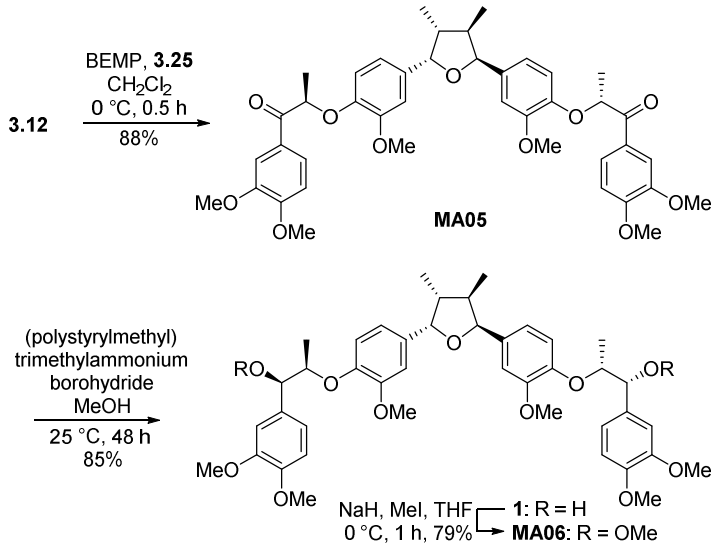

Scheme 25: Synthesis of C7/C7‴ keto and methoxy analogues

3.2.2.4 Synthesis of Desmethyl and De-oxo Analogues

To define the role of C8/C8''' methyl groups and reduce the structural complexity of manassantin side chains, we prepared C8/C8''' desmethyl analogues (**MA07–MA09**) and C8/C8''' desmethyl and C7/C7''' de-oxo analogue (**MA10**). Alkylation of tetrahydrofuran core **3.12** with α-bromoketone **3.39** (Scheme 23) provided **MA07** in modest yield (Scheme 26). Asymmetric Corey–Bakshi–Shibata reduction[117] of **MA07** afforded **MA08** as a single diastereomer, which was further converted to **MA09** by methylation with NaH and MeI. To further reduce the complexity of manassantins, we removed both C8/C8''' methyl and C7/C7''' hydroxyl groups. We prepared **MA10** by coupling **3.12** with the commercially available 4-(2-bromoethyl)-veratrole **3.40**. In addition to reducing the structural complexity, removal of the benzylic hydroxyl groups

would reduce the number of hydrogen-bonding donors and influence PK/PD parameters by improving permeability and absorption, and removing the potential metabolism site (phase-2 conjugation).[118]

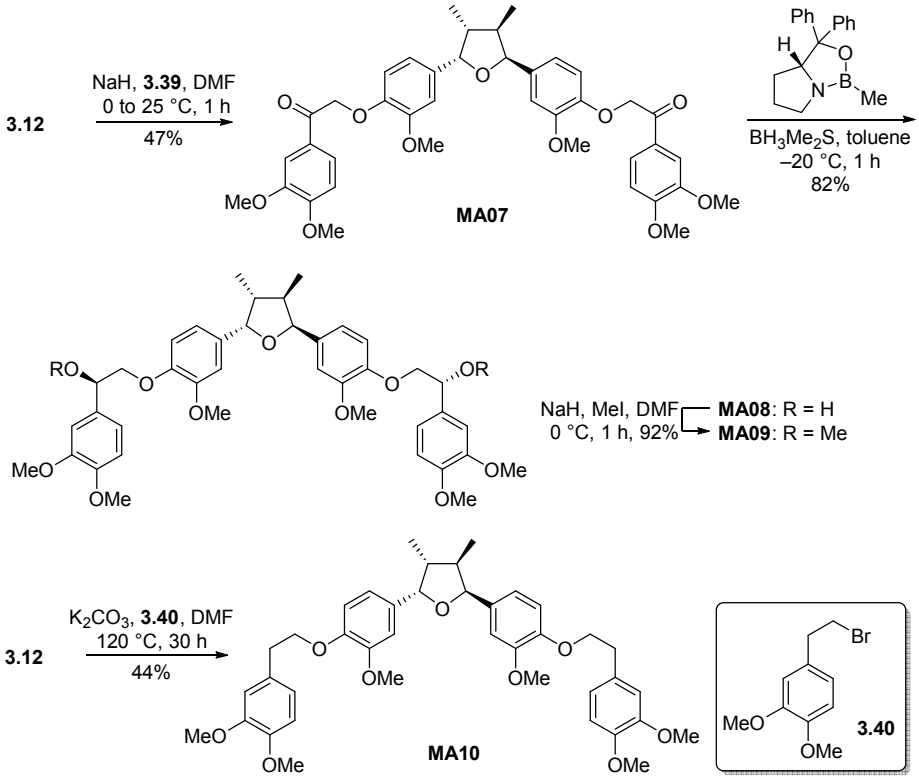

Scheme 26: Synthesis of C8/C8‴ desmethyl and C7/C7‴ de-oxo analogues

3.2.2.5 Synthesis of Hydroxy and Phenyl Analogues

Previously, it was reported that a reduction in potency was observed with the replacement of the C4 methoxy group in the distal phenyl rings of manassantins A (**1**) and B (**2**) with a hydroxyl group as in 4-*O*-demethylmanassantin B (**3**).[107c] To characterize the role of the methoxy groups on the distal phenyl rings, we prepared C3/C3''' hydroxy

analogue **MA01** (the intermediate to **MA02**, Scheme 23) and phenyl analogues **MA11** and **MA12** (Scheme 27). Asymmetric dihydroxylation of the commercially available (*E*)-1-propenyl-benzene **3.41** provided diol **3.42**. Selective DDQ oxidation of the benzylic hydroxyl group of **3.43** followed by tosylation smoothly proceeded to afford tosylate **3.44**. BEMP-mediated coupling of **3.12** with **3.44** successfully provided **MA11**, which was reduced stereoselectively to give **MA12**.

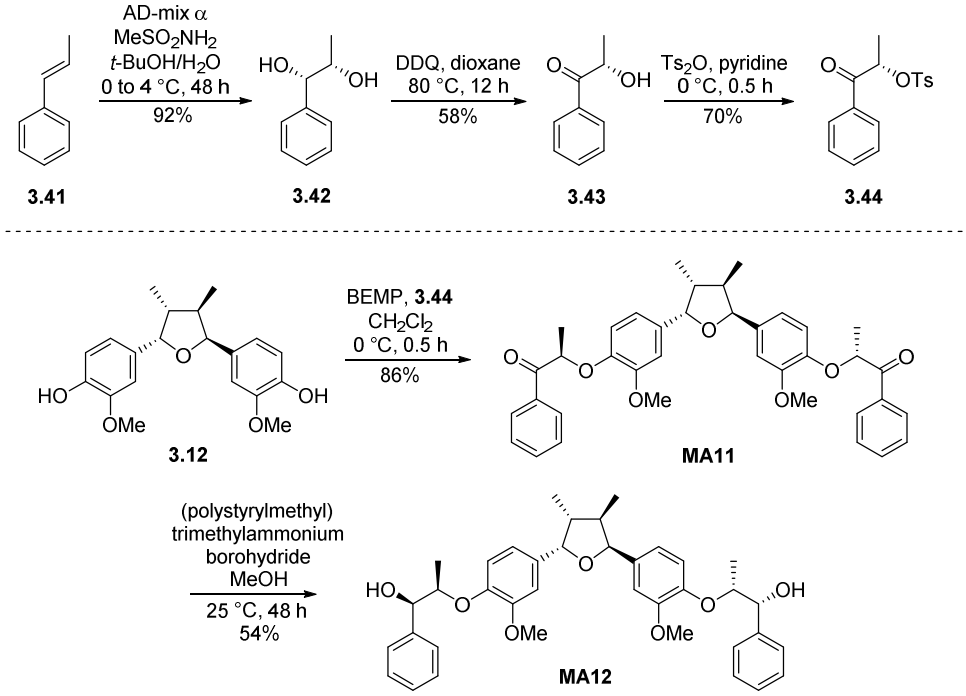

Scheme 27: Synthesis of phenyl analogues

3.2.3 Biological Evaluation of 1st Generation Analogues

After the completion of the analogue synthesis, we performed a HIF-1 luciferase-reporter assay to assess the effect of **MA01–MA12** (Figure 24) on HIF-1 activity (Figure

25). The luciferase assay was achieved by our collaborator, the Lee group at Kyungpook National University in South Korea.

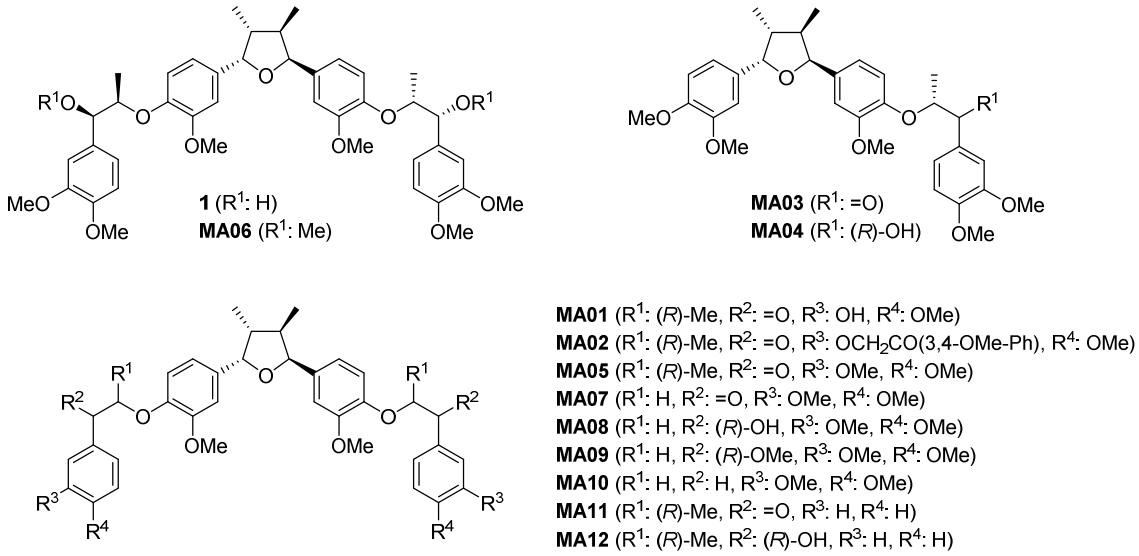

Figure 24: Structure of manassantin analogues (MA10–MA12)

The luciferase-reporter assays were used as initial *in vitro* tests to identify active compounds for further evaluation. The assay was performed with HEK-293T cells transiently transfected with both pGL3-5HRE-Luc (pGL3-HRE-Luc) and pRL-SV40 encoding Renilla-luciferase (pRen-Luc) vectors to investigate the effect of manassantin analogues (**MA01–MA12**) on HIF-1 transactivation activity (Figure 25).

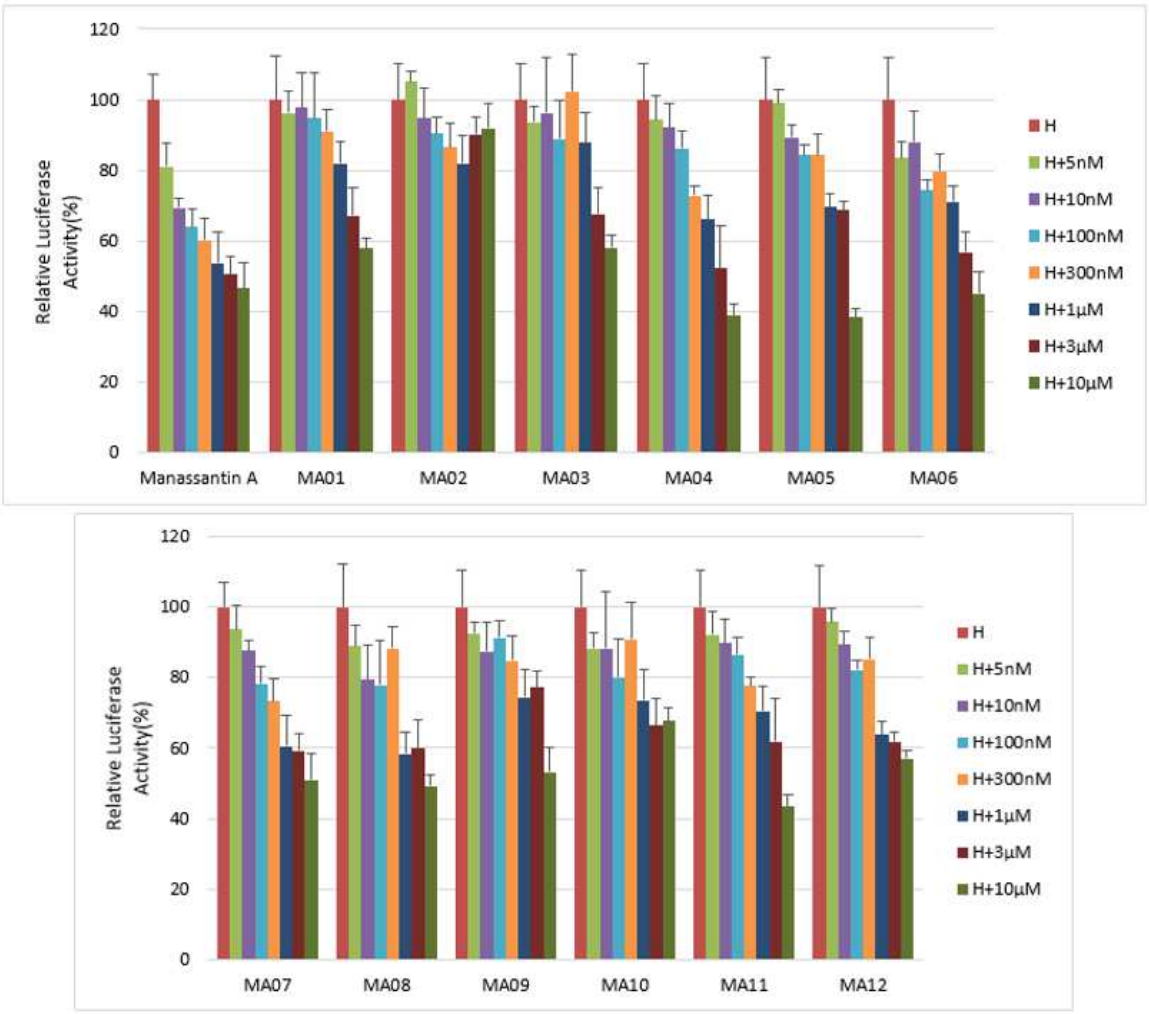

Figure 25: Manassantin analoges (MA01–MA12) suppress hypoxia-induced reporter gene activity in HEK-293T cells (H: hypoxia). After 24-hour incubation, HEK-293 cells were treated with hypoxia (1% O_2) and serially diluted compounds (MA01–MA12) for 24 h. To measure the firefly luminescence signals, Dual-Glo® reagent was added and the luminescence signals were measured by using a dual-color luminescence detection system. Luciferase expression/activity was detected, normalized to the activity of Renilla luciferase and quantified as relative luciferase units (RLUs). Data are mean values of three independent experiments.

We generated a reporter vector, pGL3-hypoxia-responsive element (HRE)-luciferase plasmid containing five copies of HRE sequences identical to that in the

human VEGF promoter gene. HEK-293T cells were seeded in a 96-well plate at a density of 5×10^3 cells/well. After 24-hour incubation, cells were treated with hypoxia (1% O_2) and serially diluted compounds (**MA01–MA12)** for 24 h. To measure the firefly luminescence signals, Dual-Glo® reagent was added and the luminescence signals were measured by using a dual-color luminescence detection system. Luciferase expression/activity was detected, normalized to the activity of Renilla luciferase and quantified as relative luciferase units (RLUs). Data are mean values of three independent experiments. We also obtained IC_{50} of the analogues based on the luciferase assay results (Table 4).

Table 4: IC_{50} values of manassantin A (1) and analogues MA01–MA12

Compound	IC_{50} (nM)
1	11
MA01	1934
MA02	>10000
MA03	2632
MA04	331
MA05	742
MA06	399
MA07	253
MA08	428
MA09	1660
MA10	1440
MA11	561
MA12	589

The luciferase assay provided several valuable insights into SAR. First, the extended analogue **MA02** was significantly less potent than manassantin A (**1**). This data demonstrated the importance of the length of the side chains of manassantins in HIF-1 inhibitory activity. To our surprise, **MA04** (4-*O*-methylsaucerneol), which was one of the truncated analogues we prepared, was less potent than **1**, but it still showed a good potency. Originally, Zhou and co-workers reported that a dramatic effect was observed with the absence of one side chain phenylpropyl unit, as in 4-*O*-methylsaucerneol.[107c] Although **MA04** possesses a lower potency relative to **1**, its simplified structure increases the ligand efficiency, which is a very important metric in lead selection.[119] Analogues with the C7/C7''' keto groups (**MA03**, **MA05**) showed lower activities than analogues with hydroxyl groups at the same positions (**MA03** vs **MA04**, **MA05** vs **1**), suggesting that the C7/C7''' hydroxyl groups are critical for the HIF-1 inhibitory activity of **1**. In addition, methylation of the C7/C7''' hydroxyl groups significantly reduced the potency (**MA06** vs **1**, **MA09** vs **MA08**), confirming the importance of these hydroxyl groups of manassantins in HIF-1 inhibition. Removal of C9/C9''' methyl groups also reduced the activity of the analogues (**MA08** vs **1**, **MA09** vs **MA06**). However, **MA07** showed a good potency. **MA07** possesses a reduced structural complexity by removing the C9/C9''' methyl groups and replacing the C7/C7''' hydroxyl groups with carbonyl groups, which enables more simplified synthesis. Interestingly, the analogues **MA11** and **MA12** with phenyl substituents showed a good potency, suggesting that removal of

both of the methoxy groups in the distal phenyl rings does not significantly affect the activity. Given methoxy groups can be metabolically labile,[120] this result is noteworthy because it provides SAR evidence to guide optimization of PK parameters.

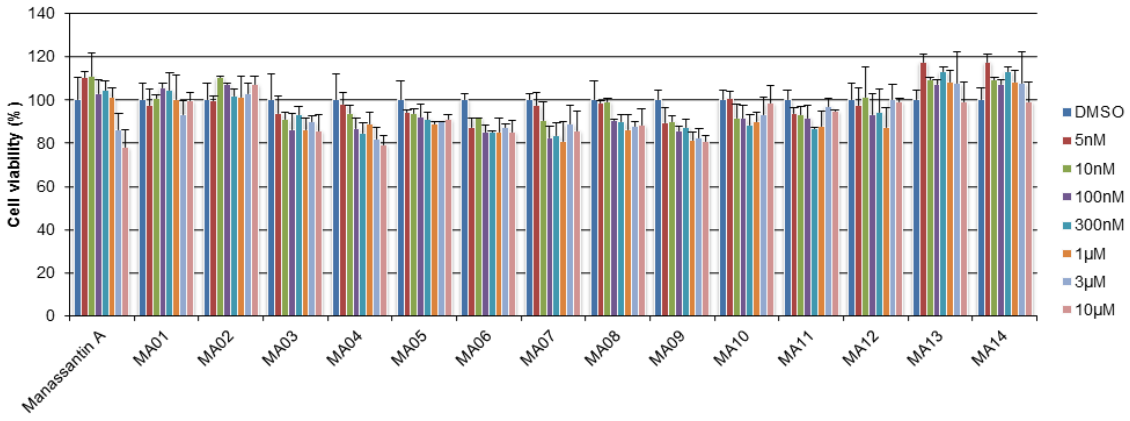

Figure 26: Effects of manassantin A and its analogues on cell viability (HEK-293T) in the MTT assay. HEK-293T cells were seeded in a 96-well plate and treated with serially diluted MA01–MA12 (0.005–10 μM) for 24 h. After 24-hour treatment, cells were washed with PBS and MTS/PMS were added. The absorbance of the formazan was detected at 490 nm.

General toxicity of manassantin analogues was examined using the MTT assay, a standard colorimetric cytotoxicity assay (Figure 26). The MTT assay was also accomplished by our collaborator, the Lee group at Kyungpook National University in South Korea. HEK-293T cells were seeded in a 96-well plate and treated with serially diluted **MA01–MA12** (0.005–10 μM) for 24 h. After 24-hour treatment, cells were washed with PBS and MTS/PMS were added following manufacturer's protocol. The absorbance of the formazan was detected at 490 nm. The MTT assay results revealed that manassantin A (**1**) and analogues **MA01–MA12** exhibited relatively low general

toxicities. Up to the highest concentration examined (10 μM), cells had > ~80 % survival rate in HEK-293T.

Following the initial luciferase assays, we used Western blots to further examine the down-regulation of HIF-1α by manassantin analogues. We selected a subset of manassantin analogues (**MA04**, **MA07**, and **MA11**) based on their potency (from luciferase-reporter based assay) and general toxicity (from MTT assay). The Western blots were also achieved by our collaborator, the Lee group at Kyungpook National University in South Korea. After incubating HEK-293T cells under hypoxia (1% O_2) for 24 h with or without compounds (1 μM), total protein lysate was extracted. Western blots were performed following the standard procedures. The expression levels of HIF-1α, HIF-1β, and Cdk6 were determined with β-actin as an internal control.

The Western blot analysis revealed that compounds **1**, **MA04**, **MA07**, and **MA11** significantly downregulated the expression level of HIF-1α in HEK-293T cells under hypoxia (Figure 27). To determine whether **1**, **MA04**, **MA07**, or **MA11** regulates HIF-1β, a transcription partner of HIF-1α, we performed western blot analysis with antibody against HIF-1β. Compounds **1**, **MA04**, **MA07**, and **MA11** did not regulate HIF-1β, suggesting that **1**, **MA04**, **MA07**, and **MA11** regulate HIF-1α, but not HIF-1β. The expression level of cyclin-dependent kinase 6 (Cdk6), which is a HIF-1 target molecule and regulates cell cycle progression, was also inhibited by **1**, **MA04**, **MA07**, and **MA11**.

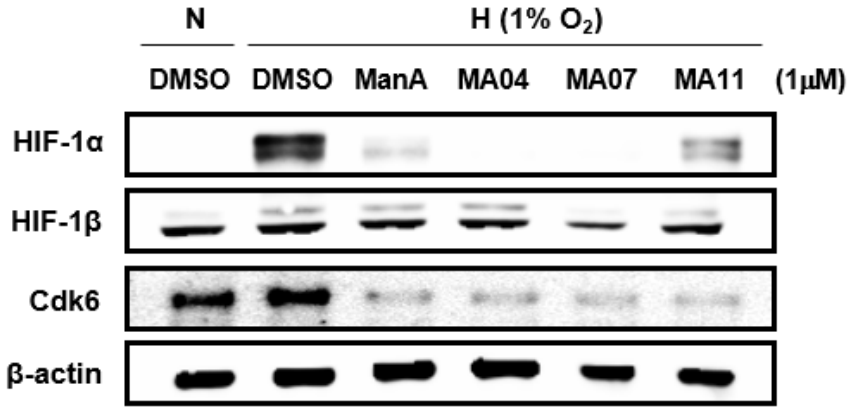

Figure 27: Manassantin A (1), MA04, MA07, and MA11 inhibit the expression of hypoxia induced HIF-1α and Cdk6 (N: normoxia, H: hypoxia). After incubating HEK-293T cells under hypoxia (1% O_2) for 24 h with or without compounds (1 μM), total protein lysate was extracted. The expression levels of HIF-1α, HIF-1β, and Cdk6 were determined by Western blot analysis with β-actin as an internal control.

Next, we examined the effect of these four compounds on the expression level of VEGF, which is a key angiogenic factor and a main target for HIF-1, to further confirm their effect on HIF-1 activity. Relative expression of VEGF mRNA was determined by real-time PCR after treatment of cells with compounds (**1**, **MA04**, **MA07**, and **MA11**) under hypoxic conditions for 24 h. Relative expression of VEGF was normalized against β-actin. Upon treatment of **1**, **MA04**, **MA07**, or **MA11** (1μM), VEGF was decreased under hypoxic conditions at the mRNA level, confirming the effect of **1**, **MA04**, **MA07**, and **MA11** on HIF-1 activity (Figure 28).

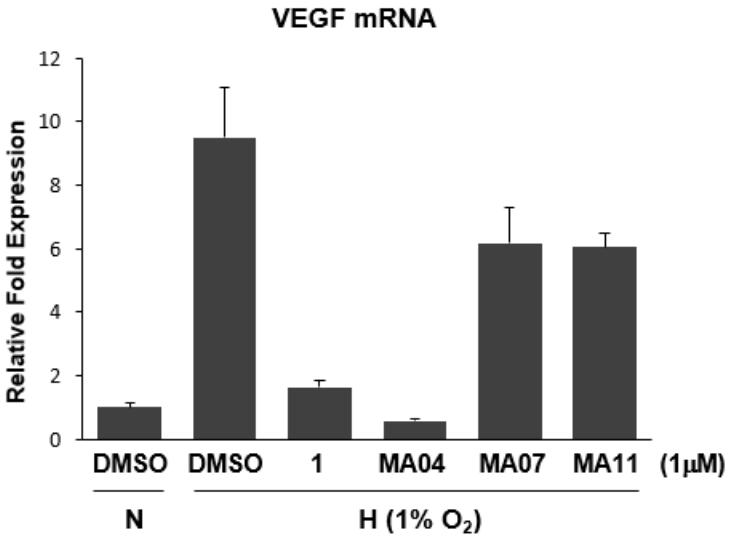

Figure 28: Manassantin A (1), MA04, MA07, and MA11 inhibit VEGF at the mRNA level (N: normoxia, H: hypoxia). Relative expression of VEGF mRNA was determined by real-time PCR after treatment of cells with compounds (1, MA04, MA07, and MA11) under hypoxic conditions for 24 h. Relative expression of VEGF was normalized against β-actin.

All together, these data demonstrate that **1**, **MA04**, **MA07**, and **MA11** are highly potent inhibitors of HIF-1 activity as well as potential lead compounds for future *in vivo* animal and preclinical studies for anticancer drug development.

3.2.4 Synthesis of 2nd Generation Analogues

3.2.4.1 Bioisosterism

Bioisosteres are chemical substituents or groups with similar physical or chemical properties which produce broadly similar biological properties to another chemical compound.[121] The purpose of exchanging one bioisostere for another is to

enhance the desired biological or physical properties of a compound without making significant changes in chemical structure.[122] In medicinal chemistry, bioisosteric replacements are used for many reasons: greater selectivity for a determined receptor or enzymatic isoform subtype, fewer undesirable side effects and decreased toxicity, increased metabolic stability, simplified synthesis, and improved pharmacokinetics.

The success of this strategy in developing new compounds that are used by the pharmaceutical industry has been observed (Figure 29). 5-Substituted tetrazole is the most popular bioisostere for the carboxylic acid.[123] Tetrazole contains an acidic proton and its anion is 10 times more lipophilic than a carboxylic acid, which can enhance absorption of a drug. The replacement of the carboxylic acid in EXP7711 with tetrazole ring led to losartan, an antihypertensive agent, with good absorption.[121, 124] A H_1-antagonist carbinoxamine was developed from diphenhydramine by replacement of benzene with pyridine and substitution of hydrogen with chlorine.[125] One example of the bioisosteric replacement to optimize PK/PD properties of drugs can be found in chlorpropamide.[126] The chlorine in chlorpropamide can block metabolic oxidation and may have a longer half-life than that of tolbutamide. Substitution of hydrogen with fluorine is one of the most common isosteric replacements because these two atoms are sterically quite similar.[127] With the strongest electronegativity of fluorine, replacement of hydrogen with flourine alters the biological activity. One representative example is the development of an anticancer drug, 5-flurouracil from uracil.[128] The increased reactivity

of 5-fluorouracil is due to the inductive effect of fluorine which results in its covalent binding to thymidylate synthase and inhibition of the enzyme activity. Thymidylate synthase is an enzyme involved in the conversion of uridylic acid to thymidylic acid and critical for DNA synthesis. The use of ring bioisosterism of celecoxib, a non-steroidal anti-inflammatory drug (NSAID), resulted in analogues with retention of its activity.[121]

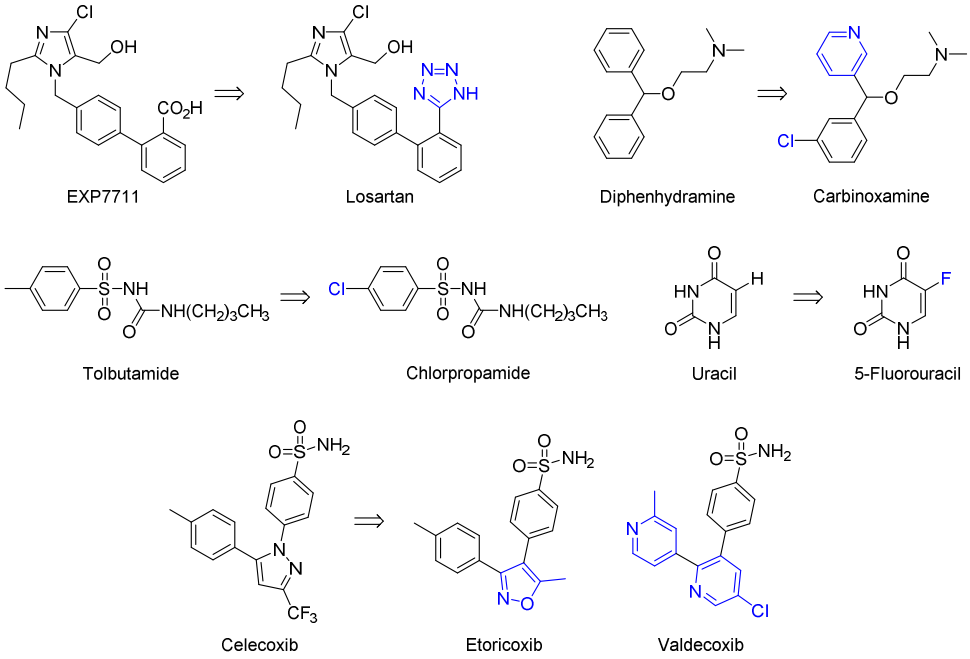

Figure 29: Therapeutic agents from the successful bioisosteric replacements

Manassantin A (**1**) possesses the potency at cellular level (IC_{50} 10–100 nM) which is already in a clinically relevant range. Because its molecular target is unknown, structure-based drug design is not feasible. Thus, we used the bioisosterism strategy to guide the design and synthesis of 2nd generation analogues to improve drug-like properties. Despite its potent activity, **1** has some potential negative factors in terms of

druglikeness such as large molecular weight, high log P, high number of rotatable bonds, and potential metabolic sites. Therefore, we tried to synthesize analogues with reduced molecular weight, enhanced hydrophilicity, reduced number of rotatable bonds, and reduced number of metabolic sites. In the subsequent sections, synthesis of 2nd generation analogues with the bioisosteric replacements will be described. Truncation of one of side chains did not result in a significant loss of activity, leading us to prepare 2nd generation analogues not only in the symmetrical forms but also in the truncated forms.

3.2.4.2 Synthesis of 4-Chloro-3-methoxyphenyl Analogues

The aromatic rings with electron-donating methoxy groups in **1** is potential phase-1 metabolic sites. Thus, we prepared 4-chloro-3-methoxyphenyl analogues in which methoxy group is substituted with chloride at C4 and/or C4''' to assess the effect of this substitution on HIF-1 inhibitory activity (Scheme 28). The synthesis of these analogues started with the preparation of tosylate **3.49** for coupling reaction. Wittig reaction and isomerization of the commercially available aldehyde **3.45** followed by asymmetric dihydroxylation of **3.46** provided diol **3.47**. Selective DDQ-oxidation of the benzylic hydroxyl group of **3.47** followed by tosylation successfully afforded **3.49**. BEMP-mediated coupling of tetrahydrofuran core **3.12** and tosylate **3.49** provided mono-

alkylated product **3.50** and bis-alkylated product **3.51**, which was further methylated and reduced stereoselectively to give **3.52** and **3.53**, respectively.

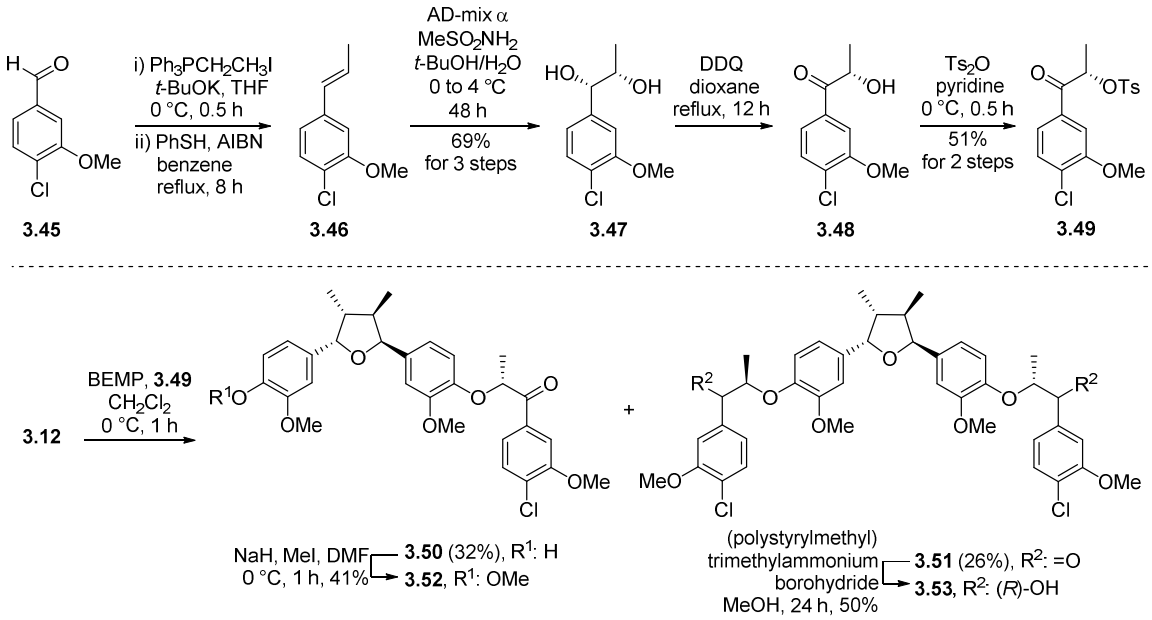

Scheme 28: Synthesis of 4-chloro-3-methoxyphenyl analogues

3.2.4.3 Synthesis of 6-Methoxypyridine Analogues

Ring bioisosterism is the most frequent relationship in drugs of different therapeutic classes.[121] We expect that the replacement of benzene rings in **1** with pyridines would make the compounds more hydrophilic, which can create more drug-like analogues. To assess the effect of this replacement on HIF-1 inhibitory activity, 6-methoxypyridine analogues were prepared as shown in Scheme 29. The commercially aldehyde **3.54** was converted to diol **3.56** through Wittig reaction, isomerization, and asymmetric dihydroxylation. Selective DDQ-oxidation of the benzylic hydroxyl group of

3.56 followed by tosylation afforded **3.58**. BEMP-mediated coupling of tetrahydrofuran core **3.12** and tosylate **3.58** provided mono-alkylated product **3.59** and bis-alkylated product **3.60**, which was further methylated and reduced to give **3.61** and **3.62**, respectively. Due to the difficulty in separation, analogue **3.62** was obtained in a diastereomeric mixture (dr = 6.4:1).

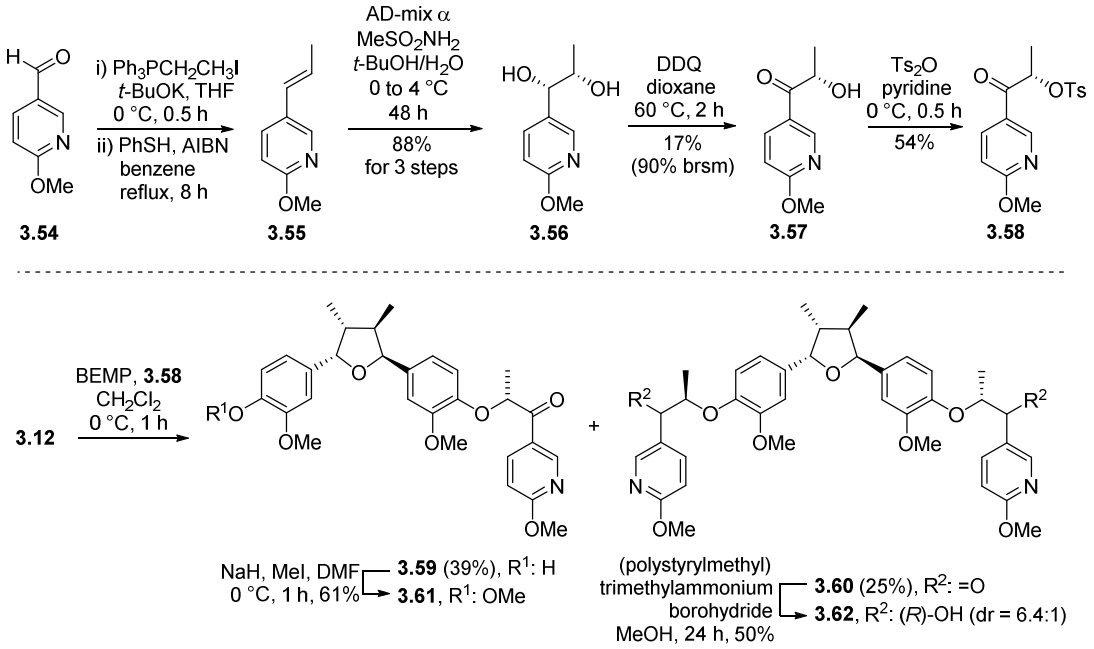

Scheme 29: Synthesis of 6-methoxypyridine analogues

3.2.4.4 Synthesis of 2-Methoxypyridine Analogues

To examine the effect of the position of substituent in methoxypyridine analogues on HIF-1 inhibitory activity, we also prepared 2-methoxypyridine analogues (Scheme 30). The commercially available aldehyde **3.63** was converted to diol **3.65** through Wittig reaction, isomerization, and asymmetric dihydroxylation. We usually

used DDQ-oxidation as a conventional method for selective oxidation of benzylic hydroxyl group. However, no reaction occurred in **3.65** even after reflux. Despite several oxidation conditions were applied to obtain hydroxy ketone **3.66**, only side products or a small amount of **3.66** were obtained. Thus, we decided to attempt tosylation of diol first, and then oxidation of benzylic hydroxyl group in **3.69**. With this strategy, diol **3.65** was subjected to tosylation with 0.75 equivalent of tosyl anhydride to form **3.69**, which was oxidized to provide **3.70**. BEMP-mediated coupling of tetrahydrofuran core **3.12** and tosylate **3.70** provided mono-alkylated product **3.71** and bis-alkylated product **3.72**, which was further methylated and reduced stereoselectively to give **3.73** and **3.74**, respectively.

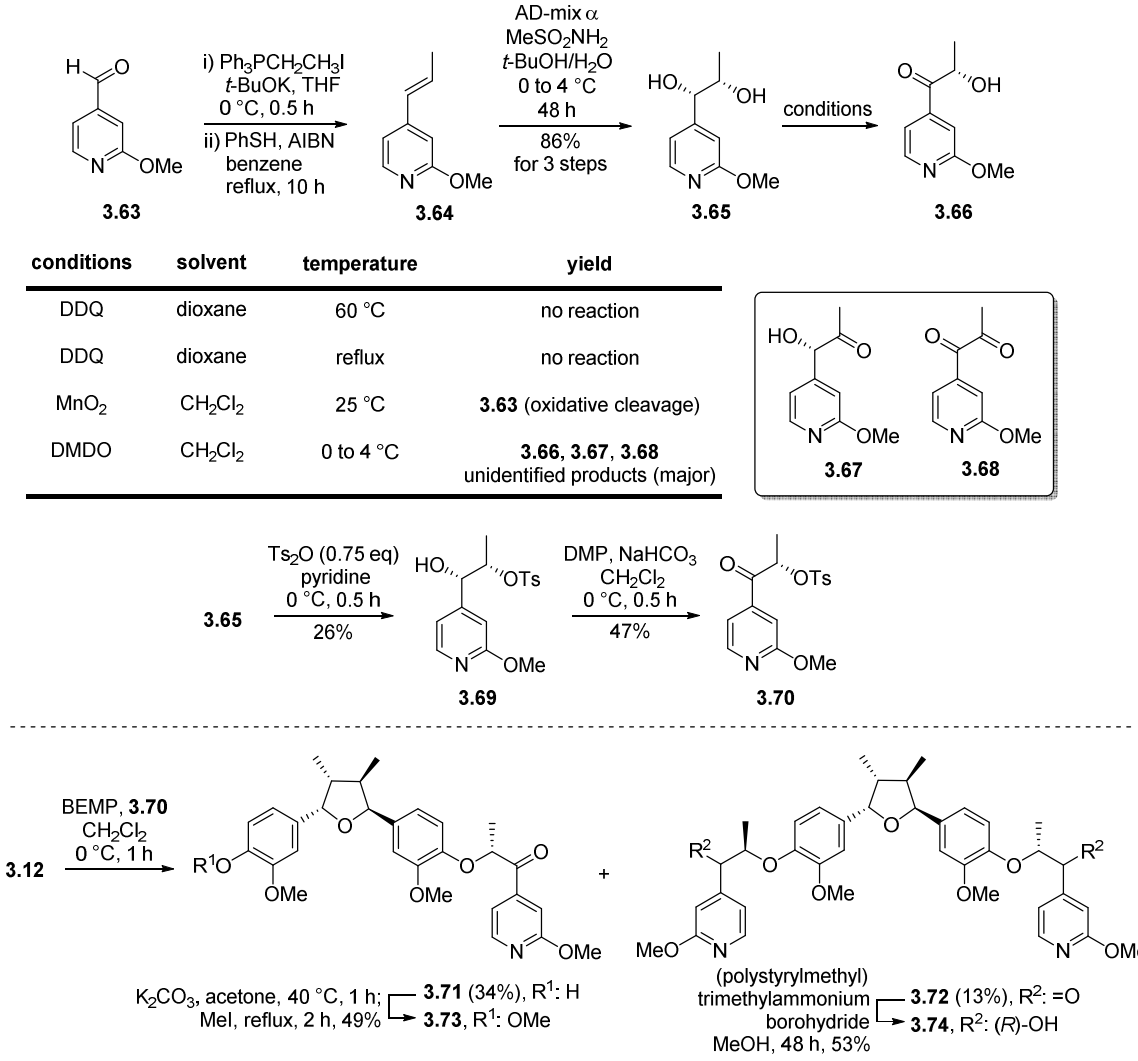

Scheme 30: Synthesis of 6-methoxypyridine analogues

3.2.4.5 Synthesis of 2-Methylpyridine Analogues

To assess the effect of replacement of methoxy group with methyl group, we prepared 2-methylpyridine analogues (Scheme 31). Wittig reaction and isomerization of the commercially available aldehyde **3.75** followed by asymmetric hydroxylation

provided diol **3.77**. Similar to the synthesis of 2-methoxypyridine analogues, **3.77** was subjected to tosylation with 1.2 equivalent of tosyl anhydride followed by oxidation to give **3.82**. BEMP-mediated coupling of tetrahydrofuran core **3.12** and tosylate **3.82** provided mono-alkylated product **3.83** and bis-alkylated product **3.84**, which was further methylated and reduced stereoselectively to give **3.85** and **3.86**, respectively. Due to the difficulty in separation, analogue **3.86** was obtained in a diastereomeric mixture (dr = 6.5:1).

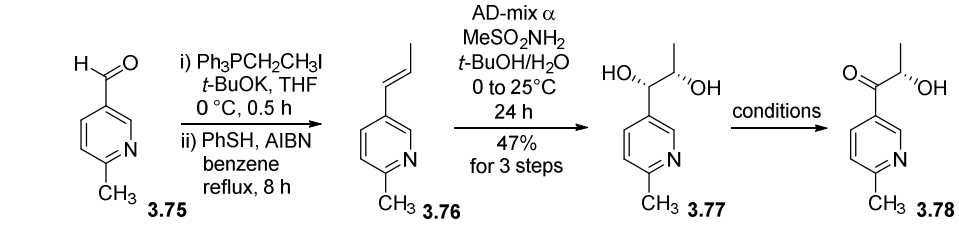

conditions	solvent	temperature	yield
DDQ	dioxane	60 °C	no reaction
DDQ	dioxane	reflux	no reaction
MnO_2	CH_2Cl_2	25 °C	**3.75** (oxidative cleavage)
DMDO	CH_2Cl_2	0 to 4 °C	**3.78**, **3.79**, **3.80** unidentified products (major)

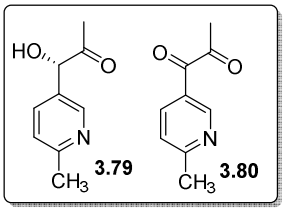

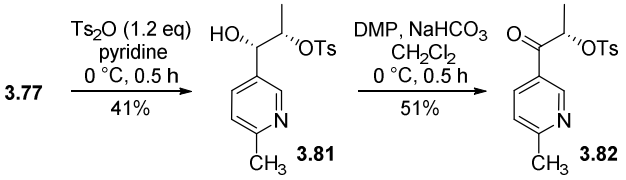

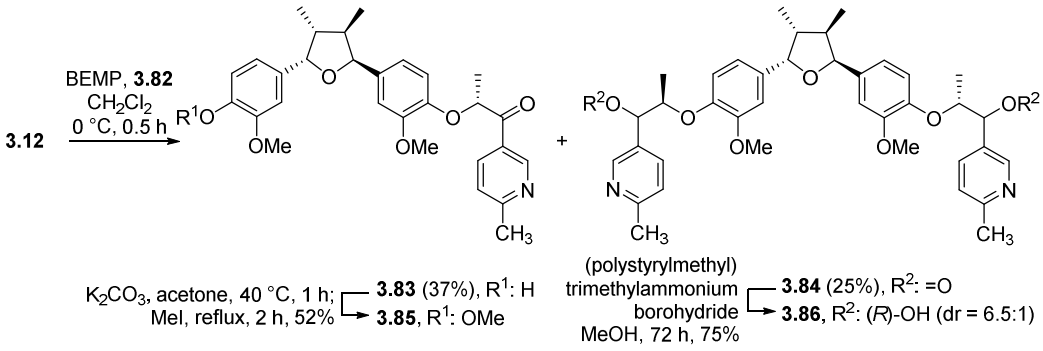

Scheme 31: Synthesis of 2-methylpyridine analogues

In summary, we have designed and prepared the 2nd generation analogues using the bioisosterism strategy to improve drug-like properties of analogues. The evaluation of the effect of these analogues on HIF-1 activity is in progress.

3.2.5 Development of Photoactivable Probes

3.2.5.1 Photoaffinity Labeling (PAL)

Despite a variety of target identification techniques introduced to date, small molecule affinity chromatography is the most widely used method.[129] This approach have led to the discovery of important drug targets. In particular, the approach can be very effective when a probe possesses a photo cross-linking group to form a covalent linkage to its target proteins.

Photoaffinity labeling (PAL) was initiated using diazocarbonyl derivatives in 1962[130] and it is a powerful tool for investigating ligand–receptor interaction. In this technique, ligands possessing photoactivable group (photophore) are irradiated with UV light after the formation of the ligand–receptor complex. Photolysis results in the creation of highly reactive intermediate, which form covalent bonds with receptor proteins at their binding site (Figure 30).

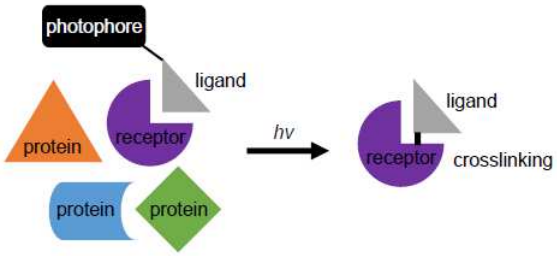

Figure 30: Schematic representation of photoaffinity labeling

PAL studies focus on how to design an efficient photoactivable probe satisfying following requirements. Strong and specific binding with a target protein, high

photospecificity to allow the efficient formation of a covalent bond between the ligand and its target protein, and high sensitivity of detection. In particular, benzophenones, aromatic azides, aliphatic and aromatic diazirines have been widely used as photophores in photoaffinity labeling (Figure 31). Each of these groups possesses advantages and disadvantages. A major drawback of aryl azides is that their maximum absorption wavelength is <300 nM, which can cause substantial damage to the biomolecules. However, aryl azides are relatively small, and can be easily prepared and incorporated into a ligand. In contrast, benzophenones are typically excited at 350–360 nm, therefore no significant damage to the biological system is expected. Furthermore, they are commercially available and commonly used building blocks. However, benzophenones are notoriously bulky functional groups, which could prevent proper interactions between the photoactivable probe and its biological targets. Finally, diazirines are photoactivated at 350–380 nm (i.e., similar to benzophenones). In addition, diazirines are stable to a wide range of chemical conditions including strong basic, strong acidic, oxidizing, and reducing agents. Nevertheless, one disadvantage of diazirines is that their syntheses can be somewhat lengthy and complicated. It has been reported that the photolysis of diazirines can cause diazo isomerization, providing undesired intermediates in PAL. Diazo isomerization can be suppressed by introduction of a trifluoromethyl group into a diazirinyl ring.[131]

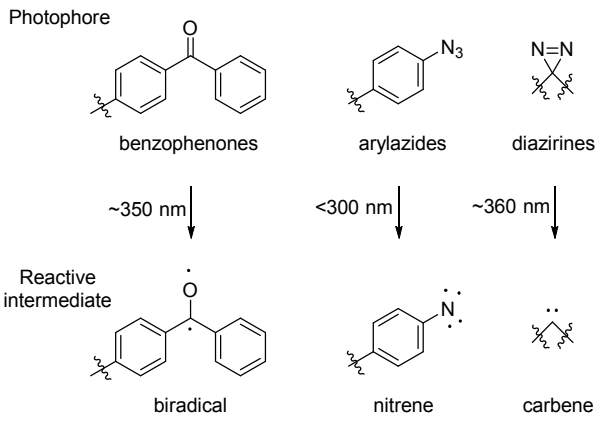

Figure 31: Three types of photoreactive groups and their reactive intermediates

In order to facilitate the isolation of photolabeled products, reporter groups such as radioactive isotopes (e.g., ^{125}I, ^{3}H), biotin, epitope tags (e.g., FLAG peptide), or fluorophores are often directly incorporated into the photoactivable probe.[132] Radioactive tags are advantageous because they are relatively small in size, highly sensitive, and easy to detect. However, radioactive tags are harmful, undergo relatively fast degradation, and require special handling. Biotin, epitope tags, and flurophores allow easy enrichment, isolation, and/or detection of photolabeled products. However, they are relatively large in size, cell impermeable, and may negatively affect biological activity by sterically disrupting key interactions between the photoactivable probe and its biological targets.

To address these advantages, photoactivable probes are synthesized containing either a terminal alkyne or aliphatic azide as a clickable handle.[133] Following covalent bond formation between the ligand and its target via photoirradiation, bioorthogonal

conjugation reactions such as the Staudinger-Bertozzi ligation[134] or copper catalyzed Huisgen 1,3-dipolar cycloaddition (click reaction)[135] are used to attach a tag specifically to the aliphatic azide or terminal alkyne within the probe. This strategy is advantageous because aliphatic azides and terminal alkynes are relatively small and easily installable functional groups that are less likely to negatively affect biological activity by disrupting key ligand–target interactions. In addition, these functional groups are biologically compatible and the approach allows for tag flexibility, high-throughput analysis, and use *in vivo*.

In 2013, Lee and co-workers identified malate dehydrogenase 2 (MDH2) as a target protein of the HIF-1 inhibitor LW6 (**3.87** in Figure 32) using chemical probes.[136] Cellular images and direct protein interactions of **3.87** were examined in living cells with a series of chemical probes, which were designed based on the SAR of **3.87**. Probe **3.88** was used to explore the intracellular localization of **3.87**, visualized through click reaction using an azide-linked fluorescent dye. Subsequently, trifluromethyl diazirine was installed to **3.88**, generating the photoactivable probe **3.89**. Photoaffinity labeling was performed in the HCT116 cells using ultraviolet irradiation and click conjugation with a fluorescent dye (Cy5 for probe **3.89** and Cy3 for probe **3.90**). Cellular proteins were separated by sodium dodecyl sulfate-polyacrylamide gel electrophoresis (SDS-PAGE), visualized by in-gel fluorescent scanning, and a Cy5 specific band was detected. The proteins bound to **3.89** and **3.90** were separated by two-dimensional gel

electrophoresis (2DE), followed by in-gel trypsin digestion and mass spectrometry. As a result, MDH2 was identified as a protein bound to probe **3.89**. To confirm the binding of **3.87** to MDH2, biotin probes were synthesized. In the affinity pull-down assays, MDH2 bound to **3.92**, compared with a negative control **3.91**. In addition, binding of biotinylated **3.87** to MDH2 was attenuated by addition of non-biotinylated **3.87**, supporting an interaction between **3.87** and MDH2.

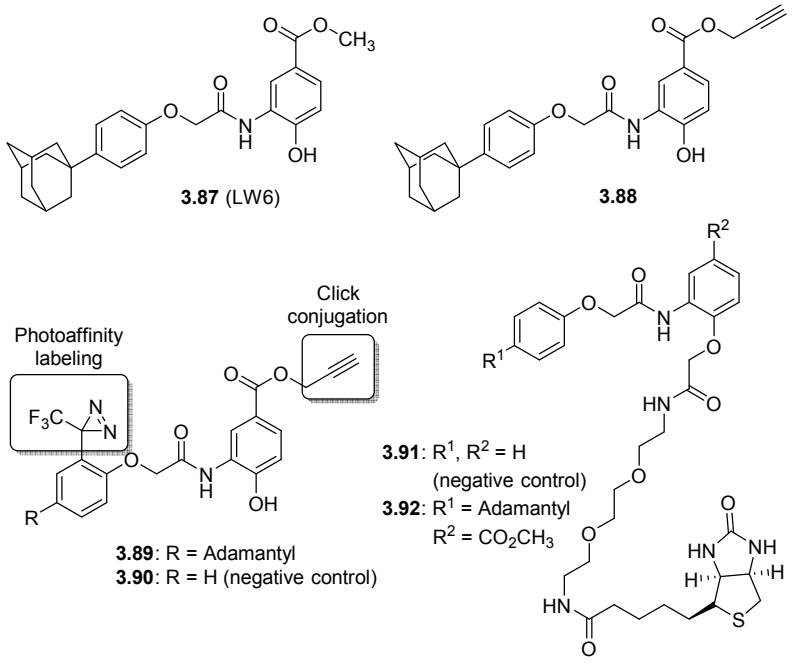

Figure 32: Chemical probes of LW6

3.2.5.2 Synthesis of Photoactivable Probes

Aiming for target identification of manassantin A, we designed alkyne-containing probe **MA13** and biotinylated probe **MA14** based on the SAR of the natural product and synthetic efficiency (Figure 33).

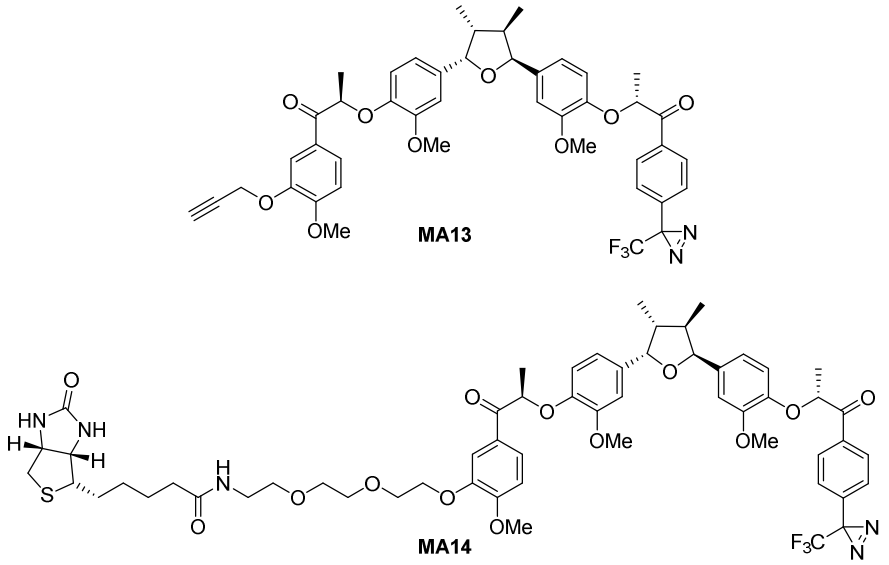

Figure 33: Manassantin A-derived photoactivable probes

Synthesis of these probes started with the preparation of tosylate **3.105** (Scheme 32). Trifluoroacetylation of the known bromide **3.93**[137] provided **3.94** which was converted to corresponding diaziridine **3.97** via oxime by conventional procedures. The diaziridine **3.97** was oxidized with freshly prepared Ag_2O to give diazirine **3.98**. Asymmetric dihydroxylation of **3.98** provided diol **3.99**, which was then subjected to several oxidation conditions to obtain **3.100**. DDQ oxidation resulted in the formation of **3.101** by oxidation of diazirine moiety. MnO_2 oxidation afforded the undesired oxidative

cleavage product **3.102**. Finally, **3.199** was treated with DMDO to give **3.100** which was tosylated to obtain **3.105**.

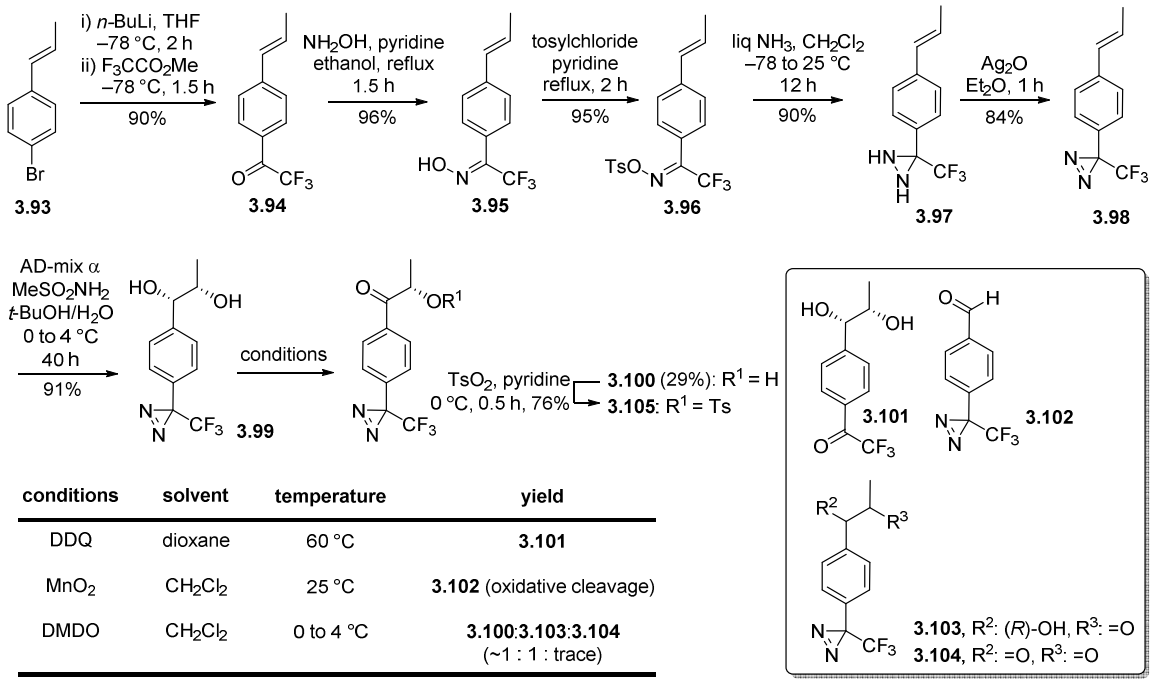

conditions	solvent	temperature	yield
DDQ	dioxane	60 °C	**3.101**
MnO_2	CH_2Cl_2	25 °C	**3.102** (oxidative cleavage)
DMDO	CH_2Cl_2	0 to 4 °C	**3.100**:**3.103**:**3.104** (~1 : 1 : trace)

Scheme 32: Synthesis of tosylate 3.105

Preparation of alkyne-containing probe **MA13** is depicted in Scheme 33. BEMP-mediated coupling of **3.12** with 1 equivalent of **3.36** (Scheme 23) provided mono-alkylated product **3.106** which was TBDPS-protected to provide **3.107**. Bn-deprotection and alkylation with propargyl bromide successfully afforded alkyne **3.109**. TBDPS-deprotection of **3.109** followed by coupling with diazirine-containing tosylate **3.105** provided **MA13**.

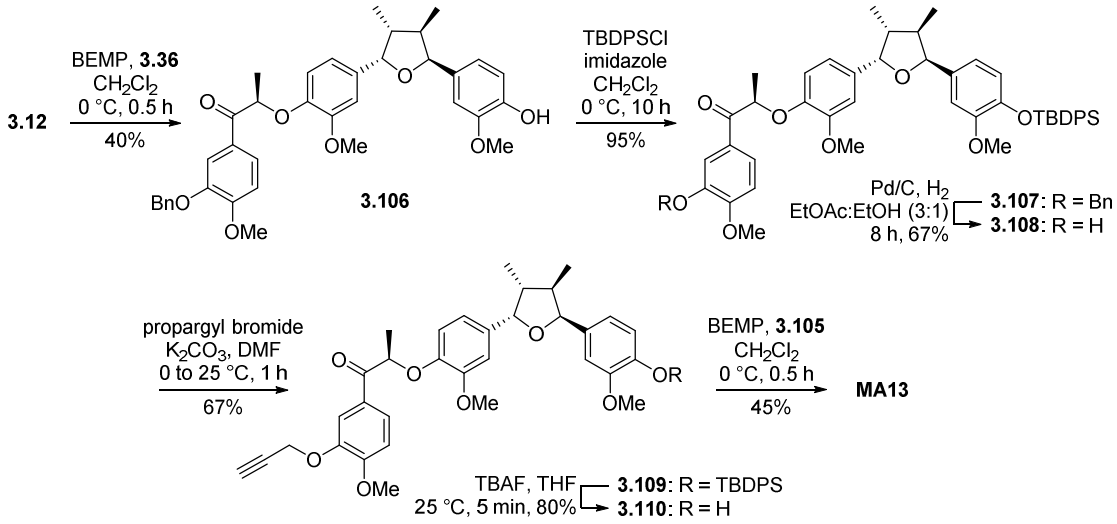

Scheme 33: Synthesis of alkyne-containing probe MA13

To prepare biotinylated probe **MA14** (Figure 31), the phenol **3.108** was alkylated with the known polyether bromide[138] (Scheme 34). Interestingly, TBDPS-deprotection was observed under the alkylation condition. BEMP-mediated coupling of **3.112** with tosylate **3.105** provided **3.113**. Boc-deprotection of **3.113** followed by acylation with biotin *N*-hydroxysuccinimide ester to yield the biotinylated probe **MA14**.

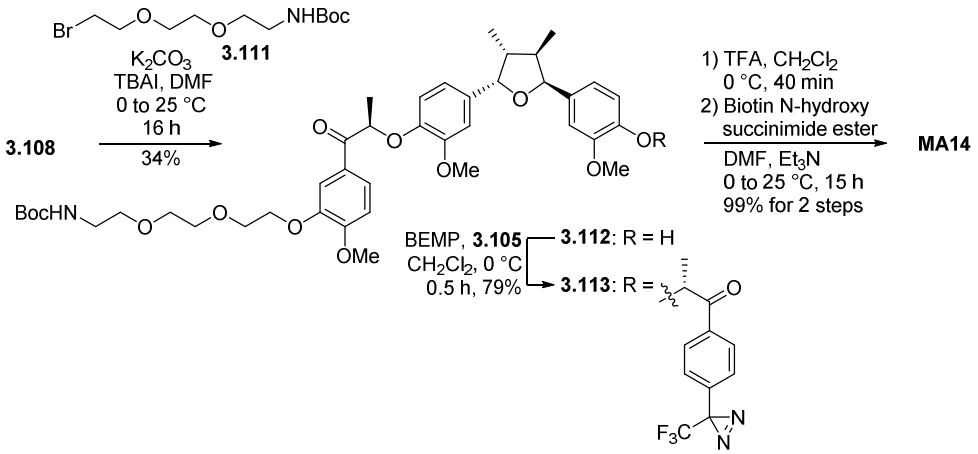

Scheme 34: Synthesis of biotinylated probe MA14

Following the preparation of probes, we sought to determine their HIF-1 inhibitory activity. Using the same HIF-1 luciferase-reporter assay system previously described for the assessment of manassantin analogues, the probes were analyzed and their IC_{50} values were obtained (Figure 34). The luciferase assay was accomplished by Lee group at Kyungpook National University in South Korea. In accordance with our SAR results, **MA13** showed good potency, suggesting that **MA13** would be a good photoactivable probe for affinity pull-down approach to identify the molecular target of manassantin A.

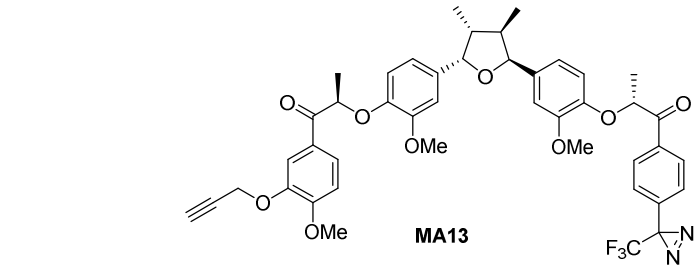

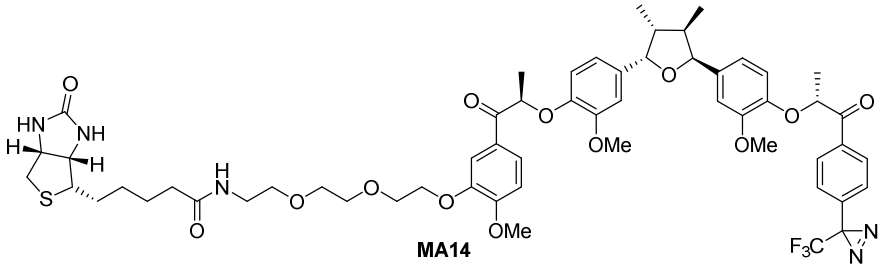

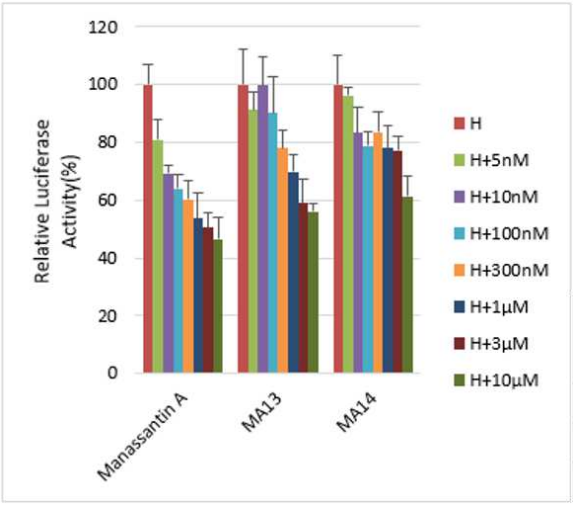

Compound	IC_{50} (nM)
Manassantin A (**1**)	11
MA13	636
MA14	>2000

Figure 34: Manassantin A (1) and probes (MA13 and MA14) suppress hypoxia-induced reporter gene activity in HEK-293T cells (H: hypoxia). After 24-hour incubation, HEK-293 cells were treated with hypoxia (1% O_2) and serially diluted compounds (MA13, MA14) for 24 h. To measure the firefly luminescence signals, Dual-Glo® reagent was added and the luminescence signals were measured by using a dual-color luminescence detection system. Luciferase expression/activity was detected, normalized to the activity of Renilla luciferase and quantified as relative luciferase units (RLUs). IC_{50} values of manassantin A (1), MA13, and MA14 are shown in the table. Data are mean values of three independent experiments.

In summary, we have designed, prepared, and evaluated alkyne-containing probe **MA13** and biotinylated probe **MA14** based on the SAR of manassantin A and the synthetic efficiency of trifluoromethyl diazirine photophore. In particular, **MA13** demonstrated a good activity in HIF-1 inhibition. We plan to use **MA13** as a chemical probe for photoaffinity pull-down approach to determine the molecular target of manassantin A.

3.3 Future Work

With the prepared analogues, we will examine their potency, cytotoxicity, effects on HIF-1 target genes, HIF-1 signaling specificity, and pharmacological properties. The luciferase-reporter assays will be used as initial *in vitro* tests to identify active compounds for further evaluation. In parallel, cytotoxic effect of manassantin analogues will be examined using the MTT assay. Based on their potency and cytotoxicity, we will select a subset of analogues, which will be further examined by Western blot and ELISA. Microarray will be used to evaluate HIF-1 signaling specificity of manassantin A and its analogues. On-target effects are the genes whose expression are induced under hypoxia and repressed by the treatment of manassantin A. In addition, microarray will be used to define off-target effects of manassantin A and its analogues. Off-target effcts are the genes whose expression are changed with the treatment of manassantin A under hypoxia, but not induced by hypoxia. The other source of off-target effects is the gene

expression in response to the treatment of manassantin A. For pharmacological characterization of manassantin analogues, we will examine their solubility, permeability, and stability. Through these efforts, we will find the most potent and selective HIF-1 inhibitors with desirable drug-like properties. Furthermore, we will use affinity pull-down approach with the photoactivable probes to identify the molecular target of manassantin A.

3.4 Conclusion

We have prepared and evaluated a series of manassantin analogues for HIF-1α inhibition. The SAR study of manassantin analogues provided valuable insights into the role/function of the side chains of manassantins and their effects on hypoxia signaling. More importantly, our medicinal chemistry efforts identified **MA04**, **MA07**, and **MA11**, which possesses a reduced structural complexity, as lead compounds for further development. These analogues down-regulated hypoxia-induced HIF-1α protein stabilization. In addition, they reduced the levels of Cdk6 and VEGF under hypoxia. We expect that **MA04**, **MA07**, and **MA11** will be potential lead compounds for future preclinical studies and the help design of more potent and selective manassantin analogues for novel therapeutic development for cancers.

We also prepared the 2nd generation analogues by bioisosteric replacements. The evaluation of their effects on HIF-1 activity is in progress. In addition, we designed and

synthesized manassantin A-derived chemical probes by incorporating a photoactivable moiety and a clickable tag or biotin tag. Biological evaluation of these probes demonstrated that **MA13** would be a good probe for the photoaffinity labeling, which has recently been applied in the development of several drugs and drug targets. We expect that **MA13** will play a crucial role in identification of the molecular target of manassantin A.

3.5 Experimental Section

General Methods

All reactions were conducted in oven-dried glassware under nitrogen. Unless otherwise stated all reagents were purchased from Sigma–Aldrich, Acros, or Fisher and were used without further purification. All solvents were ACS grade or better and used without further purification except tetrahydrofuran (THF) which was freshly distilled from sodium/benzophenone each time before use. Analytical thin layer chromatography (TLC) was performed with glass backed silica gel (60 Å) plates with fluorescent indication (Whatman). Visualization was accomplished by UV irradiation at 254 nm and/or by staining with *para*-anisaldehyde solution. Flash column chromatography was performed by using silica gel (particle size 230–400 mesh, 60 Å). All ^{1}H NMR and ^{13}C NMR spectrum were recorded with a Varian 400 (400 MHz) and a Bruker 500 (500 MHz) spectrometer in $CDCl_3$ by using the signal of residual $CHCl_3$, as an internal standard. All

NMR δ values are given in ppm, and all J values are in Hz. Electrospray ionization (ESI) mass spectra (MS) were recorded with an Agilent 1100 series (LC/MSD trap) spectrometer and were performed to obtain the molecular masses of the compounds. Infrared (IR) absorption spectra were determined with a Thermo–Fisher (Nicolet 6700) spectrometer. Optical rotation values were measured with a Rudolph Research Analytical (A21102. API/1W) polarimeter.

Preparation of Benzyl Ether 3.33

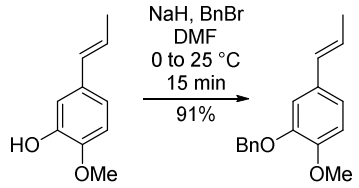

3.32 **3.33**

To a cooled (0 °C) solution of the known phenol **3.32**[114] (867 mg, 5.28 mmol) in dry DMF (13 mL, 0.4 M) were added NaH (60% dispersion in mineral oil, 304 mg, 7.92 mmol) and BnBr (0.63 mL, 5.28 mmol). The reaction mixture was allowed to warm to 25 °C. After stirring for 15 min, the reaction was quenched by addition of H_2O and extracted with EtOAc. The combined organic layers were washed with brine, dried over anhydrous Na_2SO_4, and concentrated *in vacuo*. The residue was purified by column chromatography (silica gel, hexanes/EtOAc, 20/1) to afford **3.33** as a white powder (1.22 g, 91%): ^{1}H NMR (400 MHz, $CDCl_3$) δ 7.50 (d, J = 8.0 Hz, 2H), 7.41 (t, J = 8.0 Hz, 2H), 7.35 (d, J = 7.2 Hz, 1H), 6.98 (s, 1H), 6.92 (d, J = 7.2 Hz, 1H), 6.85 (d, J = 8.4 Hz, 1H), 6.34 (d, J = 15.6 Hz, 1H),

6.07 (dq, J = 6.8, 15.6 Hz, 1H), 5.19 (s, 2H), 3.89 (s, 3H), 1.89 (d, J = 6.8 Hz, 3H); ^{13}C NMR (125 MHz, $CDCl_3$) δ 148.9, 148.2, 137.2, 131.1, 130.6, 128.5, 127.4, 127.3, 123.6, 119.2, 111.8, 111.5, 71.0, 55.9, 18.3; IR (neat) 2932, 1510, 1258, 1136, 1024, 962 cm^{-1}; HRMS (ESI) m/z 255.1389 [$(M+H)^+$, $C_{17}H_{18}O_2$ requires 255.1380].

Preparation of Diol 3.34

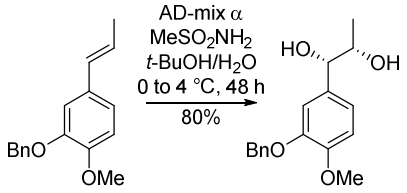

3.33 **3.34**

To a cooled (0 °C) solution of AD-mix-α (5.06 g, 1.4 g/mmol of substrate) and $MeSO_2NH_2$ (344 mg, 3.62 mmol) in t-BuOH/H_2O (1/2, 31.5 mL) was added dropwise alkene **3.33** (920 mg, 3.62 mmol) in EtOAc/t-BuOH (1/2, 16 mL). The reaction mixture was stirred for 48 h at 4 °C. The reaction was quenched by addition of sodium sulfite (5.42 g, 1.5 g/mmol of substrate), diluted with EtOAc, and stirred for 30 min at 25 °C. The layers were separated, and the aqueous layer was extracted with EtOAc. The combined organic layers were washed with 2 N KOH and brine, dried over anhydrous Na_2SO_4, and concentrated *in vacuo*. The residue was purified by column chromatography (silica gel, hexanes/EtOAc, 1/1) to afford **3.34** as a colorless oil (834 mg, 80%): ^{1}H NMR (400 MHz, $CDCl_3$) δ 7.42 (d, J = 7.2 Hz, 2H), 7.35 (t, J = 7.2 Hz, 2H), 7.29 (d, J = 7.2 Hz), 6.87–6.85 (m, 3H) 4.21 (d, J = 7.6 Hz, 1H), 3.86 (s, 1H), 3.72 (dq, J = 6.4, 14.0 Hz, 1H), 2.71 (bs, 2H), 0.94

(d, J = 6.4 Hz, 3H); ^{13}C NMR (125 MHz, $CDCl_3$) δ 149.4, 147.9, 136.9, 133.7, 128.4, 127.8, 127.5, 119.9, 113.0, 111.6, 79.1, 72.1, 71.0, 55.9, 18.7; IR (neat) 3383, 2970, 1733, 1513, 1256, 1134, 1021 cm^{-1}; HRMS (ESI) m/z 311.1244 [$(M+Na)^+$, $C_{17}H_{20}O_4$ requires 311.1254].

Preparation of Hydroxy Ketone 3.35

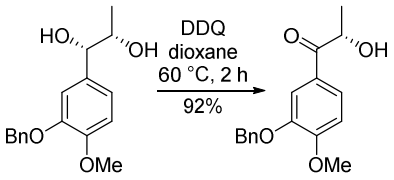

3.34 **3.35**

To a solution of diol **3.34** (834 mg, 2.89 mmol) in dioxane (29 mL, 0.1 M) was added DDQ (1.31 g, 5.78 mmol) at 25 °C. The reaction mixture was heated to 60 °C and stirred for 2 h at the same temperature. The reaction mixture was cooled to 0 °C, quenched by addition of saturated aqueous sodium thiosulfate and saturated aqueous $NaHCO_3$, diluted with CH_2Cl_2, and stirred vigorously for 1 h. The layers were separated, and the aqueous layer was extracted with CH_2Cl_2. The combined organic layers were washed with brine, dried over anhydrous Na_2SO_4, and concentrated *in vacuo*. The residue was purified by column chromatography (silica gel, hexanes/EtOAc, 2/1) to afford **3.35** as a yellow oil (762 mg, 92%): ^{1}H NMR (400 MHz, $CDCl_3$) δ 7.56–7.52 (m, 2H), 7.47–7.45 (m, 2H), 7.39 (dd, J = 7.2, 8.0 Hz, 2H), 7.33 (d, J = 7.6 Hz, 1H), 6.93 (d, J = 8.4 Hz, 1H), 5.20 (s, 2H), 5.04 (q, J = 7.2 Hz, 1H), 3.96 (s, 3H), 1.37 (d, J = 7.2 Hz); ^{13}C NMR (125 MHz, $CDCl_3$) δ 200.7, 154.2, 148.3, 136.5, 128.7, 128.2, 127.5, 126.1, 123.8, 113.5, 110.8, 71.1, 68.9; IR (neat) 3459, 2976, 1667,

1594, 1512, 1263, 1114, 1016, 861 cm^{-1}; HRMS (ESI) *m*/*z* 287.1269 [$(M+H)^+$, $C_{17}H_{18}O_4$ requires 287.1278].

Preparation of Tosylate 3.36

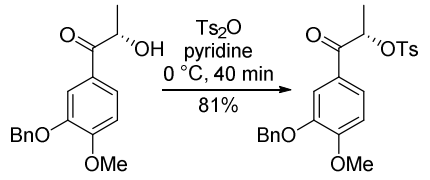

3.35 **3.36**

To a cooled (0 °C) solution of hydroxy ketone **3.35** (750 mg, 2.62 mmol) in pyridine (25 mL, 0.1 M) was added Ts_2O (1.28 g, 3.93 mmol). After stirring for 40 min at the same temperature, the reaction was quenched by addition of saturated aqueous NH_4Cl and extracted with CH_2Cl_2. The combined organic layers were washed with brine, dried over anhydrous Na_2SO_4, and concentrated *in vacuo*. The residue was purified by column chromatography (silica gel, hexanes/EtOAc, 2/1) to afford **3.36** as a white powder (935 mg, 81%): ^1H NMR (400 MHz, $CDCl_3$) δ 7.71 (d, *J* = 8.4 Hz, 2H), 7.54 (dd, *J* = 2.0, 8.8 Hz, 1H), 7.46–7.41 (m, 3H), 7.36–7.32 (m, 2H), 7.30–7.28 (m, 1H), 7.22 (d, *J* = 8.4 Hz, 2H), 6.86 (d, *J* = 8.8 Hz, 1H), 5.69 (q, *J* = 7.2 Hz, 1H), 5.12 (s, 2H), 3.90 (s, 3H), 2.36 (s, 3H), 1.48 (d, *J* = 7.2 Hz, 3H); ^{13}C NMR (125 MHz, $CDCl_3$) δ 192.9, 154.7, 148.3, 145.0, 136.5, 133.6, 129.8, 128.6, 128.1, 127.9, 127.6, 126.5, 123.9, 113.4, 110.7, 77.2, 71.0, 56.2, 21.6, 18.9; IR (neat) 2961, 1684, 1594, 1515, 1265, 1175, 1013, 932 cm^{-1}; HRMS (ESI) *m*/*z* 441.1356 [$(M+H)^+$, $C_{24}H_{24}O_6S$ requires 441.1366].

Preparation of 3.37

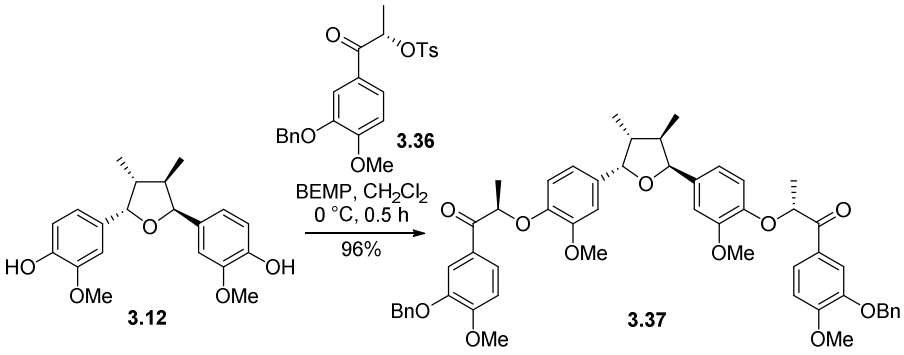

To a cooled (0 °C) solution of the known bis-phenol **3.12**[108] (54 mg, 0.16 mmol) in dry CH_2Cl_2 (2 mL, 0.08 M) was added dropwise 2-*tert*-butylimino-2-diethylamino-1,3-dimethylperhydro-1,3,2-diazaphosphorine (BEMP, 0.09 mL, 0.31 mmol). The resulting mixture was stirred at the same temperature for 10 min before tosylate **3.36** (207.2 mg, 0.47 mmol) in CH_2Cl_2 (2 mL, 0.23 M) was added. After stirring for 30 min at 0 °C, the reaction was quenched by addition of saturated aqueous NH_4Cl and extracted with CH_2Cl_2. The combined organic layers were washed with brine, dried over anhydrous Na_2SO_4, and concentrated *in vacuo*. The residue was purified by column chromatography (silica gel, hexanes/EtOAc, 2/1) to afford **3.37** as a white foam (133 mg, 96%): ^{1}H NMR (400 MHz, $CDCl_3$) δ 7.82–7.76 (m, 4H), 7.46 (d, *J* = 7.6 Hz, 4H), 7.36 (dd, *J* = 7.2, 8.0 Hz, 4H), 7.31 (dd, *J* = 2.4, 7.2 Hz, 2H), 6.89 (d, *J* = 8.4 Hz, 2H), 6.82 (dd, *J* = 2.0, 10.0 Hz, 2H), 6.76–6.73 (m, 2H), 6.69 (dd, *J* = 1.6, 8.4 Hz, 2H), 5.36–5.32 (m, 4H), 5.17 (s, 4H), 3.92 (s, 6H), 3.83 (s, 6H), 2.23–2.17 (m, 2H), 1.64 (d, *J* = 6.8 Hz, 6H), 0.62 (d, *J* = 6.4 Hz, 6H); ^{13}C NMR (125 MHz, $CDCl_3$) δ 197.5, 154.2, 150.0, 147.9, 145.8, 136.6, 135.6, 128.6, 128.0, 127.6,

127.3, 123.9, 118.5, 115.7, 113.9, 110.6, 110.5, 83.4, 78.3, 70.8, 56.0, 44.0, 19.1, 14.8; IR (neat) 2961, 1684, 1593, 1509, 1265, 1137, 1020, 867 cm^{-1}; HRMS (ESI) *m*/*z* 898.4169 [$(M+NH_4)^+$, $C_{54}H_{56}O_{11}$ requires 898.4161].

Preparation of MA01

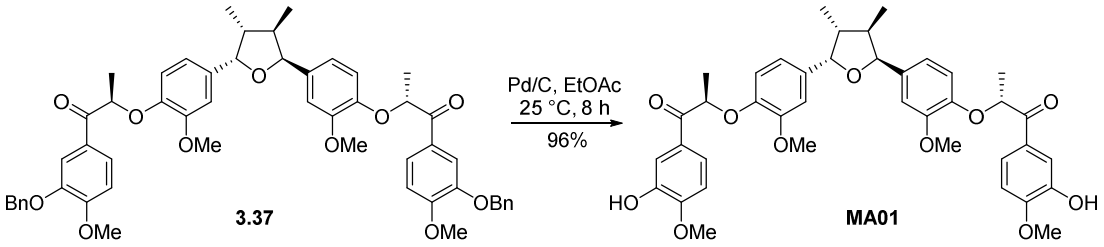

To a stirred solution of bis-benzyl ether **3.37** (29 mg, 0.03 mmol) in EtOAc (2 mL, 0.02 M) was added 10% Pd–C (6 mg, 20 wt %). The resulting mixture was stirred under H_2 atmosphere at 25 °C for 8 h. The reaction mixture was then filtered through Celite with EtOAc and concentrated *in vacuo*. The residue was purified by column chromatography (silica gel, hexanes/EtOAc, 3/2) to afford **MA01** as a white foam (22.1 mg, 96%): $[\alpha]^{25.2}_D$ = –19.9 (*c* 0.73, $CHCl_3$); ^1H NMR (400 MHz, $CDCl_3$) δ 7.73–7.68 (m, 4H), 6.87 (dd, *J* = 1.6, 8.4 Hz, 2H), 6.80 (dd, *J* = 1.6, 6.0 Hz, 2H), 6.77–6.73 (m, 2H), 6.67 (dd, *J* = 1.6, 8.4 Hz, 2H), 5.71 (bs, 2H), 5.40 (ddd, *J* = 6.8, 6.8, 6.8 Hz, 2H), 5.34 (d, *J* = 6.0 Hz), 3.93 (s, 6H), 3.83 (s, 6H), 2.20–2.16 (m, 2H), 1.67 (dd, *J* = 2.4, 6.8 Hz, 6H), 0.61 (d, *J* = 6.4 Hz, 6H); ^{13}C NMR (125 MHz, $CDCl_3$) δ 197.8, 151.1, 150.0, 146.0, 145.6, 135.8, 128.3, 122.7, 118.6, 116.4, 116.1, 115.2, 110.8, 110.1, 83.6, 78.2, 56.2, 44.1, 19.2, 14.8; IR (neat) 3404, 2962, 1684, 1608, 1509,

1272, 1139, 1028, 866 cm^{-1}; HRMS (ESI) *m*/*z* 701.2951 [$(M+H)^+$, $C_{40}H_{44}O_{11}$ requires 701.2956].

Prepration of MA02

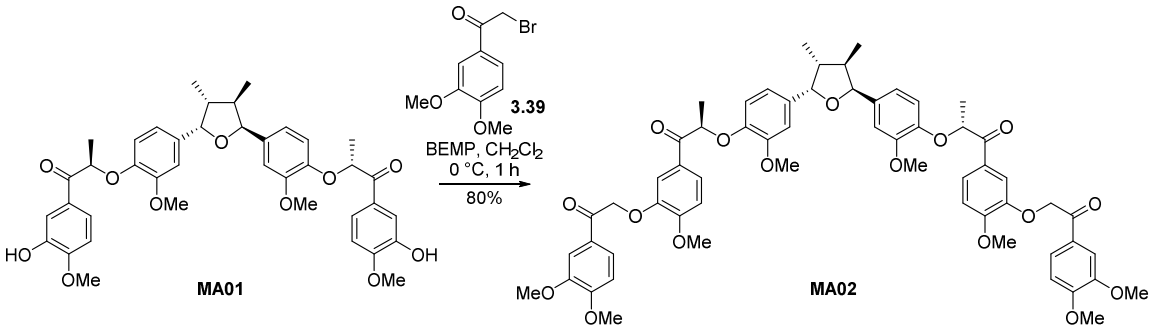

To a cooled (0 °C) solution of bis-phenol **3.12** (44 mg, 0.06 mmol) in dry CH_2Cl_2 (1.5 mL, 0.04 M) was added dropwise BEMP (0.04 mL, 0.13 mmol). The resulting mixture was stirred at the same temperature for 10 min before the known bromide **3.39**[116] (65 mg, 0.25 mmol) in CH_2Cl_2 (1.5 mL, 0.17 M) was added. After stirring for 1 h at 0 °C, the reaction was quenched by addition of saturated aqueous NH_4Cl and extracted with CH_2Cl_2. The combined organic layers were washed with brine, dried over anhydrous Na_2SO_4, and concentrated *in vacuo*. The residue was purified by column chromatography (silica gel, hexanes/EtOAc, 1/2) to afford **MA02** as a yellow foam (52.6mg, 80%): $[\alpha]^{22.6}_D$ = 7.9 (*c* 0.66, $CHCl_3$); ^{1}H NMR (400 MHz, $CDCl_3$) δ 7.86–7.82 (m, 2H), 7.61 (dd, *J* = 2.0, 6.4 Hz, 4H), 7.54 (s, 2H), 6.90 (dd, *J* = 6.0, 8.8 Hz, 4H), 6.79 (dd, *J* = 1.6, 8.8 Hz, 2H), 6.73 (dd, *J* = 4.8, 8.4 Hz, 2H), 6.68–6.64 (m, 2H), 5.40–5.31 (m, 8H), 3.95–3.92 (m, 18H), 3.80 (s, 6H), 2.19–2.15 (m, 2H), 1.65 (d, *J* = 6.8 Hz, 6H), 0.60 (d, *J* = 6.4 Hz, 6H); ^{13}C NMR (125 MHz, $CDCl_3$) δ 197.4,

192.2, 154.2, 154.0, 149.8, 149.4, 147.5, 145.8, 135.7, 127.8, 127.4, 124.7, 122.7, 118.5, 116.0, 113.8, 110.9, 110.7, 110.4, 110.3, 83.4, 78.3, 71.1, 56.2, 44.0, 19.1, 14.8; IR (neat) 2932, 1685, 1595, 1513, 1266, 1134, 1021, 870 cm^{-1}; HRMS (ESI) *m*/*z* 1074.4497 [$(M+NH_4)^+$, $C_{60}H_{64}O_{17}$ requires 1074.4482].

Preparation of MA03

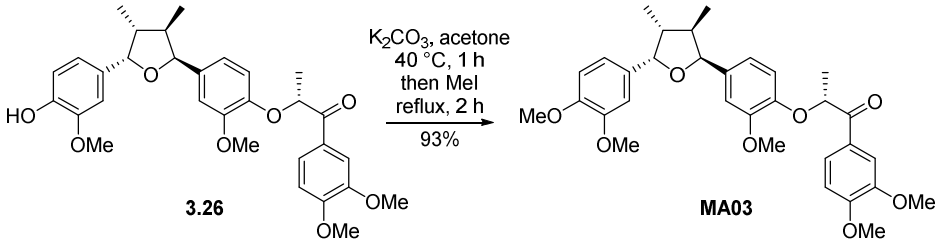

To a solution of the known phenol **3.26**[108] (32 mg, 0.06 mmol) in acetone (3 mL, 0.02 M) was added K_2CO_3 (16.6 mg, 0.12 mmol) at 25 °C. After stirring for 1 h at 40 °C, the reaction mixture was cooled to 25 °C and treated with MeI (0.02 mL, 0.24 mmol) at the same temperature. After stirring for 2 h at reflux, the reaction mixture was cooled to 25 °C, diluted with EtOAc, and rinsed with saturated aqueous NH_4Cl. The layers were separated, and the aqueous layer was extracted with EtOAc. The combined organic layers were washed with brine, dried over anhydrous Na_2SO_4, and concentrated *in vacuo*. The residue was purified by column chromatography (silica gel, hexanes/EtOAc, 1/1) to afford **MA03** as a white foam (31 mg, 93%): $[\alpha]^{22.4}_D$ = –22.5 (*c* 0.13, EtOAc); ^1H NMR (400 MHz, $CDCl_3$) δ 7.84–7.80 (m, 1H), 7.68–7.66 (m, 1H), 6.87–6.67 (m, 7H), 5.44–5.36 (m, 3H), 3.93 (s, 3H), 3.91 (s, 3H), 3.87 (s, 3H), 3.86 (s, 3H), 3.85 (s, 3H), 2.25–2.19 (m,

2H), 1.71 (d, *J* = 6.8 Hz, 3H), 0.65 (dd, *J* = 6.4, 7.2 Hz, 3H); ^{13}C NMR (125 MHz, $CDCl_3$) δ 197.9, 153.7, 149.8, 149.1, 148.7, 148.0, 146.4, 145.9, 135.8, 134.0, 127.6, 123.7, 118.6, 115.9, 111.4, 110.9, 110.7, 110.2, 109.7, 109.0, 83.6, 78.5, 56.1, 44.2, 19.3, 14.9; IR (neat) 2960, 1682, 1593, 1512, 1261, 1136, 1023, 799 cm^{-1}; HRMS (ESI) *m*/*z* 551.2631 [$(M+H)^+$, $C_{32}H_{38}O_8$ requires 551.2639].

Preparation of MA04

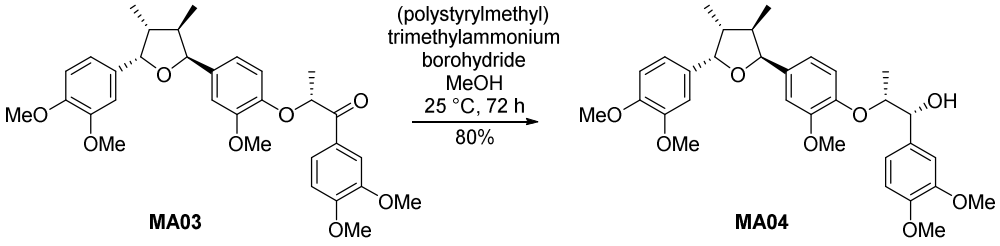

To a stirred solution of **MA03** (31 mg, 0.06 mmol) in MeOH (2 mL, 0.02 M) was added polymer-supported borohydride (2 mmol BH_4/g resin, 560 mg, 1.12 mmol). The reaction mixture was stirred with gentle agitation at 25 °C for 72 h. The polymer beads were then removed by filtration and the filtrate was purified by column chromatography (silica gel, hexanes/EtOAc, 4/1) to afford **MA04** as a colorless oil (25 mg, 80%): $[\alpha]^{22.5}_D$ = –78.3 (*c* 0.52, $CHCl_3$); ^{1}H NMR (400 MHz, $CDCl_3$) δ 7.00–6.82 (m, 9H), 5.45 (d, *J* = 6.0 Hz, 2H), 4.64 (d, *J* = 8.4 Hz, 1H), 4.15–4.08 (m, 1H), 3.92 (s, 3H), 3.89 (s, 3H), 3.88 (s, 6H), 3.87 (s, 3H), 2.22–2.31 (m, 2H), 1.17 (d, *J* = 6.4 Hz, 3H), 0.71 (d, *J* = 6.4 Hz, 3H), 0.69 (dd, *J* = 6.4, 6.4 Hz, 3H); ^{13}C NMR (125 MHz, $CDCl_3$) δ 150.7, 149.1, 149.0, 148.8, 148.0, 146.6, 136.8, 134.0, 132.7, 120.1, 118.8, 118.5, 111.0, 110.9, 110.3, 110.2, 109.7, 84.3, 83.6, 83.5, 78.5, 56.0, 44.2,

17.2, 14.9; IR (neat) 3453, 2930, 1510, 1256, 1138, 1027, 811, 733 cm^{-1}; HRMS (ESI) *m*/*z* 570.3072 [$(M+NH_4)^+$, $C_{32}H_{40}O_8$ requires 570.3061].

Preparation of MA06

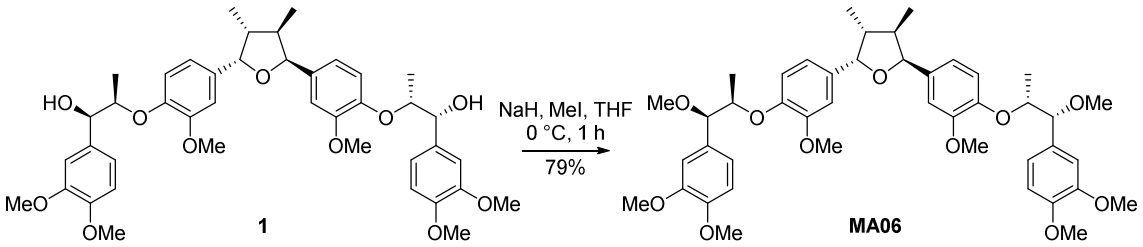

To a cooled (0 °C) solution of **1** (manassantin A)[108] (25 mg, 0.03 mmol) in THF (2 mL, 0.02 M) were added NaH (60% dispersion in mineral oil, 10.5 mg, 0.27 mmol) and MeI (0.02 mL, 0.34 mmol). After stirring for 1 h at the same temperature, the reaction was quenched by addition of H_2O and extracted with EtOAc. The combined organic layers were washed with brine, dried over anhydrous Na_2SO_4, and concentrated *in vacuo*. The residue was purified by column chromatography (silica gel, hexanes/EtOAc, 2/1) to afford **MA06** as a colorless oil (23 mg, 79%): $[\alpha]^{23.2}_D$ = –49.9 (*c* 0.3, $CHCl_3$); ^1H NMR (400 MHz, $CDCl_3$) δ 6.97–6.77 (m, 12H), 5.42 (d, *J* = 6.4 Hz, 2H), 4.53–4.46 (m, 2H), 4.32 (d, *J* = 6.4 Hz, 2H), 3.90 (s, 6H), 3.89 (s, 6H), 3.85 (s, 6H), 3.29 (s, 6H), 2.28–2.22 (m, 2H), 1.06 (d, *J* = 6.4 Hz, 6H), 0.68 (d, *J* = 6.4 Hz, 6H); ^{13}C NMR (125 MHz, $CDCl_3$) δ 150.5, 149.2, 148.9, 146.8, 135.1, 131.4, 120.5, 118.7, 116.6, 110.8, 110.6, 86.6, 83.7, 79.0, 57.3, 56.2, 56.1, 44.2, 16.5, 15.0; IR (neat) 2933, 1508, 1271, 1028 cm^{-1}; HRMS (ESI) *m*/*z* 778.4153 [$(M+NH_4)^+$, $C_{44}H_{56}O_{11}$ requires 778.4161].

Preparation of MA07

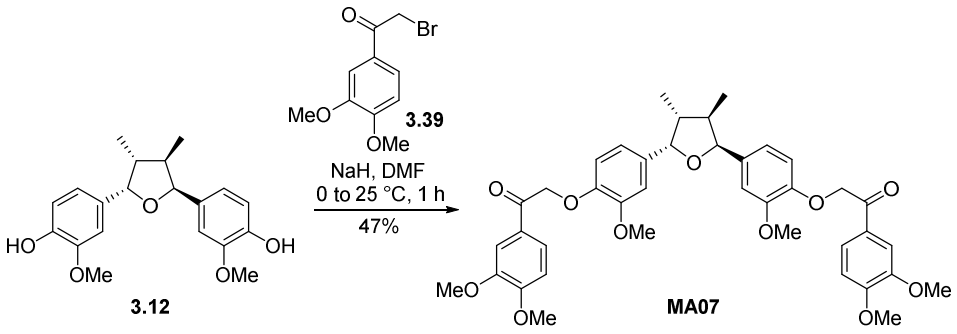

To a cooled (0 °C) solution of the known bis-phenol **3.12**[108] (90 mg, 0.26 mmol) in dry DMF (2 mL, 0.13 M) was added NaH (60% dispersion in mineral oil, 30 mg, 0.78 mmol). After stirring for 5 min, the reaction mixture was treated with the known bromide **3.39**[116] (271 mg, 1.04 mmol) in DMF (4 mL, 0.26 M) and stirred for 40 min. The resulting mixture was allowed to warm to 25 °C for 1 h. At 0 °C, the reaction was quenched by addition of saturated aqueous NH_4Cl and extracted with EtOAc. The combined organic layers were washed with brine, dried over anhydrous Na_2SO_4, and concentrated *in vacuo*. The residue was purified by column chromatography (silica gel, hexanes/EtOAc, 1/1) to afford **MA07** as a colorless oil (90 mg, 47%): $[\alpha]^{25.0}_D$ = –25.7 (*c* 0.4, EtOAc); ^{1}H NMR (400 MHz, $CDCl_3$) δ 7.67 (dd, *J* = 2.0, 8.4 Hz, 2H), 7.59 (s, 2H), 6.90–6.73 (m, 8H), 5.40 (d, *J* = 6.0 Hz, 2H), 5.28 (s, 4H), 3.95 (s, 6H), 3.93 (s, 6H), 3.89 (s, 6H), 2.26–2.20 (m, 2H), 0.66 (d, *J* = 6.4 Hz, 6H); ^{13}C NMR (125 MHz, $CDCl_3$) δ 193.5, 153.9, 149.5, 149.3, 146.6, 135.7, 128.0, 122.9, 118.5, 114.5, 110.6, 110.4, 110.2, 83.5, 72.4, 56.2, 56.1, 44.2, 14.9; IR (neat) 2931, 1689, 1512, 1261, 1163, 1021 cm^{-1}; HRMS (ESI) *m/z* 701.2959 [$(M+H)^+$, $C_{40}H_{44}O_{11}$ requires 701.2956].

Preparation of MA08

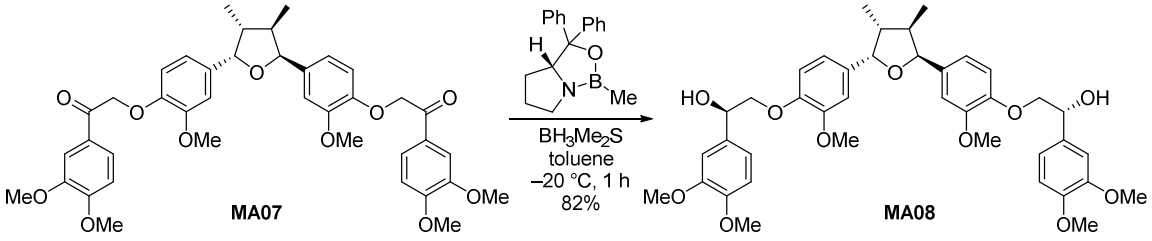

To a cooled (–20 °C) solution of (*R*)-(+)-2-methyl-CBS-oxazaborolidine (0.69 mg, 2.5 μmol) and BH_3Me_2S (5 μL, 0.05 mmol) in toluene (1 mL, 0.05 M) was added dropwise ketone **MA07** (35 mg, 0.05 mmol) in toluene (2 mL, 0.03 M). After stirring for 1 h at the same temperature, the reaction was quenched by addition of MeOH followed by 1 N HCl. The aqueous layer was extracted with EtOAc, dried over anhydrous Na_2SO_4, and concentrated *in vacuo*. The residue was purified by column chromatography (silica gel, hexanes/EtOAc, 1/2) to afford **MA08** as a colorless oil (29 mg, 82%): $[\alpha]_D$ = –32.9 (*c* 0.4, EtOAc); ^{1}H NMR (400 MHz, $CDCl_3$) δ 7.01–6.80 (m, 12H), 5.44 (d, *J* = 6.0 Hz, 2H), 5.05 (dd, *J* = 2.8, 9.2 Hz, 2H), 4.15 (dd, *J* = 3.2, 10.4 Hz, 2H), 3.96 (t, *J* = 10.0 Hz, 2H), 3.894 (s, 6H), 3.89 (s, 6H), 3.87 (s, 6H), 3.30 (bs, 2H), 2.31–2.23 (m, 2H), 0.69 (d, *J* = 6.4 Hz, 6H); ^{13}C NMR (125 MHz, EtOAc) δ 149.9, 149.2, 148.9, 146.9, 135.8, 132.3, 118.8, 118.7, 115.6, 111.1, 110.2, 109.5, 83.5, 76.5, 72.2, 56.0, 44.2, 14.9; IR (neat) 3481, 2922, 1514, 1262, 1027, 810 cm^{-1}; HRMS (ESI) *m*/*z* 722.3523 [$(M+NH_4)^+$, $C_{40}H_{48}O_{11}$ requires 722.3535].

Preparation of MA09

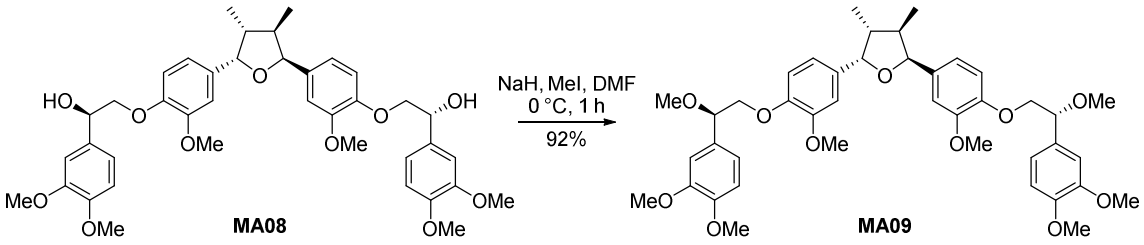

To a cooled (0 °C) solution of alcohol **MA08** (24 mg, 0.03 mmol) in dry DMF (3 mL, 0.01 M) were added NaH (60% dispersion in mineral oil, 20.5 mg, 0.55 mmol) and MeI (0.04 mL, 0.68 mmol). After stirring for 1 h at the same temperature, the reaction was quenched by addition of H_2O and extracted with EtOAc. The combined organic layers were washed with brine, dried over anhydrous Na_2SO_4, and concentrated *in vacuo*. The residue was purified by column chromatography (silica gel, hexanes/EtOAc, 2/3) to afford **MA09** as a white foam (23 mg, 92%): $[\alpha]^{22.0}_D$ = –43.2 (*c* 0.38, EtOAc); ^{1}H NMR (400 MHz, $CDCl_3$) δ 6.95–6.75 (m, 12H), 5.41 (d, *J* = 5.6 Hz, 2H), 4.60 (dd, *J* = 3.2, 7.6 Hz, 2H), 4.18 (dd, *J* = 8.0, 10.8 Hz, 2H), 4.02 (dd, *J* = 3.6, 6.8 Hz, 2H), 3.90 (s, 6H), 3.88 (s, 6H), 3.86 (s, 6H), 3.35 (s, 6H), 2.26–2.20 (m, 2H), 0.66 (d, *J* = 6.4 Hz, 6H); ^{13}C NMR (125 MHz, $CDCl_3$) δ 149.6, 149.3, 149.0, 135.0, 131.4, 119.6, 118.5, 114.1, 111.1, 110.5, 109.9, 83.6, 82.2, 74.0, 57.2, 56.1, 56.0, 44.2, 14.9; IR (neat) 2932, 1513, 1261, 1137, 1028 cm^{-1}; HRMS (ESI) *m*/*z* 750.3846 [$(M+NH_4)^+$, $C_{42}H_{52}O_{11}$ requires 750.3848].

Preparation of MA10

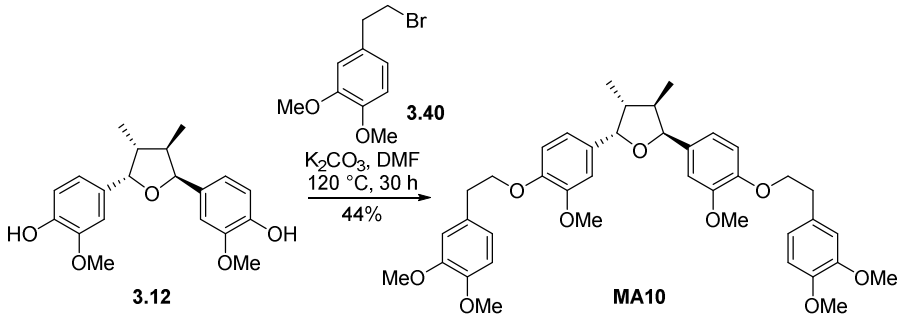

To a solution of the known bis-phenol **3.12**[108] (20 mg, 0.06 mmol) in dry DMF (1.5 mL, 0.04 M) were added K_2CO_3 (32 mg, 0.23 mmol) and 3,4-dimethoxyphenethyl bromide **3.40** (143 mg, 0.58 mmol) at 25 °C. The reaction mixture was heated to 120 °C and stirred for 30 h at the same temperature. The reaction was quenched by addition of saturated aqueous NH_4Cl and extracted with EtOAc. The combined organic layers were washed with brine, dried over anhydrous Na_2SO_4, and concentrated *in vacuo*. The residue was purified by column chromatography (silica gel, hexanes/EtOAc, 3/1) to afford **MA10** as a yellow oil (18 mg, 44%): $[\alpha]^{21.8}_D$ = –6.79 (*c* 0.28, EtOAc); ^{1}H NMR (400 MHz, $CDCl_3$) δ 6.87–6.82 (m, 12H), 5.43 (d, *J* = 6.0 Hz, 2H), 4.19 (t, *J* = 7.2 Hz, 4H), 3.88–3.87 (m, 18H), 3.10 (t, *J* = 7.2 Hz, 4H), 2.29–2.22 (m, 2H), 0.68 (d, *J* = 6.0 Hz, 6H); ^{13}C NMR (125 MHz, $CDCl_3$) δ 149.2, 149.0, 147.8, 147.3, 134.5, 130.9, 121.1, 118.6, 112.9, 112.6, 111.4, 110.3, 83.6, 70.2, 56.2, 56.1, 55.9, 56.2, 56.1, 55.9, 44.2, 35.6, 14.9; IR (neat) 2928, 1507, 1229, 1138, 1026 cm^{-1}; HRMS (ESI) *m*/*z* 690.3632 [$(M+NH_4)^+$, $C_{40}H_{48}O_9$ requires 690.3637].

Preparation of Diol 3.42

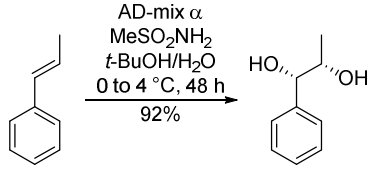

3.41 **3.42**

To a cooled (0 °C) solution of AD-mix-α (5.4 g, 1.4g/mmol of substrate) and $MeSO_2NH_2$ (367 mg, 3.85 mmol) in *t*-BuOH/H_2O (1/2, 30 mL) was added dropwise *trans*-β-methylstyrene **3.41** (0.5 mL, 3.85 mmol) in *t*-BuOH (10 mL). The reaction mixture was stirred for 48 h at 4 °C. The reaction was quenched by addition of sodium sulfite (5.78 g, 1.5g/mmol of substrate), diluted with EtOAc, and stirred for 30 min at 25 °C. The layers were separated, and the aqueous layer was extracted with EtOAc. The combined organic layers were washed with 2 N KOH and brine, dried over anhydrous Na_2SO_4, and concentrated *in vacuo*. The residue was purified by column chromatography (silica gel, hexanes/EtOAc, 3/1) to afford **3.42** as a colorless oil (539 mg, 92%): ^{1}H NMR (400 MHz, $CDCl_3$) δ 7.33–7.23 (m, 5H), 4.25 (d, *J* = 7.6 Hz, 1H), 4.02 (bs, 2H), 3.77 (dq, *J* = 6.4, 13.6 Hz, 1H), 0.95 (d, *J* = 6.4 Hz, 3H); ^{13}C NMR (125 MHz, $CDCl_3$) δ 141.2, 128.4, 128.0, 127.0, 79.5, 72.1; IR (neat) 3362, 2973, 1454, 1265, 1128, 1036, 870 cm^{-1}; HRMS (ESI) *m*/*z* 135.0804 [M+H–H_2O, $C_9H_{12}O_2$ requires 135.0804].

Preparation of Hydroxy Ketone 3.43

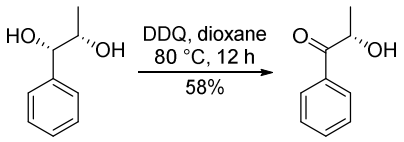

3.42 **3.43**

To a solution of diol **3.42** (539 mg, 3.54 mmol) in dioxane (35 mL, 0.1 M) was added DDQ (1.6 g, 7.08 mmol) at 25 °C. The reaction mixture was heated to 80 °C and stirred for 12 h at the same temperature. The reaction mixture was cooled to 0 °C, quenched by addition of saturated aqueous sodium thiosulfate and saturated aqueous $NaHCO_3$, diluted with CH_2Cl_2, and stirred vigorously for 1 h. The layers were separated, and the aqueous layer was extracted with CH_2Cl_2. The combined organic layers were washed with brine, dried over anhydrous Na_2SO_4, and concentrated *in vacuo*. The residue was purified by column chromatography (silica gel, hexanes/EtOAc, 2/1) to afford **3.43** as a colorless crystal (308 mg, 58%): ^{1}H NMR (400 MHz, $CDCl_3$) δ 7.92 (dd, *J* = 1.2, 8.4 Hz, 2H), 7.63–7.58 (m, 1H), 7.49 (dt, *J* = 1.6, 7.6, 14.0 Hz, 2H), 5.16 (q, *J* = 7.2 Hz, 1H), 3.73 (bs, 1H), 1.44 (d, *J* = 7.2 Hz, 3H); ^{13}C NMR (125 MHz, $CDCl_3$) δ 202.6, 134.1, 133.5, 128.9, 69.5, 22.4; IR (neat) 3455, 2979, 1679, 1597, 1268, 1126, 1025, 968 cm^{-1}; HRMS (ESI) *m*/*z* 133.0647 [$(M+H-H_2O)^+$, $C_9H_{10}O_2$ requires 133.0648].

Preparation of Tosylate 3.44

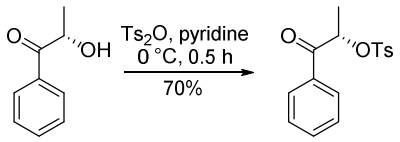

3.43 **3.44**

To a cooled (0 °C) solution of hydroxy ketone **3.43** (308 mg, 2.05 mmol) in pyridine (20 mL, 0.1 M) was added Ts_2O (1 g, 3.08 mmol). After stirring for 30 min at the same temperature, the reaction was quenched by addition of saturated aqueous NH_4Cl and extracted with CH_2Cl_2. The combined organic layers were washed with brine, dried over anhydrous Na_2SO_4, and concentrated *in vacuo*. The residue was purified by column chromatography (silica gel, hexanes/EtOAc, 2/1) to afford **3.44** as a white powder (437 mg, 70%): ^{1}H NMR (400 MHz, $CDCl_3$) δ 7.87 (dd, *J* = 1.2, 8.4 Hz, 2H), 7.75 (dd, *J* = 1.2, 8.4 Hz, 2H), 7.61–7.56 (m, 1H), 7.45 (dt, *J* = 1.6, 8.0, 13.6 Hz, 2H), 7.26 (d, *J* = 8.0 Hz, 2H), 5.78 (q, *J* = 7.2 Hz, 1H), 2.40 (s, 3H), 1.59 (d, *J* = 7.2 Hz, 3H); ^{13}C NMR (125 MHz, $CDCl_3$) δ 194.9, 145.2, 134.0, 133.8, 133.6, 129.9, 128.9, 128.0, 77.5, 21.7, 18.8; IR (neat) 2960, 1699, 1597, 1360, 1175, 1017, 919 cm^{-1}; HRMS (ESI) *m*/*z* 305.0836 [$(M+H)^+$, $C_{16}H_{16}O_4S$ requires 305.0842].

Preparation of MA11

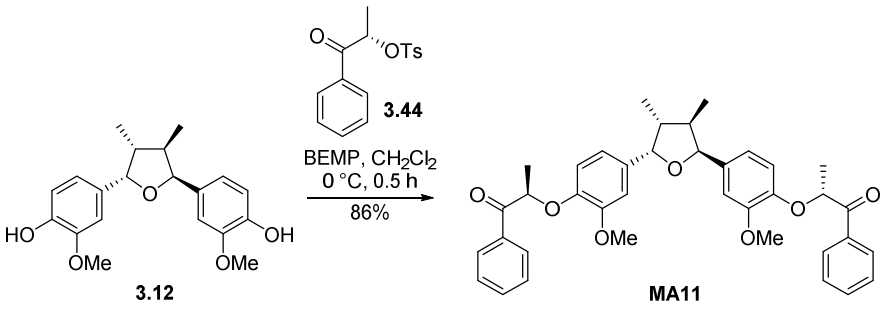

To a cooled (0 °C) solution of the known bis-phenol **3.12**[108] (30 mg, 0.09 mmol) in dry CH_2Cl_2 (1.5 mL, 0.06 M) was added dropwise BEMP (0.05 mL, 0.17 mmol). The resulting mixture was stirred at the same temperature for 10 min before tosylate **3.44** (106 mg, 0.35 mmol) in CH_2Cl_2 (1.5 mL, 0.23 M) was added. After stirring for 30 min at 0 °C, the reaction was quenched by addition of saturated aqueous NH_4Cl and extracted with CH_2Cl_2. The combined organic layers were washed with brine, dried over anhydrous Na_2SO_4, and concentrated *in vacuo*. The residue was purified by column chromatography (silica gel, hexanes/EtOAc, 4/1) to afford **MA11** as a colorless oil (45.5 mg, 86%): $[\alpha]^{23.4}_D$ = –27.57 (*c* 0.5, $CHCl_3$); ^{1}H NMR (400 MHz, $CDCl_3$) δ 8.11–8.08 (m, 4H), 7.58–7.54 (m, 2H), 7.45 (dd, *J* = 6.0, 7.2 Hz, 4H), 6.82–6.77 (m, 4H), 6.70–6.66 (m, 2H), 5.46 (dq, *J* = 4.0, 6.8 Hz, 2H), 5.35 (d, *J* = 6.0 Hz, 2H), 3.82 (s, 6H), 2.22–2.16 (m, 2H), 1.70 (d, *J* = 7.2 Hz, 6H), 0.62 (d, *J* = 6.4 Hz, 6H); ^{13}C NMR (125 MHz, $CDCl_3$) δ 199.3, 150.0, 145.9, 136.0, 134.8, 133.5, 129.1, 128.7, 118.6, 116.7, 116.5, 110.7, 83.5, 78.5, 56.1, 44.2, 30.0, 19.0, 14.9; IR (neat) 2962, 1697, 1508, 1269, 1221, 1142, 1034, 966 cm^{-1}; HRMS (ESI) *m*/*z* 626.3107 [$(M+NH_4)^+$, $C_{38}H_{40}O_7$ requires 626.3112].

Preparation of MA12

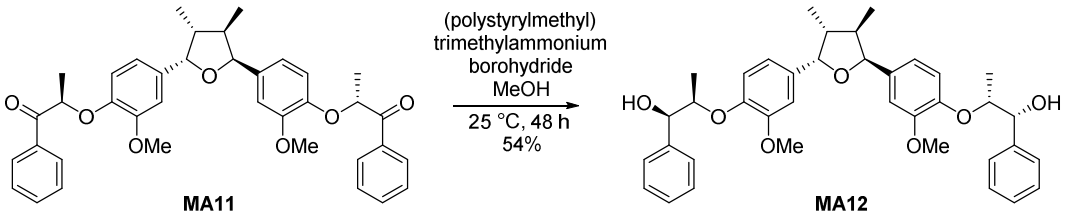

To a stirred solution of **MA11** (42 mg, 0.07 mmol) in MeOH (4.5 mL, 0.02 M) was added polymer-supported borohydride (2 mmol BH_4/g resin, 690 mg, 1.38 mmol). The reaction mixture was stirred with gentle agitation at 25 °C for 48 h. The polymer beads were then removed by filtration and the filtrate was purified by column chromatography (silica gel, hexanes/EtOAc, 2/1) to afford **MA12** as a colorless oil (23 mg, 54%): $[\alpha]^{22.7}_D$ = –62.14 (*c* 0.4, EtOAc); ^{1}H NMR (400 MHz, $CDCl_3$) δ 7.41–7.28 (m, 10H), 7.00–6.81 (m, 6H), 5.46 (d, *J* = 6.0 Hz, 2H), 4.70 (d, *J* = 8.0 Hz, 2H), 4.18–4.09 (m, 3H), 3.93 (s, 6H), 2.32–2.26 (m, 2H), 1.17 (dd, *J* = 2.0, 6.4 Hz, 6H), 0.72 (d, *J* = 6.4 Hz, 6H); ^{13}C NMR (125 MHz, $CDCl_3$) δ 150.7, 146.6, 140.2, 136.7, 128.5, 128.2, 127.5, 119.0, 118.8, 110.3, 84.3, 83.5, 78.8, 56.0, 44.3, 17.1, 15.0; IR (neat) 3481, 2964, 1508, 1258, 1036 cm^{-1}; HRMS (ESI) *m*/*z* 630.3447 [$(M+NH_4)^+$, $C_{38}H_{44}O_7$ requires 630.3425].

Preparation of Diol 3.47

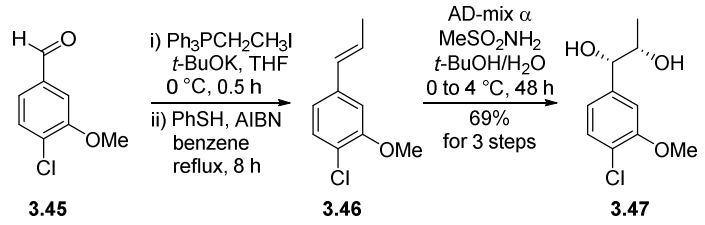

[**Wittig reaction**] To a cooled (0 °C) suspension of ethyltriphenylphosphonium iodide (1.84 g, 4.39 mmol) in THF (25 mL) was added dropwise *t*-BuOK (1.0 M in THF, 3.65 mL, 3.65 M). The resulting mixture was stirred at the same temperature for 30 min before aldehyde **3.45** (250 mg, 1.46 mmol) in THF (5 mL, 0.29 M) was added dropwise. After stirring for 30 min at 0 °C, the reaction was quenched by addition of saturated aqueous NH_4Cl and extracted with EtOAc. The combined organic layers were washed with brine, dried over anhydrous Na_2SO_4, and concentrated *in vacuo*. The residue was purified by column chromatography (silica gel, hexanes/EtOAc, 15/1) to afford *E*/*Z* (1/5) mixture of **3.46**. [**Isomerization**] To a solution of the mixture **3.46** (213 mg, 1.17 mmol) and PhSH (0.06 mL, 0.58 mmol) in refluxing benzene (25 mL, 0.05 M) was added AIBN (115 mg, 0.7 mmol) in four portions over a period of 8 h. The solvent was evaporated and the crude mixture was purified by column chromatography (silica gel, hexanes/EtOAc, 15/1) to afford alkene **3.46**: ^{1}H NMR (400 MHz, $CDCl_3$) δ 7.27–7.25 (m, 1H), 6.88–6.85 (m, 2H), 6.35 (dd, *J* = 1.2, 15.6 Hz, 1H), 6.23 (dq, *J* = 6.4, 15.6 Hz, 1H), 3.91 (s, 3H), 1.88 (dd, *J* = 1.2, 6.4 Hz, 3H). [**Dihydroxylation**] To a cooled (0 °C) solution of AD-mix-α (1.3 g, 1.4 g/mmol of substrate) and $MeSO_2NH_2$ (89 mg, 0.93 mmol) in *t*-BuOH/H_2O (1/2, 10.5 mL)

was added dropwise alkene **3.47** (170 mg, 0.93 mmol) in *t*-BuOH (3.5 mL, 0.27 M). The reaction mixture was stirred for 48 h at 4 °C. The reaction was quenched by addition of sodium sulfite (1.39 g, 1.5 g/mmol of substrate), diluted with EtOAc, and stirred for 30 min at 25 °C. The layers were separated, and the aqueous layer was extracted with EtOAc. The combined organic layers were washed with 2 N KOH and brine, dried over anhydrous Na_2SO_4, and concentrated *in vacuo*. The residue was purified by column chromatography (silica gel, hexanes/EtOAc, 1/1) to afford **3.47** as a white crystal (218 mg, 69% for 3 steps): ^{1}H NMR (400 MHz, $CDCl_3$) δ 7.30 (d, *J* = 8.0 Hz, 1H), 6.90 (d, *J* = 1.6 Hz, 1H), 6.80 (d, *J* = 2.0, 8.0 Hz, 1H), 4.27 (d, *J* = 7.6 Hz, 1H), 3.87 (s, 3H), 3.80–3.73 (m, 1H), 3.34 (bs, 1H), 2.94 (bs, 1H), 1.02 (d, *J* = 6.4 Hz, 3H).

Preparation of Tosylate 3.49

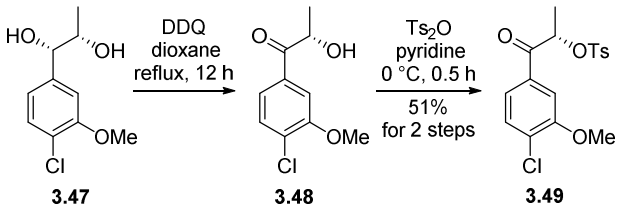

3.47 **3.48** **3.49**

[**Oxidation**] To a solution of diol **3.47** (134 mg, 0.62 mmol) in dioxane (6 mL, 0.1 M) was added DDQ (280 mg, 1.24 mmol) at 25 °C. After stirring for 12 h at reflux, the reaction mixture was cooled to 0 °C, quenched by addition of saturated aqueous sodium thiosulfate and saturated aqueous $NaHCO_3$, diluted with CH_2Cl_2, and stirred vigorously for 1 h. The layers were separated, and the aqueous layer was extracted with CH_2Cl_2.

The combined organic layers were washed with brine, dried over anhydrous Na_2SO_4, and concentrated *in vacuo*. The residue was purified by column chromatography (silica gel, hexanes/EtOAc, 2/1) to afford **3.48**. [**Tosylation**] To a cooled (0 °C) solution of hydroxy ketone **3.48** (100 mg, 0.46 mmol) in pyridine (5 mL, 0.09 M) was added Ts_2O (456 mg, 1.4 mmol). After stirring for 30 min at the same temperature, the reaction was quenched by addition of saturated aqueous NH_4Cl and extracted with CH_2Cl_2. The combined organic layers were washed with brine, dried over anhydrous Na_2SO_4, and concentrated *in vacuo*. The residue was purified by column chromatography (silica gel, hexanes/EtOAc, 4/1) to afford **3.49** as a yellow crystal (116 mg, 51% for 2 steps): ^{1}H NMR (400 MHz, $CDCl_3$) δ 7.75 (d, *J* = 8.4 Hz, 1H), 7.47–7.44 (m, 3H), 7.29 (d, *J* = 8.4 Hz, 2H), 5.74–5.68 (m, 1H), 3.95 (s, 3H), 2.43 (s, 3H), 1.57 (d, *J* = 6.8 Hz, 3H).

Preparation of 3.50 and 3.51

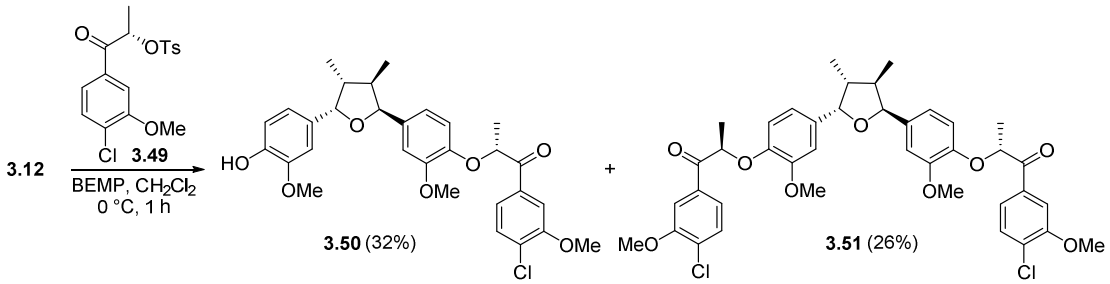

To a cooled (0 °C) solution of the known bis-phenol **3.12**[108] (20 mg, 0.06 mmol) in dry CH_2Cl_2 (1 mL, 0.06 M) was added dropwise BEMP (0.02 mL, 0.06 mmol). The resulting mixture was stirred at the same temperature for 10 min before tosylate **3.49** (21.4 mg,

0.06 mmol) in CH_2Cl_2 (0.5 mL, 0.12 M) was added. After stirring for 1 h at 0 °C, the reaction was quenched by addition of saturated aqueous NH_4Cl and extracted with CH_2Cl_2. The combined organic layers were washed with brine, dried over anhydrous Na_2SO_4, and concentrated *in vacuo*. The residue was purified by column chromatography (silica gel, hexanes/EtOAc, 1/1) to afford **3.50** (10 mg, 32%) and **3.51** (11 mg, 26%): [**For 3.50**] ^{1}H NMR (400 MHz, $CDCl_3$) δ 7.72–7.70 (m, 2H), 7.42 (d, *J* = 8.8 Hz, 1H), 6.90–6.69 (m, 6H), 5.52 (s, 1H), 5.40–5.34 (m, 3H), 3.94 (s, 3H), 3.89 (s, 3H), 3.83 (s, 3H), 2.26–2.18 (m, 2H), 1.70 (d, *J* = 6.8 Hz, 3H), 0.66 (dd, *J* = 6.4, 10.8 Hz, 6H). [**For 3.51**] ^{1}H NMR (400 MHz, $CDCl_3$) δ 7.71–7.68 (m, 4H), 7.42 (d, *J* = 8.8 Hz, 2H), 6.83–6.77 (m, 4H), 6.72–6.67 (m, 2H), 5.40–5.35 (m, 4H), 3.94 (s, 6H), 3.82 (s, 6H), 2.23–2.17 (m, 2H), 1.69 (d, *J* = 6.8 Hz, 6H), 0.62 (d, *J* = 5.6 Hz, 6H).

Preparation of 3.52

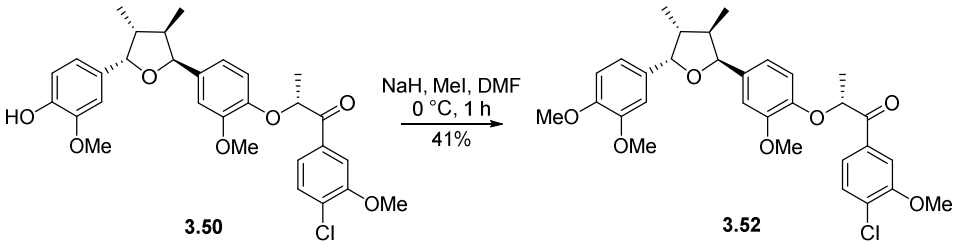

To a cooled (0 °C) solution of phenol **3.50** (7.2 mg, 0.01 mmol) in dry DMF (1 mL, 0.01 M) were added NaH (60% dispersion in mineral oil, 4.1 mg, 0.11 mmol) and MeI (0.01 mL, 0.16 mmol). After stirring for 1 h at the same temperature, the reaction was quenched by addition of H_2O and extracted with EtOAc. The combined organic layers were washed

with brine, dried over anhydrous Na_2SO_4, and concentrated *in vacuo*. The residue was purified by column chromatography (silica gel, hexanes/EtOAc, 3/1) to afford **3.52** (3.0 mg, 41%): ^{1}H NMR (400 MHz, $CDCl_3$) δ 7.76–7.69 (m, 2H), 7.43 (d, *J* = 8.8 Hz, 1H), 6.86–6.78 (m, 5H), 6.72 (ddd, *J* = 1.6, 8.4, 8.4 Hz, 1H), 5.42–5.35 (m, 3H), 3.94 (d, *J* = 1.2 Hz, 3H), 3.89 (s, 3H), 3.88 (s, 3H), 3.84 (s, 3H), 2.26–2.20 (m, 2H), 1.70 (d, *J* = 6.8 Hz, 3H), 0.66 (dd, *J* = 6.4, 10.8 Hz, 6H).

Preparation of 3.53

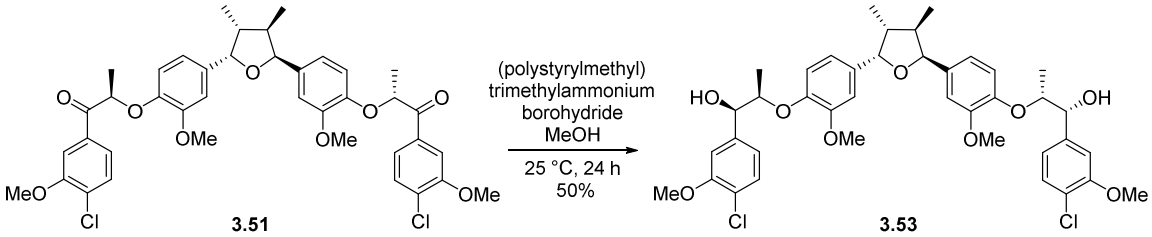

To a stirred solution of ketone **3.51** (8 mg, 0.01 mmol) in MeOH (1.5 mL, 0.01 M) was added polymer-supported borohydride (2 mmol BH_4/g resin, 108 mg, 0.22 mmol). The reaction mixture was stirred with gentle agitation at 25 °C for 24 h. The polymer beads were then removed by filtration and the filtrate was purified by column chromatography (silica gel, hexanes/EtOAc/MeOH, 1/1/0.01) to afford **3.53** (4.0 mg, 50%): ^{1}H NMR (400 MHz, $CDCl_3$) δ 7.32 (d, *J* = 8.0 Hz, 2H), 7.00–6.97 (m, 4H), 6.93–6.90 (m, 4H), 6.85–6.82 (m, 2H), 5.46 (d, *J* = 5.6 Hz, 2H), 4.67 (d, *J* = 7.6 Hz, 2H), 4.24–4.21 (m, 2H), 4.13–4.06 (m, 2H), 3.93 (s, 6H), 3.91 (s, 6H), 2.32–2.26 (m, 2H), 1.19 (dd, *J* = 2.0, 6.4 Hz, 6H), 0.72 (d, *J* = 6.4 Hz, 6H).

Preparation of Diol 3.56

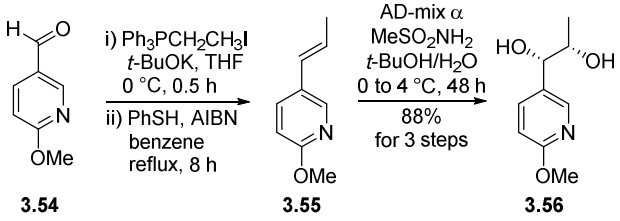

3.54 **3.55** **3.56**

[**Wittig reaction**] To a cooled (0 °C) suspension of ethyltriphenylphosphonium iodide (1.9 g, 4.38 mmol) in THF (25 mL) was added dropwise *t*-BuOK (1.0 M in THF, 3.65 mL, 3.65 mmol). The resulting mixture was stirred at the same temperature for 30 min before aldehyde **3.54** (200 mg, 1.46 mmol) in THF (5 mL, 0.29 M) was added dropwise. After stirring for 30 min at 0 °C, the reaction was quenched by addition of saturated aqueous NH_4Cl and extracted with EtOAc. The combined organic layers were washed with brine, dried over anhydrous Na_2SO_4, and concentrated *in vacuo*. The residue was purified by column chromatography (silica gel, hexanes/EtOAc, 10/1) to afford *E*/*Z* (1/4.4) mixture of **3.55**. [**Isomerization**] To a solution of the mixture **3.55** (174 mg, 1.16 mmol) and PhSH (0.06 mL, 0.06 mmol) in refluxing benzene (25 mL, 0.05 M) was added AIBN (114 mg, 0.7 mmol) in four portions over a period of 8 h. The solvent was evaporated and the crude mixture was purified by column chromatography (silica gel, hexanes/EtOAc, 10/1) to afford alkene **3.55**: ^{1}H NMR (400 MHz, $CDCl_3$) δ 8.04 (d, *J* = 2.4 Hz, 1H), 7.59 (dd, *J* = 2.4, 8.4 Hz, 1H), 6.67 (dd, *J* = 0.4, 8.8 Hz, 1H), 6.33–6.29 (m, 1H), 6.10 (dq, *J* = 6.8, 15.6 Hz, 1H), 3.91 (s, 3H), 1.86 (dd, *J* = 1.6, 6.8 Hz, 3H). [**Dihydroxylation**] To a cooled (0 °C) solution of AD-mix-α (1.3 g, 1.4 g/mmol of substrate) and $MeSO_2NH_2$ (88.3 mg, 0.93 mmol) in *t*-

BuOH/H_2O (1/2, 10.5 mL) was added dropwise alkene **3.55** (138 mg, 0.93 mmol) in *t*-BuOH (3.5 mL, 0.27 M). The reaction mixture was stirred for 48 h at 4 °C. The reaction was quenched by addition of sodium sulfite (1.39 g, 1.5 g/mmol of substrate), diluted with EtOAc, and stirred for 30 min at 25 °C. The layers were separated, and the aqueous layer was extracted with EtOAc. The combined organic layers were washed with 2 N KOH and brine, dried over anhydrous Na_2SO_4, and concentrated *in vacuo*. The residue was purified by column chromatography (silica gel, hexanes/EtOAc, 1/2) to afford **3.56** as a white powder (235 mg, 88% for 3 steps): ^{1}H NMR (400 MHz, $CDCl_3$) δ 8.10 (d, *J* = 2.0 Hz, 1H), 7.59 (dd, *J* = 2.8, 8.8 Hz, 1H), 6.75 (d, *J* = 8.8 Hz, 1H), 4.77 (bs, 2H), 4.36 (dd, *J* = 2.4, 7.6 Hz, 1H), 3.93 (s, 3H), 3.88–3.82 (m, 1H), 1.07 (d, *J* = 6.4 Hz, 3H).

Preparation of Hydroxy Ketone 3.57

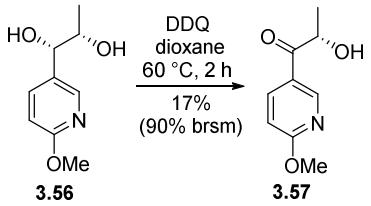

3.56 **3.57**

To a solution of diol **3.56** (218 mg, 1.19 mmol) in dioxane (10 mL, 0.12 M) was added DDQ (540 mg, 2.38 mmol) at 25 °C. The reaction mixture was heated to 60 °C and stirred for 2 h at the same temperature. The reaction mixture was cooled to 0 °C, quenched by addition of saturated aqueous sodium thiosulfate and saturated aqueous $NaHCO_3$, diluted with CH_2Cl_2, and stirred vigorously for 1 h. The layers were separated, and the

aqueous layer was extracted with CH_2Cl_2. The combined organic layers were washed with brine, dried over anhydrous Na_2SO_4, and concentrated *in vacuo*. The residue was purified by column chromatography (silica gel, hexanes/EtOAc, 2/1) to afford **3.57** as a colorless crystal (36 mg, 17%): ^{1}H NMR (400 MHz, $CDCl_3$) δ 8.76 (d, *J* = 2.8 Hz, 1H), 8.13 (dd, *J* = 2.8, 8.8 Hz, 1H), 6.84 (d, *J* = 8.8 Hz, 1H), 5.07 (p, *J* = 6.8 Hz, 1H), 4.03 (s, 3H), 3.73 (d, *J* = 6.4 Hz, 1H), 3.93 (s, 3H), 3.88–3.82 (m, 1H), 1.47 (d, *J* = 6.8 Hz, 3H).

Preparation of Tosylate 3.58

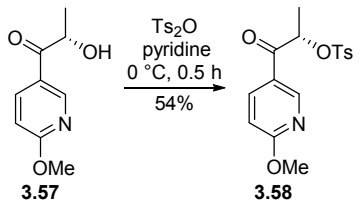

To a cooled (0 °C) solution of hydroxy ketone **3.57** (20 mg, 0.11 mmol) in pyridine (4 mL, 0.03 M) was added Ts_2O (108 mg, 0.33 mmol). After stirring for 30 min at the same temperature, the reaction was quenched by addition of saturated aqueous NH_4Cl and extracted with CH_2Cl_2. The combined organic layers were washed with brine, dried over anhydrous Na_2SO_4, and concentrated *in vacuo*. The residue was purified by column chromatography (silica gel, hexanes/EtOAc, 3/1) to afford **3.58** (20 mg, 54%): ^{1}H NMR (400 MHz, $CDCl_3$) δ 8.76 (d, *J* = 2.4 Hz, 1H), 8.07 (dd, *J* = 2.4, 8.8 Hz, 1H), 7.75 (d, *J* = 8.4 Hz, 2H), 7.28 (d, *J* = 8.0 Hz, 2H), 6.78 (d, *J* = 8.8 Hz, 1H), 5.60 (q, *J* = 6.8 Hz, 1H), 4.02 (s, 3H), 2.42 (s, 3H), 1.59 (d, *J* = 7.2 Hz, 3H).

Preparation of 3.59 and 3.60

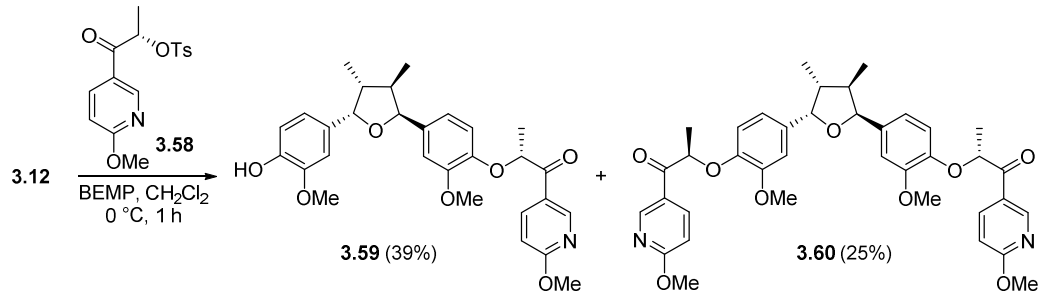

To a cooled (0 °C) solution of the known bis-phenol **3.12**[108] (25 mg, 0.07 mmol) in dry CH_2Cl_2 (1 mL, 0.07 M) was added dropwise BEMP (0.02 mL, 0.07 mmol). The resulting mixture was stirred at the same temperature for 10 min before tosylate **3.58** (24 mg, 0.07 mmol) in CH_2Cl_2 (0.9 mL, 0.07 M) was added. After stirring for 1 h at 0 °C, the reaction was quenched by addition of saturated aqueous NH_4Cl and extracted with CH_2Cl_2. The combined organic layers were washed with brine, dried over anhydrous Na_2SO_4, and concentrated *in vacuo*. The residue was purified by column chromatography (silica gel, hexanes/EtOAc, 4/1) to afford **3.59** (14 mg, 39%) and **3.60** (12 mg, 25%): [**For 3.59**] ^{1}H NMR (400 MHz, $CDCl_3$) δ 9.04 (dd, *J* = 2.4, 2.8 Hz, 1H), 8.30 (ddd, *J* = 2.4, 2.8, 8.8 Hz, 1H), 6.90–6.68 (m, 7H), 5.55 (s, 1H), 5.39 (dd, *J* = 4.4, 5.6 Hz, 2H), 5.30 (dq, *J* = 3.2, 6.8 Hz, 1H), 3.99 (s, 3H), 3.89 (s, 3H), 3.84 (s, 3H), 2.26–2.19 (m, 2H), 1.69 (dd, *J* = 1.2, 6.8 Hz, 3H), 0.66 (dd, *J* = 6.8, 10.8 Hz, 6H). [**For 3.60**] ^{1}H NMR (400 MHz, $CDCl_3$) δ 9.04–9.02 (m, 2H), 8.29 (ddd, *J* = 2.4, 2.8, 8.8 Hz, 2H), 6.83–6.72 (m, 8H), 5.36 (d, *J* = 6.0 Hz, 2H), 5.29 (dq, *J* = 2.8, 6.8, Hz, 2H), 3.99 (s, 6H), 3.83 (s, 6H), 2.23–2.17 (m, 2H), 1.68 (d, *J* = 6.8 Hz, 6H), 0.63 (d, *J* = 6.0 Hz, 6H).

Preparation of 3.61

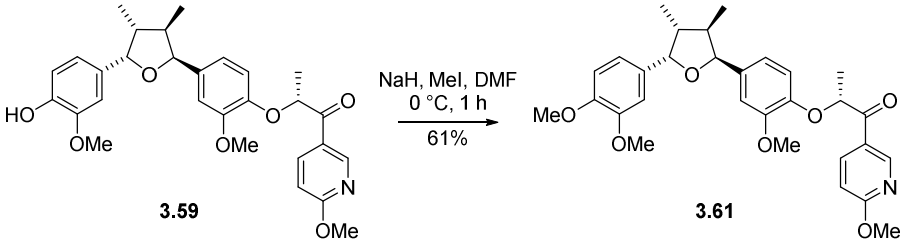

To a cooled (0 °C) solution of phenol **3.59** (14 mg, 0.03 mmol) in dry DMF (1 mL, 0.03 M) were added NaH (60% dispersion in mineral oil, 10 mg, 0.27 mmol) and MeI (0.03 mL, 0.54 mmol). After stirring for 1 h at the same temperature, the reaction was quenched by addition of H_2O and extracted with EtOAc. The combined organic layers were washed with brine, dried over anhydrous Na_2SO_4, and concentrated *in vacuo*. The residue was purified by column chromatography (silica gel, hexanes/EtOAc, 4/1) to afford **3.61** (8.6 mg, 61%): ^{1}H NMR (400 MHz, $CDCl_3$) δ 9.04 (dd, *J* = 2.4, 2.8 Hz, 1H), 8.30 (ddd, *J* = 2.4, 2.8, 8.8, Hz, 1H), 6.86–6.68 (m, 7H), 5.40 (dd, *J* = 6.4, 6.8 Hz, 2H), 5.30 (dq, *J* = 3.2, 7.2 Hz, 1H), 4.00 (s, 3H), 3.88 (d, *J* = 4.0, 6H), 3.85 (s, 3H), 2.29–2.19 (m, 2H), 1.69 (d, *J* = 6.8 Hz, 3H), 0.71–0.63 (m, 6H).

Preparation of 3.62

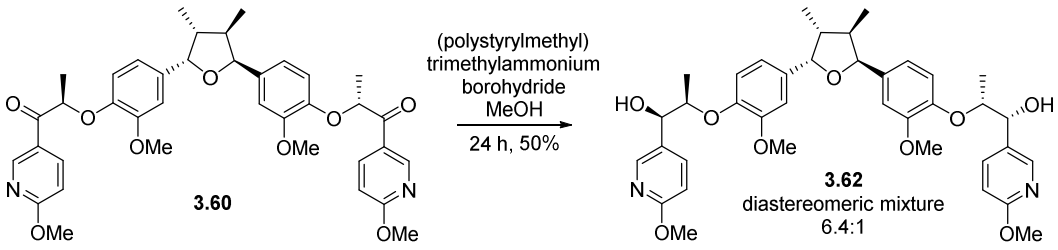

To a stirred solution of ketone **3.60** (8 mg, 0.01 mmol) in MeOH (1.5 mL, 0.007 M) was added polymer-supported borohydride (2 mmol BH_4/g resin, 119 mg, 0.24 mmol). The reaction mixture was stirred with gentle agitation at 25 °C for 24 h. The polymer beads were then removed by filtration and the filtrate was purified by column chromatography (silica gel, hexanes/EtOAc/MeOH, 1/1/0.01) to afford a 6.4:1 diastereomeric mixture of **3.62** and (7*S*, 7′′′*S*)-epimer (4 mg, 50%): ^{1}H NMR (400 MHz, $CDCl_3$) δ 8.16 (d, *J* = 2.0 Hz, 2H), 7.63 (dd, *J* = 2.4, 8.8 Hz, 2H), 6.98 (d, *J* = 8.0 Hz, 2H), 6.91–6.90 (m, 2H), 6.83 (d, *J* = 8.4 Hz, 2H), 6.74 (d, *J* = 8.4 Hz, 2H), 5.46 (d, *J* = 6.0 Hz, 2H), 4.68 (d, *J* = 8.4 Hz, 2H), 4.19 (d, *J* = 7.2 Hz, 2H), 4.15–4.08 (m, 2H), 3.94–3.91 (m, 12H), 2.32–2.26 (m, 2H), 1.20–1.16 (m, 6H), 0.72 (d, *J* = 6.4 Hz, 6H).

Preparation of Diol 3.65

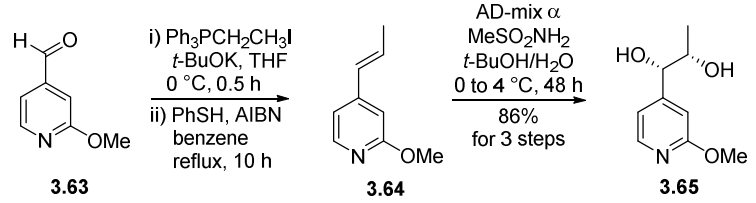

[**Wittig reaction**] To a cooled (0 °C) suspension of ethyltriphenylphosphonium iodide (2.75 g, 6.56 mmol) in THF (25 mL) was added dropwise *t*-BuOK (1.0 M in THF, 5.5 mL, 5.5 mmol). The resulting mixture was stirred at the same temperature for 30 min before aldehyde **3.63** (300 mg, 2.19 mmol) in THF (5 mL, 0.44 M) was added dropwise. After stirring for 30 min at 0 °C, the reaction was quenched by addition of saturated aqueous

NH_4Cl and extracted with EtOAc. The combined organic layers were washed with brine, dried over anhydrous Na_2SO_4, and concentrated *in vacuo*. The residue was purified by column chromatography (silica gel, hexanes/EtOAc, 10/1) to afford *E*/*Z* (1.17/1) mixture of **3.64**. [**Isomerization**] To a solution of the mixture **3.64** (261 mg, 1.75 mmol) and PhSH (0.09 mL, 0.88 mmol) in refluxing benzene (30 mL, 0.03 M) was added AIBN (172 mg, 1.05 mmol) in four portions over a period of 10 h. The solvent was evaporated and the crude mixture was purified by column chromatography (silica gel, hexanes/EtOAc, 10/1) to afford alkene **3.64**: ^{1}H NMR (400 MHz, $CDCl_3$) δ 8.1 (d, *J* = 5.6 Hz, 1H), 8.05 (d, *J* = 5.2 Hz, 1H), 6.84 (d, *J* = 5.2 Hz, 1H), 6.60 (s, 1H), 6.43 (dq, *J* = 6.4, 15.6 Hz, 1H), 6.29 (d, *J* = 15.6 Hz, 1H), 3.92 (s, 3H), 1.90 (dd, *J* = 0.8, 6.4 Hz, 3H). [**Dihydroxylation**] To a cooled (0 °C) solution of AD-mix-*α* (1.96 g, 1.4 g/mmol of substrate) and $MeSO_2NH_2$ (133 mg, 1.4 mmol) in *t*-BuOH/H_2O (1/2, 14.7 mL) was added dropwise alkene **3.64** (209 mg, 1.4 mmol) in *t*-BuOH (5.3 mL, 0.26 M). The reaction mixture was stirred for 48 h at 4 °C. The reaction was quenched by addition of sodium sulfite (2.03 g, 1.5 g/mmol of substrate), diluted with EtOAc, and stirred for 30 min at 25 °C. The layers were separated, and the aqueous layer was extracted with EtOAc. The combined organic layers were washed with 2 N KOH and brine, dried over anhydrous Na_2SO_4, and concentrated *in vacuo*. The residue was purified by column chromatography (silica gel, hexanes/EtOAc, 1/2) to afford **3.65** as a colorless crystal (345 mg, 86% for 3 steps): ^{1}H NMR (400 MHz, $CDCl_3$) δ

8.13 (d, *J* = 5.2 Hz, 1H), 6.86 (d, *J* = 5.2 Hz, 1H), 6.74 (s, 1H), 4.70 (bs, 1H), 4.36 (d, *J* = 6.8 Hz, 1H), 3.94 (s, 3H), 3.85 (p, *J* = 6.4 Hz, 1H), 1.14 (dd, *J* = 2.8, 6.4 Hz, 3H).

Preparation of 3.69

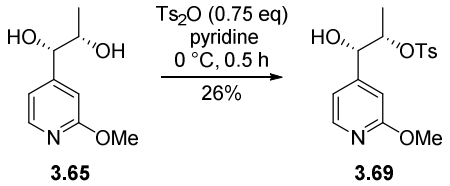

3.65 **3.69**

To a cooled (0 °C) solution of diol **3.65** (32 mg, 0.17 mmol) in pyridine (2 mL, 0.09 M) was added Ts_2O (43.5 mg, 0.13 mmol). After stirring for 30 min at the same temperature, the reaction was quenched by addition of saturated aqueous NH_4Cl and extracted with CH_2Cl_2. The combined organic layers were washed with brine, dried over anhydrous Na_2SO_4, and concentrated *in vacuo*. The residue was purified by column chromatography (silica gel, hexanes/EtOAc, 3/4) to afford **3.69** as a white foam (15 mg, 26%): ^{1}H NMR (400 MHz, $CDCl_3$) δ 8.28 (dd, *J* = 0.8, 5.2 Hz, 1H), 7.73 (d, *J* = 8.4 Hz, 2H), 7.30–7.26 (m, 2H), 7.23–7.19 (m, 1H), 7.06 (dd, *J* = 0.8, 1.6 Hz, 1H), 5.60 (q, *J* = 6.8 Hz, 1H), 3.97 (s, 3H), 2.43 (s, 3H), 1.57 (d, *J* = 7.2 Hz, 3H).

Preparation of 3.70

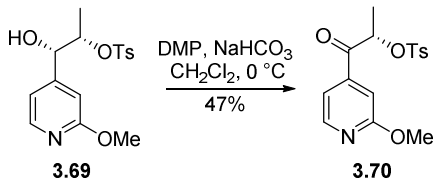

3.69 **3.70**

To a cooled (0 °C) solution of alcohol **3.69** (62 mg, 0.18 mmol) in dry CH_2Cl_2 (2 mL, 0.09 M) were added Dess–Martin periodinane (156 mg, 0.37 mmol) and $NaHCO_3$ (62 mg, 0.74 mmol). After stirring for 30 min at the same temperature, the reaction was quenched by addition of saturated aqueous $NaHCO_3$ and extracted with CH_2Cl_2. The combined organic layers were washed with brine, dried over anhydrous Na_2SO_4, and concentrated *in vacuo*. The residue was purified by column chromatography (silica gel, hexanes/EtOAc, 2/1) to afford **3.70** (29 mg, 47%): ^{1}H NMR (400 MHz, $CDCl_3$) δ 8.28 (dd, *J* = 0.8, 5.2 Hz, 1H), 7.74 (d, *J* = 8.4 Hz, 2H), 7.30–7.26 (m, 2H), 7.21 (dd, *J* = 1.6, 5.2 Hz, 1H), 7.06 (dd, *J* = 0.8, 1.6 Hz, 1H), 5.60 (q, *J* = 6.8 Hz, 1H), 3.97 (s, 3H), 2.43 (s, 3H), 1.57 (d, *J* = 6.8 Hz, 3H).

Preparation of 3.71 and 3.72

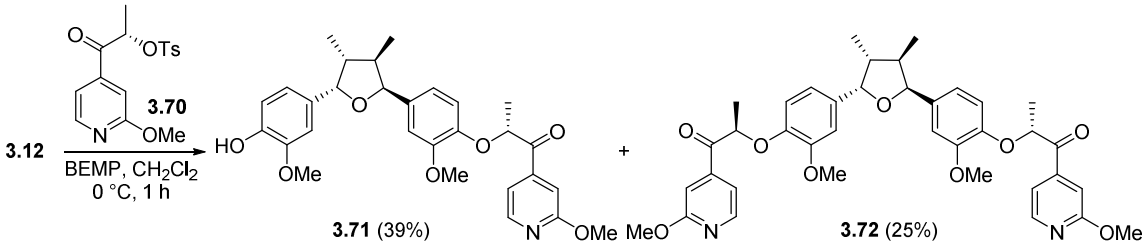

To a cooled (0 °C) solution of the known bis-phenol **3.12**[108] (20 mg, 0.06 mmol) in dry CH_2Cl_2 (1 mL, 0.06 M) was added dropwise BEMP (0.017 mL, 0.06 mmol). The resulting mixture was stirred at the same temperature for 10 min before tosylate **3.70** (19.5 mg, 0.06 mmol) in CH_2Cl_2 (0.5 mL, 0.12 M) was added. After stirring for 1 h at 0 °C, the reaction was quenched by addition of saturated aqueous NH_4Cl and extracted with

CH_2Cl_2. The combined organic layers were washed with brine, dried over anhydrous Na_2SO_4, and concentrated *in vacuo*. The residue was purified by column chromatography (silica gel, hexanes/EtOAc, 2.5/1) to afford **3.71** (10 mg, 34%) and **3.72** (5 mg, 13%): [**For 3.71**] ^{1}H NMR (400 MHz, $CDCl_3$) δ 8.28 (d, *J* = 5.2 Hz, 1H), 7.43–7.40 (m, 1H), 7.38 (d, *J* = 4.8 Hz, 1H), 6.90–6.71 (m, 6H), 5.53 (s, 1H), 5.39 (d, *J* = 4.8 Hz, 2H), 5.32 (dq, *J* = 2.4, 6.8 Hz, 1H), 3.96 (s, 3H), 3.89 (s, 3H), 3.81 (s, 3H), 2.27–2.19 (m, 2H), 1.65 (d, *J* = 6.8 Hz, 3H), 0.66 (dd, *J* = 6.4, 10.8 Hz, 6H). [**For 3.72**] ^{1}H NMR (400 MHz, $CDCl_3$) δ 8.28 (d, *J* = 5.2 Hz, 2H), 7.42–7.40 (m, 2H), 7.38 (dd, *J* = 0.8, 4.8 Hz, 2H), 6.84–6.80 (m, 4H), 6.73–6.69 (m, 2H), 5.43–5.30 (m, 4H), 3.96 (s, 6H), 3.80 (s, 6H), 2.24–2.18 (m, 2H), 1.65 (d, *J* = 6.8 Hz, 6H), 0.63 (d, *J* = 6.8 Hz, 6H).

Preparation of 3.73

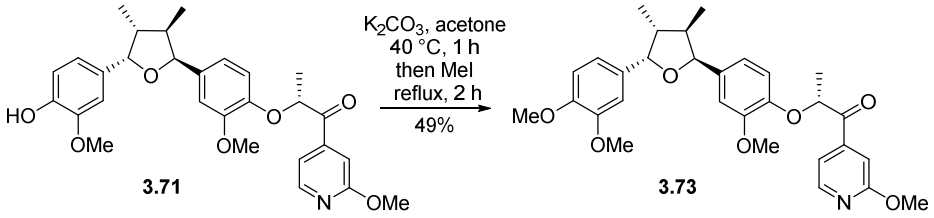

To a solution of phenol **3.71** (8 mg, 0.02 mmol) in acetone (1.5 mL, 0.01 M) was added K_2CO_3 (4.8 mg, 0.03 mmol) at 25 °C. After stirring for 1 h at 40 °C, the reaction mixture was cooled to 25 °C and treated with MeI (0.006 mL, 0.09 mmol) at the same temperature. After stirring for 2 h at reflux, the reaction mixture was cooled to 25 °C, diluted with EtOAc, and rinsed with saturated aqueous NH_4Cl. The layers were

separated, and the aqueous layer was extracted with EtOAc. The combined organic layers were washed with brine, dried over anhydrous Na_2SO_4, and concentrated *in vacuo*. The residue was purified by column chromatography (silica gel, hexanes/EtOAc, 2/1) to afford **3.73** (4 mg, 49%): ^{1}H NMR (400 MHz, $CDCl_3$) δ 8.29 (d, *J* = 5.6 Hz, 1H), 7.43–7.40 (m, 1H), 7.38 (d, *J* = 4.8 Hz, 1H), 6.86–6.71 (m, 6H), 5.41 (dd, *J* = 5.6, 5.6 Hz, 2H), 5.32 (dq, *J* = 2.8, 7.2 Hz, 1H), 3.97 (s, 3H), 3.89 (s, 3H), 3.88 (s, 3H), 3.82 (s, 3H), 2.28–2.20 (m, 2H), 1.65 (d, *J* = 7.2 Hz, 3H), 0.66 (dd, *J* = 2.8, 10.0 Hz, 6H).

Preparation of 3.72

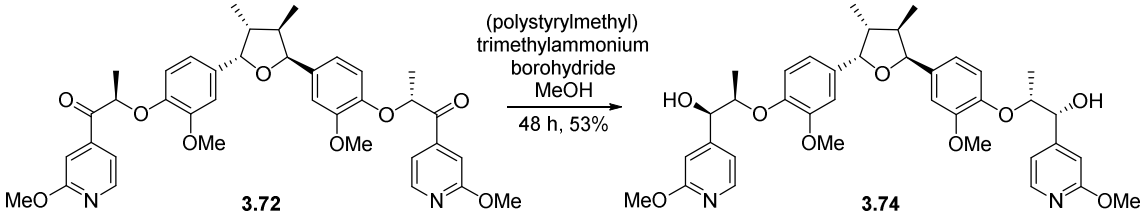

To a stirred solution of ketone **3.72** (3 mg, 0.004 mmol) in MeOH (1 mL, 0.004 M) was added polymer-supported borohydride (2 mmol BH_4/g resin, 45 mg, 0.09 mmol). The reaction mixture was stirred with gentle agitation at 25 °C for 48 h. The polymer beads were then removed by filtration and the filtrate was purified by column chromatography (silica gel, hexanes/EtOAc/MeOH, 1/1/0.01) to afford **3.74** (1.6 mg, 53%): ^{1}H NMR (400 MHz, $CDCl_3$) δ 8.12 (d, *J* = 5.6 Hz, 2H), 7.00–6.89 (m, 6H), 6.82–6.80 (m, 4H), 5.45 (d, *J* = 5.6 Hz, 2H), 4.64 (d, *J* = 8.0 Hz, 2H), 4.20–4.06 (m, 4H), 3.93 (s, 6H), 3.92 (s, 6H), 2.31–2.24 (m, 2H), 1.22 (dd, *J* = 2.0, 6.0 Hz, 6H), 0.70 (d, *J* = 6.0 Hz, 6H).

Preparation of Diol 3.77

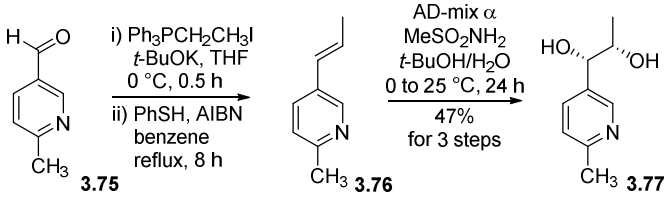

[**Wittig reaction**] To a cooled (0 °C) suspension of ethyltriphenylphosphonium iodide (2.25 g, 5.37 mmol) in THF (20 mL) was added dropwise *t*-BuOK (1.0 M in THF, 4.48 mL, 4.48 mmol). The resulting mixture was stirred at the same temperature for 30 min before aldehyde **3.75** (0.2 mL, 1.79 mmol) in THF (5 mL, 0.36 M) was added dropwise. After stirring for 30 min at 0 °C, the reaction was quenched by addition of saturated aqueous NH_4Cl and extracted with EtOAc. The combined organic layers were washed with brine, dried over anhydrous Na_2SO_4, and concentrated *in vacuo*. The residue was purified by column chromatography (silica gel, hexanes/EtOAc, 4/1) to afford *E*/*Z* (1/3.9) mixture of **3.76**. [**Isomerization**] To a solution of the mixture **3.76** (190 mg, 1.43 mmol) and PhSH (0.08 mL, 0.79 mmol) in refluxing benzene (25 mL, 0.06 M) was added AIBN (141 mg, 0.86 mmol) in four portions over a period of 8 h. The solvent was evaporated and the crude mixture was purified by column chromatography (silica gel, hexanes/EtOAc, 4/1) to afford alkene **3.76**: ^{1}H NMR (400 MHz, $CDCl_3$) δ 8.39 (d, *J* = 2.0 Hz, 1H), 7.51 (dd, *J* = 2.4, 8.0 Hz, 1H), 7.04 (d, *J* = 8.4 Hz, 1H), 6.32 (d, *J* = 16.8 Hz, 1H), 6.22 (dq, *J* = 6.4, 16.8 Hz, 1H), 2.49 (s, 3H), 1.86 (dd, *J* = 1.2, 6.4 Hz, 3H). [**Dihydroxylation**] To a cooled (0 °C) solution of AD-mix-α (1.6 g, 1.4 g/mmol of substrate) and $MeSO_2NH_2$ (109 mg, 1.15

mmol) in *t*-BuOH/H_2O (1/2, 13.5 mL) was added dropwise alkene **3.76** (152 mg, 1.15 mmol) in *t*-BuOH (4.5 mL, 0.26 M). After stirring for 24 h at 25 °C, the reaction mixture was cooled to 0 °C, quenched by addition of sodium sulfite (1.66 g, 1.5 g/mmol of substrate), diluted with EtOAc, and stirred for 30 min at 25 °C. The layers were separated, and the aqueous layer was extracted with EtOAc. The combined organic layers were washed with 2 N KOH and brine, dried over anhydrous Na_2SO_4, and concentrated *in vacuo*. The residue was purified by column chromatography (silica gel, CH_2Cl_2/MeOH, 10/1) to afford **3.77** (141 mg, 47%): ^{1}H NMR (400 MHz, $CDCl_3$) δ 8.31 (s, 1H), 7.58 (dd, *J* = 1.2, 7.6 Hz, 1H), 7.12 (d, *J* = 8.0 Hz, 1H), 4.35 (d, *J* = 7.2 Hz, 1H), 3.82 (p, *J* = 6.4 Hz, 1H), 2.49 (s, 3H), 1.06 (d, *J* = 6.0 Hz, 3H).

Preparation of 3.81

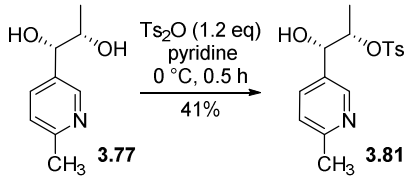

To a cooled (0 °C) solution of diol **3.77** (75 mg, 0.45 mmol) in pyridine (5 mL, 0.09 M) was added Ts_2O (176 mg, 0.54 mmol). After stirring for 30 min at the same temperature, the reaction was quenched by addition of saturated aqueous NH_4Cl and extracted with CH_2Cl_2. The combined organic layers were washed with brine, dried over anhydrous Na_2SO_4, and concentrated *in vacuo*. The residue was purified by column chromatography (silica gel, CH_2Cl_2/MeOH, 20/1) to afford **3.81** as a white foam (60 mg, 41%): ^{1}H NMR

(400 MHz, $CDCl_3$) δ 8.36 (d, *J* = 2.0 Hz, 1H), 7.75 (d, *J* = 8.4 Hz, 2H), 7.54 (dd, *J* = 2.4, 8.0 Hz, 1H), 7.31 (d, *J* = 8.0 Hz, 2H), 7.11 (d, *J* = 8.0 Hz, 1H), 4.74 (p, *J* = 6.4 Hz, 1H), 4.67 (d, *J* = 6.8 Hz, 1H), 2.53 (s, 3H), 2.45 (s, 3H), 1.15 (d, *J* = 6.4 Hz, 3H).

Preparation of 3.82

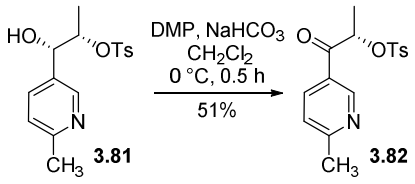

To a cooled (0 °C) solution of alcohol **3.81** (60 mg, 0.19 mmol) in dry CH_2Cl_2 (4 mL, 0.05 M) were added Dess–Martin periodinane (158 mg, 0.37 mmol) and $NaHCO_3$ (62.5 mg, 0.74 mmol). After stirring for 30 min at the same temperature, the reaction was quenched by addition of saturated aqueous $NaHCO_3$ and extracted with CH_2Cl_2. The combined organic layers were washed with brine, dried over anhydrous Na_2SO_4, and concentrated *in vacuo*. The residue was purified by column chromatography (silica gel, hexanes/EtOAc, 1/1) to afford **3.82** (30 mg, 51%): ^1H NMR (400 MHz, $CDCl_3$) δ 8.98 (d, *J* = 2.4 Hz, 1H), 8.09 (dd, *J* = 2.4, 8.0 Hz, 1H), 7.75 (d, *J* = 8.4 Hz, 2H), 7.29–7.24 (m, 3H), 5.63 (q, *J* = 6.8 Hz, 1H), 2.63 (s, 3H), 2.42 (s, 3H), 1.59 (d, *J* = 6.8 Hz, 3H).

Preparation of 3.83 and 3.84

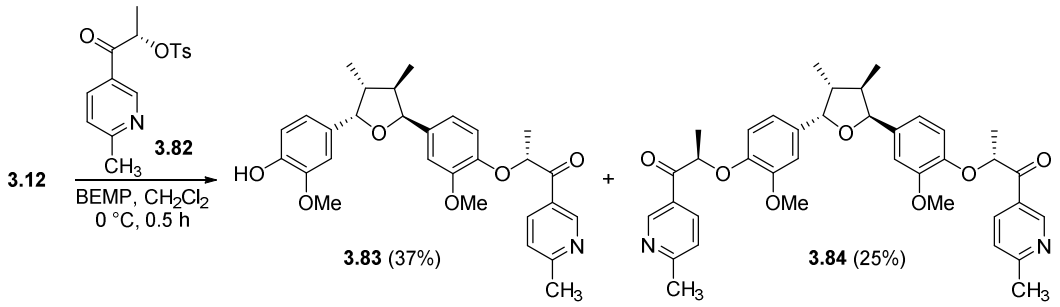

To a cooled (0 °C) solution of the known bis-phenol **3.12**[108] (19 mg, 0.06 mmol) in dry CH_2Cl_2 (1 mL, 0.06 M) was added dropwise BEMP (0.02 mL, 0.06 mmol). The resulting mixture was stirred at the same temperature for 10 min before tosylate **3.82** (18 mg, 0.06 mmol) in CH_2Cl_2 (0.5 mL, 0.12 M) was added. After stirring for 30 min at 0 °C, the reaction was quenched by addition of saturated aqueous NH_4Cl and extracted with CH_2Cl_2. The combined organic layers were washed with brine, dried over anhydrous Na_2SO_4, and concentrated *in vacuo*. The residue was purified by column chromatography (silica gel, hexanes/EtOAc, 1/1) to afford **3.83** (10 mg, 37%) and **3.84** (7 mg, 26%): [**For 3.83**] ^{1}H NMR (400 MHz, $CDCl_3$) δ 9.25 (s, 1H), 8.32–8.29 (m, 1H), 7.24 (dd, *J* = 1.6, 8.4 Hz, 1H), 6.89–6.69 (m, 6H), 5.57 (bs, 1H), 5.39 (dd, *J* = 4.0, 6.0 Hz, 2H), 5.33 (dq, *J* = 2.8, 6.8 Hz, 1H), 3.89 (s, 3H), 3.83 (s, 3H), 2.61 (s, 3H), 2.26–2.19 (m, 2H), 1.69 (d, *J* = 6.8 Hz, 3H), 0.65 (dd, *J* = 6.4, 11.6 Hz, 6H). [**For 3.84**] ^{1}H NMR (400 MHz, $CDCl_3$) δ 9.24 (s, 2H), 8.31–8.28 (m, 2H), 7.23 (d, *J* = 8.4 Hz, 2H), 6.80 (dd, *J* = 3.6, 8.0 Hz, 4H), 6.70 (dd, *J* = 9.2 Hz, 2H), 5.37–5.29 (m, 4H), 3.82 (s, 6H), 2.61 (s, 6H), 2.23–2.17 (m, 2H), 1.68 (d, *J* = 6.8 Hz, 6H), 0.62 (d, *J* = 6.0 Hz, 6H).

Preparation of 3.85

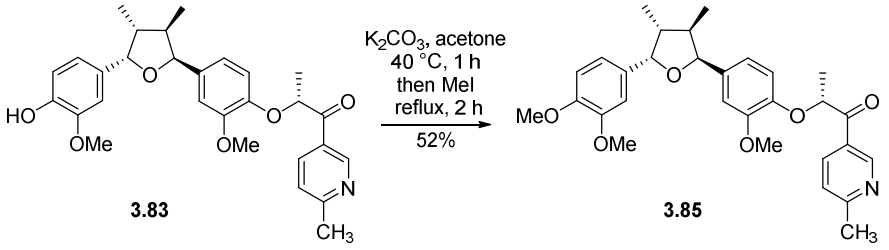

To a solution of phenol **3.83** (15 mg, 0.03 mmol) in acetone (3 mL, 0.01 M) was added K_2CO_3 (8.5 mg, 0.06 mmol) at 25 °C. After stirring for 1 h at 40 °C, the reaction mixture was cooled to 25 °C and treated with MeI (0.08 mL, 0.12 mmol) at the same temperature. After stirring for 2 h at reflux, the reaction mixture was cooled to 25 °C, diluted with EtOAc, and rinsed with saturated aqueous NH_4Cl. The layers were separated, and the aqueous layer was extracted with EtOAc. The combined organic layers were washed with brine, dried over anhydrous Na_2SO_4, and concentrated *in vacuo*. The residue was purified by column chromatography (silica gel, hexanes/EtOAc, 3/2) to afford **3.85** (8 mg, 52%): ^{1}H NMR (400 MHz, $CDCl_3$) δ 9.26 (s, 1H), 8.32–8.30 (m, 1H), 7.24–7.22 (m, 1H), 6.89–6.70 (m, 6H), 5.42–5.37 (m, 2H), 5.33 (dq, *J* = 2.4, 6.8 Hz, 1H), 3.89 (s, 3H), 3.88 (s, 3H), 3.83 (s, 3H), 2.62 (s, 3H), 2.28–2.19 (m, 2H), 1.69 (d, *J* = 6.8 Hz, 3H), 0.66 (dd, *J* = 6.0, 11.2 Hz, 6H).

Preparation of 3.86

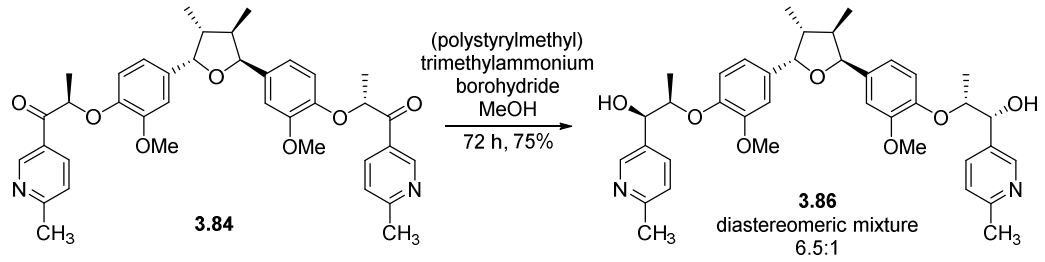

To a stirred solution of **3.84** (4 mg, 0.006 mmol) in MeOH (1.5 mL, 0.004 M) was added polymer-supported borohydride (2 mmol BH_4/g resin, 63 mg, 0.13 mmol). The reaction mixture was stirred with gentle agitation at 25 °C for 72 h. The polymer beads were then removed by filtration and the filtrate was purified by column chromatography (silica gel, CH_2Cl_2/MeOH, 35/1) to afford a 6.5:1 diastereomeric mixture of **3.86** and (7*S*, 7′′′*S*)-epimer (3 mg, 75%): ^{1}H NMR (400 MHz, $CDCl_3$) δ 8.51 (d, *J* = 2.0 Hz, 2H), 7.63 (d, *J* = 7.2 Hz, 2H), 7.15 (d, *J* = 8.0 Hz, 2H), 6.98 (d, *J* = 8.0 Hz, 2H), 6.91–6.90 (m, 2H), 6.83 (d, *J* = 8.4 Hz, 2H), 5.46 (d, *J* = 6.0 Hz, 2H), 4.71 (d, *J* = 8.4 Hz, 2H), 4.24–4.21 (m, 2H), 4.16–4.08 (m, 2H), 3.92 (s, 6H), 2.56 (s, 6H), 2.32–2.26 (m, 2H), 1.19 (dd, *J* = 2.0, 6.0 Hz, 6H), 0.71 (d, *J* = 6.8 Hz, 6H).

Preparation of Ketone 3.94

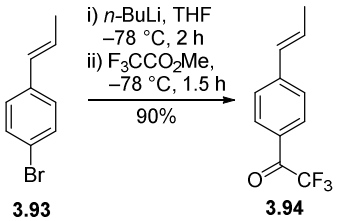

To a cooled (–78 °C) solution of the known bromide **3.93**[137] (340 mg, 1.73 mmol) in dry THF (15 mL, 0.12 M) was added dropwise *n*-BuLi (2.3 M in hexane, 1.13 mL, 2.59 mmol). The resulting mixture was stirred for 2 h at the same temperature before methylfluoroacetate (0.23 mL, 2.24 mmol) in dry THF (9 mL, 0.25 M) was added dropwise. After stirring for 1.5 h at the same temperature, the reaction was quenched by addition of saturated aqueous NH_4Cl and extracted with Et_2O. The combined organic layers were washed with brine, dried over anhydrous Na_2SO_4, and concentrated *in vacuo*. The residue was purified by column chromatography (silica gel, hexanes) to afford **3.94** (337 mg, 90%): ^{1}H NMR (400 MHz, $CDCl_3$) δ 8.00 (d, *J* = 8.0 Hz, 2H), 7.46 (d, *J* = 8.4 Hz, 2H), 6.51–6.43 (m, 2H), 1.95 (d, *J* = 5.2 Hz, 3H).

Preparation of Oxime 3.95

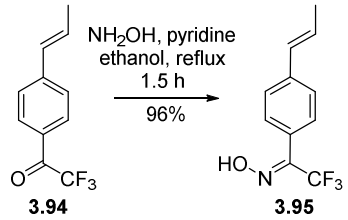

3.94 **3.95**

To a solution of ketone **3.94** in pyridine/ethanol (2/1, 6 mL) was added hydroxylamine hydrochloride (337 mg, 1.57 mmol) at 25 °C. After stirring for 1.5 h at reflux, the solvent was removed under reduced pressure. The residue was extracted with EtOAc/water mixture, dried over anhydrous Na_2SO_4, and concentrated *in vacuo*. The residue was

purified by column chromatography (silica gel, hexanes/EtOAc, 15/1) to afford **3.95** (348 mg, 96%).

Preparation of Tosyl Oxime 3.96

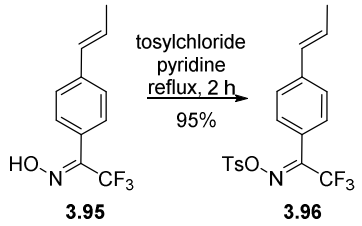

3.95 **3.96**

To a solution of oxime **3.95** (348 mg, 1.52 mmol) in pyridine (6 mL, 0.25 M) was added TsCl (434 mg, 2.28 mmol) at 25 °C. After stirring for 2 h at reflux, the solvent was removed under reduced pressure. The residue was extracted with EtOAc/water mixture, dried over anhydrous Na_2SO_4, and concentrated *in vacuo*. The residue was purified by column chromatography (silica gel, hexanes/EtOAc, 20/1) to afford **3.96** as a yellow powder (555 mg, 95%): ^{1}H NMR (400 MHz, $CDCl_3$) δ 7.91 (dd, *J* = 8.4, 14.4 Hz, 2H), 7.42–7.36 (m, 6H), 6.38 (dd, *J* = 4.0, 9.6 Hz, 2H), 2.48 (d, *J* = 5.6 Hz, 3H), 1.92 (d, *J* = 5.2 Hz, 3H).

Preparation of Diaziridine 3.97

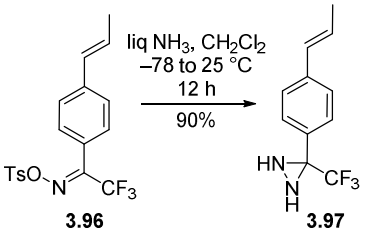

3.96 **3.97**

To a cooled (–78 °C) solution of tosyloxime **3.96** (550 1.43 mg, mmol) in CH_2Cl_2 (10 mL, 0.14 M) was bubbled NH_3 gas. The resulting mixture was stirred in a sealed tube for 5 min at –78 °C and slowly warmed to 25 °C. After stirring for 12 h at the same temperature, the reaction mixture was cooled to –78 °C, and the ammonia was evaporated for 6 h at 25 °C. The solid was removed by filtration, the filtrate was washed with water, and extracted with CH_2Cl_2. The combined organic layers were washed with brine, dried over anhydrous Na_2SO_4, and concentrated *in vacuo*. The residue was purified by column chromatography (silica gel, hexanes/EtOAc, 10/1) to afford **3.97** (296 mg, 90%): ^{1}H NMR (400 MHz, $CDCl_3$) δ 7.53–7.49 (m, 2H), 7.37–7.32 (m, 2H), 6.43–6.36 (m, 1H), 6.30 (dq, *J* = 6.4, 19.2 Hz, 1H), 2.77 (bs, 1H), 2.20 (bs, 1H), 1.91–1.86 (m, 3H).

Preparation of Diazirine 3.98

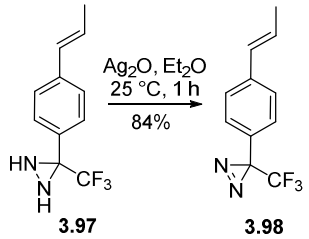

3.97 **3.98**

To a solution of diaziridine **3.97** (290 mg, 1.27 mmol) in dry Et_2O (10 mL, 0.13 M) was added a freshly prepared Ag_2O (883 mg, 3.81 mmol) at 25 °C. After stirring for 1 h at the same temperature, the reaction mixture was filtered, the organic layers were dried over anhydrous Na_2SO_4, and concentrated *in vacuo*. The residue was purified by column

chromatography (silica gel, hexanes/EtOAc, 20/1) to afford **3.98** as a yellow oil (244 mg, 84%).

Preparation of Diol 3.99

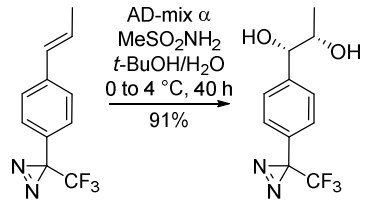

To a cooled (0 °C) solution of AD-mix-α (1.5 g, 1.4 g/mmol of substrate) and $MeSO_2NH_2$ (103 mg, 1.08 mmol) in *t*-BuOH/H_2O (1/2, 12 mL) was added dropwise alkene **3.98** (244 mg, 1.08 mmol) in *t*-BuOH (4 mL, 0.27 M). The reaction mixture was stirred for 40 h at 4 °C. The reaction was quenched by addition of sodium sulfite (1.55 g, 1.5 g/mmol of substrate), diluted with EtOAc, and stirred for 30 min at 25 °C. The layers were separated, and the aqueous layer was extracted with EtOAc. The combined organic layers were washed with 2 N KOH and brine, dried over anhydrous Na_2SO_4, and concentrated *in vacuo*. The residue was purified by column chromatography (silica gel, hexanes/EtOAc, 3/2) to afford **3.99** (255 mg, 91%): ^{1}H NMR (400 MHz, $CDCl_3$) δ 7.38 (d, *J* = 8.4 Hz, 2H), 7.18 (d, *J* = 8.4 Hz, 2H), 4.40 (d, *J* = 7.2 Hz, 1H), 3.81 (p, *J* = 6.4 Hz, 1H), 2.42 (bs, 2H), 1.07 (d, *J* = 6.4 Hz, 3H).

Preparation of Hydroxy Ketone 3.100

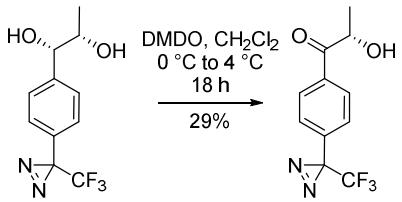

3.99 **3.100**

To a cooled (0 °C) solution of diol **3.99** (100 mg, 0.38 mmol) in CH_2Cl_2 (10 mL, 0.04 M) was added DMDO (0.1 M in acetone, 8.5 mL, 0.85 mmol). After stirring for 18 h at the same temperature, the solvent was removed under reduced pressure. The residue was purified by column chromatography (silica gel, hexanes/EtOAc, 4/1) to afford **3.100** (29 mg, 29%): ^{1}H NMR (400 MHz, $CDCl_3$) δ 7.95 (d, *J* = 8.8 Hz, 2H), 7.31 (d, *J* = 8.0 Hz, 2H), 5.14 (dq, *J* = 6.4, 6.8 Hz, 1H), 3.65 (d, *J* = 6.8, 1H), 1.44 (d, *J* = 6.8 Hz, 3H).

Preparation of Tosylate 3.105

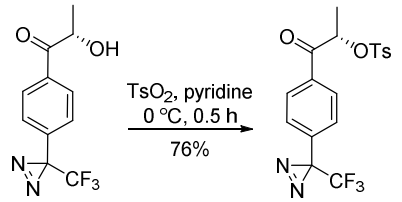

3.100 **3.105**

To a cooled (0 °C) solution of hydroxy ketone **3.100** (29 mg, 0.11 mmol) in pyridine (3 mL, 0.04 M) was added Ts_2O (55 mg, 0.17 mmol). After stirring for 30 min at the same temperature, the reaction was quenched by addition of saturated aqueous NH_4Cl and extracted with CH_2Cl_2. The combined organic layers were washed with brine, dried over

anhydrous Na_2SO_4, and concentrated *in vacuo*. The residue was purified by column chromatography (silica gel, hexanes/EtOAc, 5/1) to afford **3.105** as a white powder (36 mg, 76%): ^{1}H NMR (400 MHz, $CDCl_3$) δ 7.91 (d, *J* = 8.8 Hz, 2H), 7.72 (d, *J* = 8.4 Hz, 2H), 7.26 (dd, *J* = 8.4, 8.4 Hz, 4H), 5.67 (q, *J* = 6.8 Hz, 1H), 2.42 (s, 3H), 1.58 (d, *J* = 6.8 Hz, 3H).

Preparation of 3.106

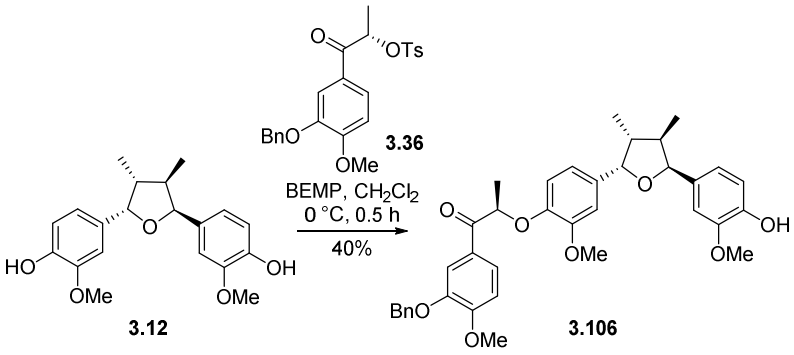

To a cooled (0 °C) solution of the known bis-phenol **3.12**[108] (35 mg, 0.1 mmol) in dry CH_2Cl_2 (1 mL, 0.1 M) was added dropwise BEMP (0.03 mL, 0.1 mmol). The resulting mixture was stirred at the same temperature for 10 min before tosylate **3.36** (45 mg, 0.1 mmol) in CH_2Cl_2 (1 mL, 0.1 M) was added. After stirring for 30 min at 0 °C, the reaction was quenched by addition of saturated aqueous NH_4Cl and extracted with CH_2Cl_2. The combined organic layers were washed with brine, dried over anhydrous Na_2SO_4, and concentrated *in vacuo*. The residue was purified by column chromatography (silica gel, hexanes/EtOAc, 1/1) to afford **3.106** (25 mg, 40%): ^{1}H NMR (400 MHz, $CDCl_3$) δ 7.82–7.76 (m, 2H), 7.47 (d, *J* = 7.2 Hz, 2H), 7.37 (dd, *J* = 7.2, 7.6 Hz, 2H), 7.31 (d, *J* = 7.6 Hz, 1H), 6.89

(dd, *J* = 6.0, 8.4 Hz, 2H), 6.83 (dd, *J* = 2.0, 13.2 Hz, 2H), 6.77–6.68 (m, 3H), 5.54 (s, 1H), 5.39 (dd, *J* = 5.2, 6.0 Hz, 2H), 5.34 (dd, *J* = 4.4, 6.8 Hz, 1H), 5.18 (s, 2H), 3.93 (s, 3H), 3.89 (s, 3H), 3.84 (s, 3H), 2.24–2.20 (m, 2H), 1.64 (d, *J* = 6.8 Hz, 3H), 0.67–0.64 (m, 6H).

Preparation of 3.107

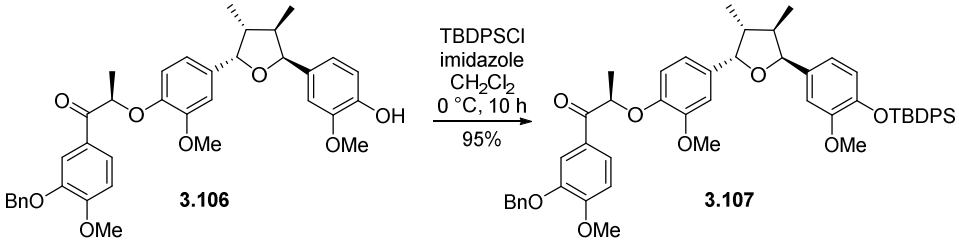

To a cooled (0 °C) solution of phenol **3.106** (18 mg, 0.03 mmol) in dry CH_2Cl_2 (2 mL, 0.02 M) were added imidazole (12 mg, 0.18 mmol) and TBDPSCl (0.02 mL, 0.09 mmol). After stirring for 10 h at the same temperature, the reaction was quenched by addition of saturated aqueous NH_4Cl and extracted with CH_2Cl_2. The combined organic layers were washed with brine, dried over anhydrous Na_2SO_4, and concentrated *in vacuo*. The residue was purified by column chromatography (silica gel, hexanes/EtOAc, 3/1) to afford **3.107** as a white foam (24 mg, 95 %): ^{1}H NMR (400 MHz, $CDCl_3$) δ 7.81–7.68 (m, 6H), 7.47–7.29 (m, 11H), 6.89 (d, *J* = 8.4 Hz, 1H), 6.82–6.66 (m, 5H), 6.53 (d, *J* = 8.4 Hz, 1H), 5.34–5.31 (m, 3H), 5.17 (s, 2H), 3.93 (s, 3H), 3.82 (s, 3H), 3.54 (s, 3H), 2.19–2.12 (m, 2H), 1.64 (d, *J* = 6.8 Hz, 3H), 1.11 (s, 9H), 0.59 (dd, *J* = 6.4, 16.0 Hz, 6H).

Preparation of 3.108

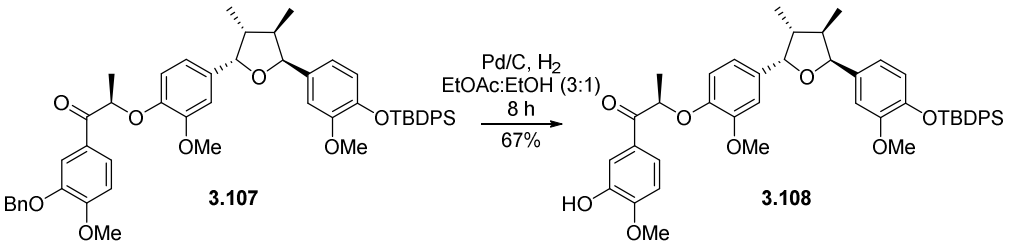

To a stirred solution of benzyl ether **3.107** (102 mg, 0.12 mmol) in EtOAc/EtOH (3/1, 12 mL, 0.1 M) was added 10% Pd–C (30 mg, 30 wt %). The resulting mixture was stirred under H_2 atmosphere at 25 °C for 8 h. The reaction mixture was then filtered through Celite with EtOAc and concentrated *in vacuo*. The residue was purified by column chromatography (silica gel, hexanes/EtOAc, 2/1) to afford **3.108** (62 mg, 67%): ^{1}H NMR (400 MHz, $CDCl_3$) δ 7.74–7.68 (m, 6H), 7.40–7.29 (m, 6H), 6.88 (dd, *J* = 2.0, 8.4 Hz, 1H), 6.81 (dd, *J* = 2.0, 6.0 Hz, 1H), 6.75 (dd, *J* = 4.4, 8.4 Hz, 1H), 6.70–6.66 (m, 3H), 6.55–6.52 (m, 1H), 5.61 (s, 1H), 5.39 (p, *J* = 6.8 Hz, 1H), 5.32 (d, *J* = 4.8 Hz, 2H), 3.95 (s, 3H), 3.84 (s, 3H), 3.54 (s, 3H), 2.18–2.12 (m, 2H), 1.68 (dd, *J* = 2.0, 6.4 Hz, 3H), 1.11 (s, 9H), 0.59 (dd, *J* = 6.4, 13.2 Hz, 6H).

Preparation of 3.109

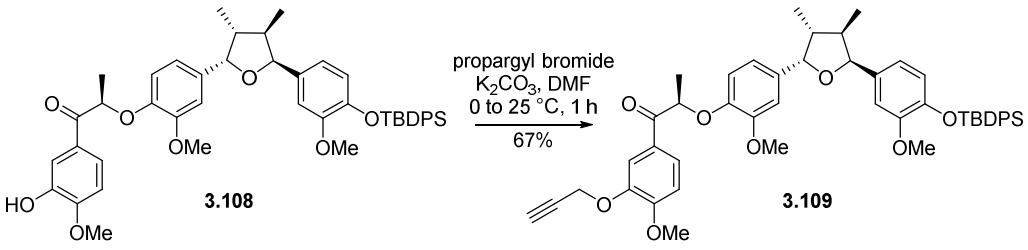

To a cooled (0 °C) solution of phenol **3.108** (20 mg, 0.03 mmol) in dry DMF (2 mL, 0.01 M) were added propargyl bromide (0.02 mL, 0.03 mmol) and K_2CO_3 (5.5 mg, 0.04 mmol). After stirring for 1h at 25 °C, the reaction was quenched by addition of water and extracted with EtOAc. The combined organic layers were washed with brine, dried over anhydrous Na_2SO_4, and concentrated *in vacuo*. The residue was purified by column chromatography (silica gel, hexanes/EtOAc, 2/1) to afford **3.109** as a white foam (14 mg, 67%): ^{1}H NMR (400 MHz, $CDCl_3$) δ 7.88–7.84 (m, 2H), 7.69 (dd, *J* = 1.6, 8.0 Hz, 4H), 7.40–7.30 (m, 6H), 6.90 (d, *J* = 8.0 Hz, 1H), 6.81 (dd, *J* = 1.6, 9.2 Hz, 1H), 6.77 (dd, *J* = 3.6, 8.0 Hz, 1H), 6.70–6.65 (m, 3H), 6.53 (dd, *J* = 1.6, 8.4 Hz, 1H), 5.37 (dq, *J* = 4.4, 6.8 Hz, 1H), 5.33–5.30 (m, 2H), 4.80 (d, *J* = 2.4 Hz, 2H), 3.93 (s, 3H), 3.84 (s, 3H), 3.54 (s, 3H), 2.51 (s, 1H), 2.19–2.12 (m, 2H), 1.71 (d, *J* = 6.8 Hz, 3H), 1.11 (s, 9H), 0.59 (dd, *J* = 6.4, 15.6 Hz, 6H).

Preparation of 3.110

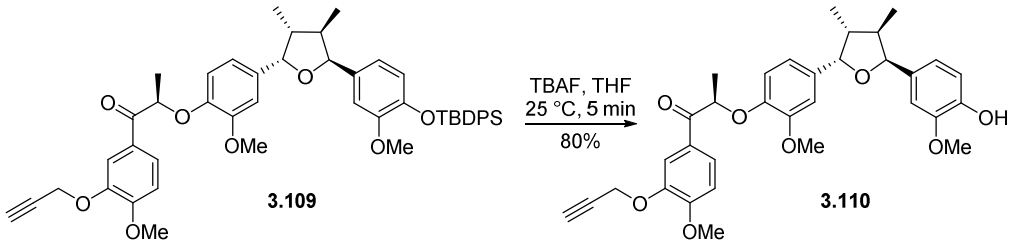

To a solution of silyl ether **3.109** (14 mg, 0.02 mmol) in dry THF (1 mL, 0.02 M) was added TBAF (1.0 M in THF, 0.04 mL, 0.04 mmol). After stirring for 5 min at 25 °C, the reaction was quenched by addition of saturated aqueous NH_4Cl and extracted with EtOAc. The combined organic layers were washed with brine, dried over anhydrous

Na_2SO_4, and concentrated *in vacuo*. The residue was purified by column chromatography (silica gel, hexanes/EtOAc, 2/1) to afford **3.110** (8 mg, 80%): ^{1}H NMR (500 MHz, $CDCl_3$) δ 7.79–7.84 (m, 2H), 6.92–6.68 (m, 7H), 5.52 (s, 1H), 5.40–5.36 (m, 3H), 4.81 (d, *J* = 2.0 Hz, 2H), 3.93 (s, 3H), 3.89 (s, 3H), 3.85 (s, 3H), 2.51 (s, 1H), 2.24–2.18 (m, 2H), 1.71 (d, *J* = 7.0 Hz, 3H), 0.67–0.64 (m, 6H).

Preparation of Alkyne-containing Probe MA13

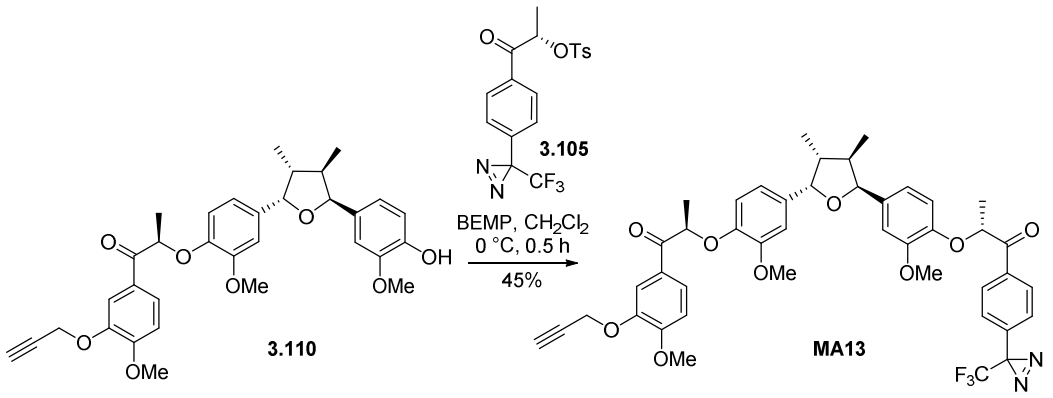

To a cooled (0 °C) solution of phenol **3.110** (8 mg, 0.01 mmol) in dry CH_2Cl_2 (1 mL, 0.01 M) was added dropwise BEMP (0.004 mL, 0.01 mmol). The resulting mixture was stirred at the same temperature for 10 min before tosylate **3.105** (7 mg, 0.02 mmol) in CH_2Cl_2 (0.5 mL, 0.04 M) was added. After stirring for 30 min at 0 °C, the reaction was quenched by addition of saturated aqueous NH_4Cl and extracted with CH_2Cl_2. The combined organic layers were washed with brine, dried over anhydrous Na_2SO_4, and concentrated *in vacuo*. The residue was purified by column chromatography (silica gel, hexanes/EtOAc, 2/1) to afford **MA13** (5 mg, 45%): ^{1}H NMR (400 MHz, $CDCl_3$) δ 8.15 (dd,

J = 4.8, 8.4 Hz, 2H), 7.88–7.84 (m, 2H), 7.23 (d, *J* = 8.4 Hz, 2H), 6.90 (d, *J* = 8.4 Hz, 1H), 6.82–6.76 (m, 4H), 6.70–6.66 (m, 2H), 5.40–5.33 (m, 4H), 4.80 (d, *J* = 2.4 Hz, 2H), 3.93 (s, 3H), 3.84 (s, 3H), 3.80 (s, 3H), 2.51 (s, 1H), 2.21–2.18 (m, 2H), 1.69 (dd, *J* = 6.8, 16.0 Hz, 6H), 0.63–0.60 (m, 6H); IR (neat) 2960, 1684, 1509, 1264, 1025 cm^{-1}; HRMS (ESI) *m*/*z* 823.2803 [$(M+Na)^+$, $C_{44}H_{43}F_3N_2O_9$ requires 823.2813].

Preparation of 3.112

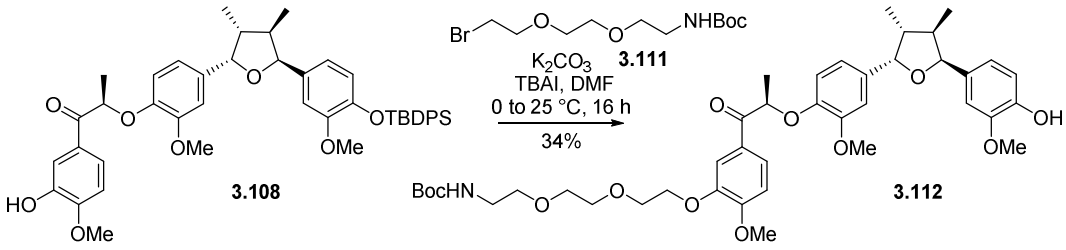

To a solution of phenol **3.108** (15 mg, 0.02 mmol) in dry DMF (2 mL, 0.01 M) was added K_2CO_3 (6 mg, 0.04 mmol) at 25 °C. After stirring for 30 min at the same temperature, the reaction mixture was cooled to 0 °C, and treated with the known polyether bromide **3.111**[138] (7.5 mg, 0.02mmol) and TBAI (0.8 mg, 0.002 mmol). After stirring for 16 h at 25 °C, the reaction was quenched by addition of water and extracted with EtOAc. The combined organic layers were washed with brine, dried over anhydrous Na_2SO_4, and concentrated *in vacuo*. The residue was purified by column chromatography (silica gel, hexanes/EtOAc, 1/2) to afford **3.112** (5 mg, 34%): ^1H NMR (400 MHz, $CDCl_3$) δ 7.82 (dd, *J* = 6.0, 8.4 Hz, 1H), 7.70 (s, 1H), 6.89–6.67 (m, 7H), 5.54 (s, 1H), 5.41–5.38 (m, 3H), 5.15 (bs, 1H), 4.23 (dd, *J* = 4.8, 4.8 Hz, 2H), 3.91–3.89 (m, 5H), 3.89 (s, 3H), 3.85 (s, 3H), 3.72 (dd, *J* =

4.0, 4.8 Hz, 2H), 3.63 (dd, *J* = 4.0, 5.2 Hz, 2H), 3.54 (dd, *J* = 4.8, 5.2 Hz, 2H), 3.31 (d, *J* = 4.8 Hz, 2H), 2.24–2.18 (m, 2H), 1.70 (d, *J* = 6.8 Hz, 3H), 1.42 (s, 9H), 0.65 (dd, *J* = 6.8, 7.2 Hz, 6H).

Preparation of 3.113

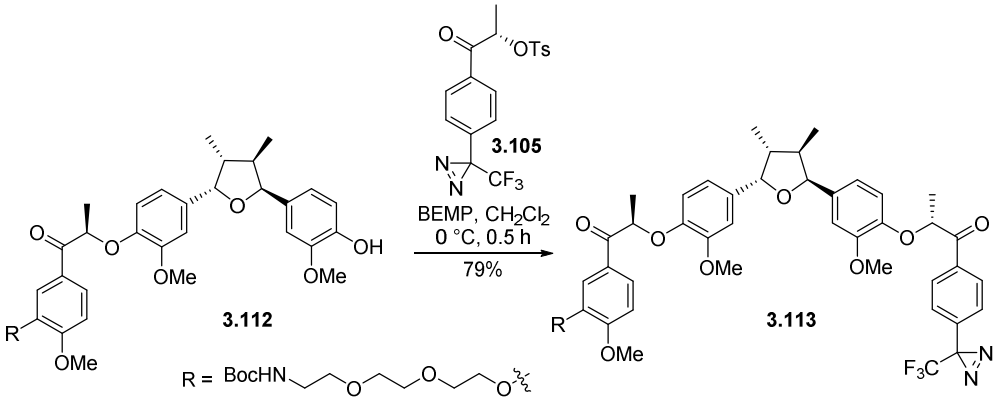

To a cooled (0 °C) solution of phenol **3.112** (24 mg, 0.03 mmol) in dry CH_2Cl_2 (2 mL, 0.02 M) was added dropwise BEMP (0.03 mL, 0.1 mmol). The resulting mixture was stirred at the same temperature for 10 min before tosylate **3.105** (39 mg, 0.1 mmol) in CH_2Cl_2 (1 mL, 0.1 M) was added. After stirring for 30 min at 0 °C, the reaction was quenched by addition of saturated aqueous NH_4Cl and extracted with CH_2Cl_2. The combined organic layers were washed with brine, dried over anhydrous Na_2SO_4, and concentrated *in vacuo*. The residue was purified by column chromatography (silica gel, hexanes/EtOAc, 2/1) to afford **3.113** (26 mg, 79%): ^{1}H NMR (400 MHz, $CDCl_3$) δ 8.15 (dd, *J* = 4.8, 8.4 Hz, 2H), 7.84–7.79 (m, 1H), 7.70 (s, 1H), 7.23 (d, *J* = 8.4 Hz, 2H), 6.87 (d, *J* = 8.4 Hz, 1H), 6.82–6.74 (m, 4H), 6.70–6.65 (m, 2H), 5.42–5.30 (m, 4H), 5.06 (bs, 1H), 4.23 (dd, *J* = 4.8, 4.8 Hz,

2H), 3.91–3.88 (m, 5H), 3.84 (s, 3H), 3.80 (s, 3H), 3.71 (dd, *J* = 4.4, 5.2 Hz, 2H), 3.63 (dd, *J* = 4.0, 4.8 Hz, 2H), 3.54 (dd, *J* = 4.8, 5.2 Hz, 2H), 3.31 (d, *J* = 4.8 Hz, 2H), 2.22–2.16 (m, 2H), 1.68 (dd, *J* = 6.8, 10.8 Hz, 6H), 1.41 (s, 9H), 0.63–0.59 (m, 6H).

Preparation of Biotin-containing Probe MA14

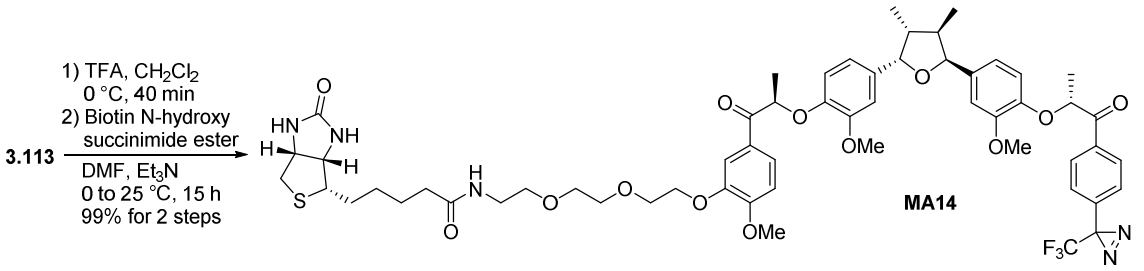

To a cooled (0 °C) solution of Boc-protected amine **3.113** (26 mg, 0.03 mmol) in dry CH_2Cl_2 (1 mL, 0.03 M) was added dropwise TFA (0.5 mL). After stirring for 40 min at the same temperature, the solvent was removed under reduced pressure. The residue was dissolved in dry DMF (1 mL, 0.03 M) and the mixture was treated with Et_3N (0.009 mL, 0.06 mmol) followed by biotin *N*-hydroxysuccinimide ester (9 mg, 0.03 mmol) in DMF (1 mL, 0.03 M) at 0 °C. After stirring for 15 h at 25 °C, the reaction was quenched by addition of water and extracted with CH_2Cl_2. The combined organic layers were washed with brine, dried over anhydrous Na_2SO_4, and concentrated *in vacuo*. The residue was purified by column chromatography (silica gel, CH_2Cl_2/MeOH, 10/1) to afford **MA14** (28 mg, 99%): ^{1}H NMR (400 MHz, $CDCl_3$) δ 8.19–8.11 (m, 2H), 7.87–7.79 (m, 1H), 7.71 (s, 1H), 7.25–7.20 (m, 2H), 6.91–6.65 (m, 7H), 6.55 (bs, 1H), 5.69 (bs, 1H), 5.42–5.30 (m, 4H), 5.07–

4.90 (m, 2H), 4.47–4.41 (m, 1H), 4.37–4.32 (m, 1H), 4.28–4.20 (m, 2H), 3.93–3.88 (m, 5H), 3.84 (s, 3H), 3.80 (s, 3H), 3.73–3.69 (m, 2H), 3.66–3.62 (m, 2H), 3.58–3.54 (m, 2H), 3.43–3.40 (m, 2H), 3.13–3.05 (m, 1H), 2.97–2.89 (m, 1H), 2.76–2.63 (m, 2H), 2.22–2.12 (m, 4H), 1.83–1.66 (m, 8H), 1.40–1.37 (m, 2H), 0.63–0.59 (m, 6H); IR (neat) 2162, 1506, 1148, 650 cm^{-1}; HRMS (ESI) *m*/*z* 1120.4541 [$(M+H)^+$, $C_{57}H_{68}F_3N_5O_{13}S$ requires 1120.4559].

References

1. Hong, J., Role of natural product diversity in chemical biology. *Current opinion in chemical biology* **2011**, *15* (3), 350–354.

2. Newman, D. J.; Cragg, G. M., Natural products as sources of new drugs over the 30 years from 1981 to 2010. *Journal of natural products* **2012**, *75* (3), 311–335.

3. Harvey, A. L.; Edrada-Ebel, R.; Quinn, R. J., The re-emergence of natural products for drug discovery in the genomics era. *Nature Reviews Drug Discovery* **2015**, 14, 111–129

4. Mishra, B. B.; Tiwari, V. K., Natural products: an evolving role in future drug discovery. *European journal of medicinal chemistry* **2011**, *46* (10), 4769–4807.

5. Wade, D. T.; Robson, P.; House, H.; Makela, P.; Aram, J., A preliminary controlled study to determine whether whole-plant cannabis extracts can improve intractable neurogenic symptoms. *Clinical Rehabilitation* **2003**, *17* (1), 21–29.

6. Nurmikko, T. J.; Serpell, M. G.; Hoggart, B.; Toomey, P. J.; Morlion, B. J.; Haines, D., Sativex successfully treats neuropathic pain characterised by allodynia: a randomised, double-blind, placebo-controlled clinical trial. *PAIN*® **2007**, *133* (1), 210–220.

7. (a) Hanson, F. R.; Eble, T. E., An antiphage agent isolated from *Aspergillus* sp. *Journal of bacteriology* **1949,** *58* (4), 527; (b) McCowen, M. C.; Callender, M. E.; Lawlis, J. F., Fumagillin (H-3), a new antibiotic with amebicidal properties. *Science* **1951**, *113* (2930), 202–203.

8. Lanternier, F.; Boutboul, D.; Menotti, J.; Chandesris, M.; Sarfati, C.; Mamzer Bruneel, M.; Calmus, Y.; Mechai, F.; Viard, J.; Lecuit, M., Microsporidiosis in solid organ transplant recipients: two *Enterocytozoon bieneusi* cases and review. *Transplant Infectious Disease* **2009**, *11* (1), 83–88.

9. Sakai, R.; Rinehart, K. L.; Guan, Y.; Wang, A., Additional antitumor ecteinascidins from a Caribbean tunicate: crystal structures and activities *in vivo*. *Proceedings of the National Academy of Sciences* **1992**, *89* (23), 11456–11460.

10. Cassier, P. A.; Dufresne, A.; Blay, J.-Y.; Fayette, J., Trabectedin and its potential in the treatment of soft tissue sarcoma. *Therapeutics and clinical risk management* **2008**, *4* (1), 109–116.

11. Baruchel, S.; Pappo, A.; Krailo, M.; Baker, K. S.; Wu, B.; Villaluna, D.; Lee-Scott, M.; Adamson, P. C.; Blaney, S. M., A phase 2 trial of trabectedin in children with recurrent rhabdomyosarcoma, Ewing sarcoma and non-rhabdomyosarcoma soft tissue sarcomas: a report from the Children's Oncology Group. *European Journal of Cancer* **2012**, *48* (4), 579–585.

12. (a) Michaelson, M.; Bellmunt, J.; Hudes, G.; Goel, S.; Lee, R.; Kantoff, P.; Stein, C.; Lardelli, P.; Pardos, I.; Kahatt, C., Multicenter phase II study of trabectedin in patients with metastatic castration-resistant prostate cancer. *Annals of oncology* **2012**, *23* (5), 1234–1240; (b) Delaloge, S.; Wolp-Diniz, R.; Byrski, T.; Blum, J.; Gonçalves, A.; Campone, M.; Lardelli, P.; Kahatt, C.; Nieto, A.; Cullell-Young, M., Activity of trabectedin in germline BRCA1/2-mutated metastatic breast cancer: results of an international first-in-class phase II study. *Annals of Oncology* **2014,** *25* (6), 1152–1158.

13. Ueda, H.; Nakajima, H.; Hori, Y.; Fujita, T.; Nishimura, M.; Goto, T.; Okuhara, M., FR901228, a novel antitumor bicyclic depsipeptide produced by *Chromobacterium violaceum* No. 968. I. Taxonomy, fermentation, isolation, physico-chemical and biological properties, and antitumor activity. *The Journal of antibiotics* **1994**, *47* (3), 301–310.

14. Nakajima, H.; Kim, Y. B.; Terano, H.; Yoshida, M.; Horinouchi, S., FR901228, a potent antitumor antibiotic, is a novel histone deacetylase inhibitor. *Experimental cell research* **1998**, *241* (1), 126–133.

15. Coiffier, B.; Pro, B.; Prince, H. M.; Foss, F.; Sokol, L.; Greenwood, M.; Caballero, D.; Morschhauser, F.; Wilhelm, M.; Pinter-Brown, L., Romidepsin for the treatment of relapsed/refractory peripheral T-cell lymphoma: pivotal study update demonstrates durable responses. *J Hematol Oncol* **2014**, *7* (11), 1–9.

16. (a) Anand, P.; Bley, K., Topical capsaicin for pain management: therapeutic potential and mechanisms of action of the new high-concentration capsaicin 8% patch. *British journal of anaesthesia* **2011**, *107* (4), 490-502; (b) Derry, S.; Rice, A. S.; Cole, P.; Tan, T.; Moore, R. A., Topical capsaicin (high concentration) for chronic neuropathic pain in adults. *The Cochrane Library* **2013**, *2*, 1–32.

17. Hong, J., Natural Product Synthesis at the Interface of Chemistry and Biology. *Chemistry-A European Journal* **2014**, *20* (33), 10204-10212.

18. Kino, T.; Hatanaka, H.; Hashimoto, M.; Nishiyama, M.; Goto, T.; Okuhara, M.; Kohsaka, M.; Aoki, H.; Imanaka, H., FK-506, a novel immunosuppressant isolated from a Streptomyces. I. Fermentation, isolation, and physico-chemical and biological characteristics. *The Journal of antibiotics* **1987**, *40* (9), 1249–1255.

19. Kino, T.; Hatanaka, H.; Miyata, S.; Inamura, N.; Nishiyama, M.; Yajima, T.; Goto, T.; Okuhara, M.; Kohsaka, M.; Aoki, H., FK-506, a novel immunosuppressant isolated from a Streptomyces. II. Immunosuppressive effect of FK-506 *in vitro*. *The Journal of antibiotics* **1987**, *40* (9), 1256–1265.

20. Faulds, D.; Goa, K. L.; Benfield, P., Cyclosporin. *Drugs* **1993**, *45* (6), 953–1040.

21. Liu, J.; Farmer, J. D.; Lane, W. S.; Friedman, J.; Weissman, I.; Schreiber, S. L., Calcineurin is a common target of cyclophilin-cyclosporin A and FKBP-FK506 complexes. *Cell* **1991**, *66* (4), 807–815.

22. Caterina, M. J.; Schumacher, M. A.; Tominaga, M.; Rosen, T. A.; Levine, J. D.; Julius, D., The capsaicin receptor: a heat-activated ion channel in the pain pathway. *Nature* **1997**, *389* (6653), 816–824.

23. Corey, E. J.; Gin, D. Y.; Kania, R. S., Enantioselective total synthesis of ecteinascidin 743. *Journal of the American Chemical Society* **1996**, *118* (38), 9202–9203.

24. (a) Endo, A.; Yanagisawa, A.; Abe, M.; Tohma, S.; Kan, T.; Fukuyama, T., Total synthesis of ecteinascidin 743. *Journal of the American Chemical Society* **2002**, *124* (23), 6552–6554; (b) Chen, J.; Chen, X.; Bois-Choussy, M.; Zhu, J., Total synthesis of ecteinascidin 743. *Journal of the American Chemical Society* **2006**, *128* (1), 87–89; (c) Zheng, S.; Chan, C.; Furuuchi, T.; Wright, B.; Zhou, B.; Guo, J.; Danishefsky, S., Stereospecific formal total synthesis of ecteinascidin 743. *Angewandte Chemie (International ed. in English)* **2006**, *45* (11), 1754–1759; (d) Fishlock, D.; Williams, R. M., Synthetic studies on Et-743. Assembly of the pentacyclic core and a formal total synthesis. *The Journal of organic chemistry* **2008**, *73* (24), 9594–9600; (e) Imai, T.; Nakata, H.; Yokoshima, S.; Fukuyama, T., Synthetic studies toward ecteinascidin 743 (Trabectedin). *Synthesis* **2012**, (17), 2743–2753; (f) Kawagishi, F.; Toma, T.; Inui, T.; Yokoshima, S.; Fukuyama, T., Total synthesis of ecteinascidin 743. *Journal of the American Chemical Society* **2013**, *135* (37), 13684–13687.

25. Le, V.; Inai, M.; Williams, R.; Kan, T., Ecteinascidins. A review of the chemistry, biology and clinical utility of potent tetrahydroisoquinoline antitumor antibiotics. *Natural product reports* **2015**, *32*, 328–347.

26. Zwenger, S.; Basu, C., Plant terpenoids: applications and future potentials. *Biotechnol Mol Biol Rev* **2008**, *3* (1), 1–7.

27. Yang, H.; Dou, Q. P., Targeting apoptosis pathway with natural terpenoids: implications for treatment of breast and prostate cancer. *Current drug targets* **2010**, *11* (6), 733–744.

28. Xia, J.; Chen, J.; Zhang, Z.; Song, P.; Tang, W.; Kokudo, N., A map describing the association between effective components of traditional Chinese medicine and signaling pathways in cancer cells *in vitro* and *in vivo*. *Drug discoveries & therapeutics* **2014**, *8* (4), 139–153.

29. (a) Yang, J.; Mao, A.; Yue, Z.; Zhu, W.; Luo, X.; Zhu, C.; Xiao, Y.; Zhang, J., A simple base-mediated synthesis of diverse functionalized ring-fluorinated 4 H-pyrans via double direct C–F substitutions. *Chemical Communications* **2015**, *51* (39), 8326–8329; (b) Wilk, W.; Waldmann, H.; Kaiser, M., γ-Pyrone natural products–A privileged compound class provided by nature. *Bioorganic & medicinal chemistry* **2009**, *17* (6), 2304–2309.

30. (a) Katoh, T., Total Synthesis of Diterpenoid Pyrones, Nalanthalide, Sesquicillin, Candelalides A–C, and Subglutinols A, B. *Studies in Natural Products Chemistry* **2014**, *43*, 1–39; (b) Lee, J. C.; Lobkovsky, E.; Pliam, N. B.; Strobel, G.; Clardy, J., Subglutinols A and B: immunosuppressive compounds from the endophytic fungus Fusarium subglutinans. *The Journal of Organic Chemistry* **1995**, *60* (22), 7076–7077; (c) Singh, S. B.; Zink, D. L.; Dombrowski, A. W.; Dezeny, G.; Bills, G. F.; Felix, J. P.; Slaughter, R. S.; Goetz, M. A., Candelalides A–C: Novel Diterpenoid Pyrones from Fermentations of Sesquicillium c andelabrum as Blockers of the Voltage-Gated Potassium Channel Kv1. 3. *Organic letters* **2001**, *3* (2), 247–250; (d) Goetz, M. A.; Zink, D. L.; Dezeny, G.; Dombrowski, A.; Polishook, J. D.; Felix, J. P.; Slaughter, R. S.; Singh, S. B., Diterpenoid pyrones, novel blockers of the voltage-gated potassium channel Kv1. 3 from fungal fermentations. *Tetrahedron Letters* **2001**, *42* (7), 1255–1257; (e) Uchida, R.; Imasato, R.; Yamaguchi, Y.; Masuma, R.; Shiomi, K.; Tomoda, H.; Omura, S., New sesquicillins, insecticidal antibiotics produced by Albophoma sp. FKI-1778. *Journal of Antibiotics* **2005**, *58* (6), 397–404.

31. Zhang, F.; Danishefsky, S. J., An Efficient Stereoselective Total Synthesis of dl-Sesquicillin, a Glucocorticoid Antagonist. *Angewandte Chemie International Edition* **2002**, *41* (8), 1434–1437.

32. (a) Watanabe, K.; Iwasaki, K.; Abe, T.; Inoue, M.; Ohkubo, K.; Suzuki, T.; Katoh, T., Enantioselective Total Synthesis of (–)-Candelalide A, a Novel Blocker of the Voltage-Gated Potassium Channel Kv1. 3 for an Immunosuppressive Agent. *Organic letters* **2005**, *7* (17), 3745–3748; (b) Oguchi, T.; Watanabe, K.; Ohkubo, K.; Abe, H.; Katoh, T., Enantioselective Total Synthesis of (−)-Candelalides A, B and C: Potential Kv1. 3 Blocking Immunosuppressive Agents. *Chemistry-A European Journal* **2009**, *15* (12), 2826–2845.

33. (a) Abe, T.; Iwasaki, K.; Inoue, M.; Suzuki, T.; Watanabe, K.; Katoh, T., Convergent and enantioselective total synthesis of (−)-nalanthalide, a potential Kv1. 3 blocking immunosuppressant. *Tetrahedron letters* **2006**, *47* (19), 3251–3255; (b) Oguchi, T.; Watanabe, K.; Abe, H.; Katoh, T., Enantioselective total synthesis of novel diterpenoid pyrones (+)-sesquicillin and (-)-nalanthalide from fungal fermentations. *Heterocycles* **2010**, *80* (1), 229–250.

34. (a) Kim, H.; Baker, J. B.; Lee, S.-U.; Park, Y.; Bolduc, K. L.; Park, H.-B.; Dickens, M. G.; Lee, D.-S.; Kim, Y.; Kim, S. H., Stereoselective synthesis and osteogenic activity of subglutinols A and B. *Journal of the American Chemical Society* **2009**, *131* (9), 3192–3194; (b) Kim, H.; Baker, J. B.; Park, Y.; Park, H. B.; DeArmond, P. D.; Kim, S. H.; Fitzgerald, M. C.; Lee, D. S.; Hong, J., Total Synthesis, Assignment of the Absolute Stereochemistry, and Structure-Activity Relationship Studies of Subglutinols A and B. *Chemistry–An Asian Journal* **2010**, *5* (8), 1902–1910.

35. Kikuchi, T.; Mineta, M.; Ohtaka, J.; Matsumoto, N.; Katoh, T., Enantioselective Total Synthesis of (–)-Subglutinols A and B: Potential Immunosuppressive Agents Isolated from a Microorganism. *European Journal of Organic Chemistry* **2011**, *2011* (26), 5020–5030.

36. Lin, R.; Kim, H.; Hong, J.; Li, Q.-J., Biological Evaluation of Subglutinol A As a Novel Immunosuppressive Agent for Inflammation Intervention. *ACS medicinal chemistry letters* **2014**, *5* (5), 485–490.

37. Lim, W.; Park, J.; Lee, Y. H.; Hong, J.; Lee, Y., Subglutinol A, an immunosuppressive α-pyrone diterpenoid from *Fusarium subglutinans*, acts as an estrogen receptor antagonist. *Biochemical and biophysical research communications* **2015**, *461* (3), 507–512.

38. (a) Kikuchi, H.; Hoshi, T.; Kitayama, M.; Sekiya, M.; Katou, Y.; Ueda, K.; Kubohara, Y.; Sato, H.; Shimazu, M.; Kurata, S., New diterpene pyrone-type compounds, metarhizins A and B, isolated from entomopathogenic fungus, *Metarhizium*

flavoviride and their inhibitory effects on cellular proliferation. *Tetrahedron* **2009**, *65* (2), 469–477; (b) Katou, Y.; Endo, N.; Suzuki, T.; Yu, J.; Kikuchi, H.; Oshima, Y.; Homma, Y., Metarhizin A suppresses cell proliferation by inhibiting cytochrome c oxidase activity. *Life sciences* **2014**, *103* (1), 1–7.

39. Gupta, S.; Krasnoff, S. B.; Renwick, J.; Roberts, D. W.; Steiner, J. R.; Clardy, J., Viridoxins A and B: novel toxins from the fungus *Metarhizium flavoviride*. *The Journal of Organic Chemistry* **1993**, *58* (5), 1062–1067.

40. Klein, L. L., Convenient Synthesis of 2, 5-Dimethyl-2-Furoic Acid. *Synthetic Communications* **1986**, *16* (4), 431–435.

41. Suzuki, K.; Kuwahara, A.; Yoshida, H.; Fujita, S.; Nishikiori, T.; Nakagawa, T., NF00659A1, A2, A3, B1 and B2, novel antitumor antibiotics produced by *Aspergillus* sp. NF 00659. I. Taxonomy, fermentation, isolation and biological activities. *The Journal of antibiotics* **1997**, *50* (4), 314–317.

42. Suzuki, K.; Kuwahara, A.; Nishikiori, T.; Nakagawa, T., NF00659A1, A2, A3, B1 and B2, novel antitumor antibiotics produced by *Aspergillus* sp. NF 00659. II. Structural elucidation. *The Journal of antibiotics* **1997**, *50* (4), 318–324.

43. Pavia, D.; Lampman, G.; Kriz, G.; Vyvyan, J., *Introduction to spectroscopy*. Cengage Learning: 2008, pp 242.

44. (a) Guerriero, A.; D'Ambrosio, M.; Cuomo, V.; Vanzanella, F.; Pietra, F., Novel Trinor-eremophilanes (Dendryphiellin B, C, and D), Eremophilanes (Dendryphiellin E, F, and G), and Branched C9-Carboxylic Acids (Dendryphiellic Acid A and B) from the Marine Deuteromycete *Dendryphiella salina* (SUTHERLAND) PUGH*et* NICOT. *Helvetica Chimica Acta* **1989**, *72* (3), 438–446; (b) Akao, H.; Kiyota, H.; Nakajima, T.; Kitahara, T., Synthesis of dendryphiellin C, a trinor-sesquiterpene from a marine source. *Tetrahedron* **1999**, *55* (25), 7757–7770; (c) Kim, S.-k.; Hatori, M.; Ojika, M.; Sakagami, Y.; Marumo, S., KM-01, a brassinolide inhibitor, its production, isolation and structure from two fungi *Drechslera avenae* and *Pycnoporus coccineus*. *Bioorganic & medicinal chemistry* **1998**, *6* (11), 1975–1982.

45. Hagiwara, H.; Uda, H., Optically pure (4aS)-(+)-or (4aR)-(-)-1, 4a-dimethyl-4, 4a, 7, 8-tetrahydronaphthalene-2, 5 (3H, 6H)-dione and its use in the synthesis of an inhibitor of steroid biosynthesis. *The Journal of Organic Chemistry* **1988**, *53* (10), 2308–2311.

46. Ardon-Jimenez, A.; Halsall, T. G., The reactions of 5α-allyl-1, 1-ethylenedioxy-5β, 9β-dimethyl-trans-decalin-6-one, a potential intermediate in the synthesis of friedolabdanes. *Journal of the Chemical Society, Perkin Transactions 1* **1978**, (12), 1461–1470.

47. (a) Kane, V. V.; Doyle, D. L.; Ostrowski, P. C., A novel transformation of 7-membered ring lactones to β-keto ethers. *Tetrahedron Letters* **1980**, *21* (27), 2643–2646; (b) Nicolaou, K. C.; Shi, G.-Q.; Gunzner, J.; Gärtner, P.; Yang, Z., Palladium-catalyzed functionalization of lactones via their cyclic ketene acetal phosphates. Efficient new synthetic technology for the construction of medium and large cyclic ethers. *Journal of the American Chemical Society* **1997**, *119* (23), 5467–5468.

48. Bird, C.; Hormozi, N., The scope of a new approach to tetrahydrooxepanol synthesis. *Tetrahedron Letters* **1990**, *31* (24), 3501–3504.

49. Peczuh, M. W.; Snyder, N. L., Carbohydrate-based oxepines: ring expanded glycals for the synthesis of septanose saccharides. *Tetrahedron letters* **2003**, *44* (21), 4057–4061.

50. Peng, J.; Clive, D. L., Synthesis of Dihydrooxepin Models Related to the Antitumor Antibiotic MPC1001. *Organic letters* **2007**, *9* (15), 2939–2941.

51. (a) Schmidt, B., Ruthenium-catalyzed olefin metathesis double-bond isomerization sequence. *The Journal of organic chemistry* **2004**, *69* (22), 7672–7687; (b) Nicolaou, K.; Postema, M. H.; Claiborne, C. F., Olefin metathesis in cyclic ether formation. Direct conversion of olefinic esters to cyclic enol ethers with Tebbe-type reagents. *Journal of the American Chemical Society* **1996**, *118* (6), 1565–1566.

52. Murelli, R. P.; Snapper, M. L., Ruthenium-catalyzed tandem cross-metathesis/Wittig olefination: Generation of conjugated dienoic esters from terminal olefins. *Organic letters* **2007**, *9* (9), 1749–1752.

53. Takai, K.; Kakiuchi, T.; Kataoka, Y.; Utimoto, K., A novel catalytic effect of lead on the reduction of a zinc carbenoid with zinc metal leading to a geminal dizinc compound. Acceleration of the Wittig-type olefination with the RCHX2-TiCl4-Zn systems by addition of lead. *The Journal of Organic Chemistry* **1994**, *59* (10), 2668–2670.

54. Iyer, K.; Rainier, J. D., Olefinic ester and diene ring-closing metathesis using a reduced titanium alkylidene. *Journal of the American Chemical Society* **2007**, *129* (42), 12604–12605.

55. Sutton, A. E.; Seigal, B. A.; Finnegan, D. F.; Snapper, M. L., New tandem catalysis: preparation of cyclic enol ethers through a ruthenium-catalyzed ring-closing metathesis-olefin isomerization sequence. *Journal of the American Chemical Society* **2002**, *124* (45), 13390–13391.

56. Bandyopadhyay, A.; Pal, B. K.; Chattopadhyay, S. K., A short route to *N*-protected furanomycin, 5'-*epi*-furanomycin and isofuranomycin derivatives. *Tetrahedron: Asymmetry* **2008**, *19* (16), 1875–1877.

57. Allwein, S. P.; Cox, J. M.; Howard, B. E.; Johnson, H. W.; Rainier, J. D., C-Glycosides to fused polycyclic ethers. *Tetrahedron* **2002**, *58* (10), 1997–2009.

58. Bovicelli, P.; Mincione, E.; Antonioletti, R.; Bernini, R.; Colombari, M., Selective halogenation of aromatics by dimethyl-dioxirane and halogen ions. *Synthetic Communications* **2001**, *31* (19), 2955–2963.

59. Rainier, J. D.; Allwein, S. P.; Cox, J. M., C-Glycosides to fused polycyclic ethers. A formal synthesis of (±)-Hemibrevetoxin B. *The Journal of organic chemistry* **2001**, *66* (4), 1380–1386.

60. Inanaga, J.; Hirata, K.; Saeki, H.; Katsuki, T.; Yamaguchi, M., A rapid esterification by means of mixed anhydride and its application to large-ring lactonization. *Bulletin of the chemical society of Japan* **1979**, *52* (7), 1989–1993.

61. Yoshida, M.; Takai, H.; Mitsuhashi, C.; Shishido, K., Concise and efficient synthesis of 4-hydroxy-2-pyrones from pentane-2, 4-diones. *Heterocycles* **2010**, *82* (1), 881–886.

62. Hagiwara, H.; Kobayashi, K.; Hoshi, T.; Suzuki, T.; Ando, M., A new protocol for synthesis of 3-hydroxymethyl-4-methoxy-2H-pyrone derivatives. *Tetrahedron* **2001**, *57* (24), 5039–5043.

63. Appel, R., Tertiary phosphane/tetrachloromethane, a versatile reagent for chlorination, dehydration, and P–N linkage. *Angewandte Chemie International Edition in English* **1975**, *14* (12), 801–811.

64. Hosomi, A.; Sakurai, H., Conjugate addition of allylsilanes to α,β-enones. A new method of stereoselective introduction of the angular allyl group in fused cyclic α,β-enones. *Journal of the American Chemical Society* **1977**, *99* (5), 1673–1675.

65. Minassi, A.; Cicione, L.; Koeberle, A.; Bauer, J.; Laufer, S.; Werz, O.; Appendino, G., A Multicomponent Carba-Betti Strategy to Alkylidene Heterodimers–Total Synthesis and Structure–Activity Relationships of Arzanol. *European Journal of Organic Chemistry* **2012**, *2012* (4), 772–779.

66. Petroski, R. J., Improved preparation of halopropyl bridged carboxylic ortho esters. *Org Commun* **2008**, *1*, 48–53.

67. Semenza, G. L., Targeting HIF-1 for cancer therapy. *Nature reviews cancer* **2003**, *3* (10), 721–732.

68. Guzy, R. D.; Schumacker, P. T., Oxygen sensing by mitochondria at complex III: the paradox of increased reactive oxygen species during hypoxia. *Experimental physiology* **2006**, *91* (5), 807–819.

69. Bertout, J. A.; Patel, S. A.; Simon, M. C., The impact of O_2 availability on human cancer. *Nature Reviews Cancer* **2008**, *8* (12), 967–975.

70. Semenza, G. L., Oxygen sensing, hypoxia-inducible factors, and disease pathophysiology. *Annual Review of Pathology: Mechanisms of Disease* **2014**, *9*, 47–71.

71. Semenza, G. L.; Nejfelt, M. K.; Chi, S. M.; Antonarakis, S. E., Hypoxia-inducible nuclear factors bind to an enhancer element located 3' to the human erythropoietin gene. *Proceedings of the National Academy of Sciences* **1991**, *88* (13), 5680–5684.

72. Wang, G. L.; Jiang, B.-H.; Rue, E. A.; Semenza, G. L., Hypoxia-inducible factor 1 is a basic-helix-loop-helix-PAS heterodimer regulated by cellular O_2 tension. *Proceedings of the national academy of sciences* **1995**, *92* (12), 5510–5514.

73. Zhao, J.; Du, F.; Shen, G.; Zheng, F.; Xu, B., The role of hypoxia-inducible factor-2 in digestive system cancers. *Cell death & disease* **2015**, *6* (1), e1600.

74. (a) Tian, H.; McKnight, S. L.; Russell, D. W., Endothelial PAS domain protein 1 (EPAS1), a transcription factor selectively expressed in endothelial cells. *Genes & development* **1997**, *11* (1), 72–82; (b) Ema, M.; Taya, S.; Yokotani, N.; Sogawa, K.; Matsuda, Y.; Fujii-Kuriyama, Y., A novel bHLH-PAS factor with close sequence similarity to hypoxia-inducible factor 1α regulates the VEGF expression and is potentially involved in lung and vascular development. *Proceedings of the National Academy of Sciences* **1997**, *94* (9), 4273–4278; (c) Flamme, I.; Fröhlich, T.; von Reutern, M.; Kappel, A.; Damert, A.; Risau, W., HRF, a putative basic helix-loop-helix-PAS-domain transcription factor is

closely related to hypoxia-inducible factor-1α and developmentally expressed in blood vessels. *Mechanisms of development* **1997**, *63* (1), 51–60.

75. Wiesener, M. S.; Jürgensen, J. S.; Rosenberger, C.; Scholze, C. K.; Hörstrup, J. H.; Warnecke, C.; Mandriota, S.; Bechmann, I.; Frei, U. A.; Pugh, C. W., Widespread hypoxia-inducible expression of HIF-2α in distinct cell populations of different organs. *The FASEB Journal* **2003**, *17* (2), 271–273.

76. Holmquist-Mengelbier, L.; Fredlund, E.; Löfstedt, T.; Noguera, R.; Navarro, S.; Nilsson, H.; Pietras, A.; Vallon-Christersson, J.; Borg, Å.; Gradin, K., Recruitment of HIF-1α and HIF-2α to common target genes is differentially regulated in neuroblastoma: HIF-2α promotes an aggressive phenotype. *Cancer cell* **2006**, *10* (5), 413–423.

77. Mole, D. R.; Blancher, C.; Copley, R. R.; Pollard, P. J.; Gleadle, J. M.; Ragoussis, J.; Ratcliffe, P. J., Genome-wide association of hypoxia-inducible factor (HIF)-1α and HIF-2α DNA binding with expression profiling of hypoxia-inducible transcripts. *Journal of biological chemistry* **2009**, *284* (25), 16767–16775.

78. (a) Fraisl, P.; Mazzone, M.; Schmidt, T.; Carmeliet, P., Regulation of angiogenesis by oxygen and metabolism. *Developmental cell* **2009**, *16* (2), 167–179; (b) Florczyk, U.; Czauderna, S.; Stachurska, A.; Tertil, M.; Nowak, W.; Kozakowska, M.; Poellinger, L.; Jozkowicz, A.; Loboda, A.; Dulak, J., Opposite effects of HIF-1α and HIF-2α on the regulation of IL-8 expression in endothelial cells. *Free Radical Biology and Medicine* **2011**, *51* (10), 1882–1892; (c) Covello, K. L.; Simon, M. C.; Keith, B., Targeted replacement of hypoxia-inducible factor-1α by a hypoxia-inducible factor-2α knock-in allele promotes tumor growth. *Cancer research* **2005**, *65* (6), 2277–2286; (d) Branco-Price, C.; Zhang, N.; Schnelle, M.; Evans, C.; Katschinski, D. M.; Liao, D.; Ellies, L.; Johnson, R. S., Endothelial cell HIF-1α and HIF-2α differentially regulate metastatic success. *Cancer cell* **2012**, *21* (1), 52–65.

79. Gordan, J. D.; Bertout, J. A.; Hu, C.-J.; Diehl, J. A.; Simon, M. C., HIF-2α promotes hypoxic cell proliferation by enhancing *c-myc* transcriptional activity. *Cancer cell* **2007**, *11* (4), 335–347.

80. Gan, B.; Melkoumian, Z. K.; Wu, X.; Guan, K.-L.; Guan, J.-L., Identification of FIP200 interaction with the TSC1–TSC2 complex and its role in regulation of cell size control. *The Journal of cell biology* **2005**, *170* (3), 379–389.

81. Choi, H.; Chun, Y.-S.; Kim, T.-Y.; Park, J.-W., HIF-2α enhances β-catenin/TCF-driven transcription by interacting with β-catenin. *Cancer research* **2010**, *70* (24), 10101–10111.

82. (a) Cummins, E. P., HIF-2α-a mediator of stem cell altruism? *Stem cell research & therapy* **2012**, *3* (6), 52; (b) Das, B.; Bayat-Mokhtari, R.; Tsui, M.; Lotfi, S.; Tsuchida, R.; Felsher, D. W.; Yeger, H., HIF-2α Suppresses p53 to Enhance the Stemness and Regenerative Potential of Human Embryonic Stem Cells. *Stem Cells* **2012**, *30* (8), 1685–1695.

83. (a) Brugarolas, J.; Lei, K.; Hurley, R. L.; Manning, B. D.; Reiling, J. H.; Hafen, E.; Witters, L. A.; Ellisen, L. W.; Kaelin, W. G., Regulation of mTOR function in response to hypoxia by REDD1 and the TSC1/TSC2 tumor suppressor complex. *Genes & development* **2004**, *18* (23), 2893–2904; (b) Koshiji, M.; Kageyama, Y.; Pete, E. A.; Horikawa, I.; Barrett, J. C.; Huang, L. E., HIF-1α induces cell cycle arrest by functionally counteracting Myc. *The EMBO journal* **2004**, *23* (9), 1949–1956.

84. Zhang, P.; Yao, Q.; Lu, L.; Li, Y.; Chen, P.-J.; Duan, C., Hypoxia-inducible factor 3 is an oxygen-dependent transcription activator and regulates a distinct transcriptional response to hypoxia. *Cell reports* **2014**, *6* (6), 1110–1121.

85. Zhang, P.; Lu, L.; Yao, Q.; Li, Y.; Zhou, J.; Liu, Y.; Duan, C., Molecular, functional, and gene expression analysis of zebrafish hypoxia-inducible factor-3α. *American Journal of Physiology-Regulatory, Integrative and Comparative Physiology* **2012**, *303* (11), R1165–R1174.

86. (a) Maynard, M. A.; Evans, A. J.; Hosomi, T.; Hara, S.; Jewett, M. A.; Ohh, M., Human HIF-3α4 is a dominant-negative regulator of HIF-1 and is down-regulated in renal cell carcinoma. *The FASEB journal* **2005**, *19* (11), 1396–1406; (b) Makino, Y.; Cao, R.; Svensson, K.; Bertilsson, G.; Asman, M.; Tanaka, H.; Cao, Y.; Berkenstam, A.; Poellinger, L., Inhibitory PAS domain protein is a negative regulator of hypoxia-inducible gene expression. *Nature* **2001**, *414* (6863), 550–554; (c) Yamashita, T.; Ohneda, O.; Nagano, M.; Iemitsu, M.; Makino, Y.; Tanaka, H.; Miyauchi, T.; Goto, K.; Ohneda, K.; Fujii-Kuriyama, Y., Abnormal heart development and lung remodeling in mice lacking the hypoxia-inducible factor-related basic helix-loop-helix PAS protein NEPAS. *Molecular and cellular biology* **2008**, *28* (4), 1285–1297.

87. Bruick, R. K.; McKnight, S. L., A conserved family of prolyl-4-hydroxylases that modify HIF. *Science* **2001**, *294* (5545), 1337–1340.

88. Semenza, G. L., Hydroxylation of HIF-1: oxygen sensing at the molecular level. *Physiology* **2004**, *19* (4), 176–182.

89. Lisy, K.; Peet, D., Turn me on: regulating HIF transcriptional activity. *Cell Death & Differentiation* **2008**, *15* (4), 642–649.

90. Dayan, F.; Roux, D.; Brahimi-Horn, M. C.; Pouyssegur, J.; Mazure, N. M., The oxygen sensor factor-inhibiting hypoxia-inducible factor-1 controls expression of distinct genes through the bifunctional transcriptional character of hypoxia-inducible factor-1α. *Cancer research* **2006**, *66* (7), 3688–3698.

91. Maxwell, P.; Salnikow, K., HIF-1, an oxygen and metal responsive transcription factor. *Cancer biology & therapy* **2004**, *3* (1), 29–35.

92. (a) Hagen, T.; Taylor, C. T.; Lam, F.; Moncada, S., Redistribution of intracellular oxygen in hypoxia by nitric oxide: effect on HIF1α. *Science* **2003,** *302* (5652), 1975-1978; (b) Sandau, K. B.; Fandrey, J.; Brüne, B., Accumulation of HIF-1α under the influence of nitric oxide. *Blood* **2001**, *97* (4), 1009–1015.

93. Guzy, R. D.; Hoyos, B.; Robin, E.; Chen, H.; Liu, L.; Mansfield, K. D.; Simon, M. C.; Hammerling, U.; Schumacker, P. T., Mitochondrial complex III is required for hypoxia-induced ROS production and cellular oxygen sensing. *Cell metabolism* **2005**, *1* (6), 401–408.

94. Bárdos, J. I.; Ashcroft, M., Hypoxia-inducible factor-1 and oncogenic signalling. *Bioessays* **2004**, *26* (3), 262–269.

95. Jiang, B.-H.; Jiang, G.; Zheng, J. Z.; Lu, Z.; Hunter, T.; Vogt, P. K., Phosphatidylinositol 3-kinase signaling controls levels of hypoxia-inducible factor 1. *Cell growth and differentiation* **2001**, *12* (7), 363–369.

96. Sang, N.; Stiehl, D. P.; Bohensky, J.; Leshchinsky, I.; Srinivas, V.; Caro, J., MAPK signaling up-regulates the activity of hypoxia-inducible factors by its effects on p300. *Journal of Biological chemistry* **2003**, *278* (16), 14013–14019.

97. Vaupel, P. In *Tumor microenvironmental physiology and its implications for radiation oncology*, Seminars in radiation oncology, Elsevier: 2004; pp 198–206.

98. (a) Brizel, D. M.; Sibley, G. S.; Prosnitz, L. R.; Scher, R. L.; Dewhirst, M. W., Tumor hypoxia adversely affects the prognosis of carcinoma of the head and neck.

International Journal of Radiation Oncology Biology* Physics* **1997**, *38* (2), 285–289; (b) Höckel, M.; Schlenger, K.; Aral, B.; Mitze, M.; Schäffer, U.; Vaupel, P., Association between tumor hypoxia and malignant progression in advanced cancer of the uterine cervix. *Cancer research* **1996**, *56* (19), 4509–4515; (c) Moon, E. J.; Brizel, D. M.; Chi, J.-T. A.; Dewhirst, M. W., The potential role of intrinsic hypoxia markers as prognostic variables in cancer. *Antioxidants & redox signaling* **2007**, *9* (8), 1237–1294.

99. Semenza, G. L., Evaluation of HIF-1 inhibitors as anticancer agents. *Drug discovery today* **2007**, *12* (19), 853–859.

100. (a) Aebersold, D. M.; Burri, P.; Beer, K. T.; Laissue, J.; Djonov, V.; Greiner, R. H.; Semenza, G. L., Expression of hypoxia-inducible factor-1α a novel predictive and prognostic parameter in the radiotherapy of oropharyngeal cancer. *Cancer research* **2001**, *61* (7), 2911–2916; (b) Moeller, B. J.; Cao, Y.; Li, C. Y.; Dewhirst, M. W., Radiation activates HIF-1 to regulate vascular radiosensitivity in tumors: role of reoxygenation, free radicals, and stress granules. *Cancer cell* **2004**, *5* (5), 429–441.

101. Koukourakis, M. I.; Giatromanolaki, A.; Sivridis, E.; Simopoulos, C.; Turley, H.; Talks, K.; Gatter, K. C.; Harris, A. L.; Tumour; Group, A. R., Hypoxia-inducible factor (HIF1α and HIF2α), angiogenesis, and chemoradiotherapy outcome of squamous cell head-and-neck cancer. *International Journal of Radiation Oncology* Biology* Physics* **2002**, *53* (5), 1192–1202.

102. Comerford, K. M.; Wallace, T. J.; Karhausen, J.; Louis, N. A.; Montalto, M. C.; Colgan, S. P., Hypoxia-inducible factor-1-dependent regulation of the multidrug resistance (MDR1) gene. *Cancer research* **2002**, *62* (12), 3387–3394.

103. Zhang, X.; Kon, T.; Wang, H.; Li, F.; Huang, Q.; Rabbani, Z. N.; Kirkpatrick, J. P.; Vujaskovic, Z.; Dewhirst, M. W.; Li, C.-Y., Enhancement of hypoxia-induced tumor cell death in vitro and radiation therapy in vivo by use of small interfering RNA targeted to hypoxia-inducible factor-1α. *Cancer research* **2004**, *64* (22), 8139–8142.

104. (a) Giaccia, A.; Siim, B. G.; Johnson, R. S., HIF-1 as a target for drug development. *Nature reviews Drug discovery* **2003**, *2* (10), 803–811; (b) Lin, X.; David, C. A.; Donnelly, J. B.; Michaelides, M.; Chandel, N. S.; Huang, X.; Warrior, U.; Weinberg, F.; Tormos, K. V.; Fesik, S. W., A chemical genomics screen highlights the essential role of mitochondria in HIF-1 regulation. *Proceedings of the National Academy of Sciences* **2008**, *105* (1), 174–179; (c) Zhang, H.; Qian, D. Z.; Tan, Y. S.; Lee, K.; Gao, P.; Ren, Y. R.; Rey, S.; Hammers, H.; Chang, D.; Pili, R., Digoxin and other cardiac glycosides inhibit HIF-1α synthesis and block tumor growth. *Proceedings of the National Academy of Sciences* **2008**, *105* (50), 19579–

19586; (d) Ellinghaus, P.; Heisler, I.; Unterschemmann, K.; Haerter, M.; Beck, H.; Greschat, S.; Ehrmann, A.; Summer, H.; Flamme, I.; Oehme, F., BAY 87-2243, a highly potent and selective inhibitor of hypoxia-induced gene activation has antitumor activities by inhibition of mitochondrial complex I. *Cancer medicine* **2013**, *2* (5), 611–624; (e) Lee, K.; Kang, J. E.; Park, S.-K.; Jin, Y.; Chung, K.-S.; Kim, H.-M.; Lee, K.; Kang, M. R.; Lee, M. K.; Song, K. B., LW6, a novel HIF-1 inhibitor, promotes proteasomal degradation of HIF-1α via upregulation of VHL in a colon cancer cell line. *Biochemical pharmacology* **2010**, *80* (7), 982–989.

105. Chandel, N.; Maltepe, E.; Goldwasser, E.; Mathieu, C.; Simon, M.; Schumacker, P., Mitochondrial reactive oxygen species trigger hypoxia-induced transcription. *Proceedings of the National Academy of Sciences* **1998**, *95* (20), 11715–11720.

106. Swarnkar, S.; Singh, S.; Mathur, R.; Patro, I.; Nath, C., A study to correlate rotenone induced biochemical changes and cerebral damage in brain areas with neuromuscular coordination in rats. *Toxicology* **2010**, *272* (1), 17–22.

107. (a) Rao, K. V.; Alvarez, F. M., Manassantins A/B and saucerneol: novel biologically active lignoids from Saururus cernuus. *Tetrahedron letters* **1983**, *24* (45), 4947–4950; (b) Hodges, T. W.; Hossain, C. F.; Kim, Y.-P.; Zhou, Y.-D.; Nagle, D. G., Molecular-Targeted Antitumor Agents: The Saururus c ernuus Dineolignans Manassantin B and 4-O-Demethylmanassantin B Are Potent Inhibitors of Hypoxia-Activated HIF-1. *Journal of natural products* **2004**, *67* (5), 767–771; (c) Hossain, C. F.; Kim, Y.-P.; Baerson, S. R.; Zhang, L.; Bruick, R. K.; Mohammed, K. A.; Agarwal, A. K.; Nagle, D. G.; Zhou, Y.-D., *Saururus cernuus* lignans–Potent small molecule inhibitors of hypoxia-inducible factor-1. *Biochemical and biophysical research communications* **2005**, *333* (3), 1026–1033.

108. Kim, H.; Kasper, A. C.; Moon, E. J.; Park, Y.; Wooten, C. M.; Dewhirst, M. W.; Hong, J., Nucleophilic addition of organozinc reagents to 2-sulfonyl cyclic ethers: stereoselective synthesis of manassantins A and B. *Organic letters* **2008**, *11* (1), 89–92.

109. Hanessian, S.; Reddy, G. J.; Chahal, N., Total synthesis and stereochemical confirmation of manassantin A, B, and B1. *Organic letters* **2006**, *8* (24), 5477–5480.

110. Lee, A.-L.; Ley, S. V., The synthesis of the anti-malarial natural product polysphorin and analogues using polymer-supported reagents and scavengers. *Organic & biomolecular chemistry* **2003**, *1* (22), 3957–3966.

111. (a) Basha, A.; Lipton, M.; Weinreb, S. M., A mild, general method for conversion of esters to amides. *Tetrahedron letters* **1977**, *18* (48), 4171–4172; (b) Shimizu, T.; Osako, K.;

Nakata, T.-i., Efficient method for preparation of *N*-methoxy-*N*-methyl amides by reaction of lactones or esters with Me_2AlCl-MeONHMe·HCl. *Tetrahedron letters* **1997**, *38* (15), 2685–2688.

112. Kasper, A. C.; Moon, E. J.; Hu, X.; Park, Y.; Wooten, C. M.; Kim, H.; Yang, W.; Dewhirst, M. W.; Hong, J., Analysis of HIF-1 inhibition by manassantin A and analogues with modified tetrahydrofuran configurations. *Bioorganic & medicinal chemistry letters* **2009**, *19* (14), 3783–3786.

113. Shoemaker, R. H., The NCI60 human tumour cell line anticancer drug screen. *Nature Reviews Cancer* **2006**, *6* (10), 813–823.

114. Qu, M. N.; Zhou, L.; Cao, X. P., First synthesis of a series of new natural glucosides. *Chinese Journal of Chemistry* **2006**, *24* (11), 1625–1630.

115. Kolb, H. C.; VanNieuwenhze, M. S.; Sharpless, K. B., Catalytic asymmetric dihydroxylation. *Chemical Reviews* **1994**, *94* (8), 2483–2547.

116. Moreno, I.; Tellitu, I.; Domínguez, E.; SanMartín, R., A simple route to new phenanthro-and phenanthroid-fused thiazoles by a PIFA-mediated (hetero) biaryl coupling reaction. *European Journal of Organic Chemistry* **2002**, *2002* (13), 2126–2135.

117. Corey, E.; Bakshi, R. K.; Shibata, S., Highly enantioselective borane reduction of ketones catalyzed by chiral oxazaborolidines. Mechanism and synthetic implications. *Journal of the American Chemical Society* **1987**, *109* (18), 5551–5553.

118. Kerns, E.; Di, L., *Drug-like properties: concepts, structure design and methods: from ADME to toxicity optimization*. Academic Press: 2010.

119. (a) Andrews, P.; Craik, D.; Martin, J., Functional group contributions to drug-receptor interactions. *Journal of medicinal chemistry* **1984,** *27* (12), 1648-1657; (b) Kuntz, I.; Chen, K.; Sharp, K.; Kollman, P., The maximal affinity of ligands. *Proceedings of the National Academy of Sciences* **1999**, *96* (18), 9997–10002.

120. Zanger, U. M.; Schwab, M., Cytochrome P450 enzymes in drug metabolism: regulation of gene expression, enzyme activities, and impact of genetic variation. *Pharmacology & therapeutics* **2013**, *138* (1), 103–141.

121. Lima, L. M.; Barreiro, E. J., Bioisosterism: a useful strategy for molecular modification and drug design. *Current medicinal chemistry* **2005**, *12* (1), 23–49.

122. Ertl, P., *In silico* identification of bioisosteric functional groups. *Current opinion in drug discovery & development* **2007**, *10* (3), 281–288.

123. Biot, C.; Bauer, H.; Schirmer, R. H.; Davioud-Charvet, E., 5-Substituted tetrazoles as bioisosteres of carboxylic acids. Bioisosterism and mechanistic studies on glutathione reductase inhibitors as antimalarials. *Journal of medicinal chemistry* **2004**, *47* (24), 5972–5983.

124. Meanwell, N. A., The influence of bioisosteres in drug design: tactical applications to address developability problems. In *Tactics in Contemporary Drug Design*, Springer: 2015; pp 283–381.

125. Ohtaka, H.; Fujita, T., Structural modification patterns from agonists to antagonists and their application to drug design–A new serotonin (5-HT_3) antagonist series. In *Progress in Drug Research/Fortschritte der Arzneimittelforschung/Progrès des recherches pharmaceutiques*, Springer: 1993; pp 313–357.

126. Melander, A.; Sartor, G.; Wåhlin, E.; Schersten, B.; Bitzén, P.-O., Serum tolbutamide and chlorpropamide concentrations in patients with diabetes mellitus. *BMJ* **1978**, *1* (6106), 142–144.

127. Bunch, L., Bioisosteres in Medicinal Chemistry. Edited by Nathan Brown. Wiley Online Library: 2013.

128. Patani, G. A.; LaVoie, E. J., Bioisosterism: a rational approach in drug design. *Chemical reviews* **1996**, *96* (8), 3147–3176.

129. Sleno, L.; Emili, A., Proteomic methods for drug target discovery. *Current opinion in chemical biology* **2008**, *12* (1), 46–54.

130. Singh, A.; Thornton, E. R.; Westheimer, F., The photolysis of diazoacetylchymotrypsin. *Journal of Biological Chemistry* **1962**, *237* (9), PC3006–PC3008.

131. Brunner, J.; Senn, H.; Richards, F., 3-Trifluoromethyl-3-phenyldiazirine. A new carbene generating group for photolabeling reagents. *Journal of Biological Chemistry* **1980**, *255* (8), 3313–3318.

132. (a) Tomohiro, T.; Hashimoto, M.; Hatanaka, Y., Cross-linking chemistry and biology: development of multifunctional photoaffinity probes. *The Chemical Record* **2005**,

5 (6), 385–395; (b) Dubinsky, L.; Krom, B. P.; Meijler, M. M., Diazirine based photoaffinity labeling. *Bioorganic & medicinal chemistry* **2012**, *20* (2), 554–570.

133. Lapinsky, D. J., Tandem photoaffinity labeling–bioorthogonal conjugation in medicinal chemistry. *Bioorganic & medicinal chemistry* **2012**, *20* (21), 6237–6247.

134. Saxon, E.; Bertozzi, C. R., Cell surface engineering by a modified Staudinger reaction. *Science* **2000**, *287* (5460), 2007–2010.

135. Rostovtsev, V.; Green, L.; Fokin, V.; Sharpless, K., A stepwise Huisgen cycloaddition process: Copper (I)-catalyzed regioselective "ligation" of azides and terminal alkynes. *Angew. Chem. Int. Ed* **2002**, *41*, 2596–2599.

136. Lee, K.; Ban, H. S.; Naik, R.; Hong, Y. S.; Son, S.; Kim, B. K.; Xia, Y.; Song, K. B.; Lee, H. S.; Won, M., Identification of malate dehydrogenase 2 as a target protein of the HIF-1 inhibitor LW6 using chemical probes. *Angewandte Chemie International Edition* **2013**, *52* (39), 10286–10289.

137. McGuigan, C.; Bidet, O.; Derudas, M.; Andrei, G.; Snoeck, R.; Balzarini, J., Alkenyl substituted bicyclic nucleoside analogues retain nanomolar potency against varicella zoster virus. *Bioorganic & medicinal chemistry* **2009**, *17* (8), 3025–3027.

138. Hatanaka, Y.; Hashimoto, M.; Kanaoka, Y., A novel biotinylated heterobifunctional cross-linking reagent bearing an aromatic diazirine. *Bioorganic & medicinal chemistry* **1994**, *2* (12), 1367–1373.

Biography

Do Yeon Kwon was born on February 6, 1982 in Daegu, South Korea. She graduated *magna cum laude* with a Bachelor of Science degree in Pharmacy from the department of pharmacy at Duksung Women's University, South Korea in February of 2005. After she had worked as a pharmacist for 2 years, she began her master program at Seoul National University and received her Master of Science degree in Pharmacy in February of 2009.

In the fall of 2010, she began her Ph.D. program in the department of chemistry at Duke University and received her Doctor of Philosophy in organic chemistry in July of 2015.

Honors & Awards:

Graduate School Travel Grant, Duke University	2015
C.R. Hauser Memorial Fellowship, Duke University	2013
Burroughs Wellcome Fellowship, Duke University	2012
Chemistry Departmental Fellowship, Duke University	2010–2014
Brain Korea (BK) scholarship, Korean Government	2007–2009
Magna Cum Laude graduate (B.S.), Duksung Women's University	2005
Academic scholarship for excellent GPA, Duksung Women's University	2000–2004
Namhae scholarship, Duksung Women's University	2000

Publications:

1. Zachary Lee Johnson, Jun-Ho Lee, Kiyoun Lee, Minhee Lee, **Do-Yeon Kwon**, Jiyong Hong, Seok-Yong Lee, "Structural basis of nucleoside and nucleoside drug selectivity by concentrative nucleoside transporters" *eLife*, **2014**, *3*, e03604.

2. Ben C. Chung, Jinshi Zhao, Robert A. Gillespie, **Do-Yeon Kwon**, Ziqiang Guan, Pei Zhou, Jiyong Hong, Seok-Yong Lee, "Crystal Structure of MraY, an Essential Membrane Enzyme for Bacterial Cell Wall Synthesis" *Science*, **2013**, *341*, 1012-1016.

3. Funan Li, Nam-Jung Kim, Seung-Mann Paek, **Do-Yeon Kwon**, Kyung Hoon Min, Yeon-Su Jeong, Sun-Young Kim, Young-Ho Park, Hee-Doo Kim, Hyeung-Geun Park, and Young-Ger Suh, "Design, synthesis, and biological evaluation of novel diarylalkyl amides as TRPV1 antagonists" *Bioorg. Med. Chem*. **2009**, *17*, 3557-3567.

4. Chan-Hee Park, Jongwon Lee, Hwi Young Jung, Min Ji Kim, Sun Ha Lim, Hyung Tae Yeo, Eung Chil Choi, Eun Jeong Yoon, Kyu Won Kim, Jong Ho Cha, Seok-Ho Kim, Dong-Jo Chang, **Do-Yeon Kwon**, Funan Li and Young-Ger Suh, "Identification, biological activity, and mechanism of the anti-ischemic Quinolone analog" *Bioorg. Med. Chem*. **2007**, *15*, 6517-6526.

Presentations:

1. **Do-Yeon Kwon**, Kyunghye Park, Douglas H. Weitzel, Chen-Ting Lee, Tesia N. Stephenson, Hyeri Park, Michael C. Fitzgerald, Jen-Tsan Chi, Robert A. Mook Jr., Mark W. Dewhirst, You Mie Lee, Jiyong Hong, "Design, Synthesis, and biological evaluation of manassantin analogues for HIF-1α inhibition" WiSE Symposium, Duke University, Durham, NC, United States, April 10, **2015**. (Poster Presentation)

2. **Do-Yeon Kwon**, Kyunghye Park, Douglas H. Weitzel, Chen-Ting Lee, Tesia N. Stephenson, Hyeri Park, Michael C. Fitzgerald, Jen-Tsan Chi, Robert A. Mook Jr., Mark W. Dewhirst, You Mie Lee, Jiyong Hong, "Design, Synthesis, and biological evaluation of manassantin analogues for HIF-1α inhibition, 249th ACS National Meeting, Denver, CO, United States, March 22–26, **2015**. (Oral Presentation)